

Evolution of developmental gene regulatory networks in echinoids

Thesis by
Eric M. Erkenbrack

In Partial Fulfillment of the Requirements for the
degree of
Doctor of Philosophy

The Caltech logo, consisting of the word "Caltech" in a bold, orange, sans-serif font.

CALIFORNIA INSTITUTE OF TECHNOLOGY
Pasadena, California

2016
Defended 7 April 2016

© 2016

Eric M. Erkenbrack
ORCID: [0000-0001-9375-3279]

All rights reserved except where otherwise noted

ACKNOWLEDGEMENTS

There have been hundreds of people who have contributed to my personal, intellectual and professional development. This is an incomplete list; and you have my sincerest apologies if my memory failed me during this retrospection.

To my family and friends, you have endlessly supported me and have made all of this possible. To my brilliant and loving wife, Jennifer, and my precocious, beautiful daughter, Eleanor: you two have made all the difference. Jennifer—tireless mother, successful biotech trailblazer and overachiever—you inspire me and have made me a better scientist and father. To my Minnesota family—Mom, Troy, Andrea, Amy, Storm, Matt, Ciara, Emily, Jacob and Louis—who understood that I needed to go out into the world and find my passion, I couldn't have done it without your support! I am forever grateful for that. For my father, who is no longer with us and who silently developed in me strength, fortitude and resilience, I will always remember what you did for me and how you lived your life. To my Connecticut Family—Bill, Lynda, Terry, Lori, Jimmy, Sarah, Clark, Jack—thank you for helping me find the time to write. For Bill, who recently left us and didn't get to read this monstrous thesis, thank you for welcoming me into your family and for your subsequent encouragement. I will not forget that.

To my friends who entered the program at Caltech with me, Drs. Weston Nichols, Michael Rome, Jon Valencia, and Alexandre Webster, we had so much fun during our critical incubation in academia. Never forget: "Do it right, and you'll have the time of your life!"

To my friends and colleagues who spent so many nights in the basement of Kerckhoff, including Drs. Stefan Materna, Sagar Damle, and Miao Cui: Thank you all for everything. We laughed, cried, suffered and discovered together. Truly stories that will last for lifetimes.

To my friends at Caltech whom I met and engaged with along the way: Georgi Marinov, Nate Pierce, Paul Minor, Tobias Heinen and Danielle Heinen, Cory Tobin, Ned Perkins. I learned so much from all of you.

To my colleagues in the Davidson Lab: Drs. Andy Ransick, Andy Cameron, Feng Gao, Jongmin Nam, Joel Smith, Julius Barsi, Enhu Li, Smadar Ben-Tabou de-Leon, Roberto Feuda, and Professor Michael Collins. My supporting friends and technical staff in Lab: Deanna Thomas, Erika Vielmas, Miki Yun, Carlzen Balagot, Pat Leahy,

and many more. A special shout out to my students who worked beside me: Elise Cai, Neal Desai, Rebekkah Kitto, Ellora Sarkar.

I am grateful to all of the individuals who helped me directly and indirectly working on bioinformatics of echinoderms at the Center for Computational Regulatory Genomics at the Beckman Institute.

To my extended California family, Dr. Rome's wife and my friend, Tara, and the Rome Family: Thank you for welcoming me and for those intellectual conversations, good fun and good times.

To my academic family and friends, who have written letters, called offices, and much more, your help was critical to my endeavor. At Shakopee High School, Mr. Tim Kelly arraigned me in front of my peers, accusing me of being a "pretend student"; you were right, and thank you for doing that. At Normandale Community College, biology faculty Drs. Jim "JE²" Erickson and Joseph McCulloch taught me about biological systems and helped me take my first steps in academia. Also at Normandale, Drs. Linda Tetzlaff, Matt Dempsey and Stephen Donaho provided critical support and insight.

To my mentors at Tufts University, countless faculty members supported, motivated and influenced me in profound ways, especially Drs. Francie Chew, Susan Ernst, Juliet Fuhrman, Sergei Mirkin, and Barry Trimmer. To my advisor Dr. Jan "JP" Pechenik: Thank you for always making time for me. Lastly, my friend and mentor Dr. Colin Orians, you have had an inestimable impact on my life and have played a major role in propelling me to where I have landed. And to all of the other faculty members at Tufts who entertained me through your discussions and helped me with your letters of recommendation: Thank you.

To my mentors in Germany, Drs. Mika Tarkka and Moritz Nowack, who took the time to bring me onto their research projects and showed me how to do good science in an important time of my professional development. Your dedication to mentoring is appreciated.

This study would not have been possible without the divers who collected wild *Eucidaris tribuloides* all over the Gulf of Mexico and the Atlantic Ocean. A special thank you to Kara and Philipp Rauch of KP Aquatics (SeaLife, Inc.), who not only supplied me regularly with livestock, but also spawned and collected gravidity data for me on the reef near Key Largo. Things were a lot less frustrating with your help. I am so appreciative!

To my new mentor at Yale, Dr. Gunter Wagner. Thank you for being so supportive, for believing in me and for allowing me to finish up my "echinoderm stuff" on your dime.

To the Archaeocidaris Dream Team, Drs. David Bottjer, Feng Gao, Liz Petsios, and Jeffrey R. Thompson. Our meetings were sometimes long but never boring. They were truly fun and an interesting meeting of the minds; and we produced some good science along the way. Thank you all.

To my mentor Dr. Isabelle Peter, who was the first and the last person I worked under in the Eric's lab. That was quite a ride; I'm glad we were on it together. Your support was unending through good times and bad.

To my friend Jane Rigg, who always spoke up in my defense. Thank you for the conversations, the thoughtful wishes and the good times. You were a big part of this.

To my committee, Drs. Marianne Bronner, Isabelle Peter, Rob Phillips, Ellen Rothenberg, Paul Sternberg, I appreciate your support, guidance, criticisms and advice over these many years.

Lastly, to my friend and late mentor Eric Harris Davidson, who taught me how to do science, how to identify good and bad science, how to run a lab, how to analytically analyze offensive and defensive schemes of a football game, and so much more. Thank you for inviting me into your lab and changing my life. A glass of bourbon will never be the same. Your memory will live on.

This dissertation is dedicated to my parents, both familial and academic, who taught me so much—even though I didn't realize it until many years later.

ABSTRACT

Developmental gene regulatory networks (dGRNs) are assemblages of regulatory genes that direct embryonic development of animal body plans and their morphological structures. dGRNs exhibit recursively-wired circuitry that is encoded in the genome and executed during development. Alteration to the regulatory architecture of dGRNs causes variation in developmental programs both during the development of an individual organism and during the evolution of an individual lineage. The explanatory power of these networks is best exemplified by the global dGRN directing early development of the euechinoid sea urchin *Strongylocentrotus purpuratus*. This network consists of numerous regulatory genes engaging in hundreds of genomic regulatory transactions that collectively direct the delineation of early embryonic domains and the specification of cell lineages. Research on closely-related euechinoid sea urchins, e.g. *Lytechinus variegatus* and *Paracentrotus lividus*, has revealed marked conservation of dGRN architecture in echinoid development, suggesting little appreciable alteration has occurred since their divergence in evolution at least 90 million years ago (mya).

We sought to test whether this observation extends to all sea urchins (echinoids) and undertook a systematic analysis of over 50 regulatory genes in the cidaroid sea urchin *Eucidaris tribuloides*, surveying their regulatory activity and function in a sea urchin that diverged from euechinoid sea urchins at least 268 mya. Our results revealed extensive alterations have occurred to all levels of echinoid dGRN architecture since the cidaroid-euechinoid divergence. Alterations to mesodermal subcircuits were particularly striking, including functional differences in specification of non-skeletogenic mesenchyme (NSM), skeletogenic mesenchyme (SM), and endomesodermal segregation. Specification of endomesodermal embryonic domains revealed that, while their underlying network circuitry had clearly diverged, regulatory states established in pregastrular embryos of these two groups are strikingly similar. Analyses of *E. tribuloides* specification leading to the establishment of dorsal-ventral (aboral-oral) larval polarity indicated that regulation of regulatory genes expressed in mesodermal embryonic domains had incurred significantly more alterations than those expressed in endodermal and ectodermal domains. Taken together, this study highlights the ability of dGRN architecture to buffer extensive alterations in the evolution and early development of echinoids and adds further support to the notion that alterations can occur at all levels of dGRN architecture and all stages of embryonic development.

PUBLISHED CONTENT AND CONTRIBUTIONS

Erkenbrack, E. M. (2016). “Evolution of gene regulatory network topology and dorsal-ventral axis specification in early development of sea urchins (Echinoidea)”. In: doi: 10.1101/044149. URL: <http://biorxiv.org/content/early/2016/03/16/044149>.
 E.M.E. designed and performed research, analyzed data, and wrote the manuscript.
 Submitted to *PLOS Genetics* on 16 March 2016.

Erkenbrack, E. M., K. Ako-Asare, et al. (2016). “Ancestral state reconstruction by comparative analysis of a GRN kernel operating in echinoderms”. In: *Dev Genes Evol* 226.1, pp. 37–45. ISSN: 1432-041X (Electronic) 0949-944X (Linking). doi: 10.1007/s00427-015-0527-y. URL: <http://www.ncbi.nlm.nih.gov/pubmed/26781941>.
 E.M.E. participated in research design, performed research, participated in data analysis, and wrote the manuscript.

Erkenbrack, E. M. and E. H. Davidson (2015). “Evolutionary rewiring of gene regulatory network linkages at divergence of the echinoid subclasses”. In: *Proc Natl Acad Sci U S A* 112.30, E4075–84. ISSN: 1091-6490 (Electronic) 0027-8424 (Linking). doi: 10.1073/pnas.1509845112. URL: <http://www.ncbi.nlm.nih.gov/pubmed/26170318>.
 E.M.E. participated in research design, performed research, participated in data analysis, and participated in writing the manuscript.

Erkenbrack, E. M., E. H. Davidson, and I. S. Peter (2016). “Divergent developmental gene regulatory networks establish conserved endomesodermal regulatory states in echinoids”. In:
 E.M.E. participated in research design, performed research, participated in data analysis and manuscript writing. *In preparation*.

TABLE OF CONTENTS

Acknowledgements	iii
Abstract	vi
Published Content and Contributions	vii
Table of Contents	viii
List of Illustrations	x
List of Tables	xiii
Chapter I: Introduction	1
1.1 Brief historical sketch of sea urchin research milestones from experimental embryology to modern developmental biology	2
1.2 Notes on developmental evolution in light of gene regulatory networks	10
1.3 History of embryological research on <i>Eucidaris tribuloides</i>	11
1.4 Précis of dissertation chapters	12
Chapter II: Divergent developmental gene regulatory networks establish conserved endomesodermal regulatory states in echinoids	21
2.1 Abstract	22
2.2 Introduction	22
2.3 Results	25
2.4 Discussion	41
2.5 Materials and Methods	48
2.6 Acknowledgements	50
Chapter III: Evolutionary rewiring of gene regulatory network linkages at divergence of the echinoid subclasses	55
3.1 Abstract	56
3.2 Significance	56
3.3 Introduction	57
3.4 Results	60
3.5 Discussion	72
3.6 Materials and Methods	78
3.7 Acknowledgements	81
Chapter IV: Ancestral state reconstruction by comparative analysis of a GRN kernel operating in echinoderms	86
4.1 Abstract	87
4.2 Introduction	87
4.3 Results and Discussion	90
4.4 Materials and Methods	100
4.5 Acknowledgements	101
Chapter V: Evolution of gene regulatory network topology and dorsal-ventral axis specification in sea urchins (Echinoidea)	105
5.1 Abstract	106

5.2	Introduction	107
5.3	Results	111
5.4	Discussion	125
5.5	Materials and Methods	132
5.6	Acknowledgments	135
5.7	Supplemental Figures	136
5.8	Supplementary Tables	142
Appendix A: Temporal Dynamics of 63 regulatory factors in early development of <i>Eucidaris tribuloides</i>		155
Appendix B: Brief notes on the gravidity of <i>Eucidaris tribuloides</i> off the coast of Key Largo, Florida, USA		164
Appendix C: Questionnaire		168
Appendix D: Consent Form		169

LIST OF ILLUSTRATIONS

<i>Number</i>	<i>Page</i>
2.1 Morphology and timing of <i>E. tribuloides</i> and <i>S. purpuratus</i> development over the first 40 hours post fertilization.	26
2.2 Gene expression matrix showing spatial distribution of <i>S. purpuratus</i> regulatory factors at five timepoints in development.	27
2.3 High-density spatiotemporal timecourse of regulatory gene expression in <i>E. tribuloides</i>	28
2.4 Spatial distribution of endomesodermal regulatory genes in <i>E. tribuloides</i> at 18 hpf.	29
2.5 Endomesodermal regulatory states in pregastrular embryos of <i>S. purpuratus</i> and <i>E. tribuloides</i> at 24 hpf and 18 hpf respectively.	30
2.6 Spatial distribution and gene expression matrix of endomesodermal regulatory genes in pregastrular embryos of <i>E. tribuloides</i> between 10 and 20 hpf.	32
2.7 Functional tests of the euechinoid NSM dGRN circuitry in <i>E. tribuloides</i>	35
2.8 Functional tests of euechinoid endodermal dGRN circuitry in <i>E. tribuloides</i>	39
2.9 Conserved and divergent dGRN circuitry between <i>E. tribuloides</i> and euechinoids revealed in this study.	42
2.10 Spatial distribution of early euechinoid endomesodermal regulatory genes in cleavage stage embryos of <i>E. tribuloides</i>	43
3.1 Spatial expression of selected skeletogenesis genes in <i>Eucidaris tribuloides</i>	61
3.2 Spatial expression of <i>delta</i> , <i>hesC</i> and <i>tbrain</i> at early gastrula stage in <i>Eucidaris tribuloides</i>	63
3.3 Morpholino perturbation of <i>Alx1</i> disrupts skeletogenesis in <i>Eucidaris tribuloides</i> larvae.	64
3.4 Timecourse of mRNA expression of <i>Strongylocentrotus purpuratus</i> double-negative gate genes in this study.	65

3.5	Functional tests for presence in <i>Eucidaris tribuloides</i> of known regulatory linkages of the <i>Strongylocentrotus purpuratus</i> skeletogenic GRN.	67
3.6	Requirement for a Wnt-signal independent β -catenin polar localization system.	70
3.7	Spatial role of <i>hesC</i> in <i>E. tribuloides</i> embryos.	73
4.1	Phylogenetic analyses of <i>Erg</i> , <i>Tgif</i> , <i>Hex</i> , and <i>Tel</i> amino acid sequences from selected deuterostomes to confirm orthology with predicted amino acid sequences from the cidaroid <i>Eucidaris tribuloides</i>	91
4.2	Spatiotemporal expression of the <i>erg-hex-tgif</i> subcircuit and the eu-echinoid skeletogenic gene <i>tel</i> in the early development of the cidaroid <i>Eucidaris tribuloides</i>	92
4.3	Co-option of the <i>erg-hex-tgif</i> subcircuit in the echinoderm clade.	99
5.1	Spatiotemporal dynamics in <i>E. tribuloides</i> of six regulatory factors involved in euechinoid dorsal ventral (D-V) axis formation.	112
5.2	Spatiotemporal dynamics in <i>E. tribuloides</i> of three regulatory factors involved in euechinoid ciliary band (CB) formation.	114
5.3	Spatiotemporal dynamics in <i>E. tribuloides</i> of six regulatory factors involved in euechinoid non-skeletogenic mesenchyme NSM domains. .	116
5.4	Early inputs and dynamics of dorsal-ventral (D-V) axis formation in <i>E. tribuloides</i> as revealed by cadherin mRNA overexpression (MOE) and development in the presence of the <i>alk4/5/7</i> small molecule inhibitor SB431542.	119
5.5	Spatial effect of SB431542 on expression of selected regulatory factors involved in ectodermal, mesodermal and ciliary band formation in <i>E. tribuloides</i>	121
5.6	Comparative analysis of relative gene expression of early GRN regulatory factors expressed in each embryonic tissue layer in three different species of echinoids.	124
5.7	Distribution plots of Spearman's rank correlation coefficients (ρ) for <i>E. tribuloides</i> and <i>S. purpuratus</i> regulatory factors binned by embryonic domain of expression.	125
5.8	Spatial expression of <i>E. tribuloides</i> regulatory factors involved in dorsal-ventral (D-V) axis formation in euechinoids.	136
5.9	Temporal dynamics of selected regulatory factors during the first 35 hpf of <i>E. tribuloides</i> development.	137

5.10	Spatial expression of <i>E. tribuloides</i> regulatory factors involved in ciliary band formation in euechinoids.	138
5.11	Microinjection data showing GFP reporter expression of <i>S. purpuratus onecut</i> BACs in <i>E. tribuloides</i>	139
5.12	Spatial expression of <i>E. tribuloides</i> regulatory factors involved in specification of non-skeletogenic mesoderm in euechinoids.	140
5.13	Ectodermal <i>gcm</i> expression and pigment cell abundance are altered in a Delta-Notch perturbed background in <i>E. tribuloides</i>	141
B.1	Gravidity of <i>Eucidaris tribuloides</i> off the coast of Key Largo, Florida and its correlation to local environmental variables.	165
B.2	Principal component analysis of environmental data against <i>Eucidaris tribuloides</i> gravidity.	166

LIST OF TABLES

<i>Number</i>		<i>Page</i>
2.1	Sequences of primer sets for qPCR detection.	49
2.2	Sequences of morpholino antisense oligonucleotides in this study.	49
3.1	Sequences of primer sets for qPCR detection.	79
3.2	Sequences of primer sets for WMISH probes.	80
3.3	Sequences of morpholino antisense oligonucleotides in this study.	80
4.1	Spatial expression patterns of <i>erg</i> , <i>hex</i> , <i>tgif</i> and <i>tel</i> in echinoderms.	93
4.2	Ancestral state reconstruction for embryos of ancestors of extant echinoderm clades by comparative analysis of spatial gene expression data from three or more taxa.	97
4.3	Sequences of primer sets for WMISH probes.	101
4.4	Sequences of primer sets for qPCR.	101
5.1	Regulatory factors in this study.	110
5.2	Enumeration of heterotopic (spatial) and heterochronic (temporal) changes to deployment of regulatory factors in echinoids since the cidaroid-euechinoid divergence 268 mya.	131
5.3	Sequences of primer sets for qPCR used in this study.	142
5.4	Sequences of primer sets for WMISH used in this study.	143
5.5	Comparative developmental timepoints in three species of echinoids used in this study	143

INTRODUCTION

The primary determining cause of development lies in the nucleus, which operates by setting up a continuous series of specific metabolic changes in the cytoplasm. This process begins during ovarian growth, establishing the external form of the egg, its primary polarity, and the distribution of substances within it. The cytoplasmic differentiations thus set up form as it were a framework within which the subsequent operations take place, in a more or less fixed course, and which itself becomes ever more complex as development goes forward.

– Edmund B. Wilson, *The Cell in Development and Inheritance*

Through the lens of the microscope, embryonic development appears straightforward and deceptively simple. A sperm cell approaches and fuses with an egg, bringing their chromosomes (genetic content or DNA) together. Shortly thereafter the single fertilized egg cell (zygote) now undergoes cellular division: one cell becomes two, then two become four, and four become eight, and so on. This process continues, with clade- and species-specific variations, giving rise to an embryo comprised of thousands of cells, of which dozens are specialized types with specific functions. This superficial series of mitotic divisions that, in the case of the sea urchin, lead to an meandering, swimming embryo do not amount to much more than this to the casual observer. However, when you begin to contemplate what you are seeing through the microscope, the complexity of this process can quickly overwhelm you. At every level of the system—cellular, macromolecular, molecular—there exists mind-bending and mind-numbing complexity that induces wonder and humility. Is acquisition of even a modest understanding of this dynamic, exceedingly complex process a reasonable expectation? Indeed, the evidence suggests it is reasonable, as E. B. Wilson's epigraph from 1896 so elegantly reminds us.

Since the appearance of Wilson's groundbreaking treatise *The Cell in Development and Inheritance*, vigorous and undaunted research effort over the last 120 years has revealed much about embryonic development. With the dawn of the 'Omics' Era, we are learning more and more about it each day. Indeed, trying to keep

pace with newly published work is akin to drinking water from a fire hydrant. Yet, astoundingly and humbly, what we know about development is merely a few pages in a tome that comprises millions of volumes. That is not to say what we have observed and what we have learned are not significant. Quite to the contrary, discoveries and observations of those researchers that tirelessly labored before us are incredibly profound: So much so that Wilson's epigraph about early embryonic developmental systems is stunningly accurate and still true today.

To begin, I briefly outline seminal discoveries that have occurred in the past century of research on sea urchin embryonic development as they relate to the modern concept of gene regulatory networks. The style is intentionally a narrative that attempts to avoid jargon with events listed mostly in chronological order. Then, I offer a brief history of embryological research on *Eucidaris tribuloides*, the sea urchin that is the subject of this dissertation. Lastly, there is an informal discussion of the topics covered in each chapter of the dissertation, explaining how and why each research topic was approached.

1.1 Brief historical sketch of sea urchin research milestones from experimental embryology to modern developmental biology

Sea urchin embryology and the chromosome theory, 1875-1933

We have come to look upon the problem of heredity as identical with the problem of development.

– Thomas H. Morgan (1910)

One of the outstanding biological problems being debated in the decades leading up to the turn of the twentieth century was the location of causal factors in the cell that contributed to development and heredity. As Wilson described it, there were two camps in this debate (E. B. Wilson, 1896): those that argued for the importance of the chromatin or the nucleus, and those that argued for preformed causal factors exclusively in the cytoplasm of the egg. Both positions were readily defended, since the arguments for them were based on experimental results from very different developmental systems.

An early piece of evidence in the nucleus-cytoplasm debate came from the observation, detailed by Oscar Hertwig in 1875, that fertilization in the sea urchin resulted

in the union of two different sexual nuclei—one from sperm and one from egg—both of which contributed nuclear chromatin to the zygote¹. Sea urchin eggs lent themselves readily to this important observation due to their relative transparency and the fact that sperm can fuse with them at any region of the surface. In subsequent experiments, Oscar and his brother Richard showed that vigorous shaking of sea urchins eggs led to an assortment of egg fragments, which contained varying amounts of cytoplasm and nuclear material (O. Hertwig and R. Hertwig, 1887). They then showed that sperm would readily fuse with enucleated fragments, which would subsequently begin to undergo cleavage. Additionally, the Hertwigs revealed that more than one sperm could, under certain conditions, fuse with an egg, resulting in dispermic or polyspermic zygotes (O. Hertwig and R. Hertwig, 1887). These results laid the groundwork for a series of ingenious experiments and discoveries by Theodor Boveri.

Boveri was interested in the causal factors of development and heredity, and in the late 1880s he undertook with sea urchins a series of "natural experiments", with which he would be closely involved for the rest of his life until his untimely death in 1916 (Laubichler and Davidson, 2008). The first set of experiments, the hybrid merogony experiments, attempted to show the role of the nucleus in development. Briefly, the idea was the following: Begin with two species of sea urchins that exhibit different larval forms; vigorously shake sea urchin eggs of one form to acquire a mixed population of egg fragments, some of which will contain a nucleus and others of which will not; then fertilize the egg fragments with sperm from the second species, and follow their development to see if different larval forms result from the nucleated and enucleated fragments. To Boveri, the results were clear:

¹Interestingly, Hertwig explicitly stated the advantages of conducting research on early sea urchin development in his tenure dissertation (*venia docendi*) at Universität Jena (now Friedrich Schiller University):

Für meine Zwecke fand ich ein ganz vorzügliches Object in den Eiern der Seeigel ... *Toxopneustes* [*Paracentrotus*] *lividus*. Abgesehen von dem Umstande, dass es leicht ist, täglich frisches, reichliches Material zu erhalten, lässt sich bei den Seeigeln die künstliche Befruchtung ohne jede Schwierigkeiten ausführen; die Entwicklung geht leicht und rasch von Statten, die Eier sind relativ klein und durchsichtig; die beträchtliche Menge, die man von einem einzigen Individuum erhalten kann, erleichtert sehr die Anwendung von Reagentien, Vortheile, die bei der Beobachtung sehr zu Statten kommen. (O. Hertwig, 1875)

In this passage, Hertwig states the advantages (Vortheile) of working with sea urchins that contemporary developmental biologists herald today: a light animal, for which fresh and ample material can be obtained daily; and for which (artificial) fertilization can be followed in sea urchins without difficulty; relatively small and transparent eggs, of which [a researcher] can obtain substantial amounts from one individual...advantages which greatly benefit observation.

The nucleus and not the cytoplasm contained the hereditary material and the causal factors that directed development. Subsequently, serious questions were raised about the reproducibility and technical difficulties of Boveri's hybrid merogone experiment (Morgan, 1895; Driesch, 1903; Seeliger, 1894), but at the time the result was still revealing and strongly suggested nuclear control of development and inheritance.

Boveri continued his efforts to show the importance of the nucleus and the chromatin in development and at the turn of the twentieth century carried out his famous polyspermy experiments with sea urchin embryos (Boveri, 1902; Boveri, 1905). These experiments followed up on his previous results (Boveri, 1889) and the advances of Hertwig and Hertwig (1887). Taking advantage of the fact that more than one sperm would fuse with a sea urchin egg, Boveri tested a proposition that was of keen interest: What was the importance to an embryo of a "normal" set² of chromosomes? That is to say, if individual chromosomes contain qualitatively distinct factors that are required in each cell or for development, will it proceed as normal if the quantity of these factors is altered? The assay was simple and perfect for the sea urchin system: Isolate sea urchins eggs that had fused with one, two, and three sperm; follow the initial cleavage events, especially the formation of the aster and spindle apparatus; determine the proportion of embryos that gastrulate and become plutei. Clearly exhibiting the necessity of a complete set of chromosomes

for development to proceed normally, these experiments provided a giant leap in conceptual clarity for early twentieth century embryologists; and, when later combined with Sutton's results (Sutton, 1902), they became an essential feature of the Sutton-Boveri chromosome theory, paving the way for the search for the causal, qualitative factors associated with chromosomes that dramatically affect embryonic development.

With the facts now pointing towards the chromosomes as carriers of particulates affecting development, researchers turned their efforts towards understanding how

²Of course the definition of "normal" is an important distinction. Most metazoan animals possess a diploid set of chromosomes, meaning two of each individual chromosome in the somatic cells, and these sets are reunited when the sperm fuses with the egg. However, there are many cases of metazoans that undergo development with haploid sets of chromosomes. For instance, in the Hymenoptera (bee, wasps, and ants), the dominant mode of sex determination is a haploid set of chromosomes for males and a diploid set for females (Heimpel and Boer, 2008). Indeed, in sea urchins it has long been known that artificial parthenogenesis of sea urchin eggs (whereby eggs are induced to begin cleavage without fertilization and are thus haploid) results in embryos that gastrulate normally and become larvae (Loeb, 1899). Conversely, experiments carried out on enucleated sea urchin eggs that were fertilized with a single sperm, producing a haploid embryo, developed into dwarf plutei (Chambers and Ohshima, 1922). Of course, now we understand the genetic basis of the requirement of at least one set of chromosomes, making Boveri's point a prescient one.

this process occurs. Not long after Boveri and Sutton, Thomas Hunt Morgan reported inheritance of a white-eyed phenotype in the fly *Drosophila melanogaster* as a sex-linked trait (Morgan, 1910). The intervening years saw a tremendous increase in research on the particulate units associated with chromosomes (*genes*) that affected embryonic development, especially on those traits that led to phenotypic abnormalities in adult structures, e.g. white eyes, or notched wings, or wingless adults. This was important for the directions of research in embryology and genetics. From a contemporary research perspective this is still sometimes the case today, as mutations to genes that affect early development will frequently have pleiotropic and catastrophic effects on embryogenesis, whereas mutations that have no or little effect in early development—affecting essentially only adult structures—will gain more attention simply due to the fact that those types of "late-effect" mutants are more accessible to perturbation and manipulation. In the early days of developmental genetics, however, this now well-known fact of research created a gulf between embryologists and geneticists, resulting in two camps of research efforts: those researchers ("pure embryologists") that continued to work on comparative early development and gross morphological traits of developmental systems as a whole—work mostly descriptive in nature—and those that worked exclusively on the transmission of traits and those traits that affected phenotypes that arose very late in development (Morgan, 1926). Indeed, embryology and genetics became more and more at odds with each other, resulting in a separation that would last for decades to come (Gilbert, 2000).

The early modern period of developmental biology, 1933-1982

Concerning the manner of functioning of the genes during development...assume that different batteries of genes come into action as development proceeds...[as] it is known that the protoplasm [cytoplasm] of different parts of the egg is somewhat different...the initial differences in the protoplasmic regions may be supposed to affect the activity of the genes. The genes will then in turn affect the protoplasm, which will start a new series of reciprocal reactions. In this way we can picture to ourselves the gradual elaboration and differentiation of the various regions of the embryo.

— Thomas H. Morgan, *Embryology and Genetics*

Extensive research from the 1870s to the 1940s into the mechanics of early sea

urchin development, as evidenced by a thorough review of the literature up to that time (Horstadius, 1939), provided an impressive knowledge base for sea urchin embryological research. However, the *Zeitgeist* was drifting towards molecular-chemical based research methods and consequently moving away from descriptive, phenomenologically-based methods. This was a necessary shift, since, as Morgan suggested, the activity of genes was somehow affecting the cytoplasm, which was then seen as the location of metabolic reactions effecting differentiation of the embryo (Morgan, 1934). Not long after Morgan's summation of the knowledge gained about embryogenesis up to 1934, a string of seismic results on the chemical nature and structure of nuclear and cytoplasmic molecular constituents forever altered the course of biological thought (Beadle and Tatum, 1941; Avery, MacLeod, and McCarty, 1944; Hershey and Chase, 1952; Watson and Crick, 1953). While a few embryologists called very early in this period for mapping the associations between genotype and phenotype (Waddington, 2012), embryology during this time remained largely a sea of phenomenology—interspersed, however, with islands of quantitative, mechanistic refugia.

There were, however, notable exceptions of embryologists utilizing sea urchins to understand how molecular and chemical changes were occurring in early development. Throughout the 1930s and 1940s in Belgium, Jean Brachet was studying the dynamics of nucleic acids in early animal development (Brachet, 1933; Brachet, 1944), frequently utilizing sea urchins during the course of his investigations. During this time (and also during World War II), Brachet made numerous remarkable observations regarding the subcellular locations and synthesis of nucleic acids and proteins, including the presence of maternal RNA in the sea urchin egg, the relative constancy of the amount of RNA relative to the increasing amount of DNA in the early embryo, and the location of nucleic acids and "ribonucleoproteins" in the cell. As pointed out in an excellent review on the topic (Ernst, 2011), Brachet's work allowed him to conclude as early as 1945:

the content of thymonucleic acid [DNA] in the nucleus regulates the amount of ribonucleoproteins in the cytoplasm... The ribonucleoproteins of the ergastoplasm [endoplasmic reticulum] are bound to the granules... These various substances probably collaborate to synthesize proteins: the amino acids might be arranged on the surface of the granule in a precise pattern.

Additionally, Brachet pointed out that the differential expression of variable gene activity in early development may be linked to the problem of differentiation (Brachet, 1949). At this time, additional evidence was being furnished for the variable gene activity theory in development (Stedman and Stedman, 1950; Mirsky, 1951). Thus it was increasingly clear by the mid twentieth century that the synthesis of proteins in the cell depended upon the synthesis and location of nucleic acids in the cell, and that this process likely effects embryonic development. Research on these questions intensified in the late 1950s and early 1960s as researchers discovered new ways to manipulate molecular dynamics in these systems. An important discovery relating to embryonic development came with the revelation that inhibition of RNA synthesis with actinomycin-D did not significantly affect protein synthesis in early embryonic development, suggesting there were large stores of maternally deposited RNA in the egg (Gross and Cousineau, 1963). At about the same time, researchers were beginning to unravel the composition and complexity of maternally deposited RNAs and their affect on early development (Davidson, 1986), which led to clues as to the association of cleavage events and the localization of these deposited molecules.

The arrival of Jacob and Monod's bacterial operon system (Jacob and Monod, 1961) brought some of the first evidence as to how genetic control systems in a cell function. However, whereas there were some attempts to directly translate features of the operon system to eukaryotes (Moore, 1962; Jacob and Monod, 1963), it was quickly realized that metazoan genetic control systems likely operate in very distinct, yet related, ways (Davidson, 1968). A constant stream of evidence appeared throughout the 1950s and 1960s that began to reveal mechanistic features of eukaryotic genomes and the tissue types to which development gives rise, including differential biochemical activity of the chromosomes (Allfrey and Mirsky, 1958), differential localization of active and inactive nuclear chromatin in eukaryotic genomes (Littau et al., 1964), and differential expression of RNAs in eukaryotic tissues (Paul and Gilmour, 1966; Paul and Gilmour, 1968).

At the end of the 1960s, in a series of landmark publications, Eric Davidson and Roy Britten laid out how the eukaryotic genetic control system may function and evolve (Britten and Davidson, 1969; Britten and Davidson, 1971). The theory was an early attempt to bring molecular data from observations on disparate eukaryotic organisms—mostly of measurements of genome size and repetitive DNA sequences—under the umbrella of a theoretical framework that could be used to interpret evolutionary and developmental phenomena. Around this time, it was generally thought

that large amounts of nucleic acids do not leave the nucleus (in contrast to the messenger nucleic acids) (Ehret and Haller, 1963; Ohno, 1972), giving rise to the term "junk DNA". But Davidson and others argued against this supposition, asserting that the repetitive nature of non-coding DNA increases the likelihood that it is functional (Zuckerkandl, 1974; Cavalier-Smith, 1978). The observation by King and Wilson that amino acid sequences were nearly identical between human and chimpanzee amino acid sequences, suggesting that alterations in regulatory sequences likely account for a disproportionate number of species-specific differences, further added to the attractiveness of the Britten-Davidson model (King and A. C. Wilson, 1975).

Coming of age: Sea urchins as model systems for embryonic development, 1982-present

The development of novel molecular biology techniques during the 1970s and 1980s opened up new avenues of research for developmental biology—indeed, for all of biology. Research on early development of embryos throughout the 1970s slowly began to reveal the kinetics of molecules in eggs and embryos, and repeat DNA sequences in genomes were highly suggestive of a functional capacity for these elements (Davidson, 1986). The publication by Davidson, Hough-Evans, and Britten in 1982 reintroducing the basic embryology of *Strongylocentrotus purpuratus* and the recently revealed dynamics of its nucleic acid constituents during early development speaks to the air of renewed interest in embryonic development circulating in the early 1980s (Davidson, Hough-Evans, and Britten, 1982).

Numerous technological advances propelled research on embryonic development forward during this time, including development of radiolabeling *in situ* hybridization to reveal the spatial distribution of individual RNA transcripts in fixed sea urchin cells (L. M. Angerer and R. C. Angerer, 1981), a microinjection method to introduce nucleic acid constructs and other reagents (Mcmahon et al., 1985), the use of fluorescent reporter molecules to trace the cell lineage of each sea urchin blastomere during development (R. A Cameron et al., 1987), and the introduction of cloned non-coding DNA fused to reporter genes to assay regulatory activity (Flytzanis, Britten, and Davidson, 1987). This last development was of particular importance, as introduction of reporter constructs allowed the first *in vivo* glimpses of functional, *cis*-regulatory control elements and DNA-protein interactions in the genome (Calzone et al., 1988).

These advances meant non-coding regulatory DNA could be assayed during em-

bryogenesis, and this led to systematic *cis*-regulatory analysis studies revealing the elaborate genetic regulatory control systems operating during development (Hough-Evans et al., 1990; Kirchhamer and Davidson, 1996). In the years following discoveries of distinct spatial and temporal enhancers regulating genes involved in larval skeletogenesis, *cis*-regulatory analysis rapidly matured and was very successfully applied to unravel the spatial and temporal regulatory logic utilized to control the *endo16* gene during development (Yuh, Bolouri, and Davidson, 1998; Yuh, Bolouri, and Davidson, 2001). In the early 2000s, morpholino antisense oligonucleotides—a small DNA oligonucleotide reagent injected into the embryo that targets specific messenger RNA molecules and blocks their translation into protein at the ribosome—were introduced, and researchers began with great success the perturbation of genes functioning in early development, affording the first glimpses of the large-scale regulatory circuitry involved in controlling differentiation events in embryonic development (Davidson, Rast, et al., 2002).

The arrival in 2006 of the first draft sequence of the *Strongylocentrotus purpuratus* genome greatly accelerated research on gene regulatory networks and developmental systems biology. Around this time, large-scale sequencing projects of DNA and RNA in closely-related species *Lytechinus variegatus*, *Strongylocentrotus franciscanus*, and others rapidly advanced the discovery of conserved *cis*-regulatory elements and validated, in some cases, gene regulatory network linkages (Brown et al., 2002; Yuh, Dorman, et al., 2004; Revilla-i-Domingo, Minokawa, and Davidson, 2004; Oliveri and Davidson, 2004).

Since the late-2000s, the general procedure for approaching gene regulatory network analysis has been codified in protocols and well-established methodologies (J. Smith, 2008; Materna and Oliveri, 2008). The dedication to this research program by hundreds of researchers over the last few decades has helped realize a first approximation of the global gene regulatory network directing early development of *Strongylocentrotus purpuratus*. This gene regulatory network is the first of its kind in developmental biology, and proffers molecular explanations for gross morphological observations made over the last century of embryological research. The power of the network to explain how development works cannot be understated. For instance, an example of the logical muscle exercised by this intellectual achievement lies in its ability to explain observations made by early experimental embryologists. One example of this is the numerous observations of blastomere lineage tracing and the surgical, "operative" methods explained by Sven Hörstadius in his long course

of study of sea urchin embryogenesis (Horstadius, 1939).

1.2 Notes on developmental evolution in light of gene regulatory networks

Though the ancestors of modern animals are extinct the evidence of how they worked is not. The evidence is swimming, walking and flying around outside, in the DNA of modern bilaterians. What happened in evolution will emerge from knowledge of the regulatory pathways of development... Comparative sets of genomic network "wiring" diagrams will emerge. Strange as it may seem, it is these that will tell us what the Bilateria are and where they came from.

– Eric H. Davidson, *Genomic Regulatory Systems*

The theoretical framework of gene regulatory networks and the data supporting it are important structural supports of the edifice of modern research programs now known by the various monikers of evo-devo, evolutionary developmental biology, and developmental evolution. Excellent reviews on the intellectual and technological development of this research program are covered elsewhere (Gilbert, Opitz, and Raff, 1996; Maienschein and Laublich, 2006; Carroll, Grenier, and Weatherbee, 2001). While the scope of this section is limited, I desire to emphasize briefly here how the previously discussed sea urchin research converges on present day investigations of gene regulatory networks in evolution and development of echinoderms.

In 1971, Britten and Davidson stressed the importance of their theory of gene regulation in higher cells in terms of evolutionary change (Britten and Davidson, 1971). The implications for development and evolution of this biological structure—should it exist—were plain, yet the molecular tools were not in place to investigate it. Clearly the import of this idea was not lost in the intervening years between the publication of the network theory in 1969 and the influential Dahlem Conference on development and evolution in Berlin in 1981, as it was discussed at length (Bonner, 1982). However, between the Dahlem Conference and the late 1990s, interest in the evolutionary import of the theory waned, as citations decreased from 1981-2001. Then, technological advances and a resurgence of interest in gene regulatory network analysis breathed second life into the gene network theory as its implications became testable; comparative gene regulatory network analysis became a reality.

We now understand that, while the minute details that Britten and Davidson set forth in the seminal 1969 article did not all hit the mark, the overarching principles of their framework alter our thinking of evolution and development in profound ways. For example, we understand now that the modularity predicted by the gene regulatory network theory impacts both the development of individual organisms and the evolution of lineages themselves. Additionally, the topic of constraint in developmental systems has long been a topic of interest (J. M. Smith et al., 1985). Observations made clear that diversification of morphological structures and of animal body plans occur at different rates (Davidson and Erwin, 2006), though sound data were rarely presented to support this view. An understanding of the architecture and process of gene regulatory networks in development makes clear how and why constraint occurs during evolution: alteration to network linkages occur at different rates in different processes of development. While alterations do occur at all levels of network circuitry and at all developmental times during embryogenesis, there must be an over-representation of changes occurring at the periphery of the networks. Thus, as we move forward with comparative analyses of gene regulatory network architecture and function in more and more diverse organisms, we will begin to understand how these architectures came to be over the past several hundred million years and why they will persist for many million years more.

1.3 History of embryological research on *Eucidaris tribuloides*

The formal description and classification of *Eucidaris tribuloides* was published by Jean-Baptiste Lamarck as 'Cidarite tribuloides' in the third volume of his opus on invertebrate animals (Lamarck, 1816). The earliest description of the rate and morphological characteristics of its embryonic development were given by David Tennent as *Cidaris tribuloides* (Tennent, 1914; Tennent, 1922). Tennent's description in 1914 is noteworthy as he compares the early embryonic development of *E. tribuloides*, a cidaroid sea urchin, with that of a euechinoid sea urchin, *Lytechinus variegatus* (*Toxopneustes* in his description):

The earliest striking difference between the two forms is the time and place of mesenchyme formation, *Cidaris* in this respect resembling the crinoids more closely than the echinoids. No mesenchyme is formed until the archenteron has pushed well into the blastocoele. (Tennent, 1914)

Tennent concerned himself with inter-species—in this case, inter-subclass—hybridization experiments, from which interpretations on the effect of paternal and maternal characteristics were inherited during embryonic development.

In 1981, Thomas Schroeder formally described the early development of *E. tribuloides* and was the first to point out the interesting observation, among others, of irregularities in the number and size of its micromeres at the vegetal plate (Schroeder, 1981). It was already known that in euechinoids the micromere lineage was fated very early in development to give rise to the embryonic skeleton (Okazaki, 1975). Thus, the natural query was to determine if this was also the case in a distantly-related sea urchin that developed with a variable micromere lineage.

Two studies that addressed the fate of micromeres in *E. tribuloides* appeared in 1988. In one study, embryo "donors" were labeled using tracer dyes and, using microsurgical techniques, the micromeres were subsequently removed. When implanted on and co-cultured in a different *E. tribuloides* "host" embryo, it was determined that the micromere-descendants contributed specifically to and participated in the larval skeletogenesis (Wray and McClay, 1988). The authors made a convincing argument as to the homology of cidaroid micromere descendants and euechinoid primary mesenchyme cells. In the second study, tracer dye was injected directly into the micromeres at the 16-cell stage and similar conclusions were reached (Urben, Nislow, and Spiegel, 1988).

These preliminary studies are in accord with what is presented in Chapter 3 and throughout this thesis.

1.4 Précis of dissertation chapters

The goals of this project were initially modest: we aimed to determine whether or not a few interesting euechinoid regulatory circuits also operated during the development of *E. tribuloides*. We started with two endomesodermal genes, *wnt8* and *blimp1*, and four mesodermal genes, *alx1*, *delta*, *ets1/2*, and *tbrain*. Of course, we knew the projects were going to grow as we learned more and more. But certainly none of us fathomed these modest projects would be so thoroughly and deeply developed. Indeed, when we first started, we could not even reliably obtain gametes from *E. tribuloides*, so it was not at all clear that this was even going to get off the ground in a more than limited way. However, with a little resolve, we managed through the frustrations of seasonal gametes (see Appendix B). And with this difficulty behind us, we were then able to move on to our grandiose objectives, which are the subjects of the next four chapters.

In Chapter 2, we set out to assay in *E. tribuloides* the spatial and temporal expression and functional relations of the euechinoid regulatory genes that sit at or near the top of the endomesodermal gene regulatory network hierarchy. Our approach of high-density *in situ* data combined with perturbation data revealed the very interesting observation that terminal pregastrular regulatory states, i.e. the total set of regulatory genes that comprise a particular embryonic domain and their boundaries seem to be more conserved in echinoids than the underlying network circuitry that produces them. This study revealed many divergent as well as conserved aspects of endomesodermal specification circuitry at all levels of gene regulatory network architecture, including the observation that Delta/Notch signaling likely does not function to specify non-skeletogenic mesoderm in this sea urchin in contrast to its well-established role in euechinoids. Other observations aside, the import clearly is that two distinct developmental programs are executed in early development of euechinoids and cidaroids that produce similar regulatory states just before the onset of gastrulation. This is an interesting biological case where the ends justify a variety of means.

In Chapter 3, we took an in-depth look in *E. tribuloides* at specification of one exceedingly interesting developmental event in early development of euechinoids: the double-negative gate. Very early in this research program we were shocked when we discovered that we could not ferret out an ortholog of *pmar1*, one of the central regulatory genes of this process in euechinoids. Our search took us first from transcriptomic RNA sequences and later to genomic DNA sequences; still we found nothing. Thus we characterized the other regulatory genes involved in this developmental event, viz. *alx1*, *delta*, *ets1*, *hesc*, and *tbrain*, and identified numerous heterochronic and heterotopic changes to their deployment and regulation. Along with perturbation and experimental data, these results indicated that extensive rewiring of this circuitry has occurred since the cidaroid-euechinoid divergence at least 268 million years ago. In this study, we found our first clue that the role of Delta/Notch signaling in *E. tribuloides* was very different. In this sea urchin, the Delta ligand is expressed in the skeletogenic lineage just as it is in euechinoids; but as mentioned in the previous summary for Chapter 2, rather than activating non-skeletogenic mesenchyme, it acts to repress the skeletogenic fate in the surrounding cells by activating the Delta/Notch responsive regulatory gene *hesc*. Now, in euechinoids, HesC is responsible for repressing the skeletogenic fate in all parts of the embryo except for where the repressor of HesC, *pmar1*, is upregulated; this is the double-negative gate. What's more, in *E. tribuloides*, HesC also represses the skeletogenic fate, just in a much more localized manner. Thus, there are very

interesting parallels in the way these long-separated regulatory components work—certainly abundant research opportunities to further explore.

Chapter 4 approaches developmental evolution with the following question: what can we say about embryonic development of ancestors from our comparative, contemporary surveys of gene expression in extant taxa? We sought to display the utility of spatial and temporal gene expression data to make phylogenetically meaningful inferences not only about extant tips or crowns of clades but also about the nodes, i.e. the long dead ancestors. The study advances the idea of ancestral state reconstruction of developmental events and shows how this is possible by interpreting gene expression data from three or more taxa. Utilizing this technique we were able to make numerous statements about the embryos of echinoderm ancestors.

In Chapter 5, we undertook a comparative analysis of regulatory gene usage in embryonic territories of *E. tribuloides* for which we had no or little gene expression data. This study looks broadly at development of dorsal-ventral (aboral-oral) polarity in *E. tribuloides* and how it has diverged since the cidaroid-euechinoid divergence. Thus, by surveying gene expression in ectodermal embryonic domains, we obtained not only an interesting perspective on the evolution of dorsal-ventral axis specification in echinoids, but also we consequently obtained gene expression data for every embryonic domain in early development. By perturbing dorsal-ventral axis specification in *E. tribuloides* we came to the conclusion that, with a few important and intriguing exceptions, ectodermal specification events are highly conserved in echinoids. Perturbation of dorsal-ventral axis specification suggests that the underlying regulatory circuitry specifying ectodermal polarity is more conserved than that mesodermal circuitry. Further, comparative analyses with euechinoid species of initiation of regulatory genes in particular embryonic domains of *E. tribuloides* added further support to the idea that regulatory circuitry directing specification and delineation of ectodermal and endodermal embryonic domains is more impervious to change than the circuitry of mesodermal domains.

When considering the body of work as a whole, it seems clear that gene regulatory networks specifying and directing mesodermal domains have undergone extensive alterations of gene regulatory network architecture at all levels of their topology—much more so than in circuitry directing endodermal and ectodermal domains. At least for endoderm and mesoderm, this is an observation that my mentor Eric Davidson and I reached very early in our speculative musings about the evolution of early development in echinoids. Studies in the ectoderm were added only later, and sadly

without Eric's input. While our experiments did not reveal the direct, genomically encoded linkages one demands when making statements of gene regulatory network evolution, we firmly are of the opinion that these studies lay the groundwork to facilitate future research efforts. A major conclusion of this dissertation is that mesodermal lineages have diverged disproportionately relative to endodermal and ectodermal lineages. In regards to this, one could suggest that, given there is an overt difference in the number and formation of micromeres in early cleavage stage morphology between cidaroids and euechinoids, one could suggest even before the start of the study that the gene regulatory networks specifying the embryonic territories around the micromeres (mesoderm) would have been very different from that in euechinoids. However, there was no evidential reason *a priori* to believe that this would be the case. In principle the whole gene regulatory network in cidaroids could have worked exactly as it does in euechinoids even with their different morphologies of early development. But it doesn't!

This study serves as an example of just how much insight we can gain when we look at a single taxon in an intriguing phylogenetic position that also has had multiple taxa around it. Whether conserved or divergent, nearly every data point is interesting. It also represents why we should continue to look in non-model organisms. The important point is that we had to look to see how it works. And I am certainly glad we did.

References

Allfrey, V. G. and A. E. Mirsky (1958). "Some effects of substituting the deoxyribonucleic acid of isolated nuclei with other polyelectrolytes". In: *Proceedings of the National Academy of Sciences* 44.10, pp. 981–991.

Angerer, L. M. and R. C. Angerer (1981). "Detection of poly A+ RNA in sea urchin eggs and embryos by quantitative in situ hybridization". In: *Nucleic Acids Research* 9.12, pp. 2819–2840.

Avery, O. T., C. M. MacLeod, and M. McCarty (1944). "Studies on the chemical nature of the substance inducing transformation of pneumococcal types induction of transformation by a deoxyribonucleic acid fraction isolated from pneumococcus type III". In: *The Journal of experimental medicine* 79.2, pp. 137–158.

Beadle, G. W. and E. L. Tatum (1941). "Genetic control of biochemical reactions in *Neurospora*". In: *Proceedings of the National Academy of Sciences* 27.11, pp. 499–506.

Bonner, J. T. (1982). *Evolution and Development: Report on the Dahlem Workshop on Evolution and Development Berlin 1981, May 10-17, Vol 22*. ed: J. T. Bonner. Berlin: Springer Verlag.

Boveri, T. (1902). “Über mehrpolige mitosen als mittel zur analyse des zellkerns”. In:

- (1905). *Zellen-studien*. Vol. 5. G. Fischer.

Brachet, J. (1933). “Eecherches sur la synthèse de l’acide thymonucléique pendant le développement de l’oeuf d’oursin”. In: *Archives de biologie* 44, pp. 519–576. URL: <http://hdl.handle.net/2013/ULB-DIPOT:oai:dipot.ulb.ac.be:2013/173380>.

- (1944). *Chemical embryology*. Paris: Masson & Cie.
- (1949). “L’hypothese des plasmagènes dans le développement et la différenciation”. In: *Pubbl. Staz. zool. Napoli* 21, pp. 77–195.

Britten, R. J. and E. H. Davidson (1969). “Gene regulation for higher cells: a theory”. In: *Science* 165.3891, pp. 349–357.

- (1971). “Repetitive and Non-Repetitive DNA Sequences and a Speculation on Origins of Evolutionary Novelty”. English. In: *Quarterly Review of Biology* 46.2, pp. 111–138. DOI: [Doi10.1086/406830](https://doi.org/10.1086/406830). URL: [%3CGo%20to%20ISI%3E://WOS:A1971J953500001](https://doi.org/10.1086/406830).

Brown, C. T. et al. (2002). “New computational approaches for analysis of cis-regulatory networks”. In: *Developmental biology* 246.1, pp. 86–102.

Calzone, F. J. et al. (1988). “Developmental appearance of factors that bind specifically to cis-regulatory sequences of a gene expressed in the sea urchin embryo.” In: *Genes & development* 2.9, pp. 1074–1088.

Cameron, R. A et al. (1987). “Lineage and fate of each blastomere of the eight-cell sea urchin embryo”. In: *Genes & Development* 1.1, pp. 75–85.

Carroll, S. B., J. K. Grenier, and S. D. Weatherbee (2001). *From DNA to diversity: molecular genetics and the evolution of animal design*. John Wiley & Sons.

Cavalier-Smith, T. (1978). “Nuclear volume control by nucleoskeletal DNA, selection for cell volume and cell growth rate, and the solution of the DNA C-value paradox”. In: *Journal of Cell Science* 34.1, pp. 247–278.

Chambers, R. and H. Ohshima (1922). “Merogony experiments on sea-urchin eggs”. In: *Experimental Biology and Medicine* 19.7, pp. 320–321.

Davidson, E. H. (1968). *Gene activity in early development*. 1st. New York: Academic Press.

- (1986). *Gene activity in early development*. 3rd. New York: Academic Press.

Davidson, E. H. and D. H. Erwin (2006). “Gene regulatory networks and the evolution of animal body plans.” In: *Science (New York, N.Y.)* 311.5762, pp. 796–800. ISSN: 1095-9203. doi: 10.1126/science.1113832. URL: <http://www.ncbi.nlm.nih.gov/pubmed/16469913>.

Davidson, E. H., B. R. Hough-Evans, and R. J. Britten (1982). “Molecular biology of the sea urchin embryo”. In: *Science* 217.4554, pp. 17–26.

Davidson, E. H., J. P. Rast, et al. (2002). “A genomic regulatory network for development.” In: *Science* 295.5560, pp. 1669–78. ISSN: 1095-9203. doi: 10.1126/science.1069883. URL: <http://www.ncbi.nlm.nih.gov/pubmed/11872831>.

Driesch, H. (1903). “Über Seeigelbastarde”. In: *Development Genes and Evolution* 16.4, pp. 713–722.

Ehret, C. F. and G. De Haller (1963). “Origin, development, and maturation of organelles and organelle systems of the cell surface in *Paramecium*”. In: *Journal of Ultrastructure Research* 9, pp. 1–42.

Ernst, S. G. (2011). “Offerings from an urchin”. In: *Developmental biology* 358.2, pp. 285–294.

Flytzanis, C. N., R. J. Britten, and E. H. Davidson (1987). “Ontogenic activation of a fusion gene introduced into sea urchin eggs”. In: *Proceedings of the National Academy of Sciences* 84.1, pp. 151–155.

Gilbert, S. F. (2000). *Developmental Biology*. Sunderland, MA: Sinauer Associates.

Gilbert, S. F., J. M. Opitz, and R. A. Raff (1996). “Resynthesizing evolutionary and developmental biology”. In: *Developmental biology* 173.2, pp. 357–372.

Gross, P. R. and G. H. Cousineau (1963). “Effects of actinomycin D on macromolecule synthesis and early development in sea urchin eggs”. In: *Biochemical and biophysical research communications* 10.4, pp. 321–326.

Heimpel, G. E. and J. G. de Boer (2008). “Sex determination in the Hymenoptera”. In: *Annu. Rev. Entomol.* 53, pp. 209–230.

Hershey, A. D. and M. Chase (1952). “Independent functions of viral protein and nucleic acid in growth of bacteriophage”. In: *The Journal of general physiology* 36.1, pp. 39–56.

Hertwig, O. (1875). *Beiträge zur Kenntniss der Bildung, Befruchtung und Theilung des thierischen Eies*. W. Engelmann. URL: <https://books.google.com/books?id=NtY0AQAAQAAJ>.

Hertwig, O. and R. Hertwig (1887). “Über den Befruchtungs-und Teilungsvorgang des tierischen Eies unter dem Einfluss äusserer Agentien”. In:

Horstadius, S. (1939). “The mechanics of sea urchin development, studied by operative methods”. In: *Biological Reviews* 14.2, pp. 132–179.

Hough-Evans, B. R. et al. (1990). "Negative spatial regulation of the lineage specific CyIIIa actin gene in the sea urchin embryo". In: *Development* 110.1, pp. 41–50.

Jacob, F. and J. Monod (1961). "Genetic regulatory mechanisms in the synthesis of proteins". In: *Journal of molecular biology* 3.3, pp. 318–356.

– (1963). "Cytodifferentiation and macromolecular synthesis". In: 21, pp. 30–64.

King, M. C. and A. C. Wilson (1975). "Evolution at two levels in humans and chimpanzees". In: *Science* 188.4184, p. 107.

Kirchhamer, C. V. and E. H. Davidson (1996). "Spatial and temporal information processing in the sea urchin embryo: modular and intramodular organization of the CyIIIa gene cis-regulatory system". In: *Development* 122.1, pp. 333–348.

Lamarck, Jean-Baptiste de Monet de (1816). *Histoire naturelle des animaux sans vertèbres, présentant les caractères généraux et particuliers de ces animaux, Tome 3*. Deterville.

Laubichler, M. D. and E. H. Davidson (2008). "Boveri's long experiment: Sea urchin merogones and the establishment of the role of nuclear chromosomes in development". English. In: *Developmental biology* 314.1, pp. 1–11. doi: 10.1016/j.ydbio.2007.11.024. URL: %3CGo%20to%20ISI%3E : //WOS:000253031100001.

Littau, V. C. et al. (1964). "Active and inactive regions of nuclear chromatin as revealed by electron microscope autoradiography". In: *Proceedings of the National Academy of Sciences* 52.1, pp. 93–100.

Loeb, J. (1899). "On the nature of the process of fertilization and the artificial production of normal larvae (plutei) from the unfertilized eggs of the sea urchin". In: *American Journal of Physiology–Legacy Content* 3.3, pp. 135–138.

Maienschein, J. and M. Laublicher (2006). *From embryology to evo-devo*. Cambridge, MA: MIT Press.

Materna, S. C. and P. Oliveri (2008). "A protocol for unraveling gene regulatory networks". In: *Nature Protocols* 3.12, pp. 1876–1887.

Mcmahon, A. P. et al. (1985). "Introduction of Cloned DNA into Sea-Urchin Egg Cytoplasm - Replication and Persistence during Embryogenesis". English. In: *Developmental biology* 108.2, pp. 420–430. doi: Doi10.1016/0012-1606(85)90045-4. URL: %3CGo%20to%20ISI%3E : //WOS:A1985AGA6800016.

Mirsky, A. E. (1951). *Genetics in the Twentieth Century*. ed: L. C. Dunn. New York: MacMillan.

Moore, J. A. (1962). "Nuclear transplantation and problems of specificity in developing embryos". In: *Journal of Cellular and Comparative Physiology* 60.S1, pp. 19–34.

Morgan, T. H. (1895). "Studies of the 'partial' larvae of *Sphaerechinus*". In: *Development Genes and Evolution* 2.1, pp. 81–126.

Morgan, T. H. (1910). "Sex limited inheritance in *Drosophila*". In: *Science* 32.812, pp. 120–122.

- (1926). *The Theory of the Gene*. Yale University Press.
- (1934). *Embryology and genetics*. New York: Columbia University Press.

Ohno, S. (1972). "So much "junk" DNA in our genome". In: *Brookhaven Symp Biol.* Vol. 23, pp. 366–370.

Okazaki, K. (1975). "Spicule formation by isolated micromeres of the sea urchin embryo". In: *American Zoologist* 15.3, pp. 567–581.

Oliveri, P. and E. H. Davidson (2004). "Gene regulatory network controlling embryonic specification in the sea urchin". In: *Current opinion in genetics & development* 14.4, pp. 351–360.

Paul, J. and R. S. Gilmour (1966). "Restriction of deoxyribonucleic acid template activity in chromatin is organ-specific." In: *Nature* 210.5040, p. 992.

- (1968). "Organ-specific restriction of transcription in mammalian chromatin". In: *Journal of molecular biology* 34.2, pp. 305–316.

Revilla-i-Domingo, R., T. Minokawa, and E. H. Davidson (2004). "R11: a cis-regulatory node of the sea urchin embryo gene network that controls early expression of SpDelta in micromeres". English. In: *Developmental biology* 274.2, pp. 438–451. doi: 10.1016/j.ydbio.2004.07.008. URL: %3CGo%20to%20ISI%3E://WOS:000224166000017.

Schroeder, T. E. (1981). "Development of a 'primitive' sea urchin (*Eucidaris tribuloides*): irregularities in the hyaline layer, micromeres, and primary mesenchyme". In: *Biological Bulletin* 161.1, pp. 141–151.

Seeliger, O. (1894). "Giebt es geschlechtlich erzeugte Organismen ohne mütterliche Eigenschaften?" In: *Development Genes and Evolution* 1.2, pp. 203–223.

Smith, J. (2008). "A protocol describing the principles of cis-regulatory analysis in the sea urchin". In: *Nature Protocols* 3.4, pp. 710–718.

Smith, J. M. et al. (1985). "Developmental constraints and evolution: a perspective from the Mountain Lake conference on development and evolution". In: *Quarterly Review of Biology*, pp. 265–287.

Stedman, E. and E. Stedman (1950). "Cell specificity of histones". In: *Nature* 166.4227, pp. 780–781.

Sutton, W. S. (1902). "On the morphology of the chromosome group in *Brachystola magna*". In: *The Biological Bulletin* 4.1, pp. 24–39.

Tennent, D. H. (1914). "The early influence of the spermatozoan upon the characters of echinoid larvae". In: *Carn Inst Wash Publ* 182, pp. 129–138.

- (1922). "Studies on the hybridization of echinoids". In: *Part I. Embryology and hybridization of *Cidaris**. *Carn Inst Wash Publ* 312, pp. 3–43.

Urben, S., C. Nislow, and M. Spiegel (1988). “The origin of skeleton forming cells in the sea urchin embryo”. In: *Roux's archives of developmental biology* 197.8, pp. 447–456. doi: 10.1007/BF00385678. url: <http://link.springer.com/article/10.1007/BF00385678>.

Waddington, C. H. (2012). “The epigenotype”. In: *International journal of epidemiology* 41.1, pp. 10–13.

Watson, J. D. and F. H. C. Crick (1953). “Molecular structure of nucleic acids”. In: *Nature* 171.4356, pp. 737–738.

Wilson, E. B. (1896). *The Cell in Development and Inheritance*.

Wray, G. A. and D. R. McClay (1988). “The origin of spicule-forming cells in a ‘primitive’ sea urchin (*Eucidaris tribuloides*) which appears to lack primary mesenchyme cells”. In: *Development* 103.2, pp. 305–315. url: <http://www.ncbi.nlm.nih.gov/pubmed/3066611>.

Yuh, C. H., H. Bolouri, and E. H. Davidson (1998). “Genomic cis-regulatory logic: experimental and computational analysis of a sea urchin gene”. In: *Science* 279.5358, pp. 1896–1902.

– (2001). “Cis-regulatory logic in the endo16 gene: switching from a specification to a differentiation mode of control”. In: *Development* 128.5, pp. 617–629.

Yuh, C. H., E. R. Dorman, et al. (2004). “An otx cis-regulatory module: a key node in the sea urchin endomesoderm gene regulatory network”. In: *Developmental biology* 269.2, pp. 536–551.

Zuckerkandl, E. (1974). “A possible role of “inert” heterochromatin in cell differentiation. Action of and competition for “locking” molecules”. In: *Biochimie* 56.6-7, pp. 937–954.

DIVERGENT DEVELOPMENTAL GENE REGULATORY
NETWORKS ESTABLISH CONSERVED ENDOMESODERMAL
REGULATORY STATES IN ECHINOIDS

Erkenbrack, E. M., E. H. Davidson, and I. S. Peter (2016). “Divergent developmental gene regulatory networks establish conserved endomesodermal regulatory states in echinoids”. In:

2.1 Abstract

Animal body plans and morphological structures are the outputs of developmental gene regulatory networks (dGRNs), and alteration of morphology as lineages evolve requires rewiring dGRNs during embryogenesis. Examples of the mechanisms and consequences of alteration of this important process are lacking in the literature. The endomesodermal dGRN of euechinoid sea urchins is the best described and researched of these networks, but remarkably research in three euechinoid species separated by 90 million years (my) of evolution has revealed that little change has occurred since the split of camarodont sea urchins. Thus, we undertook a systematic effort of characterizing the roles and functions of 12 endomesodermal regulatory factors in the more distantly-related sea urchin *Eucidaris tribuloides*, a cidaroid sea urchin removed at least 268 my from euechinoids. Analyses of regulatory state dynamics and functional perturbations revealed extensive alterations have occurred to the endomesodermal dGRN since the cidaroid-euechinoid divergence. Surprisingly, the pregastrular endomesodermal embryonic domains of *E. tribuloides* become populated with orthologous regulatory genes, in spite of numerous clear differences in installation and regulatory transactions that setup these states. Thus, conservation of regulatory states is an underappreciated principle in dGRN evolution. Further-more, our survey of endomesodermal regulatory genes indicates that endodermal circuitry is more likely to be conserved than mesodermal circuitry. We provide an illuminating example of how dGRNs are rewired in evolutionary time to achieve a very particular end by any means necessary.

2.2 Introduction

A critical process in early embryogenesis of metazoans is the installation of sets of regulatory factors, or regulatory states, in particular embryonic domains and subdomains. Regulatory states are distinct sets of regulatory factors that are expressed in spatially delimited domains in the embryo and endow cells with a particular identity. As development proceeds, the complexity of regulatory states both in terms of the number of regulatory factors and cell-type specific domains increases, delineating spatial territories that later develop into canonical larval or adult morphological structures and phenotypes. The apparatus driving these processes are genetically-encoded developmental gene regulatory networks (dGRNs) (Peter and Davidson, 2015). Our understanding of how these complex systems change in evolutionary time is limited by a scarcity of highly detailed dGRNs that can be used for comparative analysis to reconstruct ancestral states and evolutionary events. And yet, from

the scant exemplary cases in the literature, it is clear that dGRNs exhibit a hierarchical organization that likely biases rates of evolutionary change and morphological evolution of animal body plans (Davidson and Erwin, 2006; Peter and Davidson, 2011b). To place this fundamental concept on firm ground, systematic microdissection of evolutionarily diverged dGRNs in distantly-related taxa is required and will provide insight into the mechanisms and frequency of change of these networks during evolution.

The most validated dGRN currently researched is the endomesodermal dGRN of the euechinoid sea urchin *Strongylocentrotus purpuratus*. This network causally explains the installation of numerous regulatory states in the *S. purpuratus* pregastral embryo and is comprised of over 50 regulatory factors that execute hundreds of experimentally-validated regulatory transactions (Peter, Faure, and Davidson, 2012). Surprisingly, although numerous euechinoids have been the subject of considerable research focusing on early developmental regulatory systems biology, comparative analyses of other euechinoid sea urchins, e.g. *Lytechinus variegatus* and *Paracentrotus lividus*, have revealed that since the split of these three lineages approximately 90 million years ago (mya) the wiring and organization of this dGRN are remarkably conserved (Martik, Lyons, and McClay, 2016; A. B. Smith et al., 2006; Kroh and A. B. Smith, 2010). Sea urchins (class Echinoidea) are a large, ancient taxa comprised of two subclasses: cidaroids and the euechinoids. These subclasses, which diverged from each other at least 268 mya (Thompson et al., 2015), offer ample research opportunities in clades that are developmentally, anatomically, and ecologically rich in their diversity (Hopkins and A. B. Smith, 2015). Attesting to this is recent experimental data from the distantly-related cidaroid sea urchin *Eucidaris tribuloides*, which exhibits conserved and divergent wiring of its skeletogenic mesoderm (SM) (Erkenbrack and Davidson, 2015; Erkenbrack et al., 2016a). The promising results from these studies suggest that comparative analyses of euechinoid dGRNs with those operating in *E. tribuloides* would provide much needed insight into how these networks have diverged in deep time. As it has long been known that early cleavage events at the vegetal pole differ considerably between cidaroids and euechinoids (Schroeder, 1981), we sought to understand whether the underlying spatial regulatory states and dGRN circuitry specifying endomesodermal domains also differs in *E. tribuloides*.

We systematically examined the activity of regulatory factors from the endomesodermal dGRN of *S. purpuratus* that perform critical developmental roles in partitioning

spatial embryonic domains in euechinoids (Ettensohn et al., 2003; Oliveri, Carrick, and Davidson, 2002; Oliveri, Walton, et al., 2006; Revilla-i-Domingo, Oliveri, and Davidson, 2007; J. Smith, Kraemer, et al., 2008; Peter and Davidson, 2010; Peter and Davidson, 2011a; Ransick and Davidson, 2006; Materna and Davidson, 2012). In this analysis we included a cohort of 12 regulatory genes that represent five euechinoid endomesodermal regulatory states: *alx1* and *delta* in SM; *ets1/2* and *glial cells missing (gcm)* in non-skeletogenic mesoderm (NSM); *blimp1*, *foxa*, *gatae* (*gata4/5/6*), and *myc* in anterior endoderm (AE); *brachyury (bra)* and *hox11/13b* in posterior endoderm (PE); and *even-skipped (eve)* and *wnt8* in perianal ectoderm (PAE). Early in *S. purpuratus* embryonic development, maternally deposited factors, including β -catenin and Otx, provide the primary inputs to initiate zygotic transcription of many of these genes in the micromere, *veg2* and *veg1* embryonic lineages (Oliveri, Carrick, and Davidson, 2002). By fifth cleavage, one of the earliest cell fate decisions has been made when mesodermal regulatory factors—e.g. *alx1*, *delta*, and *ets1/2*—are activated in the large micromeres, sealing their fate as SM and that of their neighbors as NSM, which will come to express the Delta/Notch responsive genes *gatae* and *gcm* hours later (Ransick, Rast, et al., 2002; Davidson, Rast, Oliveri, Ransick, Calestani, C. Yuh, et al., 2002). Another critical cell lineage decision is the clearance of AE factors from the NSM precursor lineage at 18 hours post fertilization (hpf) (Oliveri, Walton, et al., 2006; Peter and Davidson, 2011a). Prior to this time, endodermal and mesodermal factors are co-expressed in the cell lineage abutting SM. Delta ligand at the cell membrane of NSM interacts with Notch receptor in proximal cells to initiate upregulation of mesodermal regulatory factors (Materna and Davidson, 2012). Initially in a ring pattern surrounding the SM cells, this multiply competent endomesodermal lineage undergoes cell division, thereby creating two rings of cells at the vegetal pole. Those cells no longer in contact with the SM no longer receive the Delta ligand, and consequently expression of Delta-dependent mesodermal factors in these cells is extinguished. Thus, the replication of *veg2* descendant cells in combination with the spatial restrictions of the SM *delta* signal cause *gcm* levels to decrease in the ring of cells no longer in contact with the Delta ligand. These cells in the outer ring now become fated to AE. In this way, NSM becomes partitioned from AE. Outside of the vegetally positioned mesodermal lineages are AE and PE. By 24 hpf, segregation of these lineages is complete, with *foxa* being expressed in the AE and *hox11/13b* expressed in the PE. At the outermost vegetal regions of the *S. purpuratus* pregastrular embryo *eve* and *wnt8* are expressed, defining the region where endoderm meets ectoderm.

In previous work that appeared in these pages, we demonstrated extensive evolutionary rewiring of dGRNs in the SM lineage since the cidaroid-euechinoid divergence, including the euechinoid double-negative (D-N) gate synapomorphy and the rewiring of mesodermal regulatory factors *ets1/2*, *delta*, *hesc*, and *tbrain* (10). Here, we adopted an approach that frames our data from the vantage point of installation and processing of regulatory states in the early development of echinoids. We undertook high-density surveys of spatial and temporal gene expression of 12 regulatory factors during *E. tribuloides* development from early blastula stage to the onset of gastrulation. We experimentally interrogated the function of critical regulatory factors, all of which have well-defined roles in the *S. purpuratus* endomesodermal dGRN. Our data indicate that the pregastrular spatial complexity of endomesodermal dGRNs is markedly similar between *E. tribuloides* and euechinoids. Specifically, the five euechinoid regulatory states that define the endomesoderm also occur in *E. tribuloides*. However, our experimental data suggest that *E. tribuloides* arrives at these pregastrular regulatory states by strikingly different means. These results suggest that echinoids exhibit a conserved set of endomesodermal regulatory states that likely existed in the common ancestor of these two clades, and the wiring of which has markedly diverged since the cidaroid-euechinoid divergence. Therefore, we provide direct evidence for conserved regulatory state processing executed by distinct regulatory factors and conclude that one critical function of dGRNs in early embryogenesis of echinoids is to ensure installation of the conserved set of regulatory states, a genetic example where the ends are truly geared to overlook the means.

2.3 Results

Conservation of pregastrular endomesodermal regulatory states

Previous analyses of *E. tribuloides* regulatory state patterning in mesoderm and ectoderm indicate that temporal and spatial expression of individual regulatory genes exhibit domain-specific constraint, e.g. regulatory genes are more likely to be conserved in ectodermal patterning than in mesodermal patterning (Erkenbrack and Davidson, 2015; Erkenbrack et al., 2016a; Erkenbrack, 2016). Thus it is clear that the function of dGRNs is to control not just individual genes, but the expression of entire cell fate specific regulatory states. Therefore, we asked if this observation also holds for specification processes in endomesodermal cell fate decisions and surveyed the spatiotemporal regulatory genes in euechinoids that execute these network functions. In *S. purpuratus* embryos developing at 15°C,

gastrulation initiates at 30 hpf. By 24 hpf, these embryos express at least six distinct endomesodermal regulatory states, one of which specifies the small micromere lineage, which are set-aside cells contributing to the juvenile sea urchin but not to embryonic endomesodermal cell fates. For this reason, the small micromere-specific regulatory states were not considered in our analysis. Normal development of *E. tribuloides* occurs at 22°C and gastrulation occurs at around 22 hpf (Figure 2.1).

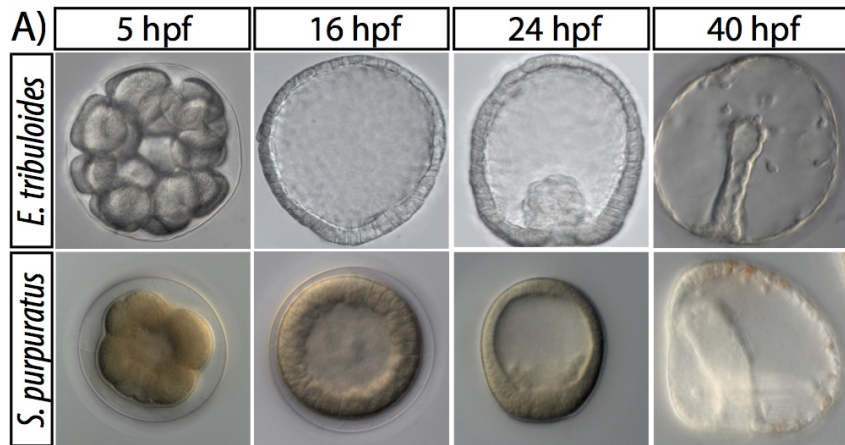


Figure 2.1: Morphology and timing of *E. tribuloides* and *S. purpuratus* development over the first 40 hours post fertilization. By 24 hpf, *E. tribuloides* has started to gastrulate and no cells are observed in the blastocoel, whereas in *S. purpuratus* skeletogenic mesenchyme has ingressed into the blastocoel and gastrulation has not begun. By 40 hpf both embryos are undergoing gastrulation and, whereas *S. purpuratus* exhibits conspicuous skeletogenic rods, *E. tribuloides* does not.

For this analysis we focused on pregastrular regulatory states of endomesodermal regulatory states in *E. tribuloides* embryos and determined the spatial expression of 12 regulatory genes representing the following regulatory states in *S. purpuratus* embryos at 24 hpf of development (Figure 2.2): *alx1* and *ets1/2* in skeletogenic mesoderm (SM); *myc* and *delta* in oral veg2 mesoderm (oral NSM); *gcm*, *gatae*, and *delta* in aboral veg2 mesoderm (aboral NSM); *foxa*, *blimp1b*, *gatae*, and *myc* in anterior endoderm (AE); and *eve*, *hox11/13b*, *brachyury*, and *wnt8* in posterior endoderm (PE).

To check whether the orthologs of these regulatory genes are also expressed during pregastrular development of *E. tribuloides* embryos, their timecourse of expression levels during pre-gastrular development was analyzed by QPCR (Figure 2.3).

Just as in *S. purpuratus* embryos, the earliest expressed regulatory genes in *E.*

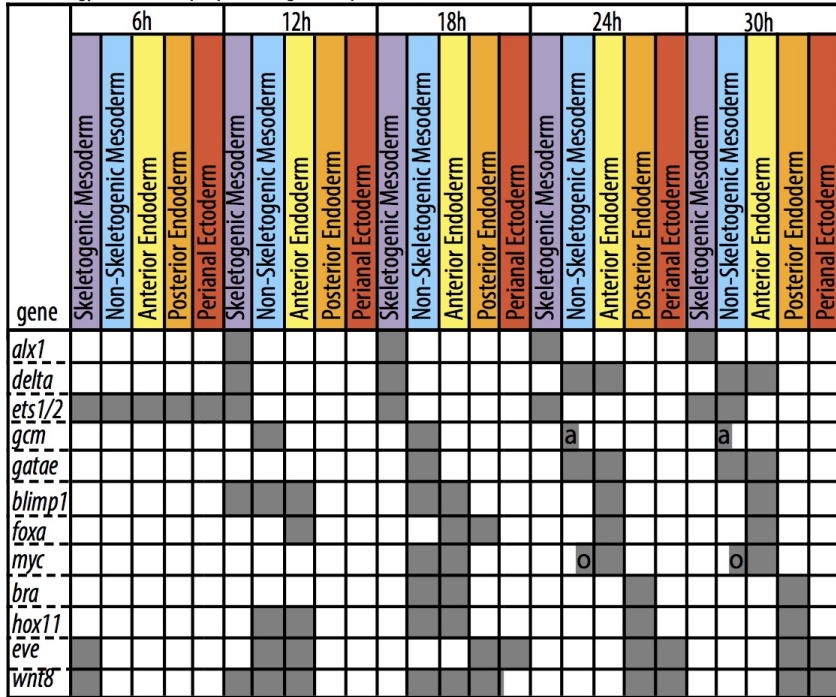
A) *Strongylocentrotus purpuratus* gene expression matrix

Figure 2.2: Gene expression matrix showing spatial distribution of *S. purpuratus* regulatory factors at five timepoints in development. Columns represent embryonic domains, and rows represent regulatory gene expression. After Peter and Davidson (2011)

tribuloides are *eve*, *wnt8*, and *blimp1*, for which in *E. tribuloides* embryos the earliest transcripts were detected by 6 hpf. All 12 regulatory genes are expressed before 15 hpf, although *alx1* expression levels remain very low. We therefore proceeded to analyze the spatial expression of these pregastrular regulatory genes in *E. tribuloides* embryos at 18 hpf, just prior to the onset of gastrulation, a stage corresponding approximately to the 24 hpf stage in *S. purpuratus*. Our results show that the spatial expression of these regulatory genes in *E. tribuloides* embryos occurs in at least four different cellular domains (Figure 2.4). The regulatory genes expressed in each of these domains in *E. tribuloides* are the following, starting from the most vegetal domain: *alx1* and *delta* (SM); *ets1/2*, *gcm*, *gatae*, and *myc* (NSM); *blimp1*, *foxa*, *myc*, *gatae*, and *hox11/13b* (AE); *brachyury*, *hox11/13b*, *eve*, and *wnt8* (PE). A direct comparison of the spatial expression of *E. tribuloides* and *S. purpuratus* regulatory genes shows that with few exceptions, the same regulatory states are expressed in the endomesodermal domains in *S. purpuratus* and *E. tribuloides* embryos (Figure 2.5). Thus, the shared regulatory states in these embryos are as follows: *alx1* in SM, *gcm*, *gatae*, and *myc* in NSM, *blimp1*, *foxa*, *gatae*, and *myc*

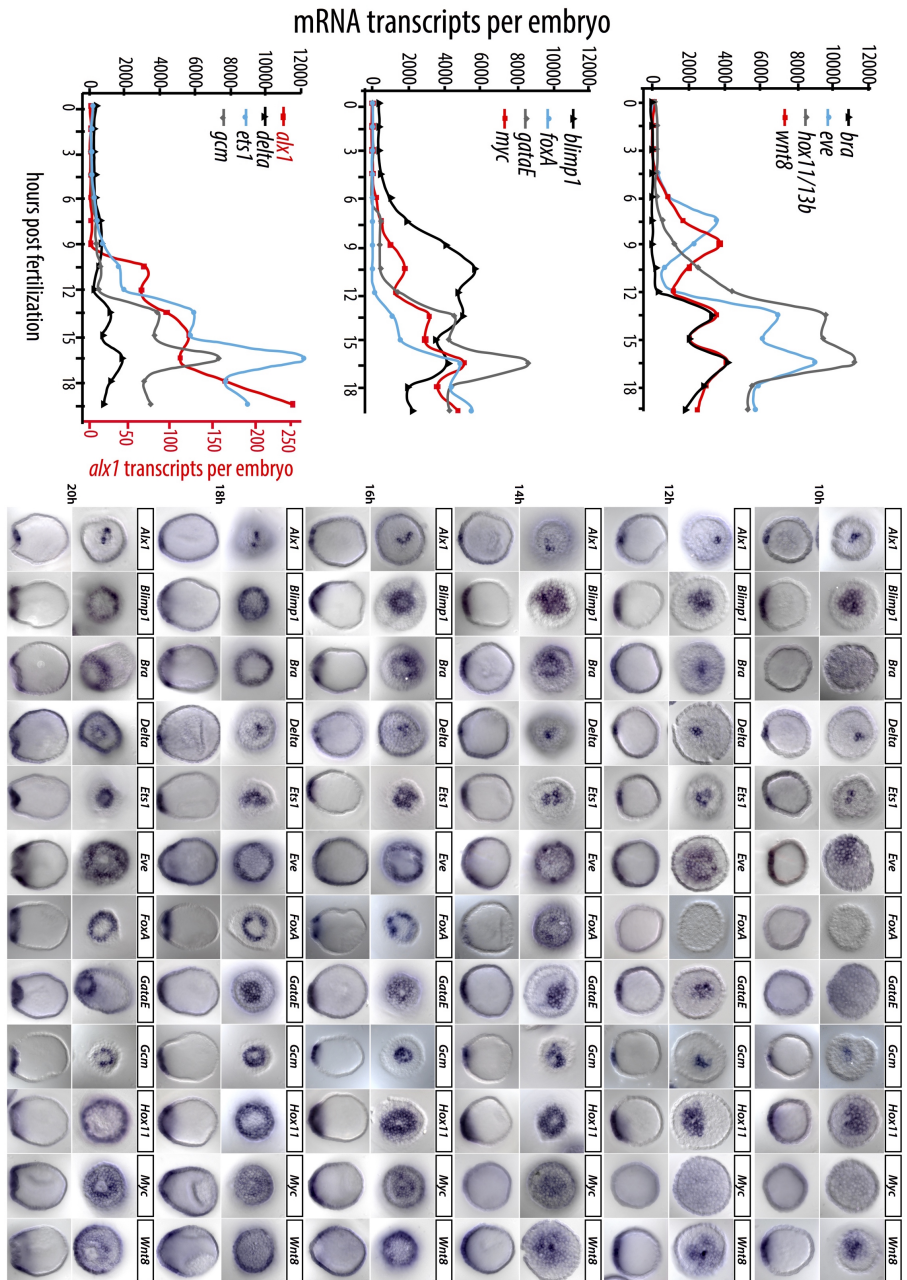


Figure 2.3: High-density spatiotemporal timecourse of regulatory gene expression in *E. tribuloides*. mRNA transcripts per embryo estimated as in Erkenbrack et al. (2016).

in AE, and *brachyury*, *hox11/13b*, *eve*, and *wnt8* in PE. Thus the only conspicuous difference in regulatory gene expression is *ets1/2* in NSM, as in *S. purpuratus* *ets1/2* is restricted to SM at 24 hpf. However, in *S. purpuratus* *ets1/2* is also expressed in oral NSM by 30 hpf; a discrepancy that can be interpreted as a heterochronic shift

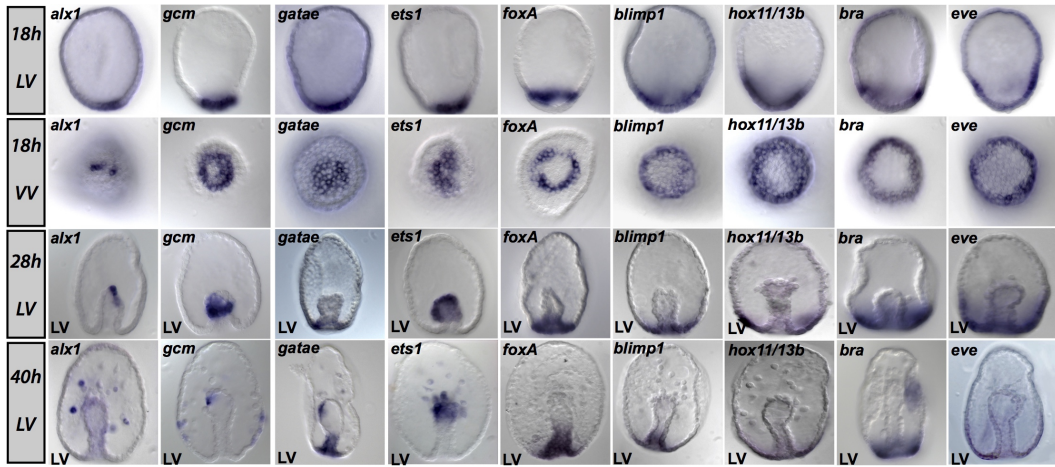


Figure 2.4: Spatial distribution of endomesodermal regulatory genes in *E. tribuloides* at 18 hpf.

in expression since the cidaroid-euechinoid divergence (Figure 2.2). Whereas in *S. purpuratus* *delta* is expressed in NSM at 24 hpf, in *E. tribuloides* *delta* is expressed in skeletogenic mesoderm; however, in *S. purpuratus* *delta* is expressed in SM at earlier stages of development and has an important role in the specification of NSM. In *E. tribuloides* *hox11/13b* is expressed in AE and PE, but expression of *hox11/13b* in *S. purpuratus* is restricted to posterior endoderm only at 24 hpf, even though *hox11/13b* is expressed in AE precursor cells during earlier development up to 21 hpf. The spatial organization of these endomesodermal domains is similar in *E. tribuloides* and *S. purpuratus* embryos, although vegetal SM cells in *S. purpuratus* embryos start to ingress into the blastocoel at 21 hpf. Furthermore, in *S. purpuratus* embryos, the *veg2* mesodermal domain is further subdivided into separate oral and aboral mesodermal domains, whereas only one NSM domain is apparent in pregastrular *E. tribuloides* embryos. To confirm that the four regulatory domains of *E. tribuloides* embryos indeed give rise to similar cell fates than their corresponding *S. purpuratus* domains, we analyzed post-gastrular expression of regulatory genes (Figure 2.4). Indeed, in *E. tribuloides* *alx1* and possibly also *ets1/2* are expressed in skeletogenic cells ingressing into the blastocoel only after invagination of the archenteron (1). In *E. tribuloides*, *gcm*, *gatae*, and *ets1/2* are expressed in NSM cells, *foxa*, *blimp1*, and *gatae* are expressed broadly in the endoderm, including in future fore- and midgut cells, while *hox11/13b* and *brachyury* are expressed in PE domains.

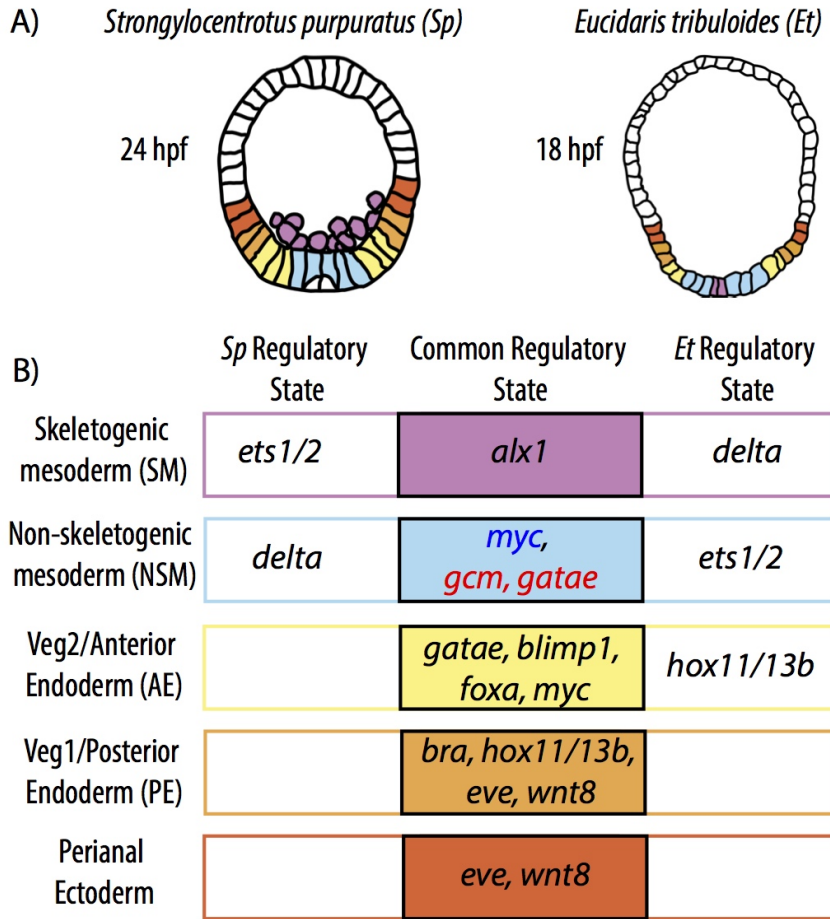


Figure 2.5: Endomesodermal regulatory states in pregastrular embryos of *S. purpuratus* and *E. tribuloides* at 24 hpf and 18 hpf, respectively. Schematic diagrams for each embryo are displayed in the top panel. Comparative differences are listed under each schematic. Shared regulatory states are listed in the center column. For NSM, blue text indicates oral NSM and red text indicates aboral NSM.

Developmental sequence of specification of regulatory state domains

We next considered the temporal sequence in which the four endomesodermal regulatory state domains are specified and the regulatory genes responsible for initially defining the location and boundaries of each domain. A timecourse analysis of gene expression levels for these endodermal and mesodermal regulatory genes indicated that *eve*, *wnt8*, and *blimp1* are the earliest regulatory genes expressed zygotically by 6 hpf, and all genes in this study have initiated transcription by 15 hpf (Figure 2.3). High-density *in situ* hybridization of these regulatory genes during pre-gastrular *E. tribuloides* specification revealed the spatial dynamics of regulatory state specification between 10-20 hpf in *E. tribuloides* embryos (Figure 2.3). In *S. purpuratus* embryos, the earliest domain showing specific expression

of zygotic regulatory genes is the SM precursor cells at the vegetal pole (Figure 2.2). *Pmar1* is exclusively transcribed in this *S. purpuratus* lineage starting at 5 hpf (Oliveri, Carrick, and Davidson, 2002; Oliveri, Tu, and Davidson, 2008). *Pmar1* encodes a repressor that functions at the top of the D-N gate, a network circuit operating to restrict the activity of the skeletogenic GRN to skeletogenic micromeres. In consequence, *alx1* and *delta* initiate zygotic expression at 9 hpf in the skeletogenic domain. While *alx1* expression persists in skeletogenic cells, *delta* stops being transcribed in these cells between 18-21 hpf. In *E. tribuloides* embryos, the expression of *alx1* and *delta* is observed specifically in skeletogenic cells at 10 hpf, and both genes are transcribed exclusively in these cells up to 20 hpf (Figure 2.6A) (Erkenbrack and Davidson, 2015). Thus in both *S. purpuratus* and *E. tribuloides* embryos, vegetally localized SM is the first domain with cell-type specific zygotic expression of regulatory genes.

By 15 hpf of development, *S. purpuratus* embryos have undergone two additional cell fate decisions, separating NSM cell fates from AE cell fates, and AE from PE (Peter and Davidson, 2010; Peter and Davidson, 2011a). The earliest expression of the mesodermal regulatory gene *gcm* in *S. purpuratus* initiates at 9 hpf in the *veg2* precursors of both NSM and AE. However, by 15 hpf these cells have given rise to two rings of cells surrounding the SM: the inner ring continuing to express *gcm* and fated to become NSM, and the outer ring ceasing to express *gcm* and fated to become AE (Peter and Davidson, 2010). In addition, both mesodermal and endodermal *veg2* lineage descendants continue to express regulatory genes associated with endodermal fate, such as *blimp1*, *foxa*, *brachyury*, and *hox11/13b*. In *E. tribuloides* embryos, expression of *gcm* initiates in a few cells before 10 hpf in the skeletogenic precursor cells, showing expanding expression to the surrounding NSM by 12 hpf (Figure 2.6A,B and Figure 2.3). On the other hand, expression of endodermal regulatory genes *blimp1*, *eve*, and *hox11/13b* initiates before 10 hpf broadly in vegetal cells including SM, NSM and AE. Thus in contrast to *S. purpuratus* embryos, where NSM and AE descend from a common *veg2* lineage initially expressing an endomesodermal regulatory state, *E. tribuloides* embryos first express a set of endodermal regulatory genes within a field of cells, some of which will turn on expression of the mesodermal regulatory genes *gcm* and *gatae* at 12 hpf and give rise to mesodermal cell fates. Endodermal cells therefore never express mesodermal regulatory genes in *E. tribuloides* embryos and do not descend from a common endomesodermal cell lineage. The result, however, is the same, which is the separation of SM, NSM, and AE expression domains. To complete the process of separating endodermal and

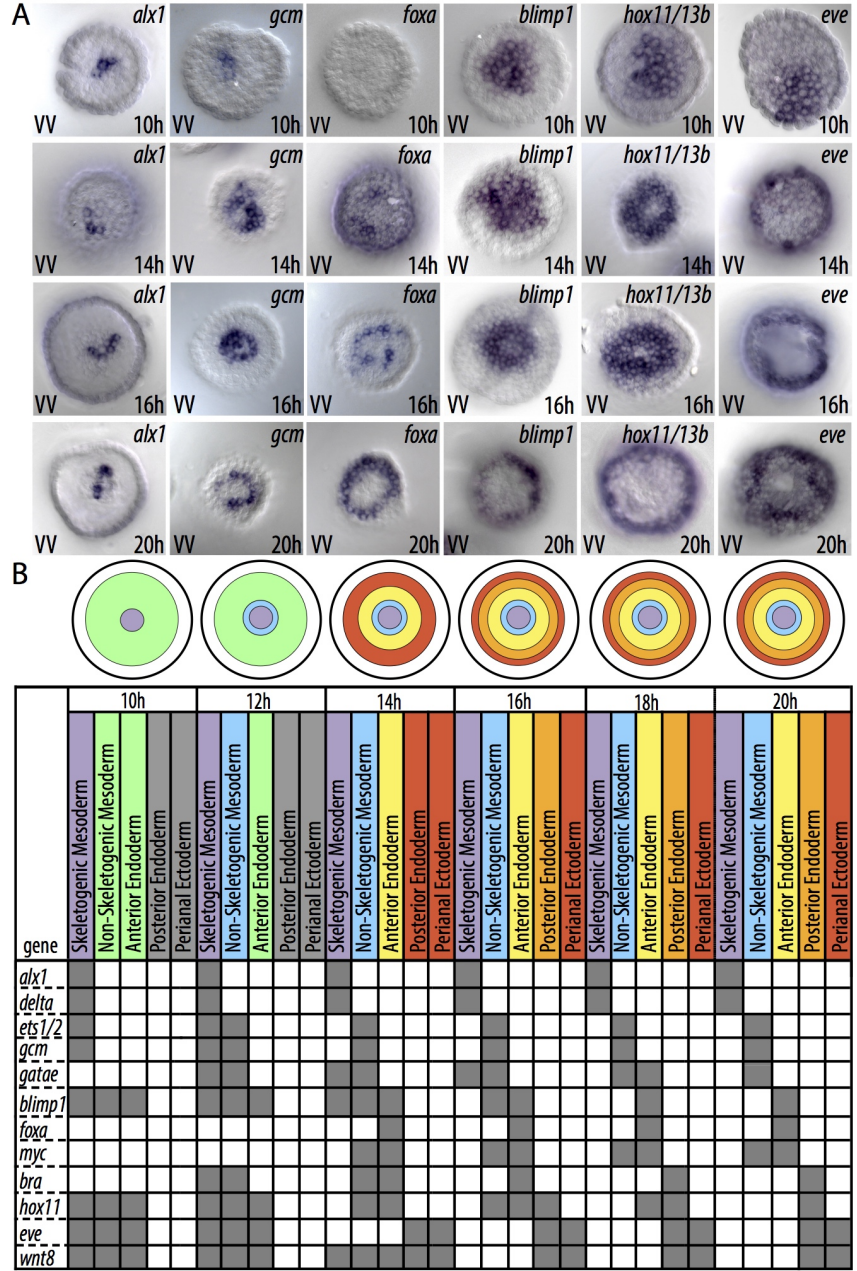


Figure 2.6: Spatial distribution and gene expression matrix of endomesodermal regulatory genes in pregastrular embryos of *E. tribuloides* between 10 and 20 hpf. (A) Spatial distribution for regulatory genes that demarcate endomesodermal cell types: *alx1*, SM; *gcm*, NSM; *foxa* and *blimp1*, AE; *hox11/13b*, PE; and *eve*, perianal ectoderm. (B) Gene expression dynamics of all regulatory genes examined in this study. Top panel: Schematic diagrams for each timepoint of dynamic regulatory gene process at the vegetal pole of *E. tribuloides*. Bottom panel: Matrix of gene expression. Shaded boxes indicate expression in an embryonic domain (column).

non-skeletogenic mesoderm gene expression, endodermal gene expression is cleared from mesodermal cells by 18 hpf in *S. purpuratus* embryos (Peter and Davidson, 2010). In *E. tribuloides* embryos, however, clearance of *blimp1* and *hox11/13b* transcripts from NSM precursors occurs later, just prior to gastrulation at 18 hpf (Figure 2.6A,B and Figure 2.3).

The separate specification of AE and PE is marked in *S. purpuratus* embryos by the expression of *eve* in PE. By 15 hpf, the entire *veg1* lineage including PE expresses *eve*, while the anterior endoderm of the *veg2* lineage expresses *blimp1*, *foxa*, *brachyury*, and *hox11/13b*. By 24 hpf, however, PE precursors also start to express *hox11/13b* and *brachyury*, while the expression of these genes clears from AE. This expression of *hox11/13b* and *brachyury* occurs specifically in PE precursors and establishes the boundary between PE and perianal ectoderm. In *E. tribuloides* embryos, *eve* expression occurs initially in cells also expressing *blimp1* and *hox11/13b*, including mesodermal and AE domains. However, by 14 hpf, *eve* transcripts have cleared from this area and are expressed in a ring of cells surrounding the domain of *hox11/13b*, similar to *S. purpuratus* embryos—though in contrast *hox11/13b* continues to be expressed in mesodermal domains. By 18 hpf in *E. tribuloides*, *hox11/13b*, and *brachyury* expression starts in a subset of *eve* expressing cells, and *brachyury* is simultaneously cleared from *blimp1*-*foxa* expressing cells, while *hox11/13b* expression is only cleared from AE by 20 hpf.

Thus the gene expression boundaries between SM and NSM; NSM and AE; AE and PE; and PE and perianal ectoderm are installed in the same temporal sequence in both embryos and are defined, with exceptions, by orthologous regulatory genes. However, no equivalent of the *S. purpuratus* endomesodermal *veg2* precursor lineage that expresses endodermal and mesodermal regulatory genes and gives rise to both cell fates exists in *E. tribuloides* embryos. Instead, expression of the regulatory gene *gcm* is superimposed within a subset of cells expressing an endodermal regulatory state, and these cells are thereby converted to mesodermal cell fates.

Evolution of regulatory mechanisms underlying specification of mesodermal fates

Specification of SM occurs very early in embryonic development of *S. purpuratus* and *E. tribuloides*, the gene regulatory interactions of which are described elsewhere (Erkenbrack and Davidson, 2015). Here we focus on the specification of pregastrular NSM cell fates. Several gene regulatory network circuitries crucial for

mesoderm specification in *S. purpuratus* embryos are resolved (Figure 2.7A), and we specifically test for similar regulatory mechanisms operating to specify mesodermal lineages in *E. tribuloides* embryonic development.

Gcm in NSM and at the top of the pigment cell lineage GRN hierarchy. In *S. purpuratus*, specification of NSM in the veg2 cell lineage initiates with the expression of *gcm* at 10 hpf in a single ring of eight veg2 daughter cells (Ransick and Davidson, 2006). Strikingly in euechinoids, these cells are simultaneously the precursors of all NSM cell fates and AE which will give rise to the foregut and aboral midgut endoderm. In the course of mesoderm specification, *gcm* is particularly important for specification of pigment cells and functions as a driver of pigment cell differentiation genes (Ransick and Davidson, 2006; Calestani and Rogers, 2010; Ransick and Davidson, 2012). *S. purpuratus* cells expressing *gcm* delaminate from the tip of the archenteron at the onset of gastrulation and incorporate into the ectoderm, where they further develop into differentiated pigment cells. In the absence of *Gcm*, *S. purpuratus* larvae lack pigment cells (Ransick and Davidson, 2006). In *E. tribuloides* embryos, *gcm* expression is first detectable at 7 hpf, but a strong increase in expression levels occurs between 12-16 hpf (Figure 2.3A). The temporal dynamics of *gcm* expression in *E. tribuloides* are consistent with *gcm* spatial expression, which is exclusively expressed by 10 hpf in precursor SM, but by 12 hpf expands to surrounding NSM cells. By 14 hpf, *gcm* expression clears from skeletogenic precursors and remains exclusively expressed in NSM (Figure 2.6A). As shown above, *gcm* expression continues in mesodermal cells in the anterior archenteron, and by 40 hpf is detectable in cells within the ectoderm (Figure 2.4). Consistent with the hypothesis that *Gcm* functions as a driver of pigment cell specification in *E. tribuloides* embryos, injection of a morpholino blocking translation of *gcm* messenger RNA resulted in albino embryos lacking pigment cells (Figure 2.7B). Thus, the functional importance of *Gcm* in pigment cell specification is a plesiomorphic trait of echinoids and suggests that it has been atop the pigment cell specification GRN for at least 268 million years.

Initial inputs controlling *gcm* expression and early mesoderm specification

The earliest expression of *gcm* in mesoderm precursor cells in *S. purpuratus* embryos is controlled by Delta/Notch signaling and is induced upon presentation of Delta ligand in adjacent SM at the vegetal pole (Ransick and Davidson, 2006). Thus by means of controlling the expression of the earliest NSM regulatory gene *gcm* and Delta/Notch signaling controls both spatial and temporal initiation of NSM

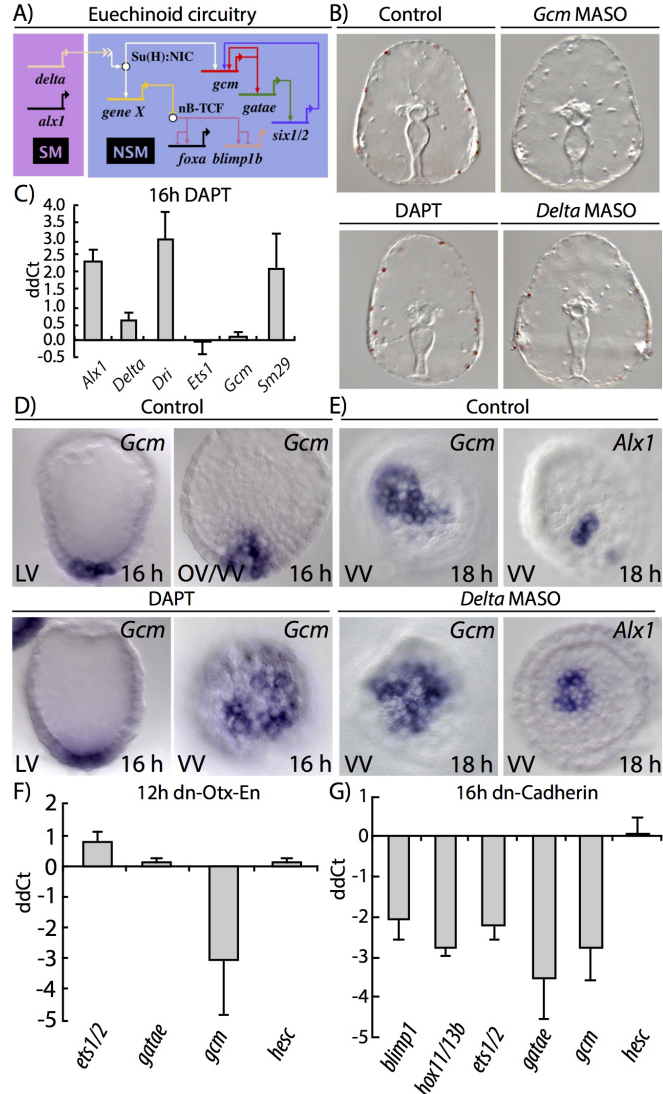


Figure 2.7: Testing the euechinoid NSM dGRN in *E. tribuloides* (A) Euechinoid NSM circuitry relevant to this study (see text). (B) Perturbation of *gcm* results in pigment-less larvae, though this is not the case in *delta* perturbation background. (C) Effect of DAPT on mesodermal regulatory genes at 16 hpf. Difference in qPCR cycle number relative to control is listed on the y-axis. Relative abundance of NSM genes *gcm* and *ets1/2* is unchanged in DAPT treatment. Upregulation of SM genes is a positive control of Notch signaling perturbation (Erkenbrack and Davidson (2015)). (D-E) *Gcm* is unchanged in two different perturbations of Delta/Notch signaling, whereas *alx1* is upregulated. (F) mRNA overexpression of a dominant-negative Otx construct decreases expression of *gcm*, but not other NSM regulatory genes. (G) mRNA overexpression of β -catenin/TCF perturbation construct reduces abundance of numerous endomesodermal regulatory genes, but not *hesc*.

specification. Interfering with Delta/Notch signaling in *S. purpuratus* embryos leads to complete loss of *gcm* expression and albino embryos (Ransick and Davidson,

2006; Materna and Davidson, 2012). Further, analysis of an early enhancer has demonstrated the direct control of *gcm* by the Delta/Notch responsive transcription factor Suppressor of Hairless (Ransick and Davidson, 2006). In *E. tribuloides* embryos, *delta* expression occurs early in development in SM, just as in *S. purpuratus* embryos. Furthermore, inhibition of Delta/Notch signaling has been shown to result in the ectopic expression of skeletogenic genes in NSM cells (Erkenbrack and Davidson, 2015). To test whether in addition, Delta/Notch signaling is required for expression of *gcm*, *E. tribuloides* embryos were treated with DAPT and expression of *gcm* and *ets1/2* was analyzed by qPCR (Figure 2.7C). Relative expression of *gcm* and *ets1/2* remain unchanged upon DAPT treatment, even though expression levels of the SM genes *alx1*, *dri* and *sm29* increased (Erkenbrack and Davidson, 2015). The spatial expression of *gcm*, when analyzed by WMISH, was also not affected by treating embryos with DAPT, or by injection of *delta* morpholino, even though interfering with Delta expression resulted in ectopic expression of *alx1* in NSM cells (Figure 2.7D,E). In addition, DAPT treatment or injection of Delta morpholino did not interfere with the specification of pigment cells, as shown in Figure 2.7B. These results demonstrate that Delta/Notch signaling is not responsible for the control of *gcm* expression in early NSM cells and is also not required for the specification of pigment cells.

If not Delta/Notch signaling, then what are the inputs driving early expression of *gcm* in *E. tribuloides* mesodermal precursor cells? The earliest expression of *gcm* in cells at the vegetal pole before expanding to adjacent cells resembles the expression of many genes of the endodermal GRN in *S. purpuratus* embryos. In these embryos, the earliest activation of endodermal genes is regulated by two maternal transcription factors, Otx and Tcf. Otx is maternally localized at the vegetal pole, and the anisotropic distribution of β -catenin turns Tcf into a transcriptional activator in cells of the vegetal pole. To test whether the orthologs of these two factors regulate expression of *gcm*, we injected *E. tribuloides* embryos with a dominant negative form of Et-Otx, in which Et-Otx is fused to an Engrailed repressor domain. When measured by QPCR, Otx-En decreased the expression of *gcm*, but not *ets1/2*, *gatae*, and *hesc*, in a dose-dependent manner (Figure 2.7F). The same experiment, when conducted in *S. purpuratus* embryos using Sp-Otx-En, did not affect the expression of *gcm* (Davidson, Rast, Oliveri, Ransick, Calestani, C. H. Yuh, et al., 2002). To perturb the activity of Tcf, we injected mRNA encoding a dominant negative form of *cadherin*, δ -cadherin, which interferes with β -catenin nuclearization. Injection of δ -cadherin mRNA led to decreased expression of *gcm*, *ets1/2*, and *gatae*, but

not of *hesc* (Figure 2.7G). Both perturbations also affect the expression of regulatory genes driving endodermal specification, which at 12 hpf are also expressed in mesodermal precursor cells. In turn, interfering with translation of two important endodermal regulators, Hox11/13b and Eve did not affect expression of *gcm*. Thus, our observations indicate that early activation of *gcm* in *E. tribuloides* is not dependent on Delta/Notch signaling, but rather is directly or indirectly downstream of early activating factors such as β -catenin and Otx. Finally, in regards to the role of *delta* in *E. tribuloides* endomesodermal segregation, we are forced to conclude its main function is to restrict SM fate to the micromere-descendants (Erkenbrack and Davidson, 2015).

Mesodermal specification downstream of *gcm*

In *S. purpuratus* embryos, after *gcm* expression is activated downstream of transient Delta/Notch input, *gcm* expression is maintained by a positive feedback circuit (Figure 2.7A). This feedback circuit is completed by Gatae and Six1/2, where Gcm activates the expression of *gatae*, and Gatae activates the expression of *six1/2*, the product of which in turn activates *gcm* (Ransick and Davidson, 2012). In addition, Gcm positively autoregulates itself, and injection of morpholino targeting *gcm* transcript leads to decreased *gcm* transcription. In contrast, introduction of *gcm* morpholino into *E. tribuloides* embryos, does not affect the expression of *gcm* during pregastrular development. Furthermore, after the onset of gastrulation, at 22 hpf, Gcm is negatively autoregulated, and injection of *gcm* morpholino leads to an expansion of *gcm* expression within NSM. Neither *gatae* nor *ets1/2* are affected by injection of *gcm* morpholino. Since all three regulatory genes are activated in mesodermal precursor cells at a similar time, about 12 hpf, they may all be controlled by similar regulatory inputs. Indeed, *gatae* expression in *E. tribuloides* is affected by injection of δ -cadherin mRNA, but not by overexpression of *otx-en* RNA, while neither of these perturbations affected the expression of *ets1/2*. Thus while *gatae* expression in Sp NSM is regulated by Otx, Gcm and Delta/Notch signaling, *gatae* expression in *E. tribuloides* is activated downstream of Tcf but not Otx. Interestingly, Tcf does provide an input controlling *gcm* expression in *S. purpuratus*, though this regulatory interaction operates within endoderm precursor cells.

Clearance of expression of regulatory genes associated with endoderm fate

An important step in the specification of mesodermal cell fates is the clearance of mRNAs encoding transcription factors associated with the endodermal fate. In *S.*

purpuratus embryos, this clearance occurs downstream of Delta/Notch signaling but independently of the mesoderm GRN at 18 hpf (Peter and Davidson, 2010; Croce and McClay, 2010). In *E. tribuloides* clearance of *blimp1* and *hox11/13b* transcripts occurs in NSM cells between 16-18 hpf, just prior to gastrulation. Interestingly, this clearance is not dependent on Delta/Notch signaling, since treatment with DAPT did not interfere with the downregulation of *blimp1* transcription in NSM (Figure 2.8A).

Taken together, perturbation analyses in *E. tribuloides* indicate that significant changes have occurred in the regulation of regulatory gene expression in NSM cells since the cidaroid-euechinoid divergence. While mesodermal specification is affected by perturbation of Tcf/ β -catenin activity in *S. purpuratus* embryos, this regulation operates indirectly through the activation of delta expression in skeletogenic cells, leading to the spatial restriction of *gcm* expression and mesodermal specification. In *S. purpuratus* embryos therefore, *delta* expression in skeletogenic cells leads to activation of Notch signaling in NSM, activating expression of *gcm* and *gatae* as well as leading to repression of endodermal regulatory genes *blimp1*, *foxa*, *hox11/13b*, and *brachyury* (Peter and Davidson, 2010). In *E. tribuloides*, delta expression in SM leads to activation of Notch signaling in NSM, however its role is to suppress expression of regulatory genes associated with SM fate (Erkenbrack and Davidson, 2015), while it does not contribute to the specification of NSM lineages such as pigment cells. In addition, utilization of a transient signaling input in the activation of *gcm* expression in *S. purpuratus* requires an immediate installment of a positive feedback circuit to ensure the maintenance of *gcm* expression, while no functionally equivalent circuit operates the expression of *gcm* in *E. tribuloides*.

Evolution of regulatory mechanisms underlying endodermal cell fate specification

Initial activation of regulatory genes in endodermal precursors

The earliest expression of regulatory genes in endodermal precursor cells occurs at 10-12 hpf in *S. purpuratus* embryos, and includes *blimp1*, *hox11/13b*, *eve*, and shortly thereafter *foxa* and *brachyury* (Peter and Davidson, 2010). The expression of all five regulatory genes is activated downstream of maternal Sp-Tcf/ β -catenin, with additional input from Otx into *blimp1*, *foxa*, and *brachyury* (Peter and Davidson, 2010; Peter and Davidson, 2011a; Cui et al., 2014; de-Leon and Davidson, 2010; J. Smith, Kraemer, et al., 2008). Similarly, in *E. tribuloides* perturbation

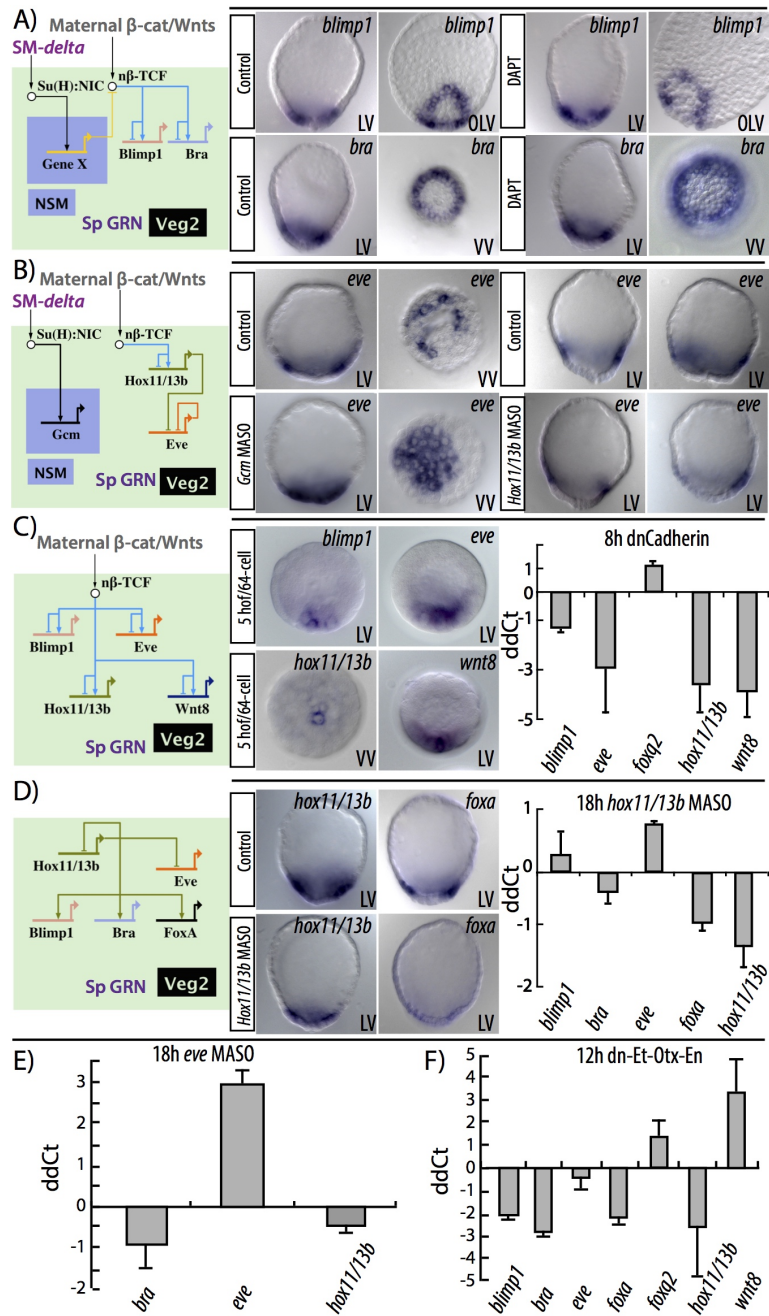


Figure 2.8: Testing the euechinoid endodermal dGRN in *E. tribuloides* Each experiment is accompanied by a euechinoid endodermal dGRN circuitry relevant to the question (see text). (A) Test for Delta/Notch signaling activity in segregation of endoderm and mesoderm. (B) Test for clearance of *eve* by endomesodermal regulatory genes. (C) Test for early initiation sensitivity to β -catenin/TCF inputs. (D) Test for role of *hox11/13b* in AE specification. (E) Test for role of *eve* in AE-PE regulatory states. (F) Test for sensitivity to Otx input.

of Tcf/β-catenin by injection of *dn-cadherin* mRNA decreased the expression of *blimp1*, *brachyury*, *eve*, *foxa*, and *hox11/13b*, indicating that the entire endodermal GRN is initially controlled downstream of maternal Tcf/β-catenin just as in *S. purpuratus* embryos (Figure 2.8C). Overexpression of *Et-otx-en* RNA leads to decreased expression of *blimp1*, *hox11/13b*, and *brachyury* at 12 hpf (Figure 2.8F).

Exclusive regulatory states in anterior and posterior endoderm

The distinction between anterior and posterior endodermal cell fates in *S. purpuratus* embryos occurs soon after the onset of zygotic gene expression in endodermal precursor cells. Thus by 15 hpf, *veg2* derived AE expresses *blimp1*, *foxa*, *brachyury*, and *hox11/13b*, whereas *veg1* derived PE expresses *eve*. The distinction between AE-PE regulatory states requires the repression of *eve* expression in AE, mediated by a combination of autorepression and repression by *Hox11/13b*. Similarly, targeting *eve* mRNA transcripts with a morpholino leads to increased levels of *eve*, consistent with a negative feedback circuit operating downstream of *Eve* (Figure 2.8E). Furthermore, *E. tribuloides* embryos injected with morpholino targeting *hox11/13b* show expression of *eve* in cells of the anterior but not posterior endoderm, indicating that *Hox11/13b* in *E. tribuloides* is responsible for the clearance of *eve* from AE (Figure 2.8B). An additional, unexpected repressive interaction of *Gcm* on *eve* ensures that vegetal cell fates do not express *eve*. Thus interfering with *gcm* translation leads to continued expression of *eve* throughout the vegetal plate, in SM and NSM (Figure 2.8B).

The anterior endoderm dGRN

In addition to the regulatory inputs provided by maternal factors, expression in *S. purpuratus* of *foxa*, *blimp1*, and *brachyury* also depends on *Hox11/13b*, activating the expression of its target genes at 18-21 hpf. However, by 21 hpf *Hox11/13b* negatively autoregulates itself, and *hox11/13b* transcripts are cleared from AE by 24 hpf. In the absence of *Hox11/13b*, *brachyury* expression is also extinguished in AE. Similarly, expression of *foxa* in *E. tribuloides*, but not *blimp1* and *brachyury*, depends on activation downstream of *Hox11/13b* (Figure 2.8D). Although the decrease in *hox11/13b* expression and the clearance of transcripts from AE precursors occurs at 18-20 hpf in *E. tribuloides* embryos, injection of morpholino targeting *hox11/13b* transcripts leads to a decrease rather than increase in *hox11/13b* expression levels (Figure 2.8D). Analysis of spatial expression of *hox11/13b*, however, shows that in *E. tribuloides* morpholino injected embryos, *hox11/13b* transcripts are detected in

AE cells, and not as in control embryos in PE precursors (Figure 2.8D). Thus the role of Hox11/13b in activating expression of *foxa* and inhibiting its own expression within the AE is a conserved regulatory interaction, although this factor displays additional functions in *S. purpuratus* embryos (Peter and Davidson, 2010).

Activation of posterior endoderm dGRN

In *S. purpuratus* embryos, the specification of PE starts with the activation of *hox11/13b* and *brachyury* expression at 21-24 hpf. The expression of *hox11/13b* and *brachyury* occurs downstream of Eve and Wnt signaling from the AE precursors, and is specific to the PE domain, thereby distinguishing prospective endoderm cell fates from the perianal ectoderm fate within the veg1 lineage (Peter and Davidson, 2011a; Cui et al., 2014; E. Li et al., 2014). In *S. purpuratus* the expression of *wnt1* and *wnt16* requires activation by Hox11/13b, and in turn *Wnt1* and *Wnt16* lead to activation of *hox11/13b* expression in PE (Cui et al., 2014). In *E. tribuloides* embryos, expression of *hox11/13b* and *brachyury* is activated in PE at 18 hpf. However, injection of morpholino targeting *eve* affects levels of neither *hox11/13b* nor *brachyury*, indicating that activation of the PE GRN occurs by different regulatory mechanisms in *S. purpuratus* and *E. tribuloides* embryos (Figure 2.8E). However, injection of *hox11/13b* morpholino does interfere with the activation of *hox11/13b* in PE precursors (Figure 2.8D), which is consistent with a regulatory circuit in which Hox11/13b expression in AE functions upstream of a signaling ligand activating *hox11/13b* expression in the adjacent PE domain.

2.4 Discussion

We show here the results of the first large-scale analysis of regulatory gene activity and regulatory state processing in the endomesoderm of the cidaroid sea urchin *E. tribuloides*. We exploited the well characterized endomesodermal dGRN of *S. purpuratus* to test whether network circuitry executing critical developmental tasks is present also in the GRN underlying *E. tribuloides* endomesodermal specification. We hypothesized that *E. tribuloides* would exhibit different genomic regulatory programs directing endomesodermal specification based on the observations of previous work on this species, demonstrating extensive rewiring of SM, NSM, and ectoderm specification and regulatory states to euechinoids (Erkenbrack and Davidson, 2015; Erkenbrack et al., 2016b; Erkenbrack, 2016), as well as the observation that cidaroid and euechinoid embryos exhibit distinct asymmetrical cleavage events at the vegetal pole in early development (Schroeder, 1981; Yamazaki, Kidachi, and

Minokawa, 2012). Importantly, we aimed to throw light on the evolutionary dynamics of dGRNs in early development of echinoids, as current evidence indicates that regulatory linkages of endomesodermal dGRNs of three euechinoid species separated by 90 million years of evolution exhibit extraordinary conservation. Thus, we conducted our analysis in a sea urchin that last shared a common ancestor with euechinoids much deeper in geological time. Documentation of the spatiotemporal dynamics of 12 regulatory factors in *E. tribuloides* development from early blastula stage to the onset of gastrulation allowed us to detail the dynamics of endomesodermal regulatory states of the pregastrular *E. tribuloides* embryo, from which we made inferences regarding potential regulatory transactions that may be facilitating delineation of domain boundaries and installation of regulatory states. Initial interpretations of these regulatory states suggested potentially conserved regulatory linkages. However, perturbation analyses revealed that distinct regulatory transactions were being utilized to install similar regulatory states in similar embryonic territories of *E. tribuloides*, suggesting extensive alterations have occurred to the endomesodermal dGRNs since these two clades split in the Middle Permian (Figure 2.9). Thus, although the terminal pregastrular regulatory states of endomesodermal

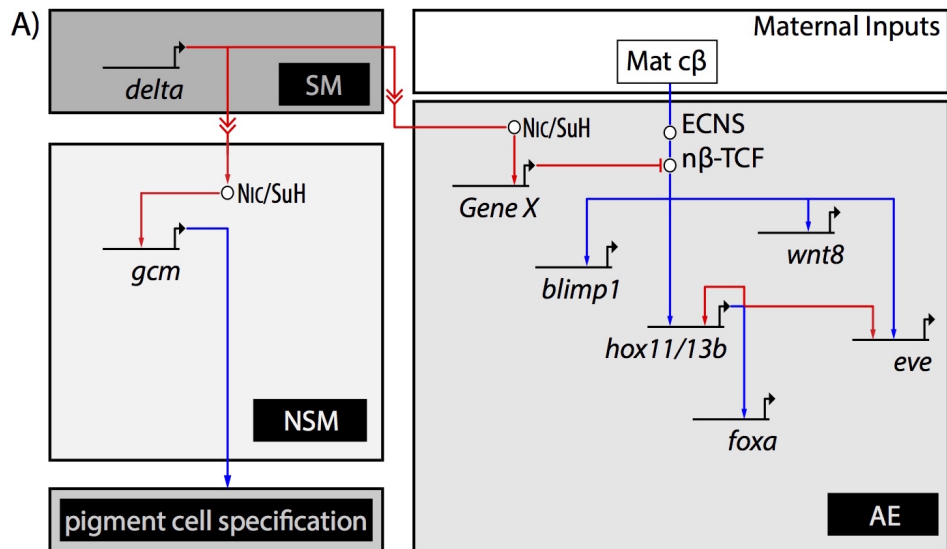


Figure 2.9: Conserved and divergent dGRN circuitry between *E. tribuloides* and euechinoids revealed in this study

domains are similar between *E. tribuloides* and euechinoids, the genomic regulatory processing that installs these sets of regulatory factors is drastically different between these clades.

Comparative analysis of regulatory state dynamics in *E. tribuloides* and euechinoids

Regulatory state dynamics in *E. tribuloides* provide an insightful developmental contrast to the seemingly evolutionarily static dynamics observed in camarodont euechinoids. As would be expected, there is an overall progression from general to specific regulatory states. In both systems we observe early activity of β -catenin responsive factors, e.g. *blimp1*, *eve*, *hox11/13b*, and *wnt8*. These observations are consistent with β -catenin nuclearization in localized vegetal pole cells in *E. tribuloides* (Erkenbrack and Davidson, 2015) and early expression of these factors in a tightly localized cluster of cells at the vegetal pole (Figure 2.10). Here, we demon-

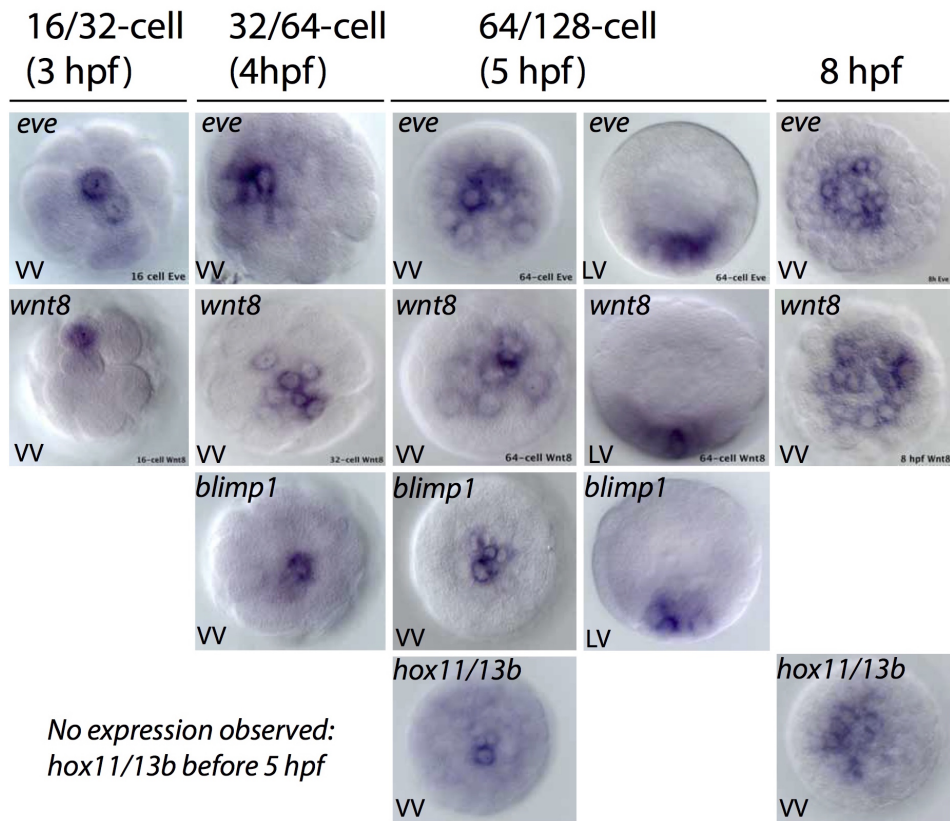


Figure 2.10: Spatial distribution of early euechinoid endomesodermal regulatory genes in cleavage stage embryos of *E. tribuloides*.

strate in this system the high sensitivity of these factors to perturbation of β -catenin nuclearization, an observation of which is consistent with that in euechinoids (J. Smith, Kraemer, et al., 2008) and are likely highly conserved regulatory interactions in all echinoderms (McCauley et al., 2015). Additionally, our data also suggest that there likely exists a conserved early regulatory input into many of these regulatory

factors from the maternal factor Otx (Davidson, Rast, Oliveri, Ransick, Calestani, C. Yuh, et al., 2002). These data are consistent with the hypothesis that in echinoids there exists conserved regulatory circuitry zygotically initiating transcription of this cohort of endomesodermal genes, which later in development engages in downstream genomic control of early endomesodermal regulatory factors. Importantly, in *E. tribuloides* we observe important differences downstream of this initial regulatory circuitry. For example, whereas in euechinoids the expression of *blimp1*, *hox11/13b* and *wnt8* is extinguished in mesodermal precursor cells relatively in quick succession, this is not the case in *E. tribuloides*, where our data indicate that expression of this cohort is maintained far longer in mesodermal precursor cells. This observation suggests that segregation of endomesoderm from mesoderm is obtained in *E. tribuloides* in spite of the sustained occupancy of endodermal regulatory factors in mesodermal lineages.

Another particularly striking distinction of regulatory state dynamics in *E. tribuloides* relative to euechinoids is the prominence of the micromere-descendants as an embryonic hub of regulatory factor initiation. In camarodont euechinoids particular endomesodermal regulatory factors are never expressed in SM, e.g. *bra*, *gatae*, *gcm*, and *foxa*. However, in *E. tribuloides* we observed three of these regulatory factors initiating zygotic expression in the micromere-descendants. Now we can clearly see that this contradistinction is a direct consequence of both Delta-dependent regulation of mesodermal regulatory factors and differential regulation of endodermal initiation in euechinoids. One hypothesis that could explain the observation that the micromere-descendants act as a hub of zygotic initiation in *E. tribuloides* is that many of these factors exhibit differential sensitivity to β -catenin nuclearization. This hypothesis is supported by observations in the sea star *Patiria miniata*, which indicate that numerous endomesodermal regulatory factors in this system exhibit dose-dependent sensitivity to β -catenin nuclearization (McCauley et al., 2015). This may also be the case in *E. tribuloides*, where we see spatially localized β -catenin nuclearization (Erkenbrack and Davidson, 2015) and sequential activation of vegetally localized regulatory factors. While we did not experimentally validate that this is the case for *E. tribuloides*, our data and other echinoderm data strongly suggest this is the case.

Role of Delta/Notch in segregating endodermal and mesodermal lineages in echinoids

In euechinoids, mesodermal regulatory factors combined with cellular division act to separate endodermal from mesodermal lineages (Oliveri, Walton, et al., 2006; Peter and Davidson, 2011a; Croce and McClay, 2010; Sethi et al., 2012). We found no evidence indicating a role for Notch signaling in segregation of endodermal and mesodermal lineages in *E. tribuloides*. However, given the limitations of our survey, we cannot preclude the possibility that Notch signaling plays a role in segregation of endoderm and mesoderm. Our data here indicate that perturbation of Notch signaling by inhibition with the small molecule antagonist DAPT had no affect on the clearance of endodermal regulatory factors *blimp1* and *bra* from NSM precursors. However, the observations that numerous endodermal regulatory factors are expressed in NSM precursor cells, that they are cleared from NSM at the time of Delta expression in proximal SM cells, and that Delta/Notch signaling plays a critical role in endodermal and mesodermal segregation in euechinoids are all highly suggestive that Delta/Notch plays a role in this process in *E. tribuloides*. Future surveys of Delta-responsive factors in NSM precursor cells will need to address this hypothesis. As of now, the only known function for Delta/Notch signaling in *E. tribuloides* early development is restriction of SM fate to micromere-descendants (Erkenbrack and Davidson, 2015).

Role of endomesodermal regulatory factors in segregating endoderm and mesoderm of EE. *tribuloides*

A striking difference between mesodermal specification in *E. tribuloides* and euechinoids is that early expression of *gcm* is not dependent on presentation of the Delta ligand in SM in spite of the fact that delta is expressed in *E. tribuloides* SM. Indeed, our data indicate that *gcm* is upregulated in micromere-descendants very early in *E. tribuloides* development and that its zygotic activation is likely driven by β -catenin nuclearization and maternal Otx. This result indicates that *gcm* possesses different functional roles in early development of *E. tribuloides*. Indeed, unexpectedly a role for *gcm* was revealed in clearing the posterior endodermal regulatory factor *eve* from mesodermal precursor cells. We found no evidence for prominent regulatory interactions that serve to segregate AE and PE of euechinoids. Surprisingly, in *E. tribuloides*, only two regulatory interactions were uncovered for Hox11/13b: positive autoregulation of itself and positive regulation of AE regulatory factor *foxa*. That Hox11/13b perturbation does not affect the expression of

AE regulators *blimp1* and *bra* was also surprising, as *hox11/13b* sits at the top of the AE GRN in euechinoids (Tsuchimoto and Yamaguchi, 2014; Wilson, Andrews, and Raff, 2005; McIntyre et al., 2013). Further, the spatiotemporal expression of *hox11/13b* in *P. baculosa* was shown to be similar to *E. tribuloides* (Yamazaki, Kidachi, and Minokawa, 2012), suggesting its function is likely a conserved feature of cidaroid endomesodermal specification. Taken together these observations suggest a limited role for *hox11/13b* in the earliest specification of anterior endoderm in *E. tribuloides*. Thus it is likely that regulatory linkages downstream of Hox11/13b into *blimp1* and *bra* were intercalated into the anterior endoderm GRN after the distinction of cidaroids and euechinoids in the lineage leading to extant euechinoids. Our perturbation data also suggest that neither *eve* nor *wnt8* exhibit prominent roles in initiating the regulation of endomesodermal genes that we surveyed, including *blimp1*, *bra*, *gatae*, *foxa*, and *hox11/13b*. This result further supports the notion that numerous endomesodermal regulatory factors are under control of maternal factors such as β -catenin nuclearization and maternal Otx.

The evolutionary origin of extant echinoid micromere lineages at the vegetal pole

In camarodont euechinoids, two asymmetric vegetal cleavage events produce a 32-cell embryo with four large micromeres and four small micromeres at 5th cleavage. The large micromeres are fated to become the SM (PMC) lineage and perform the critical task of Delta ligand presentation to proximally located anterior and posterior cells, upon which numerous downstream cell fate and specification events depend. This is contrasted to the asymmetric cleavage events at the 16-cell stage in the development of cidaroids, in which a variable number of differentially sized micromeres are produced at the vegetal pole (Schroeder, 1981; Yamazaki, Kidachi, and Minokawa, 2012). The descendants of these cells also later synthesize the larval skeleton, and it has been argued that cidaroid micromere-descendants are homologous to euechinoid PMCs (Wray and McClay, 1988; Urben, Nislow, and Spiegel, 1988). Comparative analyses of regulatory state dynamics in cidaroids and euechinoids now provide clues as to the evolutionary origins of these two cell lineages. We have demonstrated that *alx1* faithfully marks micromere-descendants in *E. tribuloides* and use it to indicate the spatial positioning of this lineage later in development. Contrary to the observed ring of euechinoid PMC cells prior to pregastrular ingress, *alx1* positive cells in *E. tribuloides* are frequently observed in disorderly, non-abutting positions at the tip of the vegetal pole. Consequently,

in cidaroids the disorganized arrangement of micromere-descendants is ill suited to provide the juxtacrine signaling mechanisms and symmetrical patterning output that is observed and affect downstream cell fate decisions in euechinoid endomesodermal domains. This hypothesis is consistent with the primary role of cleavage-stage micromere descendants as a Delta signaling hub that negatively regulates NSM from being fated as SM (Erkenbrack and Davidson, 2015). As was suggested elsewhere (Erkenbrack and Davidson, 2015), the global positive control of genes downstream of the euechinoid D-N gate circuitry is a shared derived character of euechinoids.

These observations afford insight into the evolutionary trajectories of the extant micromere lineage cell type in the two echinoid subclasses. In the ancestral echinoid embryo, the primary mechanisms controlling initiation and spatial localization of endomesodermal regulatory factors were likely spatial distribution of β -catenin nuclearization at the vegetal pole. This variable was likely fine-tuned with maternal inputs such as Otx. In this scenario, mesodermal regulatory states were initiated and stabilized by the regulatory factors that are restricted to micromere-descendants due to their β -catenin sensitivity early in development, e.g. *delta*, *ets1/2*, and *gcm*, regulatory factors which then acted as the primary inputs for downstream genes such as *alx1* and *tbrain*. This scenario outlines multiple hypotheses that can be assayed in modern cidaroid development. In the ancestral embryo of the lineage that led to extant euechinoids, there were likely numerous regulatory events that led to the precisely controlled D-N gate circuitry that we see today—chief among them being the appearance of the micromere-repressor *pmar1*. In this evolutionary scenario, at least four cis-regulatory events must have occurred: (1) *hesC* came under the control of a global positive input in the early embryo; (2) PMC regulatory factors *alx1*, *delta* and *ets1/2* acquire cis-regulatory sites for a globally expressed activator; (3) the cis-regulatory region of *pmar1* acquires binding sites for the same maternal inputs, viz. β -catenin nuclearization and Otx, as D-N gate responsive genes in extant cidaroids; and (4) the cis-regulatory region of *hesC* comes under the control of Pmar1. There is some evidence that a few of these regulatory interactions were in place at the time of the cidaroid-euechinoid split. We have already demonstrated that *alx1* transcription is repressed by HesC in NSM in *E. tribuloides* (Erkenbrack and Davidson, 2015), though this is not the case for *delta* and *ets1/2*. Furthermore, qPCR and WMISH evidence indicate that *hesC* is ubiquitously expressed early in *E. tribuloides*, suggesting this is the ancestral echinoid condition. What is still not clear, however, is the benefit to the embryo of early activation of the PMC GRN in

the large micromeres. Whatever that benefit may be, we here demonstrate the power of comparative analyses of developmental gene regulatory networks to shed light on long past evolutionary events.

2.5 Materials and Methods

Animals and Embryo Cultures

E. tribuloides sea urchins were obtained off the coast of Key Largo, FL (SeaLife, Inc.) and were maintained in room temperature aquaria. Animals were spawned by intracoelomic injection of 0.5 M KCl. Cultures were grown between 22°C and 23°C in millipore filtered sea water.

Real-time quantitative PCR

qPCR timecourse for the twelve genes-of-interest in this study was carried out at approximately 23°C over the first 20 hpf of *E. tribuloides* development. For each timepoint, 100 embryos were counted and cDNA template was obtained as described in (Erkenbrack and Davidson, 2015). To obtain per embryo transcript counts in timecourse samples, each timepoint was spiked with approximately 1000 copies of synthetic Xeno RNA (TaqMan Cells-to-Ct Kit, Life Technologies). Microinjected embryos (MASOs and constructs) were prepared as described in (Erkenbrack et al., 2016a). qPCR products for each gene were amplified using the primer sequences in Table 5.8.

Whole-mount *in situ* hybridization

Chromogenic WMISH was conducted as described in (Erkenbrack and Davidson, 2015). Embryos were prepared for double fluorescent WMISH (dfWMISH) with essentially the same protocol and were stained using the Tyramide Signal Amplification Kit (Perkin Elmer). Antibody concentration was 1:2000, and both cyanine3 and fluorescein were diluted 1:400 in manufacturer's diluent solution. Staining proceeded for approximately 5 minutes at room temperature. Stained embryos were imaged on an Axioskop II Plus equipped with an Axiocam MRc (Zeiss). WMISH primers used in this study are listed in Table S2. Additional primer sequences for are listed in Table 3.2.

Microinjection of MASOs, constructs, and RNA

Unfertilized eggs of *E. tribuloides* were prepared essentially as described in (Mcma-
hon et al., 1985). Morpholinos (MASOs) were synthesized by Gene Tools (Philo-

gene	WMISH Forward Primer	WMISH Reverse Primer
<i>blimp1</i>	TTGACCTCGTAGATGCATCG	TGTCTGCCATCGTAATTG
<i>brachyury</i>	TGGACACGTGGCTCGTATTGT	AAACGGGCTATCAGGACAGT
<i>eve</i>	CGTGACCAGCAACAGTAATCCAA	TACGCCAGGCCATTCCGA
<i>foxa</i>	AAAGTACCGAGAACGCCAGA	CAGCACAAACAAATCACGCG
<i>gatae</i>	AACCCACAACGGTCTGACGGGCTA	TGCCGTAGCCGTTCCGTAGATAA
<i>myc</i>	AGGAGGTCAAGCGAATGT	GATTACGACATGACACTGCC
<i>gcm</i>	GGCCATGCGAAACACCAACAATCA	AGACGCACACGACAAACGTTACTGA
<i>hox11/13b</i>	ATGCAGATAGGCATGGAGCA	TCGTCACAAACACATCACCACA
<i>wnt8</i>	AATGAATCGAGCCATCGAGGAGTG	AAGTTGTCGTGACCTCTAGCTGCA

Table 2.1: Sequences of primer sets for qPCR detection.

math, OR, USA), and their sequences are provided in Table S3. All MASO injection solutions were 1 mM, and each fertilized egg received approximately 10 pl of injection solution. Embryos for WMISH or qPCR were collected and processed as described above. Dominant-negative-Otx (Et-Otx-en) mRNA construct was modeled after a similar construct described in (X. Li, Wikramanayake, and Klein, 1999) and consisted of 5'- T3 RNA polymerase recognition sequence, the 5' 885 nucleotide (nt) repressor domain of the *Drosophila melanogaster* engrailed coding sequence, the 225 nt homeodomain of *E. tribuloides*, and a 21 nt nuclear localization sequence-3'. The complete coding sequence was codon-optimized and synthesized as a single gBlocks fragment (IDT; Coralville, Iowa). After addition of dATP nucleotides to the 3-prime ends, the construct was directly ligated into pGEM-T vector (Promega) and cloned into *E. coli*. Capped mRNA was synthesized using the mMessage Machine kit (Ambion, Thermo-Fisher) and microinjected into *E. tribuloides* embryos. Dominant-negative Cadherin (dnCad) RNA—which blocks β -catenin nuclearization at the vegetal pole, as described by (Logan et al., 1999)—was injected at a concentration of 1000 ng per μ l. For visualization of early, asymmetric nuclearization of β -catenin, RNA encoding a fused β -catenin:GFP product was synthesized using SP6 mMessage Machine RNA polymerase and injected at a concentration of 3 μ g per μ l. For microinjection of the 2.59 kb sp-pmar1 minimal reporter construct from (J. Smith and Davidson, 2009), 1500 molecules of reporter construct were injected per embryo, and injected embryos were scored at 26 hpf.

gene	MASO sequence	Interferes with
<i>delta</i>	ATAACATATAGCACGCCGAGAAGGC	Translation
<i>eve</i>	ATGGTGAAACCTTTCCATGTTAC	Translation
<i>gcm</i>	TGTCTCTGGACCATGTTGACCGTC	Translation
<i>hox11/13b</i>	GATTATGGATGTTGGCTTACCTGTC	Splicing

Table 2.2: Sequences of morpholino antisense oligonucleotides in this study.

Treatment with small molecule inhibitors

Embryos were treated with 1500 nM of the porcupine inhibitor C59 (C7641-2s, Cellagen Technology) as described in (Cui et al., 2014). Embryos were treated with the small molecule gamma-secretase inhibitor of the Notch pathway DAPT (GSI-IX, Selleck Chemicals, Inc.) at 10 μ M, the concentration of which was systematically determined by dilution series and the corresponding effect on skeletogenic target genes.

2.6 Acknowledgements

We thank Jonathon E. Valencia for contributing an image of an *S. purpuratus* embryo in Figure S1, Rebekah Kitto for helping with WMISH and imaging embryos, Miao Cui for providing c59 inhibitor. We are especially grateful to Andy Cameron, Parul Kudtakar, and the whole bioinformatics team at the Center for Computational Regulatory Genomics at the Beckman Institute for their professional support and computational wizardry. This work was supported by a National Science Foundation CREATIV Grant 1240626.

References

Calestani, C. and D. J. Rogers (2010). “Cis-regulatory analysis of the sea urchin pigment cell gene polyketide synthase”. In: *Developmental biology* 340.2, pp. 249–255.

Croce, J. C. and D. R. McClay (2010). “Dynamics of Delta/Notch signaling on endomesoderm segregation in the sea urchin embryo.” In: *Development* 137.1, pp. 83–91. ISSN: 1477-9129. doi: 10.1242/dev.044149. URL: <http://www.ncbi.nlm.nih.gov/pubmed/20023163> <http://www.ncbi.nlm.nih.gov/pmc/articles/PMC2796929/>.

Cui, M. et al. (2014). “Specific functions of the Wnt signaling system in gene regulatory networks throughout the early sea urchin embryo”. In: *Proc Natl Acad Sci U S A* 111.47, E5029–38. doi: 10.1073/pnas.1419141111. URL: <http://www.ncbi.nlm.nih.gov/pubmed/25385617>.

Davidson, E. H. and D. H. Erwin (2006). “Gene regulatory networks and the evolution of animal body plans.” In: *Science (New York, N.Y.)* 311.5762, pp. 796–800. ISSN: 1095-9203. doi: 10.1126/science.1113832. URL: <http://www.ncbi.nlm.nih.gov/pubmed/16469913>.

Davidson, E. H., J. P. Rast, P. Oliveri, A. Ransick, C. Calestani, C. H. Yuh, et al. (2002). “A provisional regulatory gene network for specification of endomesoderm in the sea urchin embryo”. In: *Developmental biology* 246.1, pp. 162–190.

Davidson, E. H., J. P. Rast, P. Oliveri, A. Ransick, C. Calestani, C. Yuh, et al. (2002). “A genomic regulatory network for development.” In: *Science* 295.5560, pp. 1669–78. ISSN: 1095-9203. doi: 10.1126/science.1069883. URL: <http://www.ncbi.nlm.nih.gov/pubmed/11872831>.

Erkenbrack, E. M. (2016). “Evolution of gene regulatory network topology and dorsal-ventral axis specification in early development of sea urchins (Echinoidea)”. In: *bioRxiv*, p. 044149.

Erkenbrack, E. M. and E. H. Davidson (2015). “Evolutionary rewiring of gene regulatory network linkages at divergence of the echinoid subclasses”. In: *Proc Natl Acad Sci U S A* 112.30, E4075–84. ISSN: 1091-6490 (Electronic) 0027-8424 (Linking). doi: 10.1073/pnas.1509845112. URL: <http://www.ncbi.nlm.nih.gov/pubmed/26170318>.

Erkenbrack, E. M. et al. (2016a). “Ancestral state reconstruction by comparative analysis of a GRN kernel operating in echinoderms”. In: *Dev Genes Evol* 226.1, pp. 37–45. ISSN: 1432-041X (Electronic) 0949-944X (Linking). doi: 10.1007/s00427-015-0527-y. URL: <http://www.ncbi.nlm.nih.gov/pubmed/26781941>.

– (2016b). “Ancestral state reconstruction by comparative analysis of a GRN kernel operating in echinoderms”. In: *Development Genes and Evolution* 226.1, pp. 37–45. ISSN: 0949-944X. doi: 10.1007/s00427-015-0527-y. URL: <http://link.springer.com/10.1007/s00427-015-0527-y>.

Ettensohn, C. A. et al. (2003). “Alx1, a member of the Cart1/Alx3/Alx4 subfamily of Paired-class homeodomain proteins, is an essential component of the gene network controlling skeletogenic fate specification in the sea urchin embryo”. English. In: *Development* 130.13, pp. 2917–2928. doi: 10.1242/dev.00511. URL: %3CGo%20to%20ISI%3E://WOS:000184149900009.

Hopkins, M. J. and A. B. Smith (2015). “Dynamic evolutionary change in post-Paleozoic echinoids and the importance of scale when interpreting changes in rates of evolution”. In: *Proc Natl Acad Sci U S A* 112.12, pp. 3758–3763. doi: 10.1073/pnas.1418153112. URL: <http://www.ncbi.nlm.nih.gov/pubmed/25713369>.

Kroh, A. and A. B. Smith (2010). “The phylogeny and classification of post-Palaeozoic echinoids”. English. In: *Journal of Systematic Palaeontology* 8.2, pp. 147–212. doi: Pii922467612Doi10.1080/14772011003603556. URL: %3CGo%20to%20ISI%3E://WOS:000278007400001.

de-Leon, S. Ben-Tabou and E. H. Davidson (2010). “Information processing at the foxa node of the sea urchin endomesoderm specification network”. In: *Proceedings of the National Academy of Sciences* 107.22, pp. 10103–10108.

Li, E. et al. (2014). “Encoding regulatory state boundaries in the pregastrular oral ectoderm of the sea urchin embryo.” In: *Proceedings of the National Academy of Sciences of the United States of America* 111.10, E906–13. ISSN: 1091-6490.

doi: 10.1073/pnas.1323105111. url: <http://www.ncbi.nlm.nih.gov/pubmed/24556994> %20http://www.ncbi.nlm.nih.gov/ articlerender.fcgi?artid=PMC3956148.

Li, X., A. H. Wikramanayake, and W. H. Klein (1999). “Requirement of SpOtx in cell fate decisions in the sea urchin embryo and possible role as a mediator of β -catenin signaling”. In: *Developmental biology* 212.2, pp. 425–439.

Logan, C. Y. et al. (1999). “Nuclear beta-catenin is required to specify vegetal cell fates in the sea urchin embryo”. English. In: *Development* 126.2, pp. 345–357. url: %3CGo%20to%20ISI%3E://WOS:000078613200014.

Martik, M. L., D. C. Lyons, and D. R. McClay (2016). “Developmental gene regulatory networks in sea urchins and what we can learn from them”. In: *F1000Research* 5.203. doi: 10.12688/f1000research.7381.1.

Materna, S. C. and E. H. Davidson (2012). “A comprehensive analysis of Delta signaling in pre-gastrular sea urchin embryos.” In: *Developmental biology* 364.1, pp. 77–87. issn: 1095-564X. doi: 10.1016/j.ydbio.2012.01.017. url: <http://www.ncbi.nlm.nih.gov/pubmed/22306924> %20http://www.ncbi.nlm.nih.gov/ articlerender.fcgi?artid=PMC3294105.

McCauley, B. S. et al. (2015). “Dose-dependent nuclear β -catenin response segregates endomesoderm along the sea star primary axis”. In: *Development* 142.1, pp. 207–217.

McIntyre, D. C. et al. (2013). “Short-range Wnt5 signaling initiates specification of sea urchin posterior ectoderm”. In: *Development* 140.24, pp. 4881–4889.

Mcmahon, A. P. et al. (1985). “Introduction of Cloned DNA into Sea-Urchin Egg Cytoplasm - Replication and Persistence during Embryogenesis”. English. In: *Developmental biology* 108.2, pp. 420–430. doi: Doi10.1016/0012-1606(85)90045-4. url: %3CGo%20to%20ISI%3E://WOS:A1985AGA6800016.

Oliveri, P., D. M. Carrick, and E. H. Davidson (2002). “A regulatory gene network that directs micromere specification in the sea urchin embryo”. In: *Developmental biology* 246.1, pp. 209–228.

Oliveri, P., Q. Tu, and E. H. Davidson (2008). “Global regulatory logic for specification of an embryonic cell lineage”. In: *Proc Natl Acad Sci U S A* 105.16, pp. 5955–5962. doi: 10.1073/pnas.0711220105. url: <http://www.ncbi.nlm.nih.gov/pubmed/18413610>.

Oliveri, P., K. D. Walton, et al. (2006). “Repression of mesodermal fate by foxa, a key endoderm regulator of the sea urchin embryo.” In: *Development* 133.21, pp. 4173–81. issn: 0950-1991. doi: 10.1242/dev.02577. url: <http://www.ncbi.nlm.nih.gov/pubmed/17038513>.

Peter, I. S. and E. H. Davidson (2010). “The endoderm gene regulatory network in sea urchin embryos up to mid-blastula stage.” In: *Developmental biology* 340.2, pp. 188–99. ISSN: 1095-564X. doi: 10.1016/j.ydbio.2009.10.037. URL: <http://www.ncbi.nlm.nih.gov/pubmed/19895806%20http://www.ncbi.nlm.nih.gov/articlerender.fcgi?artid=PMC3981691>.

- (2011a). “A gene regulatory network controlling the embryonic specification of endoderm”. In: *Nature* 474.7353, pp. 635–639. doi: 10.1038/nature10100. URL: <http://www.ncbi.nlm.nih.gov/pubmed/21623371>.
- (2011b). “Evolution of Gene Regulatory Networks Controlling Body Plan Development”. In: *Cell* 144.6, pp. 970–985. ISSN: 00928674. doi: 10.1016/j.cell.2011.02.017.
- (2015). *Genomic Control Process, Development and Evolution*. Oxford: Academic Press.

Peter, I. S., E. Faure, and E. H. Davidson (2012). “Predictive computation of genomic logic processing functions in embryonic development”. In: *Proc Natl Acad Sci U S A* 109.41, pp. 16434–16442. doi: 10.1073/pnas.1207852109. URL: <http://www.ncbi.nlm.nih.gov/pubmed/22927416>.

Ransick, A. and E. H. Davidson (2006). “cis-regulatory processing of Notch signaling input to the sea urchin glial cells missing gene during mesoderm specification.” In: *Developmental biology* 297.2, pp. 587–602. ISSN: 0012-1606. doi: 10.1016/j.ydbio.2006.05.037. URL: <http://www.ncbi.nlm.nih.gov/pubmed/16925988>.

- (2012). “Cis-regulatory logic driving glial cells missing: self-sustaining circuitry in later embryogenesis”. In: *Developmental biology* 364.2, pp. 259–267.

Ransick, A., J. P. Rast, et al. (2002). “New early zygotic regulators expressed in endomesoderm of sea urchin embryos discovered by differential array hybridization.” In: *Developmental biology* 246.1, pp. 132–47. ISSN: 0012-1606. doi: 10.1006/dbio.2002.0607. URL: <http://www.ncbi.nlm.nih.gov/pubmed/12027439>.

Revilla-i-Domingo, R., P. Oliveri, and E. H. Davidson (2007). “A missing link in the sea urchin embryo gene regulatory network: hesC and the double-negative specification of micromeres”. In: *Proc Natl Acad Sci U S A* 104.30, pp. 12383–12388. doi: 10.1073/pnas.0705324104. URL: <http://www.ncbi.nlm.nih.gov/pubmed/17636127>.

Schroeder, T. E. (1981). “Development of a ‘primitive’ sea urchin (*Eucidaris tribuloides*): irregularities in the hyaline layer, micromeres, and primary mesenchyme”. In: *Biological Bulletin* 161.1, pp. 141–151.

Sethi, A. J. et al. (2012). “Sequential signaling crosstalk regulates endomesoderm segregation in sea urchin embryos”. In: *Science* 335.6068, pp. 590–593.

Smith, A. B. et al. (2006). "Testing the molecular clock: molecular and paleontological estimates of divergence times in the Echinoidea (Echinodermata)." In: *Molecular biology and evolution* 23.10, pp. 1832–51. ISSN: 0737-4038. DOI: [10.1093/molbev/msl039](https://doi.org/10.1093/molbev/msl039). URL: <http://www.ncbi.nlm.nih.gov/pubmed/16777927>.

Smith, J. and E. H. Davidson (2009). "Regulative recovery in the sea urchin embryo and the stabilizing role of fail-safe gene network wiring". English. In: *Proceedings of the National Academy of Sciences of the United States of America* 106.43, pp. 18291–18296. DOI: [10.1073/pnas.0910007106](https://doi.org/10.1073/pnas.0910007106). URL: [%3CGo%20to%20ISI%3E://WOS:000271222500046](http://www.ncbi.nlm.nih.gov/pubmed/200271222500046).

Smith, J., E. Kraemer, et al. (2008). "A spatially dynamic cohort of regulatory genes in the endomesodermal gene network of the sea urchin embryo". In: *Dev Biol* 313.2, pp. 863–875. DOI: [10.1016/j.ydbio.2007.10.042](https://doi.org/10.1016/j.ydbio.2007.10.042). URL: <http://www.ncbi.nlm.nih.gov/pubmed/18061160>.

Thompson, J.R. et al. (2015). "Reorganization of sea urchin gene regulatory networks at least 268 million years ago as revealed by oldest fossil cidaroid echinoid". English. In: *Scientific Reports* 5. DOI: [ARTN1554110.1038/srep15541](https://doi.org/10.1038/srep15541). URL: [%3CGo%20to%20ISI%3E://WOS:000363122100003](http://www.ncbi.nlm.nih.gov/pubmed/263122100003).

Tsuchimoto, J. and M. Yamaguchi (2014). "Hox expression in the direct-type developing sand dollar *Peronella japonica*". In: *Developmental Dynamics* 243.8, pp. 1020–1029.

Urben, S., C. Nislow, and M. Spiegel (1988). "The origin of skeleton forming cells in the sea urchin embryo". In: *Roux's archives of developmental biology* 197.8, pp. 447–456. DOI: [10.1007/BF00385678](https://doi.org/10.1007/BF00385678). URL: <http://link.springer.com/article/10.1007/BF00385678>.

Wilson, K. A., M. E. Andrews, and R. A. Raff (2005). "Dissociation of expression patterns of homeodomain transcription factors in the evolution of developmental mode in the sea urchins *Heliocidaris tuberculata* and *H. erythrogramma*." In: *Evolution & development* 7.5, pp. 401–15. ISSN: 1520-541X. DOI: [10.1111/j.1525-142X.2005.05045.x](https://doi.org/10.1111/j.1525-142X.2005.05045.x). URL: <http://www.ncbi.nlm.nih.gov/pubmed/16174034>.

Wray, G. A. and D. R. McClay (1988). "The origin of spicule-forming cells in a 'primitive' sea urchin (*Eucidaris tribuloides*) which appears to lack primary mesenchyme cells". In: *Development* 103.2, pp. 305–315. URL: <http://www.ncbi.nlm.nih.gov/pubmed/3066611>.

Yamazaki, A., Y. Kidachi, and T. Minokawa (2012). ""Micromere" formation and expression of endomesoderm regulatory genes during embryogenesis of the primitive echinoid *Prionocidaris baculosa*." In: *Development, growth & differentiation* 54.5, pp. 566–78. ISSN: 1440-169X. DOI: [10.1111/j.1440-169X.2012.01360.x](https://doi.org/10.1111/j.1440-169X.2012.01360.x). URL: <http://www.ncbi.nlm.nih.gov/pubmed/22680788>.

EVOLUTIONARY REWIRING OF GENE REGULATORY
NETWORK LINKAGES AT DIVERGENCE OF THE ECHINOID
SUBCLASSES

Erkenbrack, E. M. and E. H. Davidson (2015). “Evolutionary rewiring of gene regulatory network linkages at divergence of the echinoid subclasses”. In: *Proc Natl Acad Sci U S A* 112.30, E4075–84. ISSN: 1091-6490 (Electronic) 0027-8424 (Linking). doi: 10.1073/pnas.1509845112. URL: <http://www.ncbi.nlm.nih.gov/pubmed/26170318>.

3.1 Abstract

Evolution of animal body plans occurs with changes in the encoded genomic programs that direct development, by alterations in the structure of encoded developmental gene regulatory networks (GRNs). However, study of this most fundamental of evolutionary processes requires experimentally tractable, phylogenetically divergent organisms that differ morphologically while belonging to the same monophyletic clade, plus knowledge of the relevant GRNs operating in at least one of the species. These conditions are met in the divergent embryogenesis of the two extant, morphologically distinct, echinoid (sea urchin) subclasses, Euechinoidea and Cidaroidea, which diverged from a common late Paleozoic ancestor. Here we focus on striking differences in the mode of embryonic skeletogenesis in a euechinoid, the well-known model *Strongylocentrotus purpuratus* vs. the cidaroid *E. tribuloides*. At the level of descriptive embryology, skeletogenesis in *S. purpuratus* and *E. tribuloides* have long been known to occur by distinct means. The complete GRN controlling this process is known for *S. purpuratus*. We carried out targeted functional analyses on *E. tribuloides* skeletogenesis to identify the presence, or demonstrate the absence, of specific regulatory linkages and subcircuits key to the operation of the *S. purpuratus* skeletogenic GRN. Remarkably, most of the canonical design features of the *S. purpuratus* skeletogenic GRN that we examined are either missing or operate differently in *E. tribuloides*. This work directly implies a dramatic reorganization of genomic regulatory circuitry concomitant with the divergence of the euechinoids, which began before the end-Permian extinction.

3.2 Significance

This work provides direct evidence of evolutionary rewiring of gene regulatory circuitry accompanying divergence of two subclasses of echinoderm: the cidaroid and euechinoid sea urchins. These forms descend from a known common Paleozoic ancestor, and their embryos develop differently, offering an opportunity to probe the basic evolutionary process by which clade divergence occurs at the gene regulatory network (GRN) level. We carried out a systematic analysis of the use of a set of particular genes participating in embryonic skeletogenic cell specification, building on an established euechinoid developmental GRN. This study revealed that the well-known and elegantly configured regulatory circuitry that underlies skeletogenic specification in modern sea urchins is largely a novel evolutionary invention. The results dramatically display extensive regulatory changes in a specific developmental GRN, underlying an incidence of cladistic divergence at the subclass level.

3.3 Introduction

The mechanisms responsible for evolutionary divergence of animal body plans, as so extensively documented in the Phanerozoic fossil record, lie in alterations of the encoded genomic regulatory programs that direct development. This has long been evident *a priori* (Britten and Davidson, 1971), and overwhelmingly, accumulating current evidence precludes any other general explanation (Peter and Davidson, 2015). But it still remains a challenge to adduce specific examples in which evolutionary rewiring of developmental GRNs can be seen to account for observed differences in morphogenetic processes that distinguish descendants of a common ancestor. Knowledge of developmental GRNs remains insufficiently extensive, and it is not trivial to locate useful examples, which require comparison within a monophyletic clade at just sufficient distance so that the diverged morphology is clearly the output of homologous networks of developmental regulatory gene interactions.

In recent years largely complete developmental GRN models have been solved that causally explain spatial specification in large domains of the embryo of the sea urchin *Strongylocentrotus purpuratus*, up to gastrulation (Peter and Davidson, 2011; Oliveri, Tu, and Davidson, 2008; Peter and Davidson, 2009). The explanatory power of these networks was demonstrated, in these pages, by a predictive computational analysis which showed that they contain sufficient information to regenerate the developmental course of events *in silico*, in automaton-like fashion (Peter, Faure, and Davidson, 2012). The present work stems from the almost irresistible opportunities that these same GRNs offer for approaching the basic evolutionary mechanisms of GRN divergence. Thus here we focus on a sea urchin clade that descends from a common ancestor with *S. purpuratus*, but in which embryonic structures are generated differently from those to which the known GRNs pertain.

Sea urchins (Class Echinoidea) are one of the five extant classes of echinoderms (the others are sea stars, brittle stars, sea cucumbers, and crinoids), and for over a century their embryos have served as major model systems for the study of early development; the initial high point was Boveri's 1902-1908 demonstration that a complete set of chromosomes is required in every nucleus of the sea urchin embryo for embryonic development to work properly (Laubichler and Davidson, 2008; Boveri, 1907). These and almost all subsequent experimental studies on sea urchin embryos, including all the recent GRN analyses cited, have been carried out on species belonging to one of the two subclasses of sea urchins surviving in the post-Paleozoic world, the Euechinoidea. Relatively little is known of any aspect of

developmental mechanism in their sister group, the subclass Cidaroidea. Although, as we briefly summarize below, the common Paleozoic ancestry of these echinoid subclasses is unequivocal, euechinoid and cidaroid sea urchins differ canonically in aspects of their body test plate organization, and in other adult skeletal structures that develop in the juvenile immediately after morphogenesis (Gao, J. R. Thompson, et al., 2015). During embryogenesis both euechinoid and cidaroid embryos produce geometrical systems of larval skeletal rods, displaying species-specific morphology. The skeleton provides the post-embryonic echinoid larva with internal structural support, and with mounting for the ciliated anterior larval arms that aid in motility and feeding. But a striking distinction between cidaroid and euechinoid modes of embryonic skeletogenesis early on drew the attention of embryologists, in that the embryonic skeletons arise very differently. In euechinoids four skeletogenic founder cells (large micromeres) segregate from all other fates near the very beginning of development, at 5th cleavage, and all descendants of these four vegetal pole cells exclusively execute skeletogenic specification and differentiation, according to a rigidly hierarchical, encoded network of regulatory gene interactions (Oliveri, Tu, and Davidson, 2008). In *S. purpuratus* embryos the cells of this lineage actively express skeletogenic genes during cleavage and blastulation (Oliveri, Tu, and Davidson, 2008). They divide exactly 3x during this period, and then well before gastrular invagination of the archenteron, they singly ingress into the blastocoel, divide one last time, and following internal ectodermal signal cues arrange themselves spatially within the blastocoel, form a syncytium, and progressively construct the skeleton during the remainder of embryogenesis (Nishita et al., 2000; Armstrong and McClay, 1994; McIntyre et al., 2014). But in cidaroid sea urchin embryos no precocious ingressions of a skeletogenic micromere lineage occurs before gastrulation (Wray and McClay, 1988; Schroeder, 1981). A variable number of micromeres is formed at the vegetal pole early in cleavage, but their ultimately skeletogenic descendants only emerge well after gastrulation is under way, together with a cloud of other mesodermal derivatives, by delamination from the tip of the mid-gastrular archenteron. As we see below, in cidaroid embryos specifically skeletogenic molecular functions are not transcriptionally executed in micromere descendants during cleavage. After emergence from the archenteron tip, the mesenchymal skeletogenic cells of cidaroid embryos migrate to the ectoderm, and late in embryogenesis proceed to construct the larval skeleton. We show here that the distinction in mode of developmental origin of the larval skeleton in euechinoid vs. cidaroid embryogenesis is anything but a trivial heterochrony: rather it is the morphological tip of an iceberg

of fundamentally distinct GRN architecture.

The extant echinoderm classes were established in the Ordovician if not earlier, and in major aspects of their body plans they have exemplified evolutionary stasis of definitive character suites for the ensuing 430 million years (Peter and Davidson, 2015; Bottjer et al., 2006). For echinoids as a whole these features include the globular test form, and developmental rearrangements of the coeloms resulting in a stacked configuration in the juvenile (Mooi and David, 1998; Peterson, Arenas-Mena, and Davidson, 2000). Within these constraints the fossil record displays a remarkable variety of Lower Paleozoic echinoid morphology. However, in the Upper Paleozoic there arose an echinoid branch that is clearly ancestral to both the modern euechinoid and cidaroid subclasses, known as the archaeocidaroid lineage (Kroh and A. B. Smith, 2010). A new high resolution paleontological analysis (J. Thompson et al., 2015) indicates that the last common archaeocidarid ancestor of both modern echinoid subclasses existed at the latest about 268 million years ago, i.e. at least 16 my prior to the Permian/Triassic extinction event which terminated the Paleozoic and many of its canonical denizens. Since the Triassic, a curious and perhaps profound difference in evolutionary flexibility distinguishes euechinoid and cidaroid subclasses. The euechinoids have radiated prodigiously, diversifying into nearly 1000 species of highly variegated morphology, while the cidaroids, comprised of only 100 species, have retained extremely conservative morphologies seemingly not far removed from their ancestral forms (Hopkins and A. B. Smith, 2015; A. B. Smith and Hollingworth, 1990). This fact generally biases the likelihood that novel features arising since divergence occurred in the euechinoid rather than the cidaroid lineage. Nonetheless, both subclasses display evolutionary innovations, i.e. subclass-specific, shared derived characters (apomorphies) with respect to the (fossilized) skeletal characters of their archaeocidarid ancestor, just as both display plesiomorphic morphological characters (Gao, J. R. Thompson, et al., 2015; A. B. Smith and Hollingworth, 1990; Gao and Davidson, 2008).

Our experimental object was to pry open the genomic program innovations that underlie observed phenomenological distinctions in embryonic skeletogenesis between euechinoids and cidaroids. To approach this problem systematically we carried out a large scale investigation of developmental regulatory gene use in the embryonic endomesoderm of the cidaroid *Eucidaris tribuloides* (results from comparing development of endoderm and non-skeletogenic mesoderm in these embryos are reported separately). *E. tribuloides* is the same species in which embryonic skeletogenic

morphogenesis had been studied earlier (Wray and McClay, 1988), and in which juvenile skeletogenesis was also investigated in our lab (Gao, J. R. Thompson, et al., 2015). Many relevant genes from the authenticated *S. purpuratus* skeletogenic specification GRN (Oliveri, Tu, and Davidson, 2008) were investigated, of which five essential participants are reported on in the following. These are the regulatory genes at the very top of the skeletogenic GRN hierarchy in *S. purpuratus*, the deployment of which our earlier work (Gao and Davidson, 2008) predicted might have been the locus of the evolutionary changes that mobilized the skeletogenic network in the micromere lineage of euechinoids. Experiments on another cidaroid species (Yamazaki, Kidachi, et al., 2014) have already cast doubt on the presence of one key component of this circuitry, the repressive paired box gene *pmar1*, which functions in a double negative transcriptional gate at the top of the skeletogenic GRN of *S. purpuratus* (Oliveri, Tu, and Davidson, 2008; Revilla-i-Domingo, Oliveri, and Davidson, 2007). As described below, we show here that the *pmar1* gene is indeed apparently not represented in the genome or in transcriptomes of *E. tribuloides*. However, this turns out to be but one probably derivative feature of a very generally different regulatory architecture. The complete structure of the *E. tribuloides* skeletogenic GRN is still a work in progress. The present study is more narrowly focused on evidence for evolutionary rewiring in this circuitry, which must have taken place at the separation of the surviving echinoid clades more than 260 million years ago.

3.4 Results

Spatial expression of five key genes of the euechinoid skeletogenic GRN in *Eucidaris tribuloides* embryos

Initial observations indicated a surprising lack of congruence between *S. purpuratus* and *E. tribuloides* in the spatial domains of expression of four regulatory genes (i.e., genes encoding transcription factors) and of an essential signaling gene. These genes are of particular interest because of the important roles they play in the skeletogenic specification GRN of *S. purpuratus*. Even though their embryonic behavior is completely different from those of the skeletogenic micromere precursors of euechinoids, it had been shown by Wray and McClay (Wray and McClay, 1988) that the micromeres appearing early in *E. tribuloides* cleavage do ultimately give rise to the post-gastrular skeletogenic cells of this embryo. Thus we could directly study expression of genes of the euechinoid GRN in known skeletogenic precursors of the cidaroid *E. tribuloides*. We note here that the behavior of early ingressing skeletogenic cells of *S. purpuratus* is typical of many euechinoids, as

supported by numerous observations on several different echinoid species, both at morphological and molecular levels.

Detailed spatial expression of none of the genes reported on here had been studied before in *E. tribuloides* embryos, and the whole mount *in situ* hybridizations of Figure 3.1 provide an important baseline for consideration of their skeletogenic (or anti-skeletogenic) functions. Each of the five genes was expressed differently in *E. tribuloides* than would have been expected from the echinoid examples.

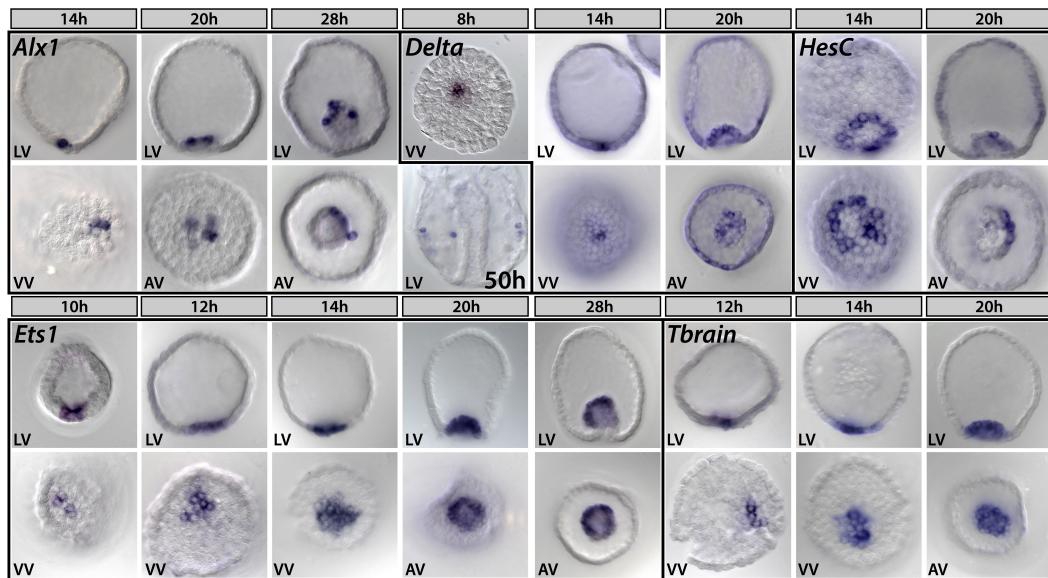


Figure 3.1: Spatial expression of selected skeletogenesis genes in *Eucidaris tribuloides*. *Alx1* expression is restricted to skeletogenic precursors throughout development; by 50 h *alx1*-positive cells are seen migrating to the vegetal lateral clusters where they will synthesize the larval skeleton. *Delta* is first expressed in micromere-descendants prior to hatching and is restricted to this lineage until late blastula stage (20 h), where it is expressed in scattered cells at the tip of the archenteron. Zygotic expression of *hesC* begins in a ring of cells that abut the micromere-descendants at the vegetal pole; by early gastrula it is asymmetrically expressed in the archenteron (20 h AV). Expression of *ets1* begins in a few cells at the vegetal pole prior to hatching and expands to demarcate the whole mesodermal domain, eventually occupying the entire mesodermal bulb by early gastrula stage. Onset of zygotic *tbrain* expression occurs at the vegetal pole shortly after that of *ets1*, to which it exhibits very similar spatial expression. h, hours post fertilization; AV, tip of archenteron/apical view; LV, lateral view; VV, vegetal view.

alx1

The *alx1* gene is a primary driver of skeletogenic specification and differentiation in sea urchin embryo and adult development, and is a member of a family of

homeodomain genes also utilized in vertebrate skeletogenesis (Gao and Davidson, 2008; Ettensohn et al., 2003; Rafiq, Cheers, and Ettensohn, 2012; Lyons et al., 2014). In euechinoids *alx1* is one of the initial set of positively acting transcriptional regulators that set up the skeletogenic regulatory state, and it is transcriptionally activated by a double negative derepression subcircuit Revilla-i-Domingo, Oliveri, and Davidson, 2007; Damle and Davidson, 2011, immediately upon segregation of the skeletogenic micromere founder cells early in cleavage (Ettensohn et al., 2003). In *S. purpuratus* this gene then participates in direct cross-regulation of the succeeding tiers of the skeletogenic specification GRN. But these features of *alx1* regulation are not likely to exist in *E. tribuloides*. Thus in *E. tribuloides* *alx1* is not even transcribed significantly until 4-6 hours after the earliest micromere-specific genes are activated (*delta* and *ets1*; Figure 3.1, 3.2), although *alx1* expression is thereafter confined to micromeres and their skeletogenic descendants. Expression of the *E. tribuloides* *alx1* gene is however ultimately required for postgastrular skeleton formation to occur (Figure 3.3), just as it is required for post-embryonic skeletogenesis in both sea urchins and sea stars (Gao and Davidson, 2008).

delta

The euechinoid *delta* gene is also an immediate transcriptional activation target of the *S. purpuratus* micromere double negative gate subcircuit, and it continues to be expressed in this lineage until blastula stage when its expression is extinguished there and instead appears in the surrounding non-skeletogenic mesoderm cells (Revilla-i-Domingo, Oliveri, and Davidson, 2007; Revilla-i-Domingo, Minokawa, and Davidson, 2004; J. Smith, Kraemer, et al., 2008). In *E. tribuloides* *delta* expression occurs early in micromeres, 4-6 hours before that of *alx1*, suggesting a primary function unconnected to later skeletogenic specification (Figure 3.1). Expression of *E. tribuloides* *delta* does not become non-skeletogenic until much later, when a complex pattern of ectodermal expression is installed (Figure 3.4).

hesC

The most dramatically different functional implications revealed by Figure 3.1 are to be seen the expression in *E. tribuloides* of the *hesC* gene. In the *S. purpuratus* GRN, HesC is the repressor controlling the initial skeletogenic regulatory state (i.e., including expression of *alx1*, *delta*, and *ets1*), and this state is controlled spatially by the transcriptional activity of the *hesC* gene. In the *S. purpuratus* GRN the skeletogenic regulatory state is installed in micromeres by specific repression of the

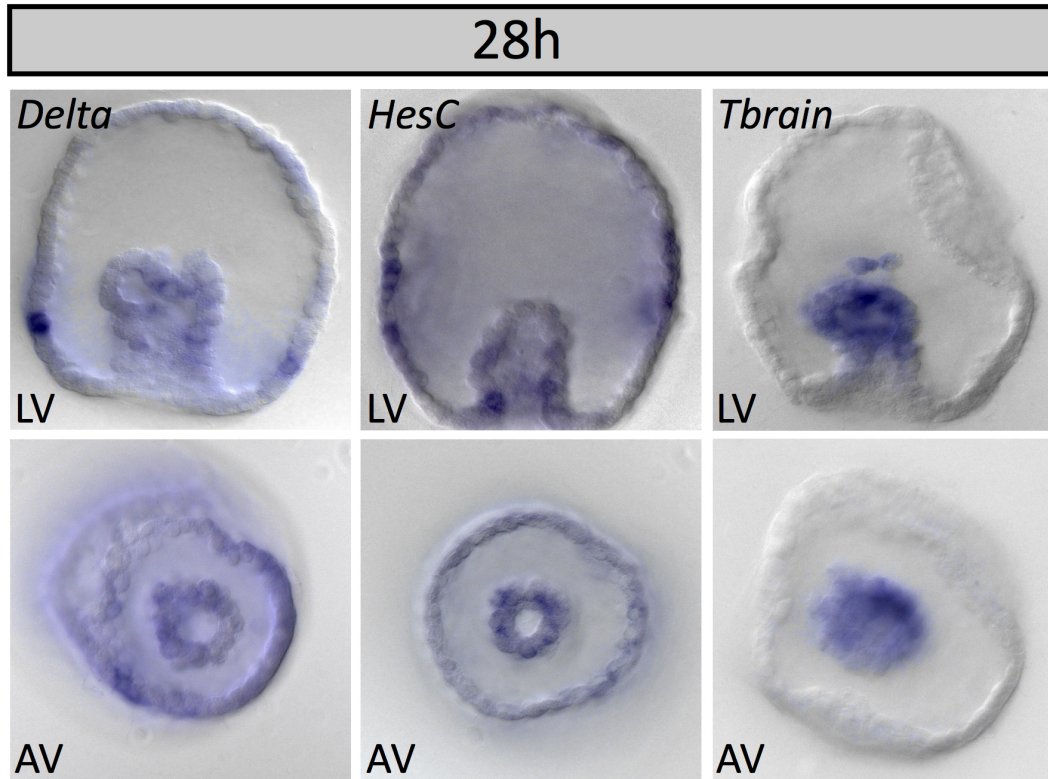


Figure 3.2: Spatial expression of *delta*, *hesC* and *tbrain* at early gastrula stage in *Eucidaris tribuloides*. *Delta* is observed in a few mesodermal cells at this stage and begins to be expressed in a scattered pattern in the ectoderm. *HesC* is expressed in the non-skeletogenic mesoderm and endoderm, is absent from the ecto-endodermal boundary, and is expressed in a diffuse, non-specific pattern in the ectoderm. *Tbrain* expression is seen throughout the mesoderm and here can be seen in the ingressing spicule precursor cells at the tip of the archenteron.

repressive *hesC* gene, executed by the micromere-specific repressor, Pmar1, thus opening the double negative gate subcircuit. *HesC* is transcriptionally expressed throughout the whole *S. purpuratus* embryo, except where this gene is turned off by *pmar1* expression in the micromeres; thus in *S. purpuratus* *hesC* transcription and skeletogenic function are Boolean exclusives (Oliveri, Tu, and Davidson, 2008; Revilla-i-Domingo, Oliveri, and Davidson, 2007; Oliveri, Davidson, and McClay, 2003). But, as Figure 3.1 shows, in *E. tribuloides*, *hesC* is expressed in micromeres at the same time as are *ets1* and *delta*, in direct contrast to its double negative gate function in *S. purpuratus*. Furthermore, the *hesC* gene is never vigorously expressed throughout the whole *E. tribuloides* embryo as it is in *S. purpuratus*, and instead is strongly expressed (by blastula stage) only in the immediately surrounding non-skeletogenic mesoderm, as we see in more detail below.

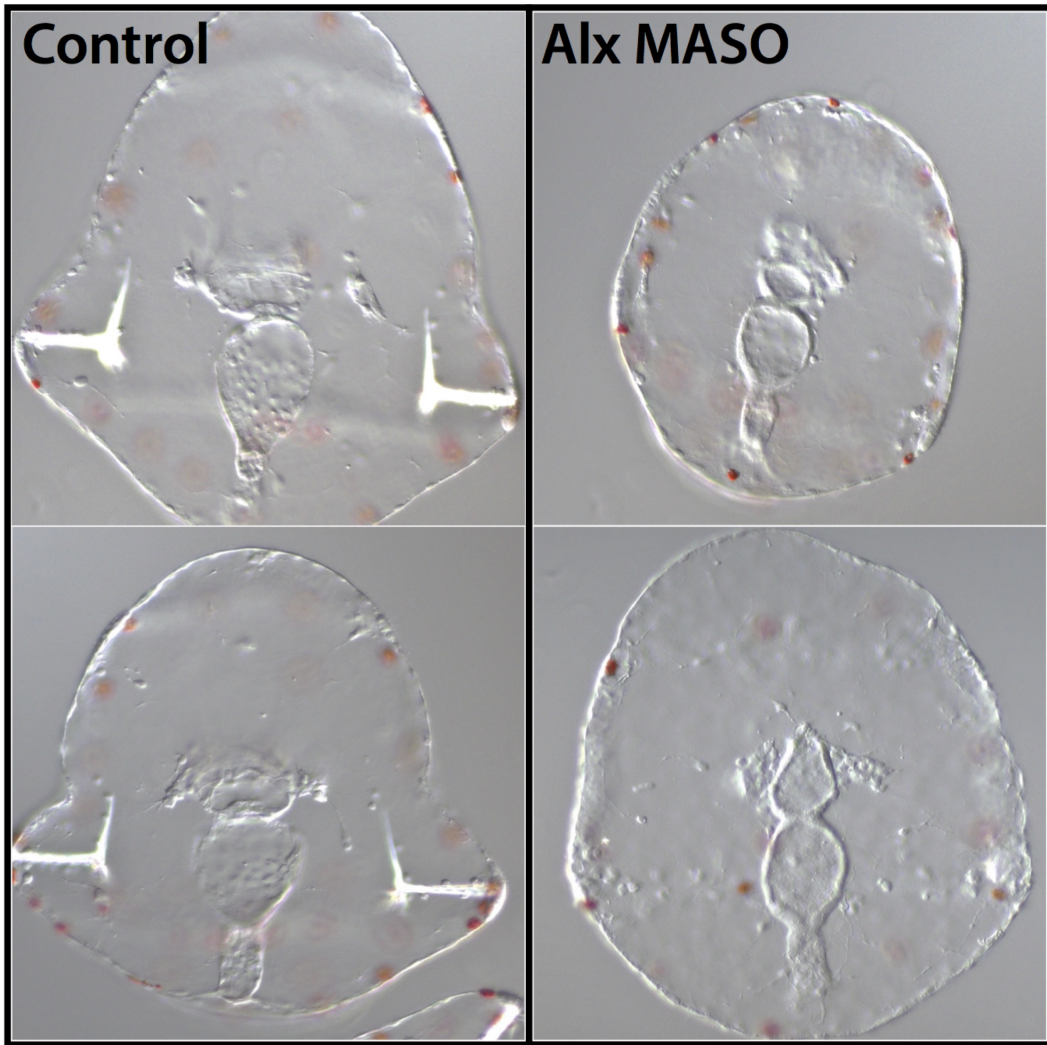


Figure 3.3: Morpholino perturbation of Alx1 disrupts skeletogenesis in *Eucidaris tribuloides* larvae. Zygotes were injected with *alx1* morpholino, cultured for five days, and scored for the presence or absence of larval skeletal rods (11 of 16 lacked skeleton). Uninjected control groups were cultured and scored simultaneously (0 of 20 lacked skeleton).

ets1

Zygotic transcription of *ets1* is turned on as the double negative gate is unlocked in early cleavage in the *S. purpuratus* GRN, and thereafter this gene provides powerful positive inputs to both regulatory and effector genes in skeletogenic specification, far into development (Rafiq, Cheers, and Ettensohn, 2012; Damle and Davidson, 2011; Revilla-i-Domingo, Minokawa, and Davidson, 2004). In *S. purpuratus* there is also a prevalent store of maternal *ets1* mRNA, but this is entirely missing in *E. tribuloides*. As in *S. purpuratus* the *ets1* gene is activated as early in the micromeres

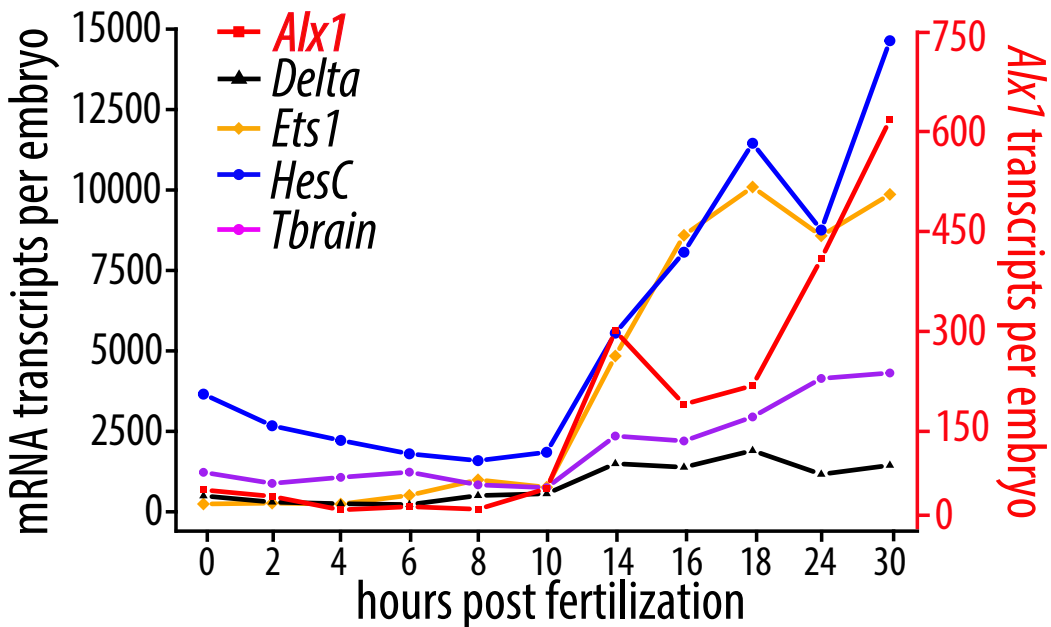


Figure 3.4: Timecourse of mRNA expression of *Strongylocentrotus purpuratus* double-negative gate genes in this study. The left ordinate shows the estimated number of transcripts per embryo as determined by quantitative PCR for *delta*, *ets1*, *hesC*, and *tbrain*. The right ordinate (shown in red) is estimated transcripts per embryo for *alx1* only. The x-axis shows the timepoints in development assayed, starting at fertilized egg (0 hpf) and ending when skeletogenic mesenchyme ingresses at early gastrula stage (30 hpf). A protocol for estimating the number of transcripts per embryo is described in Materials and Methods.

as is the *delta* gene, but strikingly, by 12-14 hours (blastula stage), *E. tribuloides ets1* expression spreads to the non-skeletogenic mesoderm, and is then extinguished in the micromere descendants altogether (Figure 3.1). Thus neither is this gene likely to function similarly in the cidaroid as in the euechinoid skeletogenic lineage.

tbrain

Finally, the *tbrain* gene, which is required for and coopted to skeletogenic function in euechinoids (Gao and Davidson, 2008; Revilla-i-Domingo, Oliveri, and Davidson, 2007; Wahl et al., 2009; Minemura, Yamaguchi, and Minokawa, 2009), is again expressed very differently in *E. tribuloides*. Though the *tbrain* gene is first activated in the micromeres, its expression quickly spreads to the entire non-skeletogenic mesodermal domain, where by double *in situ* hybridization it can be seen to totally overlap that of *ets1* (evidence not shown), and in direct contrast to *S. purpuratus*, there is no evidence from its expression pattern that it ever plays a skeletogenic role.

Descriptive patterns of gene expression can never demonstrate the existence of given regulatory linkages, but they can certainly exclude their existence. Figure 3.1 alone implies a very different cidaroid regulatory configuration than used in euechinoid skeletogenic specification.

Experimental tests for specific linkages of the euechinoid skeletogenic GRN

We now set about challenging *E. tribuloides* regulatory linkages among the above and additional genes with the specific intent of determining whether these linkages could be the same, or must be exclusive, of the linkages among these same genes in the *S. purpuratus* skeletogenic GRN.

Test for global confinement to skeletogenic lineage by HesC repression, of *alx1*, *tbrain*, and *ets1* transcription

A dramatic demonstration of the function of the skeletogenic double negative gate in *S. purpuratus* is afforded by either over-expression of the repressor Pmar1 or introduction into the egg of *hesC* morpholino (MASO), either of which results in global transformation of embryonic cells to skeletogenic fate, and in global expression of the double negative target genes delta, *alx1* and *tbrain* (Oliveri, Tu, and Davidson, 2008; Revilla-i-Domingo, Oliveri, and Davidson, 2007; Damle and Davidson, 2011; Oliveri, Davidson, and McClay, 2003; Wahl et al., 2009). In Figure 3.5A and 3.5B, left column, we see the spatial effect of *hesC* MASO on *alx1* expression in *E. tribuloides* embryos. At blastula stage (Figure 3.5B) expression of *alx1* indeed expands but (reasonably enough) only to the extent of significant *hesC* expression, which as evident from Figure 3.1 is confined to the immediately surrounding non-skeletogenic mesoderm. At gastrula stage (Figure 3.5A) *alx1* expression expands to the immediately surrounding archenteron tip (mesoderm) cells. Thus while HesC does repress *alx1*, it is not responsible for preventing *alx1* expression throughout the embryo as in *S. purpuratus*, but only in the non-skeletogenic mesoderm. In Figure 3.5B the effects of *hesC* MASO on spatial expression of *tbrain* and *ets1* are shown. Since Figure 3.1 demonstrates the overlap of expression domains of *hesC* expression with those of *ets1* and *tbrain* genes, they are unlikely to be subject to HesC repression, and indeed *hesC* MASO has no effect on their spatial expression, again in direct contrast with the case in *S. purpuratus*. In Figure 3.5C these results are substantiated quantitatively in a qPCR experiment, which shows that the only significant effects (i.e. $>1.5\times$ cycle number change, a log2 metric) are the modest increase in *alx1* expression seen spatially above, and in

hesC transcript level itself; this gene apparently depresses its own transcription.

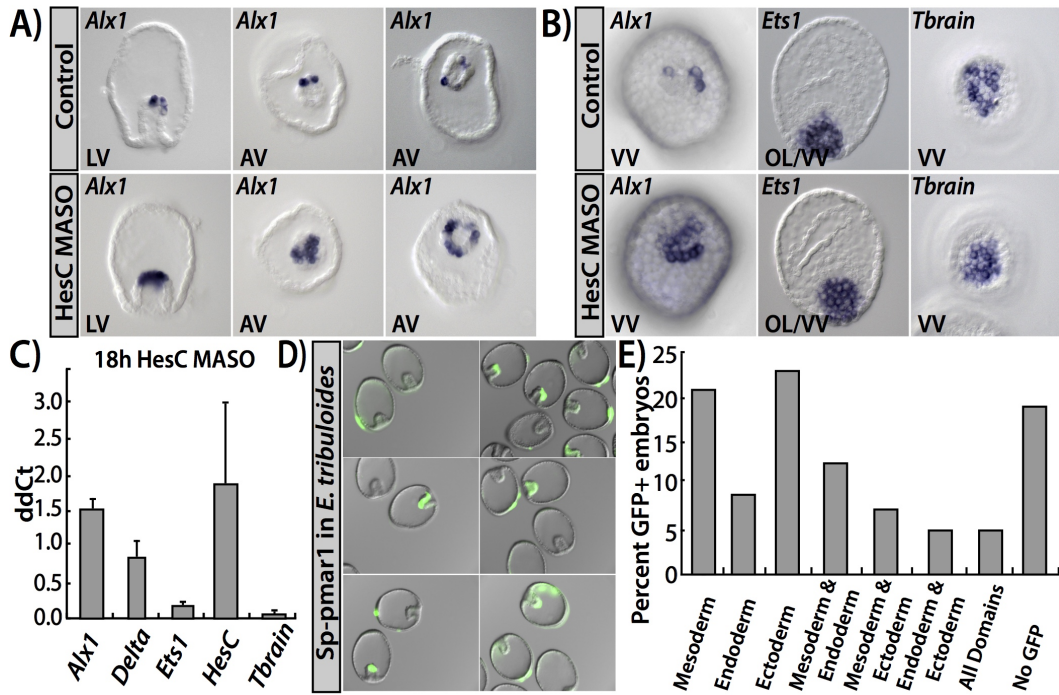


Figure 3.5: Functional tests for presence in *Eucidaris tribuloides* of known regulatory linkages of the *Strongylocentrotus purpuratus* skeletogenic GRN. **(A-C)** Test for global *HesC* repression of skeletogenic regulatory state. **(A)** 28 h embryos injected with *hesC* morpholino exhibit an expanded domain of the skeletogenic lineage marker *alx1*. **(B)** 20 h embryos injected with *hesC* morpholino showing no global expression of dominant-negative gate genes. *Alx1* expands locally only, while *ets1* and *tbrain* are unaffected. **(C)** Quantitative effects of *hesC* morpholino on mRNA abundance at 18 h on expression of skeletogenic genes *alx1*, *delta*, *ets1*, *hesc*, and *tbrain*. *Alx1* and *hesc* mRNAs are significantly upregulated. The difference in cycle number (ddCt) with respect to an uninjected control group is shown on the ordinate. Error bars represent the standard deviation of two independent experiments.

These experiments preclude the global control of skeletogenesis by *hesC* repression in *E. tribuloides*, which is its prominent role in the *S. purpuratus* skeletogenic GRN. They also preclude any control in *E. tribuloides* of either *ets1* or *tbrain* by *hesC* repression. We have already seen that neither of these genes is likely to have anything to do with skeletogenesis after cleavage in *E. tribuloides* in any case.

Lack of evidence for existence of the *pmar1* gene in *Eucidaris tribuloides*

A genomic sequence has been obtained for *E. tribuloides*, though it is not annotated and has been assembled only to contigs of several kb N50. In addition a mixed embryonic transcriptome has been sequenced and analyzed (data from Hu-

man Genome Sequence Center). Despite their incomplete nature, these genomics resources sufficed for identification of >95% of a large set of *S. purpuratus* protein coding genes. But we were unable to find any sequence whatsoever in the *E. tribuloides* databases indicating the existence of genes resembling *S. purpuratus pmar1*. The *S. purpuratus* genome includes at least six clustered paralogues of this divergent paired box gene, and two of these genes, for which *cis*-regulatory evidence has also been obtained, are directly similar to the *pmar1* transcripts that we functionally characterized earlier (Oliveri, Davidson, and McClay, 2003; J. Smith and Davidson, 2009). Since failure to identify *pmar1* genes in the *E. tribuloides* genome or embryo transcriptomes is not an entirely convincing result, we embarked on an additional, though indirect approach, and asked whether the regulatory state of *E. tribuloides* micromeres (or indeed of any polar early cleavage *E. tribuloides* cells) would support transcription of an *S. purpuratus pmar1* gene. An accurately expressing, recombinered *pmar1* BAC construct bearing a knocked-in GFP marker had earlier been constructed and authenticated in gene transfer experiments (J. Smith and Davidson, 2009). It responds at known *cis*-regulatory sites to the two transcription factors that in *S. purpuratus* constitute the localized input responsible for endogenous *pmar1* expression as soon as micromeres form (Oliveri, Tu, and Davidson, 2008). These are a Tcf input, which utilizes for its spatial activation function maternally localized β -catenin (Weitzel et al., 2004), and Otx α transcription factor, which is also transiently localized to the micromeres in *S. purpuratus* (Chuang et al., 1996). But when this *pmar1* reporter construct was injected into *E. tribuloides* eggs no localized expression could be seen, and instead the construct expressed more or less equivalently in all domains of the embryo. This result is shown in Figures 3.5D and 3.5E. Additionally we checked whether a localized Otx factor might be used for early control of the skeletogenic regulatory state in *E. tribuloides*, even if this effect were not mediated by a *pmar1* gene (or a recognizable *pmar1* gene). A sequence encoding the maternal Otx factor was truncated to produce a dominant negative form, which was shown to be functional by its effect on endoderm genes when the mRNA was injected into *E. tribuloides* eggs (data presented elsewhere). However, injection of this mRNA into *E. tribuloides* eggs had no effect whatsoever on expression levels of any of the micromere genes, such as *alx1* or *delta*, as assessed by qPCR.

The minimum conclusion from these experiments is that the combinatorial localization system that in *S. purpuratus* provides the β -catenin/Tcf and Otx α transcriptional inputs causing micromere *pmar1* expression does not exist in *E. tribuloides*. Nor in all probability does *pmar1*, the lynchpin upstream gene of the double negative

gate, even exist in the *E. tribuloides* genome. Taken together with the foregoing *hesC* MASO experiments, it can be concluded that the double negative gate circuitry of the euechinoid micromere lineage does not control the skeletogenic regulatory state in *E. tribuloides*. Absence of this circuit feature was also inferred for another cidaroid embryo (Yamazaki, Kidachi, et al., 2014).

What does specify the ultimate skeletogenic fate of micromeres in *Eucidaris tribuloides*?

The *alx1* gene is clearly not an initial regulatory mediator of skeletogenic specification in *E. tribuloides* micromeres as it is in the *S. purpuratus* skeletogenic micromere GRN, since as we show here it is not even transcribed as early as is the initial set of micromere-specific genes. However, *alx1* is ultimately just as clearly a canonical driver of later skeletogenic differentiation in *E. tribuloides* (Figure 3.3), as it is also in euechinoids (Ettensohn et al., 2003). Thus we can use its expression as a faithful indicator of skeletogenic fate, unlike genes such as *tbrain* and *ets1* which though expressed early in *E. tribuloides* micromeres apparently end up having little to do with skeletogenesis.

A not entirely unexpected clue as to the nature of the initial molecular input specifying skeletogenic fate devolves from the experiments in Figure 3.6A, though they raise as well answer a mechanistic question. As shown there, when mRNA encoding GFP-tagged β -catenin is injected into *E. tribuloides* eggs, it is ubiquitously translated, but then over the next few cleavages this protein is asymmetrically degraded (Stamos and Weis, 2013), leaving it concentrated, dramatically and ex-clusively, in the micromeres. This negative cytoplasmic localization system is mediated by the β -catenin protein sequence per se, and the behavior of the tagged construct perfectly reflects the early highly localized retention of native β -catenin in euechinoid sea urchin micromeres, as observed immunocyto logically (Logan et al., 1999) (we cannot of course be certain whether the kinetics of asymmetric clearance in *E. tribuloides* are affected by the GFP tag). The responsible localiza-tion system does not depend on asymmetric Wnt signaling in the cleavage stage embryo: thus the same localization of GFP-tagged β -catenin occurs in the presence of a potent antagonist of all canonical and non-canonical Wnt signaling, “C59” (Figure 3.6B). C59 works by inhibiting Porcupine-dependent Wnt mobilization and secretion, and is both effective and specific in sea urchin embryos (Cui et al., 2014); detailed evidence for sea urchin embryos and references to its specificity and mode of action in other bilaterian systems are to be found in this cited work. It follows

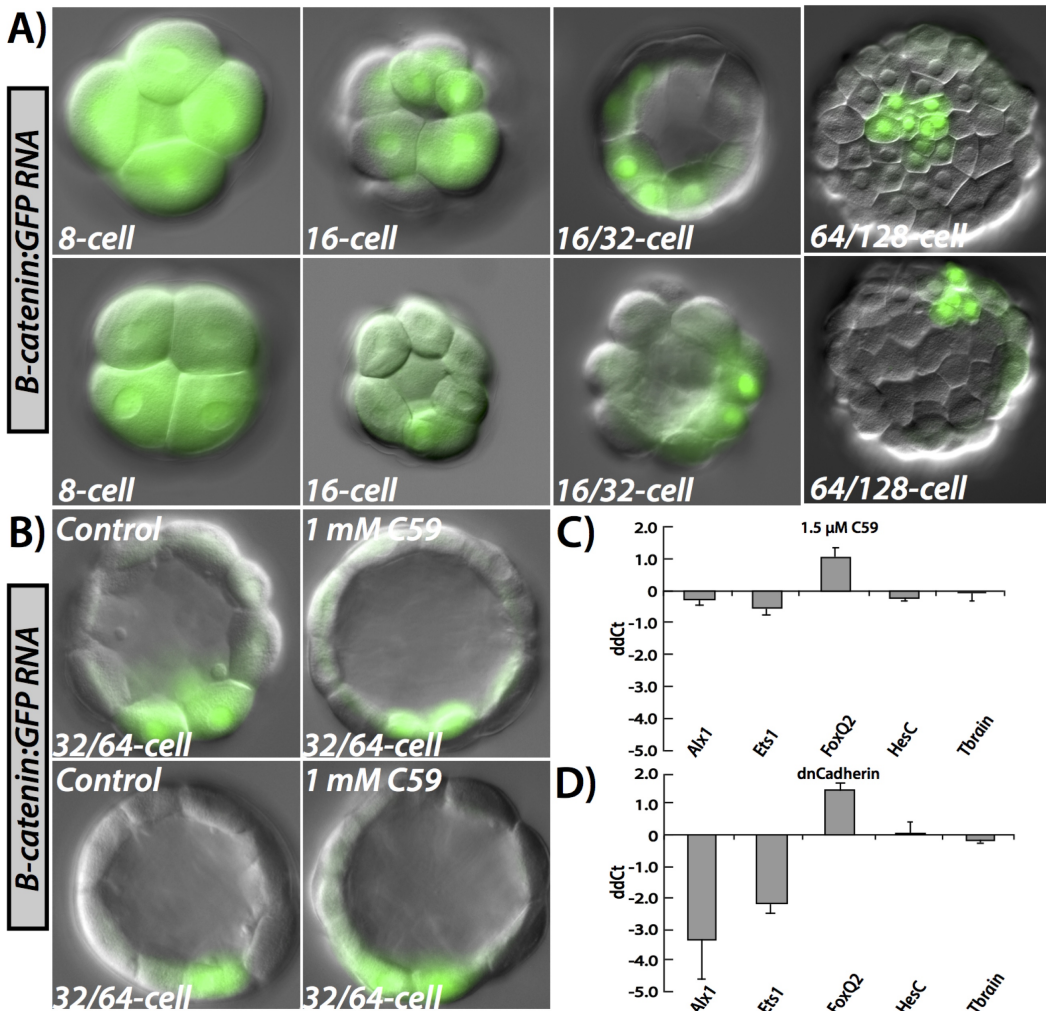


Figure 3.6: Requirement for a Wnt-signal independent β -catenin polar localization system. **(A)** Early cleavage *E. tribuloides* embryos demonstrating progressive spatial restriction of an injected β -catenin:GFP mRNA to the vegetal pole. Before 16-cell stage, this mRNA is found in all cells of the embryo. At fourth cleavage, the mRNA comes to be restricted to micromere- and micromere-abutting nuclei at the vegetal pole. Several cleavages later, it is only found in a few cells at the vegetal pole, the only likely identity of which is the micromeres since they are disposed exactly as are the cells expressing micromere genes (Figure 3.1). **(B)** Early cleavage embryos treated with C59, a reagent inhibiting porcupine-dependent Wnt signaling. C59 does not effect spatial restriction of β -catenin:GFP mRNA. **(C)** Quantitative effects, measured by qPCR, of treatment with 1.5 μ M C59 on relevant genes in 15 h *E. tribuloides* embryos. The difference in cycle number (ddCt) with respect to an uninjected control group is shown on the ordinate. Error bars represent the standard deviation of four independent experiments. **(D)** qPCR analysis of effects at 16 h in *E. tribuloides* embryos of injected dominant-negative *cadherin* mRNA. Error bars represent the standard deviation of two independent experiments.

from the results of experiments such as those reproduced in Figure 3.6A and 3.6B, that the β -catenin localization system of early *E. tribuloides* embryos is a property of the oocyte/egg cytoplasmic localization system, which falls into the category of anisotropic deposition of molecules of gene regulatory significance, a general feature of very early animal eggs (Peter and Davidson, 2015). The main import of Figure 3.6, however, is in the qPCR experiment of Figure 3.6D. Here we see that there is virtually no expression of *alx1* in micromeres (<8% of control values), if maternal β -catenin is sequestered by introduction of excess cadherin fragment, even though *alx1* transcription is a late cleavage event. Furthermore, these effects depend not at all on Wnt signaling even as late as 15h. Thus we are confronted with a missing link: β -catenin construct localization is complete in *E. tribuloides* by 7th cleavage (Figure 3.6A), and a significant time gap of several hours separates this event from activation of the *alx1* gene. The actual transcriptional mediator of *alx1* activation which responds to the localized β -catenin/Tcf cue therefore remains unknown. We cannot yet experimentally either exclude or support the possibility that the initial transducer of the β -catenin/Tcf input is the *cis*-regulatory system of the *E. tribuloides ets1* gene, which is activated hours earlier than *alx1* at about the right time. It may be significant that *cis*-regulatory analysis of *alx1* expression in Sp showed it to be subject initially to obligatory *ets1* activation (Damle and Davidson, 2011). This however remains to be demonstrated for *E. tribuloides alx1*.

The basal role of *hesC* in mesoderm specification

The relation between *hesC* and *delta* expression is a well-known constant of Notch signaling systems (Bailey and Posakony, 1995; Borggrefe and Oswald, 2009). Though there are countless variations, in simple form, the Delta ligand promotes Notch receptor activation with the consequence that the immediate transcriptional effector, Su(H), activates Notch signal transduction target genes. Among these are very often genes encoding bHLH repressors of the *hesC* family. The expression of these repressors enforces the distinction between Delta signal-sending and Notch signal-receiving genes by transcriptional exclusion of *delta* transcription in the Notch signal receiving cells. A beautiful illustration of this relationship can be seen in Figure 3.7A. As we report elsewhere, Notch signaling is taking place in the *E. tribuloides* embryo, but aside from the following negative relationship it plays no role whatsoever in specification or differentiation of skeletogenic cells per se.

Figure 3.7A shows that *hesC* expression, by this time in the surrounding non-skeletogenic mesodermal cells, is entirely dependent on Delta expression in the

immediately adjacent skeletogenic micromeres. That is, as in the canonical case, Notch signal transduction of the micromere Delta signal results in *hesc* expression in these non-skeletogenic mesodermal cells. Since, as shown above, *HesC* is the repressor excluding *alx1* expression from the non-skeletogenic mesoderm, if Delta expression is prevented, *alx1* expression spreads to the non-skeletogenic mesoderm, now involving twice as many cells (Figure 3.7B, 3.7C, and 3.7D). We perhaps see here the original role of micromere *delta* expression in sea urchin embryos, the spatial separation of skeletogenic from non-skeletogenic mesodermal specification.

3.5 Discussion

Our main and specific objective was to assess at least the minimum evolutionary divergence that took place within a thoroughly known developmental GRN, during the last major cladistic split in the evolution of the echinoids. This divergence occurred in an Upper Paleozoic time interval that is constrained in real time by the fossil record. One uncertainty that could affect dynamic interpretation of the results is the possibility that the differences we observe between the test species of this work, *S. purpuratus* and *E. tribuloides*, are actually in part the sum of changes that occurred only gradually, subsequently to the cladistic split from which emerged the modern euechinoid and cidaroid subclasses, that is, during the Mesozoic (Triassic, Jurassic, and Cretaceous). This would require, however, that the specific circuitry features we investigated vary among modern euechinoid orders that arose only gradually during the Mesozoic (18). But, though indeed incomplete, the evidence so far obviates this possibility. Thus a euechinoid belonging to a basal group (the Spangatoids) far removed from typical euechinoids such as *S. purpuratus*, also contains a *pmar1* gene and also zygotically expresses the *hesc* gene all over the embryo except for the skeletogenic micromeres (Yamazaki and Minokawa, 2015), exactly as in *S. purpuratus*, and in direct contrast to *E. tribuloides* (we refer here only to the key shared linkages of interest here, irrespective of the many and various other intra-euechinoid divergences that are also observed, but are irrelevant to skeletogenesis)(Yamazaki and Minokawa, 2015). Therefore key diagnostic features of the modern euechinoid (i.e., Sp) GRN are found in descendants of a euechinoid clade that arose anciently, perhaps at the beginning of the Jurassic (Kroh and A. B. Smith, 2010). This result leaves untested only the most basal orders of euechinoids, but since these clades emerged directly from the subclass split per se, they have less effect on the temporal argument pertaining to post divergence events. Similarly, on the cidaroid side, as noted above, the orders composing this Subclass have displayed remarkably

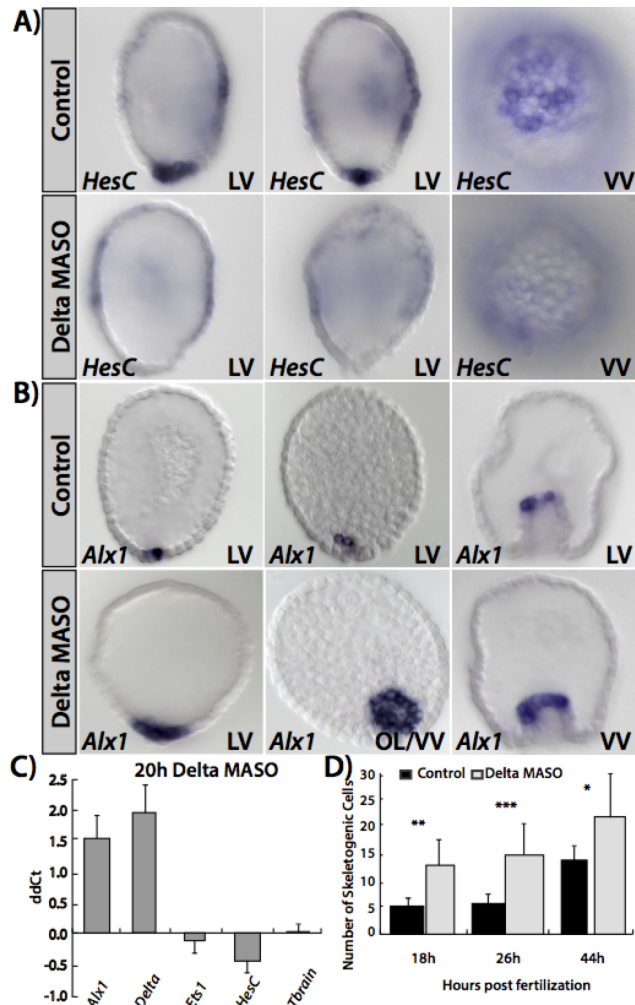


Figure 3.7: Spatial role of *hesC* in *E. tribuloides* embryos. **(A)** Effects of *delta* morpholino on *hesC* at the vegetal pole. In the presence of *delta* MASO, *hesC* expression is extinguished specifically at the vegetal pole, while its weak expression in certain regions of the ectoderm is unaffected. **(B)** Presence of *delta* MASO in *E. tribuloides* causes an expansion of the skeletogenic marker *alx1* to the surrounding non-skeletogenic mesoderm domain. **(C)** Quantitative effects of *delta* MASO measured by qPCR in 20 h embryos of *E. tribuloides*. *Delta* and *alx1* are significantly upregulated in the presence of *delta* MASO. *HesC* is barely affected due to its back-ground presence in the ectoderm. *Ets1* and *tbrain* are unaffected. The difference in cycle number (ddCt) with respect to an uninjected control group is shown on the ordinate. Error bars represent the standard deviation of three independent experiments. **(D)** Histogram shows the number of *alx1*-positive, i.e. skeletogenic, cells at three timepoints of *E. tribuloides* development in embryos injected with *delta* MASO versus uninjected controls. (18 h and 26 h, n=7, ** P < 0.001; 44 h, n=6, * P<0.05; all three as determined by Student's t-test). LV, lateral view; VV, vegetal view; OL/VV, oblique lateral/vegetal view.

invariant and conservative morphology ever since their appearance (Kroh and A. B. Smith, 2010). Consistent with this, *E. tribuloides* indeed shares with a different cidaroid the key property of lacking the double negative skeletogenic specification gate (Yamazaki, Kidachi, et al., 2014). Therefore, with the caveat of the yet unexamined most basal euechinoid orders, we can tentatively assume that we are here assaying genomic wiring features typical of the whole euechinoid subclass versus those typical of the whole cidaroid subclass, differences which indeed arose during the Upper Paleozoic at the cladistic split, differences which have ever since been inherited by descendants of the crown group ancestors of each branch.

GRN linkages of the embryonic *S. purpuratus* skeletogenic GRN shown here to be specifically absent from the embryonic *Eucidaris tribuloides* skeletogenic specification system

We can now list specific regulatory features encoded in *S. purpuratus cis*-regulatory sequence, that contribute decisively to the architecture of the *S. purpuratus* skeletogenic GRN (Peter, Faure, and Davidson, 2012), but that do not operate or operate differently in *E. tribuloides* (numbered references in the following all refer to *cis*-regulatory studies or other decisive studies in *S. purpuratus*). This provides a minimum but hard estimate of regulatory differences between the embryonic skeletogenic specification circuitries that have arisen since the last common ancestor from which these two genomes descend:

The *hesC cis*-regulatory system

First, in *S. purpuratus* the *hesC* gene responds to a powerful global embryonic activator (Revilla-i-Domingo, Oliveri, and Davidson, 2007), a feature totally lacking in *E. tribuloides*. In the latter *hesC* transcription is spatially controlled by Delta/Notch signaling from the micromeres, and hence is expressed only in mesoderm immediately adjacent to the micromeres (Delta/Notch signaling does still provide an additional *cis*-regulatory input to *hesC* in *S. purpuratus* (J. Smith and Davidson, 2009)). Second, in *S. purpuratus* the *hesC* gene is negatively controlled at the transcriptional level by *Pmar1* repression (Revilla-i-Domingo, Oliveri, and Davidson, 2007; J. Smith and Davidson, 2009). In *E. tribuloides* no *pmar1* gene or similarly functioning gene appears to exist.

The *tbrain* *cis*-regulatory system

First, in *S. purpuratus* this gene is negatively controlled by HesC and positively controlled by a ubiquitous activator (Wahl et al., 2009). Second, in *S. purpuratus* tbr is expressed in skeletogenic cells. In *E. tribuloides* none of these three inputs operates on tbr transcription.

The *ets1/2* *cis*-regulatory system

First, in *S. purpuratus* this gene is expressed maternally. Second, in later development it is expressed in differentiating skeletogenic cells (where it plays a major role in activating skeletogenic effector genes). But in *E. tribuloides* neither is true.

The *delta* *cis*-regulatory system

In *S. purpuratus* this gene is negatively controlled by HesC and positively controlled by Ets1 (Revilla-i-Domingo, Oliveri, and Davidson, 2007; Revilla-i-Domingo, Minokawa, and Davidson, 2004). In *E. tribuloides*, neither HesC nor Ets1 control *delta* expression.

The *pmarl* gene

This key gene of the *S. purpuratus* skeletogenic specification system is almost certainly absent altogether from the *E. tribuloides* genome.

The initial combinatorial *Otxα:Tcfβ*-catenin *cis*-regulatory micromere input

In *S. purpuratus* this combinatorial input is used to trigger *pmarl* transcription in micromeres (Oliveri, Tu, and Davidson, 2008; J. Smith and Davidson, 2009), while in *E. tribuloides* this combination is not functional in skeletogenic micromere specification by direct test, nor is *Otxα* utilized at all in skeletogenic specification.

In sum there are here 9 specific *cis*-regulatory inputs into genes operating in both species that function in *S. purpuratus* and are absent in *E. tribuloides*; plus a key gene missing in *E. tribuloides* (or small subfamily of genes); plus a key localized combinatorial *cis*-regulatory transcriptional input utilized in *S. purpuratus* by the gene absent in *E. tribuloides*. Assuming the euechinoid network is the evolutionary novelty (see below) each of these regulatory inputs represents appearance of a new GRN linkage that had to be encoded in *cis*-regulatory DNA of genes in the euechinoid lineage, a linkage that is lacking in the *cis*-regulatory sequences of the same genes in the cidaroid lineage. Perforce a minimum estimate, we see here something of the scale of genomic regulatory change required for architectural

network evolution, even in a small, confined GRN dedicated to specification of one cell lineage. Canonically, this type of evolutionary process is far removed from the single *cis*-regulatory module divergence easily accessed in studies of intra- and inter-specific adaptive variation (Peter and Davidson, 2015).

Plesiomorphy and polarity in the echinoid regulatory linkages

All of the changes enumerated above are gains of function with respect to the regulatory configuration of the *E. tribuloides* system, most of them multiple with respect to inputs per *cis*-regulatory module. While it is conventional to note that all such changes could also represent loss of function changes in the cidaroid lineage, meaning that the euechinoid regulatory system could equally be plesiomorphic, the evidence is no longer balanced: it is much more likely (just as intuitively assumed by past observers (Wray and McClay, 1988; Schroeder, 1981)) that the euechinoid skeletogenic GRN is the derived, novel character shared among descendants of the common euechinoid ancestor. A crucial argument that now comes into view is that the gains of function are sequentially and logically nested. That is, a given change requires particular sets of sequential changes, which imposes polarity on the process. For example, acquisition of *cis*-regulatory response to a global regulator in the *hesC* gene introduces the possibility of release of control of genes such as *alx1* from a strictly mesodermal activator to control by a general global activator, and of the delta gene from its strictly Notch dependent control also to that of a global activator. But such relaxations of domain-specific positive regulatory constraint in turn make it necessary to control micromere expression by negative rather than positive means, as executed by the euechinoid double negative gate. This is not to propose any specific pathway, but to point out that whatever the pathway, we are dealing here with an internally sequential logic train, rather than a series of independent changes which indeed individually might be considered equally likely to be gain as loss of function. A second argument concerns the cooption of the *tbrain* gene to skeletogenic function. This work shows that cooption to be a euechinoid novelty, since in *E. tribuloides* *tbrain* is not skeletogenic in function, and since we know from comparative studies that the plesiomorphic role of *tbrain* in echinoderms is not skeletogenic either (Minemura, Yamaguchi, and Minokawa, 2009). Therefore this cooption is a derived euechinoid character, and in *S. purpuratus*, *tbrain* also is driven by a ubiquitous activator (Wahl et al., 2009) so that its expression is made skeletogenesis-specific only by the double negative gate. Third, and similarly, control of *delta* gene expression is executed by the Notch response system in *E.*

tribuloides, whereas addition of a global positive control input in the *delta* gene in *S. purpuratus* (Revilla-i-Domingo, Oliveri, and Davidson, 2007) is therefore also a euechinoid derivation. We conclude that all the linkages of the skeletogenic control GRN that are found in *S. purpuratus* but are absent from *E. tribuloides* are probably shared derived characters of the euechinoids.

But if this is the case there must also remain plesiomorphic aspects of the skeletogenic program that would have been identified in this work as shared features present in both *E. tribuloides* and *S. purpuratus*. Indeed this logical expectation is fulfilled. The most prominent plesiomorphic GRN character is of course the dominant role of *alx1* as a driver of skeletogenic differentiation. The role of *alx1* is plesiomorphic for echinoderm skeletogenesis in general (Gao and Davidson, 2008; Ettensohn et al., 2003). A second major plesiomorphy in circuit wiring is indicated by the retention in both systems of negative spatial control of *alx1* by HesC repression. Similarly, a third plesiomorphic linkage is retention of negative *cis*-regulatory control of *delta* expression in *S. purpuratus* by HesC. This linkage, exactly like the HesC repression of *alx1*, is used in *S. purpuratus* for global control of expression, and in *E. tribuloides* for control of skeletogenic versus non-skeletogenic mesodermal expression.

Evolutionary assembly of the euechinoid skeletogenic GRN

Solution of the *E. tribuloides* skeletogenic GRN will facilitate a rational reconstruction of the evolutionary path by which the euechinoid skeletogenic micromere specification GRN might likely have assembled from its starting configuration. Only some general propositions can be offered at this juncture. It is clear from this work that multiple genomic regulatory changes had to be installed in the euechinoid lineage, whatever the exact pathway, and it is obvious that these cannot have entered the system all at once, nor would piecemeal alterations have had functional utility. However, in this conundrum originates the most powerful argument for the polarity of the evolutionary train of events. The presumably plesiomorphic cidaroid skeletogenesis system has a fundamental, key feature that would have allowed the accumulation of the novel GRN linkages without at the same time destroying its needed function of programming embryo/larval skeletogenesis. This feature is that development of the cidaroid micromere cell lineage is in functional terms essentially a dual process. In *E. tribuloides*, cleavage-stage micromere functions per se and skeletogenic functions per se are separate. The cleavage-stage micromeres do not execute skeletogenic specification, and instead their role is to emit Delta signals, which are used negatively in late cleavage to protect the nonskeletogenic

mesoderm from skeletogenic differentiation fate. Skeletogenic specification occurs only subsequently (in micromere descendants), when and after *alx1* is belatedly turned on. Skeletogenic differentiation takes place even later, mainly at the tip of the archenteron and subsequently in the blastocoel. Thus, the precocious skeletogenic functions controlled by the novel euechinoid skeletogenic GRN could have assembled over evolutionary time at the embryological address of the micromere lineage, during or soon after the period the cladistic cidaroid/euechinoid split was taking place, without interrupting any of the developmentally later skeletogenic functions on which the embryo of the euechinoid stem lineage would still have depended. In other words, in the plesiomorphic state the micromere lineage executed signaling but not skeletogenic functions during cleavage and blastulation, but during euechinoid divergence novel skeletogenic circuitry executed in the micromere lineage during early development could have been superimposed, without necessarily interfering with gastrular skeletogenesis until the latter became redundant.

3.6 Materials and Methods

Animals and Embryo Cultures

Eucidaris tribuloides sea urchins were obtained from SeaLife, Inc. (Key Largo, FL, USA) and were maintained in room temperature (r/t) aquaria. Animals were spawned with 0.5 M KCl. Cultures were grown in Millipore-filtered sea water (MFSW) in an incubator set to 22°C unless otherwise indicated.

Real-Time Quantitative PCR

For each MASO-treated time point, injected and uninjected embryos were counted (~70 embryos per timepoint were used), gently centrifuged, and lysed with Buffer RLT (Qiagen). Just before column chromatography, an equal amount of exogenous GFP RNA was added to both treatment and uninjected control samples to normalize for RNA preparation, which was carried out according to the manufacturer's protocol (RNeasy; Qiagen). All samples were processed in concert. cDNA was synthesized for the entire sample (iScript; Bio-Rad). Approximately one embryo per reaction was assayed in triplicate by qPCR (SYBR Green; Life Technologies). Primer sequences to amplify qPCR products in this study are presented in Table 3.1.

Whole-mount *in situ* hybridization

The following protocol is a modified from (Ransick, 2004). Digoxigenin (DIG)- or fluorescein (FLU)-labeled RNA probes were prepared by cloning purified PCR

gene	qPCR Forward Primer	qPCR Reverse Primer
<i>alx1</i>	ATCCGGGTATGAAATGCCCA	TTCTGCAGATGCGGAGCATA
<i>delta</i>	AAATGTAACGTGCCGTGTGAGCCA	TACAGCTCACATTGGTGCACCT
<i>ets1</i>	TGAGTCATCACCGAACTCGAACCA	GGTGTCCGTCAAACGTGTCAAA
<i>foxq2</i>	TACGCCTATCCTTCCACCATC	GTGAAGGCAGCGACGAATATG
<i>hesC</i>	ACGTCGAGCAAGAACG	CACTCGACTGGGTCTGTAATTCCCT
<i>tbrain</i>	ATTCTCCAAGGTAGTGGGCTGCAT	GATGCGAGGTTGGTACTTGTGCAT

Table 3.1: Sequences of primer sets for qPCR detection.

product (0.7–1.2 kb in length) into PGEM-T vector (Promega). All plasmids were sequenced to confirm insert and orientation. Primer sequences used to amplify PCR product used for this study are presented in Table 3.2. Antisense RNA probe was synthesized with T7 or SP6 RNA polymerase (Roche) and purified by column chromatography (RNeasy; Qiagen). For fixation, embryos were fixed on ice in paraformaldehyde (PFA)-maleic acid buffer (MAB) fixation buffer [4% (wt/vol) PFA, 32.5% (vol/vol) MFSW, 32.5 mM maleic acid (pH 7), 162.5 mM NaCl], left overnight (o/n) at 4°C, and brought into hybridization buffer (HyB: 50% formamide, 5× Denhardt's, 5× SSC, 1 mg/mL yeast tRNA, 100 mM NaCl, 0.1% Tween-20, and 50 µg/mL Heparin) by the following series: 10%, 25%, 50%, 75%, and 100%. Fixed embryos were washed twice in and also stored in HyB at -20°C. For WMISH, a modified version of a standard protocol (43) was used. Briefly, fixed embryos were incubated in HyB at 63°C for 1 h. DIG- or FLU-labeled probes were added to a final concentration of 0.5–1 ng/µL and incubated o/n at 63°C. Posthybridization washes were the following: HyB for 15 min, 50:50 HyB/2× SSC for 15 min, 2X SSC for 20 min, 0.2× SSC for 20 min, 0.1× SSC for 30–60 min. Embryos were washed 3× in Tris-buffered saline with Tween-20 (TBST) and blocked at r/t in blocking buffer 1 [80% TBST, 10% sheep serum, 1 mg/mL bovine serum albumin (BSA)] for 30 min, and subsequently blocking buffer 2 (89% TBST, 10% sheep serum, 0.1 mg/mL BSA) for 30 min. Anti-DIG or -FLU fab fragments (Roche) was added to a final concentration of 0.25 µg/mL, incubated for 1 h at r/t, and removed by washing 6× in TBST. Probes were detected by washing 2× in alkaline phosphatase (AP) Buffer and 1× in AP Buffer with 10% dimethylformamide and nitro blue tetrazolium (NBT)/5-chloro-4-bromo-3-indolyl phosphate (BCIP). Staining was halted with TBST/EDTA. Embryos were stored in 70% glycerol until imaging.

gene	WMISH Forward Primer	WMISH Reverse Primer
<i>alx1</i>	TGAAATGCCCATAGCTCCACGA	ATGCCCATGACTGAACGTGCT
<i>delta</i>	ACGGTGATACTAACCTTCACTGG	AGACAGGTGTACCCGTCAAGC
<i>ets1</i>	AATGAGGTTGGACCGAGTGCTGTCA	GTCCGTCAAACGTGTCAAAGGGT
<i>hesC</i>	ACGCAAACGTCGAGCAAGAAC	GCCACATTGTTGGCAGCTGTTG
<i>tbrain</i>	TGTTCCCTCAACTGGTCTCAAGC	CATAGCGCCCTTGTGATAGGAT

Table 3.2: Sequences of primer sets for WMISH probes.

Microinjection of MASOs, Constructs, and RNA

Unfertilized eggs of *Et* were prepared essentially as described (Mcmahon et al., 1985). MASOs were synthesized by Gene Tools (Philomath, OR, USA), and their sequences are provided in Table 3.3. All MASO injection solutions were 1 mM, and each fertilized egg received ~10 pL of injection solution. Embryos for WMISH or qPCR were collected and processed as described above. Dominant-negative Cadherin RNA—which blocks β -catenin nuclearization at the vegetal pole, as described (38)—was injected at a concentration of 1,000 ng/ μ L. For visualization of early, asymmetric nuclearization of β -catenin, RNA encoding a fused β -catenin:GFP product was synthesized by using SP6 mMessage Machine RNA polymerase (Life Technologies) and injected at a concentration of 3 μ g/ μ L. For microinjection of the 2.59-kb Sp-pmar1 minimal reporter construct from ref. 34, ~1,500 molecules of reporter construct were injected per embryo, and injected embryos were scored at 26 h postfertilization (hpf).

gene	MASO sequence	Interferes with
<i>alx1</i>	AGTATTTCATCGTCTCCACCTTTTC	Splicing
<i>delta</i>	ATAACATATAGCACGCCGAGAAGGC	Translation
<i>hesC</i>	AATCACAAGGTAAGACGAGGATGGT	Translation

Table 3.3: Sequences of morpholino antisense oligonucleotides in this study.

Treatment with C59 Inhibitor

The concentration of the porcupine inhibitor C59 (C7641-2s; Collagen Technology) at which to expose embryos of *Et* was established by dose–response. Shortly after fertilization, embryos were assigned to four treatment groups of the inhibitor: 0.3, 0.9, 3, and 9 μ M. Phenotypes for these groups were assessed under a dissecting microscope. Based on these observations, experiments were carried out at 1.5 μ M. Embryos were added to the C59-containing MFSW shortly after they were fertilized, cultured in the medium at 22°C until the desired time, and processed for qPCR analysis as described above.

3.7 Acknowledgements

This work was supported by NSF grant EHD.CREATIV-1-NSF.IOS1240626. We thank Dr. Isabelle Peter for excellent discussions and for her creative suggestion of injecting the minimal *Sp-pmar1* reporter construct; Dr. Joel Smith for providing the minimal *Sp-pmar1* reporter construct; Ryan Range for providing plasmid containing β -catenin:GFP insert; and Miao Cui for providing C59 inhibitor and educating us in its use. We extend a special thanks to Dr. Andy Cameron and Parul Kudtakar at the Beckman Institute’s Center for Computational Regulatory Genomics for providing support with transcriptomics in *Eucidaris tribuloides*.

References

Armstrong, N. and D. R. McClay (1994). “Skeletal pattern is specified autonomously by the primary mesenchyme cells in sea urchin embryos”. In: *Dev Biol* 162.2, pp. 329–338. doi: 10.1006/dbio.1994.1090. URL: <http://www.ncbi.nlm.nih.gov/pubmed/8150198>.

Bailey, A. M. and J. W. Posakony (1995). “Suppressor of Hairless Directly Activates Transcription of Enhancer of Split Complex Genes in Response to Notch Receptor Activity”. English. In: *Genes & Development* 9.21, pp. 2609–2622. doi: DOI10.1101/gad.9.21.2609. URL: %3CGo%20to%20ISI%3E://WOS:A1995TD88500004.

Borggrefe, T. and F. Oswald (2009). “The Notch signaling pathway: Transcriptional regulation at Notch target genes”. English. In: *Cellular and Molecular Life Sciences* 66.10, pp. 1631–1646. doi: 10.1007/s0018-009-8668-7. URL: %3CGo%20to%20ISI%3E://WOS:000268003600001.

Bottjer, D. J. et al. (2006). “Paleogenomics of echinoderms”. English. In: *Science* 314.5801, pp. 956–960. doi: DOI10.1126/science.1132310. URL: %3CGo%20to%20ISI%3E://WOS:000241896000041.

Boveri, T. (1907). *Zellenstudien VI. Die Entwicklung dispermer Seeigeleier. Ein Beitrag zur Befruchtungslehre und zur Theorie des Kerns*. Jena: Gustav Fischer.

Britten, R. J. and E. H. Davidson (1971). “Repetitive and Non-Repetitive DNA Sequences and a Speculation on Origins of Evolutionary Novelty”. English. In: *Quarterly Review of Biology* 46.2, pp. 111–138. doi: Doi10.1086/406830. URL: %3CGo%20to%20ISI%3E://WOS:A1971J953500001.

Chuang, C. K. et al. (1996). “Transient appearance of *Strongylocentrotus purpuratus* Otx in micromere nuclei: Cytoplasmic retention of SpOtx possibly mediated through an alpha-actinin interaction”. English. In: *Developmental Genetics* 19.3, pp. 231–237. doi: Doi10.1002/(Sici)1520-6408(1996)19:3<231::Aid-Dvg6>3.0.Co;2-A. URL: %3CGo%20to%20ISI%3E://WOS:A1996VV86200006.

Cui, M. et al. (2014). “Specific functions of the Wnt signaling system in gene regulatory networks throughout the early sea urchin embryo”. In: *Proc Natl Acad Sci U S A* 111.47, E5029–38. doi: 10.1073/pnas.1419141111. URL: <http://www.ncbi.nlm.nih.gov/pubmed/25385617>.

Damle, S. and E. H. Davidson (2011). “Precise cis-regulatory control of spatial and temporal expression of the alx-1 gene in the skeletogenic lineage of *s. purpuratus*”. English. In: *Developmental biology* 357.2, pp. 505–517. doi: 10.1016/j.ydbio.2011.06.016. URL: %3CGo%20to%20ISI%3E://WOS:000294834400020.

Ettensohn, C. A. et al. (2003). “Alx1, a member of the Cart1/Alx3/Alx4 subfamily of Paired-class homeodomain proteins, is an essential component of the gene network controlling skeletogenic fate specification in the sea urchin embryo”. English. In: *Development* 130.13, pp. 2917–2928. doi: 10.1242/dev.00511. URL: %3CGo%20to%20ISI%3E://WOS:000184149900009.

Gao, F. and E. H. Davidson (2008). “Transfer of a large gene regulatory apparatus to a new developmental address in echinoid evolution”. English. In: *Proceedings of the National Academy of Sciences of the United States of America* 105.16, pp. 6091–6096. doi: 10.1073/pnas.0801201105. URL: %3CGo%20to%20ISI%3E://WOS:000255356000027.

Gao, F., J. R. Thompson, et al. (2015). “Juvenile skeletogenesis in anciently diverged sea urchin clades”. In: *Dev Biol* 400.1, pp. 148–158. doi: 10.1016/j.ydbio.2015.01.017. URL: <http://www.ncbi.nlm.nih.gov/pubmed/25641694>.

Hopkins, M. J. and A. B. Smith (2015). “Dynamic evolutionary change in post-Paleozoic echinoids and the importance of scale when interpreting changes in rates of evolution”. In: *Proc Natl Acad Sci U S A* 112.12, pp. 3758–3763. doi: 10.1073/pnas.1418153112. URL: <http://www.ncbi.nlm.nih.gov/pubmed/25713369>.

Kroh, A. and A. B. Smith (2010). “The phylogeny and classification of post-Palaeozoic echinoids”. English. In: *Journal of Systematic Palaeontology* 8.2, pp. 147–212. doi: Pi1922467612Doi10.1080/14772011003603556. URL: %3CGo%20to%20ISI%3E://WOS:000278007400001.

Laubichler, M. D. and E. H. Davidson (2008). “Boveri’s long experiment: Sea urchin merogones and the establishment of the role of nuclear chromosomes in development”. English. In: *Developmental biology* 314.1, pp. 1–11. doi: 10.1016/j.ydbio.2007.11.024. URL: %3CGo%20to%20ISI%3E://WOS:000253031100001.

Logan, C. Y. et al. (1999). “Nuclear beta-catenin is required to specify vegetal cell fates in the sea urchin embryo”. English. In: *Development* 126.2, pp. 345–357. URL: %3CGo%20to%20ISI%3E://WOS:000078613200014.

Lyons, D. C. et al. (2014). "Specification to Biominerization: Following a Single Cell Type as It Constructs a Skeleton". English. In: *Integrative and Comparative Biology* 54.4, pp. 723–733. doi: 10.1093/icb/icu087. URL: %3C%20to%20ISI%3E://WOS:000343314700018.

McIntyre, D. C. et al. (2014). "Branching out: origins of the sea urchin larval skeleton in development and evolution". In: *Genesis* 52.3, pp. 173–185. doi: 10.1002/dvg.22756. URL: <http://www.ncbi.nlm.nih.gov/pubmed/24549853>.

Mcmahon, A. P. et al. (1985). "Introduction of Cloned DNA into Sea-Urchin Egg Cytoplasm - Replication and Persistence during Embryogenesis". English. In: *Developmental biology* 108.2, pp. 420–430. doi: Doi10.1016/0012-1606(85)90045-4. URL: %3C%20to%20ISI%3E://WOS:A1985AGA6800016.

Minemura, K., M. Yamaguchi, and T. Minokawa (2009). "Evolutionary modification of T-brain (tbr) expression patterns in sand dollar". English. In: *Gene Expression Patterns* 9.7, pp. 468–474. doi: 10.1016/j.gep.2009.07.008. URL: %3C%20to%20ISI%3E://WOS:000271094600002.

Mooi, R. and B. David (1998). "Evolution within a bizarre phylum: Homologies of the first echinoderms". English. In: *American Zoologist* 38.6, pp. 965–974. URL: %3C%20to%20ISI%3E://WOS:000078397500015.

Nishita, M. et al. (2000). "Interaction between Wnt and TGF-beta signalling pathways during formation of Spemann's organizer". In: *Nature* 403.6771, pp. 781–785. doi: 10.1038/35001602. URL: <http://www.ncbi.nlm.nih.gov/pubmed/10693808>.

Oliveri, P., E. H. Davidson, and D. R. McClay (2003). "Activation of pmar1 controls specification of micromeres in the sea urchin embryo". In: *Dev Biol* 258.1, pp. 32–43. URL: <http://www.ncbi.nlm.nih.gov/pubmed/12781680>.

Oliveri, P., Q. Tu, and E. H. Davidson (2008). "Global regulatory logic for specification of an embryonic cell lineage". In: *Proc Natl Acad Sci U S A* 105.16, pp. 5955–5962. doi: 10.1073/pnas.0711220105. URL: <http://www.ncbi.nlm.nih.gov/pubmed/18413610>.

Peter, I. S. and E. H. Davidson (2009). "Modularity and design principles in the sea urchin embryo gene regulatory network". In: *FEBS Lett* 583.24, pp. 3948–3958. doi: 10.1016/j.febslet.2009.11.060. URL: <http://www.ncbi.nlm.nih.gov/pubmed/19932099>.

- (2011). "A gene regulatory network controlling the embryonic specification of endoderm". In: *Nature* 474.7353, pp. 635–639. doi: 10.1038/nature10100. URL: <http://www.ncbi.nlm.nih.gov/pubmed/21623371>.
- (2015). *Genomic Control Process, Development and Evolution*. Oxford: Academic Press.

Peter, I. S., E. Faure, and E. H. Davidson (2012). "Predictive computation of genomic logic processing functions in embryonic development". In: *Proc Natl Acad Sci U S A* 109.41, pp. 16434–16442. doi: 10.1073/pnas.1207852109. URL: <http://www.ncbi.nlm.nih.gov/pubmed/22927416>.

Peterson, K. J., C. Arenas-Mena, and E. H. Davidson (2000). "The A/P axis in echinoderm ontogeny and evolution: evidence from fossils and molecules". In: *Evol Dev* 2.2, pp. 93–101. URL: <http://www.ncbi.nlm.nih.gov/pubmed/11258395>.

Rafiq, K., M. S. Cheers, and C. A. Ettensohn (2012). "The genomic regulatory control of skeletal morphogenesis in the sea urchin". English. In: *Development* 139.3, pp. 579–590. doi: 10.1242/dev.073049. URL: %3CGo%20to%20ISI%3E://WOS:000299168700015.

Ransick, A. (2004). "Detection of mRNA by In situ hybridization and RT-PCR". English. In: *Development of Sea Urchins, Ascidians, and Other Invertebrate Deuterostomes: Experimental Approaches* 74, pp. 601–620. URL: %3CGo%20to%20ISI%3E://WOS:000225592500024.

Revilla-i-Domingo, R., T. Minokawa, and E. H. Davidson (2004). "R11: a cis-regulatory node of the sea urchin embryo gene network that controls early expression of SpDelta in micromeres". English. In: *Developmental biology* 274.2, pp. 438–451. doi: 10.1016/j.ydbio.2004.07.008. URL: %3CGo%20to%20ISI%3E://WOS:000224166000017.

Revilla-i-Domingo, R., P. Oliveri, and E. H. Davidson (2007). "A missing link in the sea urchin embryo gene regulatory network: hesC and the double-negative specification of micromeres". In: *Proc Natl Acad Sci U S A* 104.30, pp. 12383–12388. doi: 10.1073/pnas.0705324104. URL: <http://www.ncbi.nlm.nih.gov/pubmed/17636127>.

Schroeder, T. E. (1981). "Development of a 'primitive' sea urchin (*Eucidaris tribuloides*): irregularities in the hyaline layer, micromeres, and primary mesenchyme". In: *Biological Bulletin* 161.1, pp. 141–151.

Smith, A. B. and N. T. J. Hollingworth (1990). "Tooth structure and phylogeny of the Upper Permian echinoid *Miocidaris keyserlingi*". In: *Proceedings of the Yorkshire Geological Society* 48, pp. 47–60.

Smith, J. and E. H. Davidson (2009). "Regulative recovery in the sea urchin embryo and the stabilizing role of fail-safe gene network wiring". English. In: *Proceedings of the National Academy of Sciences of the United States of America* 106.43, pp. 18291–18296. doi: 10.1073/pnas.0910007106. URL: %3CGo%20to%20ISI%3E://WOS:000271222500046.

Smith, J., E. Kraemer, et al. (2008). "A spatially dynamic cohort of regulatory genes in the endomesodermal gene network of the sea urchin embryo". In: *Dev Biol* 313.2, pp. 863–875. doi: 10.1016/j.ydbio.2007.10.042. URL: <http://www.ncbi.nlm.nih.gov/pubmed/18061160>.

Stamos, J. L. and W. I. Weis (2013). “The beta-Catenin Destruction Complex”. English. In: *Cold Spring Harbor Perspectives in Biology* 5.1. doi: ARTNa00789810. 1101 / cshperspect . a007898. URL: %3CGo%20to%20ISI%3E : // WOS : 000315983600008.

Thompson, J.R. et al. (2015). “Reorganization of sea urchin gene regulatory networks at least 268 million years ago as revealed by oldest fossil cidaroid echinoid”. English. In: *Scientific Reports* 5. doi: ARTN1554110. 1038 / srep15541. URL: %3CGo%20to%20ISI%3E : // WOS : 000363122100003.

Wahl, M. E. et al. (2009). “The cis-regulatory system of the tbrain gene: Alternative use of multiple modules to promote skeletogenic expression in the sea urchin embryo”. In: *Dev Biol* 335.2, pp. 428–441. doi: 10.1016/j.ydbio.2009.08.005. URL: <http://www.ncbi.nlm.nih.gov/pubmed/19679118>.

Weitzel, H. E. et al. (2004). “Differential stability of beta-catenin along the animal-vegetal axis of the sea urchin embryo mediated by dishevelled”. English. In: *Development* 131.12, pp. 2947–2956. doi: 10.1242/dev.01152. URL: %3CGo%20to%20ISI%3E : // WOS : 000222695700017.

Wray, G. A. and D. R. McClay (1988). “The origin of spicule-forming cells in a ‘primitive’ sea urchin (*Eucidaris tribuloides*) which appears to lack primary mesenchyme cells”. In: *Development* 103.2, pp. 305–315. URL: <http://www.ncbi.nlm.nih.gov/pubmed/3066611>.

Yamazaki, A., Y. Kidachi, et al. (2014). “Larval mesenchyme cell specification in the primitive echinoid occurs independently of the double-negative gate”. In: *Development* 141.13, pp. 2669–2679. doi: 10.1242/dev.104331. URL: <http://www.ncbi.nlm.nih.gov/pubmed/24924196>.

Yamazaki, A. and T. Minokawa (2015). “Expression patterns of mesenchyme specification genes in two distantly related echinoids, *Glyptocidaris crenularis* and *Echinocardium cordatum*”. In: *Gene Expr Patterns* 17.2, pp. 87–97. doi: 10.1016/j.gep.2015.03.003. URL: <http://www.ncbi.nlm.nih.gov/pubmed/25801498>.

ANCESTRAL STATE RECONSTRUCTION BY COMPARATIVE
ANALYSIS OF A GRN KERNEL OPERATING IN
ECHINODERMS

Erkenbrack, E. M. et al. (2016). “Ancestral state reconstruction by comparative analysis of a GRN kernel operating in echinoderms”. In: *Development Genes and Evolution* 226.1, pp. 37–45. ISSN: 0949-944X. doi: 10.1007/s00427-015-0527-y. URL: <http://link.springer.com/10.1007/s00427-015-0527-y>.

©2016 Springer Verlag, Berlin

Permission secured by the Career Advancement Clause of the Springer-Verlag Copyright Transfer Agreement.

4.1 Abstract

Diverse sampling of organisms across the five major classes in the phylum Echinodermata is beginning to reveal much about the structure and function of gene regulatory networks (GRNs) in development and evolution. Sea urchins are the most studied clade within this phylum, and recent work suggests there has been dramatic rewiring at the top of the skeletogenic GRN along the lineage leading to extant members of the euechinoid sea urchins. Such rewiring likely accounts for some of the observed developmental differences between the two major subclasses of sea urchins: cidaroids and euechinoid. To address effects of top-most rewiring on downstream GRN events, we cloned four downstream regulatory genes within the skeletogenic GRN and surveyed their spatiotemporal expression patterns in the cidaroid *Eucidaris tribuloides*. We performed phylogenetic analyses with homologs from other non-vertebrate deuterostomes and characterized their spatiotemporal expression by quantitative polymerase chain reaction (qPCR) and whole mount in situ hybridization (WMISH). Our data suggest that the *erg-hex-tgif* subcircuit, a putative GRN kernel, exhibits a mesoderm-specific expression pattern early in *E. tribuloides* development that is directly downstream of the initial mesodermal GRN circuitry. Comparative analysis of the expression of this subcircuit in four echinoderm taxa allowed robust ancestral state reconstruction, supporting hypotheses that its ancestral function was to stabilize the mesodermal regulatory state and that it has been co-opted and deployed as a unit in mesodermal subdomains in distantly diverged echinoderms. Importantly, our study supports the notion that GRN kernels exhibit structural and functional modularity, locking down and stabilizing clade-specific, embryonic regulatory states.

4.2 Introduction

Echinoids, or sea urchins, are constituents of the phylum Echinodermata and are comprised of two extant subclasses, the cidaroids (Cidaroidea) and the euechinoids (Euechinoidea). Fossil evidence suggests these two clades had already diverged by the middle of the Permian period at least 268 million years ago (mya) (J. Thompson et al., 2015). In addition to the conspicuous differences observed in the adult morphologies of these clades (Gao, J. R. Thompson, et al., 2015), embryological evidence also indicates numerous developmental differences between these two clades, suggesting extensive rewiring of the gene regulatory networks (GRNs) directing their development (Schroeder, 1981). Two decades of research have parsed out the elaborate circuitry of the GRNs guiding early euechinoid development (Peter

and Davidson, 2011). Thus, with an abundance of euechinoid data in hand, an auspicious opportunity presents itself not only to enumerate the observed developmental differences between these two clades at the molecular level, but also to utilize them to better understand the plasticity and role of GRNs in developmental evolution.

The most striking difference between the early development of cidaroids and euechinoids is exhibited in the skeletogenic mesenchyme. In contrast to euechinoids, which exhibit a precociously ingressing, pre-invagination skeletogenic primary mesenchyme (PMC) lineage, the skeletogenic mesenchyme of cidaroids ingresses from the tip of the archenteron well after gastrulation has begun (Wray and McClay, 1988). In euechinoids, the micromere quartet gives rise to the PMC lineage and is fated from very early in development to become embryonic skeleton (Oliveri, Tu, and Davidson, 2008). Cidaroids, in juxtaposition, exhibit a variable number of micromeres in each embryo (Schroeder, 1981), and yet in spite of this variance their micromeres were found to be homologous to euechinoid PMCs (Wray and McClay, 1988).

The skeletogenic GRN of the purple sea urchin *Strongylocentrotus purpuratus*, a euechinoid, proffers a highly detailed account of the specification and differentiation of the PMC lineage (Oliveri, Tu, and Davidson, 2008). Multiple lines of experimental evidence support the hypothesis that this developmental GRN is highly conserved amongst euechinoids (Ettensohn, 2013). Recently, similar investigations have been extended to cidaroids (Erkenbrack and Davidson, 2015; Yamazaki et al., 2014). For example, a recent study investigated expression and function of genes at the top of the euechinoid PMC GRN in the Atlantic Basin-dwelling cidaroid *E. tribuloides* (Erkenbrack and Davidson, 2015). Functional interrogation of these genes in *E. tribuloides* revealed nine specific regulatory inputs that are absent and that are likely to be gain-of-function changes that occurred during the evolution of euechinoids. More specifically, the localization mechanism of skeletogenic factors to the euechinoid PMCs—the double negative gate—was missing in this cidaroid, suggesting large-scale rewiring of this circuitry occurred in the lineage leading to extant euechinoids. Furthermore, the transcription factors *ets1/2* and *tbrain* were not spatially restricted to the *E. tribuloides* skeletogenic cells. This was also the case in the Indo Pacific-dwelling cidaroid *Prionocidaris baculosa*, suggesting a broader role in mesodermal specification for these genes in the cidaroid clade (Yamazaki et al., 2014). In euechinoids, *ets1/2* and *tbrain* are restricted to the PMCs and function as important early inputs into an *erg-tgif-hex-alx1* skeletogenic GRN circuit

(Oliveri, Tu, and Davidson, 2008). An additional function of the micromeres in *E. tribuloides* is to exclude the skeletogenic fate in the surrounding nonskeletogenic mesoderm (Erkenbrack and Davidson, 2015). Many of these findings in *E. tribuloides* are consistent with those in *Prionocidaris baculosa*, suggesting that many of these observations are conserved amongst cidaroids (Yamazaki et al., 2014). These results beg the question of how manifold the changes to the downstream circuitry are between the cidaroid skeletogenic GRN and the euechinoid PMC GRN.

In examined euechinoids, *erg*, *hex*, and *tgif* form a recursively wired subcircuit downstream of *ets1/2* and *tbrain* that plays a role in stabilizing the regulatory state of the skeletogenic lineage (Oliveri, Tu, and Davidson, 2008). There is strong evidence that in the echinoderm clade this subcircuit serves as a highly conserved, recursively wired GRN kernel that can be deployed at alternative embryonic addresses to lock down and stabilize regulatory states (McCauley, Weideman, and Hinman, 2010; Davidson and Erwin, 2006). Importantly, it is clear that there has been significant GRN rewiring in the lineage leading to euechinoids, in which much of this circuitry has been restricted to the skeletogenic mesoderm as opposed to the broader endomesodermal roles seen in the sea star *Patiria miniata* and mesodermal roles in the sea cucumber *Parastichopus parvimensis* (McCauley, Weideman, and Hinman, 2010; McCauley, Wright, et al., 2012). Comparative analyses in sea stars and euechinoid sea urchins indicate that the initial onset of this circuit differs between these clades. In euechinoids, *ets1* and *tbrain* set off the *erg-hex-tgif* regulatory cascade (Oliveri, Tu, and Davidson, 2008). However, in asteroids *tbrain* is the major driver of this subcircuit, suggesting that *ets1* is a derived input unique to euechinoids (McCauley, Weideman, and Hinman, 2010). We hypothesized that in *E. tribuloides* this conserved circuit would play roles mainly in mesoderm specification, as the drivers of this kernel—*ets1/2* and *tbrain*—are expressed throughout the mesoderm in cidaroids, as opposed to their more restricted roles in the PMCs in euechinoids. Thus we predicted that in cidaroid sea urchins the spatial expression pattern of this subcircuit would mirror more closely that of asteroids and holothuroids than that of euechinoids. To address these queries we cloned the genes from the conserved *erg-hex-tgif* subcircuit and investigated their spatiotemporal expression in *E. tribuloides*. We also present here expression dynamics of the skeletogenic GRN gene *tel*, as similar data in other echinoderms is lacking.

4.3 Results and Discussion

Cloning and phylogenetic analysis of skeletogenic genes

Homologs of *erg*, *hex*, *tgif*, and *tel* were isolated from *E. tribuloides*. Erg and Tel belong to the ETS (E-twenty six) family of related transcription factors, which is characterized by a DNA binding domain known as the ETS domain with a “winged” helix-turn-helix motif (Seidel, 2002). The PNT domain occurs rarely in subfamilies and regulates phosphorylation by serving as a docking site for kinases such as Erk2 (Seidel, 2002). In *S. purpuratus*, there are 11 members of the Ets family with at least one ortholog for each of the subfamilies that have been identified in vertebrates (with the exception of one mammal-specific subfamily) (Rizzo et al., 2006). Genes in this family interact with a diverse array of co-regulatory proteins and serve as both transcriptional activators and repressors (Mavrothalassitis and Ghysdael, 2000). In *E. tribuloides*, the full-length coding sequence of *erg* is 1,785 basepairs (bp) and encodes a 594 amino acid (aa) protein that includes a PNT domain (161-246) and an ETS (425-505) domain. The full-length coding sequence of *tel* is 2,121 bp and encodes a 706 aa protein that includes a PNT domain (42-126) and an ETS (473-554) domain. The predicted aa sequences for Erg and Tel show 69.67% and 55.06% similarity to their homologs in *S. purpuratus*, respectively.

Hex and Tgif (TG-interacting factor) belong to the HOX (homeobox) family of related transcription factors, characterized by the presence of a DNA binding homeodomain with a helix-turn-helix motif. There are 96 members belonging to various subfamilies in *S. purpuratus* (Howard-Ashby et al., 2006). A member of the NK subfamily, Hex (PRH) is known to act both as an activator and repressor of transcription (Soufi and Jayaraman, 2008); while Tgif is a member of the TALE (Three Amino-acid Loop Extension) subfamily, serving mostly to repress transcription, although it can also function as an activator. In *E. tribuloides*, the full-length coding sequence of *hex* is 885 bp and encodes a 294 aa protein that includes a HOX (151-211) domain. The full-length coding sequence of *tgif* is 1,083 bp and encodes a 360 aa protein that contains a HOX domain (44-107). The predicted aa sequences show 64.98% and 70.01% similarity to their homologs in *S. purpuratus*, respectively.

To confirm the identity of each *E. tribuloides* sequence, we carried out phylogenetic analyses in which the cephalochordate *Branchiostoma floridae* was always the out-group. In each case, our analyses resulted in a phylogenetic tree that confirmed the orthology of our sequences and their placement as anciently diverged with respect to euechinoids within a large clade consisting of ambulacrarians (i.e. echinoderms

and the hemichordate *Saccoglossus kowalevskii*) (Figure 4.1).

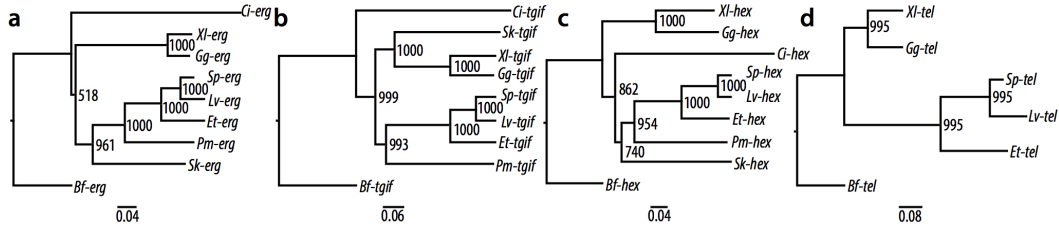


Figure 4.1: Phylogenetic analyses of Erg, Tgif, Hex, and Tel amino acid sequences from selected deuterostomes to confirm homology with predicted amino acid sequences from the cidaroid *Eucidaris tribuloides*. **a** Erg; **b** Tgif; **c** Hex; **d** Tel. N-J trees were constructed in FigTree 1.4.0 following multiple sequence alignments in ClustalX 2.1. Bootstrap values are indicated at the nodes, and scale bars beneath the trees represent the average number of substitutions per site as a measure of evolutionary distance. Species abbreviations: Et, *Eucidaris tribuloides*; Sp, *Strongylocentrotus purpuratus*; Lv, *Lytechinus variegatus*; Pm, *Patiria miniata*; Sk, *Saccoglossus kowalevskii*; Ci, *Ciona intestinalis*; XI, *Xenopus laevis*; Gg, *Gallus gallus*; Bf, *Branchiostoma floridae* (outgroup).

Characterization of spatiotemporal expression of *Et-erg*

Previous studies in *S. purpuratus* showed that *erg* is initially ubiquitous and subsequently restricted to the PMCs by 21 hours post fertilization (hpf). Upon ingress of the PMCs, *Sp-erg* is activated in the oral non-skeletogenic mesenchyme (NSM), where it functions in blastocoelar cell fate (Materna et al., 2013; Solek et al., 2013). *Pm-erg* is initially expressed at blastula stage in mesoderm precursors at the center of the vegetal pole (McCauley, Weideman, and Hinman, 2010), and is localized during gastrulation to the bulb of the archenteron with some expression in ingressing mesenchymal cells. Similar expression is also observed in the holothurian *P. parvi-mensis* (McCauley, Wright, et al., 2012). In *E. tribuloides*, our data indicate that, as in euechinoids, *erg* is not maternally expressed. Both qPCR and WMISH data indicate that zygotic expression in *E. tribuloides* begins specifically in a few cells at center of the vegetal pole 4-5 hpf prior to gastrulation (Figure 4.2a,e,e'). This localized expression is similar to that for *Sp-erg*, which begins to be expressed in the PMCs around 15 hpf (Rizzo et al., 2006). In *E. tribuloides* this restricted initial expression pattern is reminiscent of mesodermal genes at the top of the euechinoid PMC GRN that begin their expression in the micromere-descendants, including that of *alx1*, *ets1/2*, and *tbrain*, which begin to be expressed at 4 hpf, 8 hpf, and 6 hpf prior to *erg*, respectively (Erkenbrack and Davidson, 2015). *Et-erg* expression is seen in the entire mesoderm by 24 hpf; later, expression is observed in skeletogenic mes-

enchyme ingressing into the blastocoel (Figure 4.2f,f'). Moreover, staining persists at 60 hpf not only at the tip of the archenteron and in all mesenchyme, but also in 3-5 cells that have migrated to the ventral lateral clusters and which likely constitute the skeletogenic mesenchyme (Figure 4.2g').

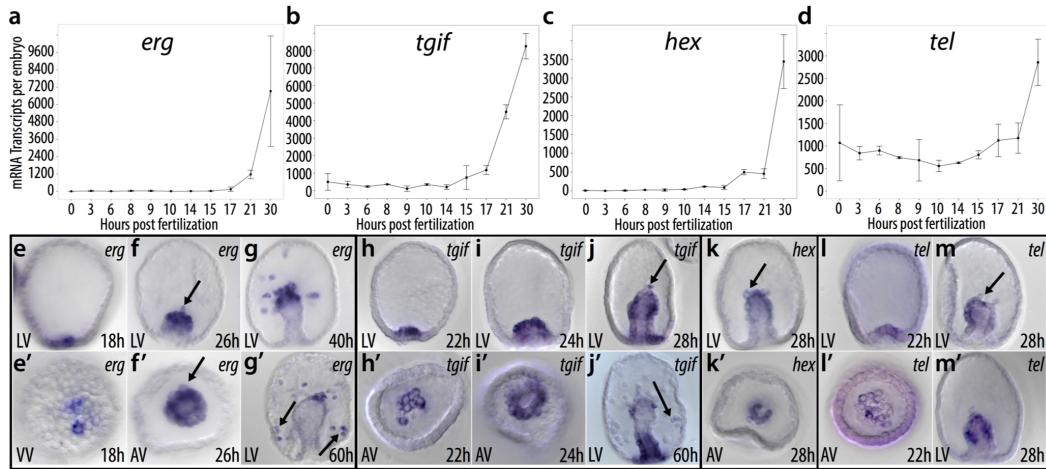


Figure 4.2: Spatiotemporal expression of the *erg-hex-tgif* subcircuit and the eu-echinoid skeletogenic gene *tel* in the early development of the cidaroid *Eucidaris tribuloides*. **a-d** High-density qPCR timecourse profiles of **a** *erg*, **b** *tgif*, **c** *hex*, and **d** *tel*. **e-m** Whole mount in situ hybridization (WMISH) of genes in this study. **e-g**, **e'-g'** WMISH of *erg*. **e**, **e'** At 18h, *erg* is expressed in a few cells at the vegetal pole. **f**, **f'** At 26h, *erg* is expressed in all invaginating cells (mesoderm) and is also expressed in skeletogenic mesenchyme (arrow). **g** At 40h, *erg* is expressed throughout the mesoderm and ingressing mesenchyme. **g'** At 60h, *erg* expression is present at the tip of the archenteron and in migrating mesenchyme, including mesenchymal cells that have migrated to the ventral lateral cluster (skeletogenic cells, arrow). **h-j**, **h'-j'** WMISH of *tgif*. **h**, **h'** At 22h, *tgif* is expressed in a few cells at the vegetal pole. **i**, **i'** At 24h, *tgif* is now seen throughout the mesoderm. **j** By 28h, *tgif* is expressed throughout the mesoderm, including skeletogenic cells (arrow), and also in the endoderm. **j'** At 60h, *tgif* is expressed at the tip of the archenteron, in the mid- and hind-gut endoderm and also in cells that have migrated to the ventral lateral clusters (arrow). *Tgif* is not, however, expressed in most migrating mesenchyme. **k**, **k'** At 28h, *hex* is expressed throughout the mesodermal domain and is also present in ingressing skeletogenic mesenchyme (arrow). **l**, **l'**, **m**, **m'** WMISH of *tel*. **l**, **l'** At 22h, *tel* is expressed in isolated mesodermal cells. **m**, **m'** At 28h, *tel* expression is seen in the majority of the mesodermal domain, but is absent from ingressing skeletogenic cells (arrow). h, hours post fertilization; LV, lateral view; VV, vegetal view; AV, apical view.

These data are consistent with the hypothesis that *Et-erg* potentially is a broad mesodermal regulator that is downstream of the first wave of mesodermal GRN circuitry (Erkenbrack and Davidson, 2015). Though the initial input of *erg* is not

known, it is highly probable there is an intermediate regulator between the initial mesodermal regulators *ets1/2* and *tbrain*, since these genes are already expressed in many more cells than the number of cells in which *erg* begins to be expressed. Minimally, these data further substantiate the claim that *erg* played an ancestral role in mesoderm specification in eleutherozoans, and possibly all echinoderms, as it is expressed in this tissue in all taxa where spatial expression data is available and thus is a crucial cog in GRN circuitry of mesodermal specification (Table 4.1).

Taxon/ Stage	gene/embryonic domain of expression			
	<i>erg</i>	<i>tgif</i>	<i>hex</i>	<i>tel</i>
Asteroids				
<i>blastula</i>	mesodermal	endo- mesodermal	endo- mesodermal	no orthologue
<i>mid-gastrula</i>	mesodermal	endodermal	endo- mesodermal	no orthologue
Ophiuroids				
<i>blastula</i>	no data	no data	no data	no data
<i>mid-gastrula</i>	no data	no data	no data	no data
Holothuroids				
<i>blastula</i>	mesodermal	mesodermal	no data	no data
<i>mid-gastrula</i>	mesodermal, skeletogenic, NSM	no data	no data	no data
Cidaroids				
<i>blastula</i>	mesodermal	mesodermal	no data	mesodermal
<i>mid-gastrula</i>	mesodermal, skeletogenic, NSM	mesodermal, endodermal	mesodermal	mesodermal
Euechinoids				
<i>blastula</i>	PMC	PMC, NSM	PMC	PMC
<i>mesenchyme blastula</i>	PMC, NSM	PMC, NSM	PMC	no data
<i>mid-gastrula</i>	NSM, PMC, coelomic pouches	NSM, endo- derm	PMC, NSM	no data

Table 4.1: Spatial expression patterns of *erg*, *hex*, *tgif*, and *tel* in echinoderms. Data for the cidaroid lineage are from this study. All other data are from previously published work, for which the references are: Asteroids, McCauley et al. (2010); Holothuroids, McCauley et al. (2012); Cidaroids, (this study); Euechinoids, Rizzo et al. (2006); Poustka et al. (2007); Howard-Ashby et al. (2006); Materna et al.(2013); Solek et al. (2013).

Characterization of spatiotemporal expression of *Et-tgif*

In *S. purpuratus*, *tgif* is a maternally deposited factor, the zygotic expression of which begins at 16 hpf, where it is initially expressed in both the PMCs and NSM (Howard-Ashby et al., 2006). After gastrulation begins, *Sp-tgif* is seen in NSM and midgut endoderm. In *P. miniata*, *tgif* expression is first observed broadly in the endomesoderm and by mid-gastrula is observed in the endoderm, whereas in *P. parvimensis*, *tgif* is expressed first in mesodermal cells and later is seen in endoderm and non-ingressed mesoderm at the tip of the archenteron (McCauley, Weideman, and Hinman, 2010; McCauley, Wright, et al., 2012). Our qPCR data indicate that *Et-tgif* is maternally expressed (Figure 4.2b). Zygotic expression begins by at least 14 hpf, indicating this is the first gene to be zygotically expressed in the *erg-hex-tgif* subcircuit. Up to gastrulation *Et-tgif* is restricted to a subset of cells in the mesoderm, after which point it comes to be expressed throughout the mesoderm by early gastrula and then subsequently in mesoderm and endoderm by mid-gastrula (Figure 4.2h,i,j). By late gastrula, very faint expression can be seen in migrating mesenchyme cells, weak expression is seen in mesodermal cells at the tip of the archenteron and strong expression occurs in the mid- and hind-gut—while expression is conspicuously absent from the foregut (Figure 4.2j'). These data indicate that, in all eleutherozoans examined, *tgif* has an early, spatially restricted role in mesodermal specification and, later, a distinct role in endoderm specification. However, only in echinozoans is *tgif* restricted to a mesodermal lineage early in development. Given that the role of *tgif* in endodermal specification appears conserved in all eleutherozoans, these data suggest that following the echinozoan-asterozoan divergence (481 mya; (Jell, 2014)) this endodermal activity was activated later in embryonic development in echinozoans and is a derived feature of this clade.

Characterization of spatiotemporal expression of *Et-hex*

Zygotic expression of *Sp-hex*, which is not maternal in *S. purpuratus*, begins prior to hatching in the early blastula and is observed in the PMCs by 20 hpf (Poustka et al., 2007). Similarly to *Sp-erg*, *Sp-hex* expression is also activated in the oral NSM upon ingress of the PMCs (Materna et al., 2013). By late gastrula stage, expression is observed in PMCs and SMCs, but not endoderm. *Pm-hex* is initially expressed at blastula stage throughout the presumptive endomesoderm at the vegetal pole. During gastrulation, *Pm-hex* continues to be weakly expressed in both the endoderm and the mesoderm with the exception of some cells at the tip of the archenteron (McCauley, Weideman, and Hinman, 2010). Our data suggest that, like in *S. purpuratus*, *hex*

is not maternally expressed in *E. tribuloides* (Figure 4.2c). Zygotic expression of *Et-hex* begins concurrently with *Et-erg* after hatching in the late blastula by 16 hpf (Figure 4.2c). By 28 hpf, spatial expression occurs broadly in mesodermal cells and also occurs in cells ingressing into the blastocoel, very likely overlapping in its expression with *Et-erg* (Figure 4.2k,k'). The spatiotemporal expression patterns of *Et-hex* are indicative of the possibility that it shares inputs with *erg*. Unlike in sea stars, however, these data indicate that *Et-hex* is not expressed in the endoderm up to the time that the skeletogenic mesenchyme ingresses at early gastrula. Indeed, this is also the case in euechinoids (Poustka et al., 2007). These data suggest that in early embryonic development of echinoids *hex* is strictly mesodermal, whereas in asteroids it functions in both endoderm and mesoderm. Additionally, even though the spatial expression pattern of *hex* is not known in *P. parvimensis*, comparative analyses of spatiotemporal expression patterns from three taxa predict that the expression pattern of *hex* in this holothuroid will mirror that of *erg* and *tgif* in *P. parvimensis*.

Initiation and conserved wiring of *erg-hex-tgif* subcircuit in *E. tribuloides*

Taken together, the spatial expression of *Et-erg*, *Et-hex* and *Et-tgif* are remarkable in their congruence, all broadly expressed in-and restricted to-the mesoderm at least until skeletogenic mesenchyme ingresses at 26 hpf. Furthermore, our data specifically show that *erg*, *hex*, and *tgif* are all expressed in the first mesenchyme to ingress in *E. tribuloides* (Figure 2f,f',j,k,k'). These observations lend strong support to the supposition that micromere-descendants in *E. tribuloides* are homologous to the PMC lineage of euechinoids (Wray and McClay, 1988). Additionally, these data suggest that many aspects of the downstream euechinoid PMC GRN circuitry was already in place at the divergence of the two extant echinoid clades. It is also important to note for *erg* and *tgif* that their initial activation in *E. tribuloides* is restricted to a few cells at the pole of the vegetal plate. While we do not present the necessary experimental evidence to claim the *erg-hex-tgif* subcircuit initiates solely in *alx1*-positive cells, our data are very suggestive that its activation begins in micromere-descendants and subsequently expands to the surrounding NSM rather than vice versa. However, this being the case, it can be said with certainty that the *erg-hex-tgif* subcircuit is running in *alx1*-positive cells at the time of skeletogenic mesenchyme ingress (28 hpf). Thus, by 22 hpf, *Et-tgif* and *Et-erg* have come on in cells that are very likely the micromere-descendants. Given that *ets1/2* and *tbrain* are known to be upstream of *erg* and *tgif* in *S. purpuratus*, their activation by

ets1/2 and *tbrain* in *E. tribuloides* must be addressed in future studies. However, the initial activation and spatial restriction of the *erg-hex-tgif* subcircuit to a few cells at the tip of the vegetal pole occurs long after *ets1/2* and *tbrain* have been initiated in the mesoderm, suggesting there are other factors at play in their activation. With that said, as soon as *erg* and *tgif* begin to run in the micromere-descendants, all of the inputs required to initiate the *erg-hex-tgif* subcircuit are in place: *ets1/2* and *tbrain* are running in the mesoderm; *erg* would feed into both *hex* and *tgif*; and *hex* would feed back into both *erg* and *tgif*. Lastly, it is worth noting that the repressive function of *erg* on *tbrain*, described in *P. miniata* (McCauley, Weideman, and Hinman, 2010), must be missing in cidaroids, as *erg* and *tbrain* are expressed in overlapping cells at least up to 40 hpf.

Characterization of spatiotemporal expression of *Et-tel*

While *tel* is not part of the *erg-hex-tgif* subcircuit, it was included in the study due to its role immediately downstream of the initial activators of the Sp PMC GRN. In *S. purpuratus*, *tel* is a maternal factor that begins to be zygotically expressed by 15 hpf in the PMCs, where it remains until at least mesenchyme blastula stage (Rizzo et al., 2006). In *P. miniata*, there is no evidence of a *tel* homolog. We found that *tel* is maternally expressed in *E. tribuloides* and that zygotic expression begins much like *erg*, *hex* and *tgif*, in a few cells at the center of the vegetal pole; thereafter it expands to be broadly mesodermal (Figure 4.2d,l,m). Interestingly, we found that ingressing skeletogenic mesenchyme cells of *E. tribuloides* were not positive for *Et-tel* even though it is clearly visible in the surrounding NSM at 30 hpf (Figure 4.2m,m'). In *S. purpuratus*, *tel* is an input into differentiation genes in the PMC GRN (Oliveri, Tu, and Davidson, 2008). In *E. tribuloides* our data indicate that, while *Et-tel* is expressed early on in skeletogenic cells, by the time the skeletogenic cells ingress into the blastocoel, *tel* expression is absent from those cells. These data suggest that the restricted, PMC-specific expression of *tel* is a euechinoid novelty and likely the result of another euechinoid co-option event.

Evolution of the *erg-hex-tgif* subcircuit in echinoderms

Comparative analysis of three or more taxa in a monophyletic clade is the gold standard for making claims regarding developmental character state evolution. This is because with only two taxa, it is impossible to establish polarity of characters, and thus determine which character states are ancestral and which are derived. Our results buttress and broaden already published data on spatiotemporal expression

patterns from three major taxa of echinoderms—asteroids, holothuroids and echinoids—members of which last shared a common ancestor over 481 mya (Jell, 2014). By comparing data from multiple taxa, we can minimally enumerate twelve statements about the embryos of the ancestors of these modern species (Table 4.2). These statements are incredibly significant, as they afford predictions regarding both timing and classification of evolutionary events that must have occurred in the various evolutionary lineages that led to extant taxa.

At least 481 mya: In ancestral embryos prior to the asterozoan – echinozoan divergence
<ol style="list-style-type: none"> 1. <i>erg</i> was a mesodermal driver at blastula stage and gastrula stage 2. <i>hex</i> was a mesodermal driver at blastula stage 3. <i>tgif</i> was a mesodermal driver at blastula stage and gastrula stage 4. <i>tgif</i> was an endodermal driver at mid-gastrula 5. <i>erg-hex-tgif</i> kernel operated in mesoderm 6. Prediction: <i>hex</i> is likely to be expressed in mesoderm of holothurians, but endodermal expression after blastula stage is unclear
At least 462 mya: In ancestral embryos prior to the holothuroid – echinoid divergence
<ol style="list-style-type: none"> 7. <i>erg</i> and <i>tgif</i> were initiated in the mesoderm and <i>tgif</i> came to be expressed in the endoderm at a later time in development, whereas <i>erg</i> remained restricted to the mesoderm throughout early embryonic development to fulfill its ancestral function, <i>tgif</i> was expressed first in the mesoderm and then in the mesoderm and the endoderm 8. <i>tgif</i> mesoderm expression at mid-gastrula stage was either lost in asteroids or gained in the lineage leading to the last common ancestor of echinozoans 9. <i>erg</i> was expressed in the skeletogenic lineage at least as late in development as mid-gastrula stage 10. <i>hex</i> endodermal expression is acquired early in asteroid embryogenesis or lost in last common ancestor of extant echinozoans
At least 268 mya: In ancestral embryos at the cidaroid – euechinoid divergence, e.g. in <i>Archaeocidaris</i> embryos
<ol style="list-style-type: none"> 11. <i>erg</i>, <i>hex</i>, and <i>tel</i> were initiated in a few cells at the center of the vegetal pole; later in the lineage leading to camarodont euechinoids following the cidaroid – euechinoid divergence, these three genes are restricted PMCs prior to PMC ingestion 12. <i>tgif</i> remains expressed in mesodermal cells that ingressed into the blastocoel (<i>tgif</i> is not expressed in mesodermal cells that have ingressed in holothuroids)

Table 4.2: Ancestral state reconstruction for embryos of ancestors of extant echinoderm clades by comparative analysis of spatial gene expression data from three or more taxa.

Data from asteroids and holothuroids allow for establishment of character polarity with regard to the spatiotemporal deployment of the *erg-hex-tgif* subcircuit in echinoids. That the deployment of the *erg-hex-tgif* subcircuit appears to be limited to the mesoderm in modern cidaroids, as it is in holothuroids (McCauley, Wright, et al., 2012), indicates that this subcircuit was likely deployed in the mesoderm of the last common ancestor of cidaroids and euechinoids, e.g. in the embryos of the taxon Archaeocidaris, which lived over 268 million years ago (J. Thompson et al., 2015). Furthermore this rigorously demonstrates that the PMC and NSM restricted expression of the *erg-hex-tgif* subcircuit in euechinoids is a derived character state and must have arisen in stem-group or early crown-group euechinoids since the euechinoid-cidaroid divergence. Although these data indicate that the broader mesodermal utilization of the *erg-hex-tgif* subcircuit in cidaroids is basal with respect to the more specific deployment in euechinoids, this is but one set of characters, and phylogenetic analyses indicate that neither the cidaroids, nor euechinoids are more ancestral than the other (J. Thompson et al., 2015).

Lastly, these results proffer a straightforward explanation as to the evolution of the spatial control of the *erg-hex-tgif* conserved GRN circuitry in echinoderms (Figure 4.3). An interesting hypothesis is that *tbrain* is the ancestral regulator of the *erg-hex-tgif* subcircuit in echinoderms. This is consistent with the observations that the embryonic spatial expression of *tbrain* grades from PMC restricted in euechinoids (Ettensohn, 2013), to broadly mesodermal in cidaroids and holothuroids (Erkenbrack and Davidson, 2015; McCauley, Wright, et al., 2012), and to mesodermal and endodermal in asteroids (McCauley, Weideman, and Hinman, 2010). That the *erg-hex-tgif* subcircuit also exhibits these expression patterns in the same clades suggests that all four of these genes may be recursively wired. Further, *tbrain* solely regulates this subcircuit in asteroids and partially regulates it in euechinoids in spite of the fact that *tbrain* is expressed at different development addresses in these clades. Taken together these observations are consistent with the hypothesis that this subcircuit is downstream of *tbrain* in eleutherozoans. Developmentally, this suggests that, as proposed by others (McCauley, Weideman, and Hinman, 2010), the ancestral function of the *erg-hex-tgif* subcircuit was to stabilize the mesodermal regulatory state.

Our data lend support to this hypothesis and also add weight to the hypothesis, put forward by Gao and Davidson (Gao and Davidson, 2008), that whole apparatus of ancestral mesodermal GRN circuitry were loaded into the micromere embryonic

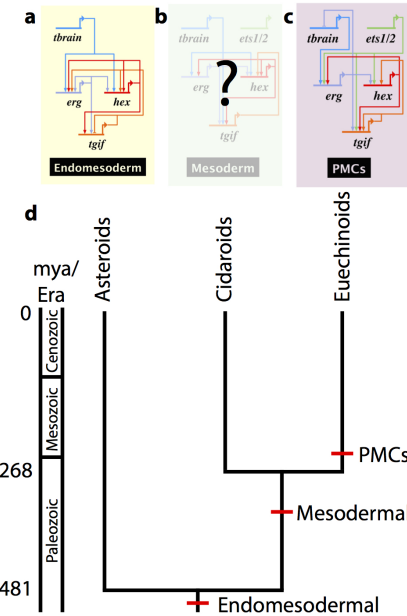


Figure 4.3: Co-option of the *erg-hex-tgif* subcircuit in the echinoderm clade. **a-c** Gene regulatory network (GRN) diagrams of the *erg-hex-tgif* subcircuit showing its wiring and embryonic domain of expression during development in three echinoderm clades. GRN diagrams were constructed using the BioTapestry online software suite (biotapestry.org). **a** GRN diagram of the *erg-hex-tgif* subcircuit in asteroids based on data presented in McCauley et al. (2010). In asteroids, this subcircuit is expressed in the endomesoderm in early blastulae and *tbrain* is its early activator. **b** Hypothetical GRN diagram of the *erg-hex-tgif* subcircuit in cidaroids, in which it is expressed exclusively in the mesoderm in pregastrular embryos. The transparency and question mark indicates that the *cis*-regulatory inputs between these genes have not been verified by perturbation analysis. The early activator of this GRN is not known. **c** GRN diagram of the *erg-hex-tgif* subcircuit in euechinoids, as presented in McCauley et al. (2010). In euechinoids this circuit is expressed exclusively in the PMCs, a population of mesodermal cells that give rise to the embryonic skeleton, and its early activators are *tbrain* and *ets1/2*. **d** Phylogeny depicting geological era of divergence and co-option events of the *erg-hex-tgif* subcircuit in three echinoderm clades in which this subcircuit has been investigated. Divergence estimates are taken from Thompson et al. (2015) for the euechinoid-cidaroid divergence and Jell (2014) for the asterozoan-echinozoan divergence. Red bars indicate a co-option event, and the embryonic address to which the subcircuit was co-opted is also indicated.

address in the lineage leading to modern euechinoids following the euechinoid-cidaroid divergence—a truly remarkable case of evolutionary co-option (Figure 4.3). Phenomena like those observed here are best explained by the observation that GRNs are fundamentally hierarchical and modular in nature (Davidson and Erwin, 2006). The *erg-hex-tgif* kernel in the early embryogenesis of these echinoderms

provides an extraordinary example of the modularity and clade-specific functions of GRNs in evolution and development. The correspondence of spatial expression of the *erg-hex-tgif* kernel to *ets1/2* and *tbrain* in these disparate clades, sea stars, sea cucumbers, and sea urchins suggests that, even though these organisms last shared a common ancestor over 481 mya, the regulatory embrace they find themselves locked in is so difficult to genetically disentangle, that during evolution they are deployed differentially around the embryo as a parcel.

4.4 Materials and Methods

Cloning and phylogenetic analyses

RNA was extracted from embryos following in vitro fertilization of eggs obtained from adult *Eucidaris tribuloides* collected by Gulf Specimens Marine Lab (Panacea, FL) or Reeftopia (Sugarloaf Key, FL). cDNA was prepared using the SMART RACE cDNA Amplification Kit. Full-length sequences of *erg*, *hex*, *tgif*, and *tel* were obtained through a combination of cloning and existing transcriptome data available in Echinobase (echinobase.org). DNA binding domains were predicted using ExPASy: Bioinformatics Resource Portal (expasy.org). Multiple sequence alignments were performed using ClustalX 2.1. Phylogenetic reconstruction was carried out using maximum likelihood methods with bootstrap confidence intervals determined by using 1000 replicates. The output was viewed using FigTree 1.4.0.

The following sequences were used to construct the phylogenetic trees: SpErg (SPU_018483), LvErg (retrieved by BLAST in Echinobase), PmErg (GU_251975), CiErg (NM_001078474), SkErg (XM_006822711), BfErg (XM_002613065), XI (AJ_224125), and GgErg (X_77159); SpHex (SPU_027215), LvHex (retrieved by BLAST in Echinobase), PmHex (GU_251972), CiHex (NM_001078262), SkHex (SQ_431047), BfHex (EU_296398), XIHex (NM_001085590), and GgHex (NM_205252); SpTel (SPU_028479), LvTel (retrieved by BLAST in Echinobase), BfTel (XP_002608583), XITel (NM_001124423), and GgTel (NM_001199273); SpTgif (SPU_018126), LvTgif (retrieved by BLAST in Echinobase), PmTgif (GU_251973), CiTgif (XP_002124000), SkTgif (NM_001164980), BfTgif (NP_001071803), XI Tgif (NP_001080420), GgTgif (NM_205379).

Whole mount *in situ* hybridization

Probes were synthesized from cDNA using the DIG RNA Labeling Kit (SP6/T7) (Roche). Primers used for WMISH probe amplification were designed from full-length coding sequences (Table 4.3). Embryos were fixed in PFA-MAB (4% PFA,

32.5% MFSW, 32.5 mM maleic acid (pH 7), 162.5 mM NaCl) solution on ice and left overnight at 4°C. Embryos were transferred into hybridization buffer (50% formamide, 5X Denhardt's, 5X SSC, 1 mg/mL yeast tRNA, 100 mM NaCl, 0.1% Tween-20, 50 µg/mL Heparin) by series (10%, 25%, 50%, 75%, 100%). Probe concentrations were 0.5-1.0 ng/µL. Probe hybridization and post-hybridization stringency washes were carried out at 63°C. Antibody concentration was 0.25 µg/mL. Detailed procedures are described elsewhere (Erkenbrack and Davidson, 2015).

gene	WMISH Forward Primer	WMISH Reverse Primer
<i>erg</i>	TCTCGGATGACCAGTCTATGT	CACGGCTCAGTTATCGTAGTT
<i>hex</i>	GTCCTGCCCCATCTCGTTGTCTCCCTTGCC	CTCCAACGATCAGACGATGGAACCTCACTCG
<i>tel</i>	GTGCTTGTCTCCCATCGGATGTAGGGCG	GGAGGAGTTCTCGCTGGACAGCGTGAAATGC
<i>tgif</i>	GGCGGGCATCGACAAGAATGTGGAATGG	CATCACCACGGCGCGAGTAGTTCTGCTC

Table 4.3: Sequences of primer sets for WMISH probes.

Real-time quantitative PCR

Eggs from two different females were used as the starting point for two timecourse cultures. From these, 100 embryos were counted at hourly intervals, gently centrifuged, and lysed with Buffer RLT. To allow quantification of mRNA transcripts, each timepoint was spiked with ~1000 transcripts of synthetic Xeno RNA (Cells-to-Ct Control Kit, Life Technologies) and harvested according to the manufacturer's protocol (RNeasy, Qiagen). Approximately 1 embryo per reaction was assayed in triplicate by qPCR (SYBR Green, Life Technologies). qPCR primers used in this study are listed in Table 4.4.

gene	qPCR Forward Primer	qPCR Reverse Primer
<i>erg</i>	TTCGACGCCCGAGGAAC	CCACTGGACCCACTGTTGA
<i>hex</i>	CTCTACCCGTACTCTAGGAATGA	ATCGTTGGAGAACCTGACTTG
<i>tel</i>	AAATTCAAGCATGAACGGGAAGGCG	TCGGTGTCTCTGATTCCTGCTCT
<i>tgif</i>	GCGAGTAGTTCTGCTCCAAA	ATGGCGAATCTCACTCTTGT

Table 4.4: Sequences of primer sets for qPCR.

4.5 Acknowledgements

This work was part of a funding initiative to enhance developmental biology research at undergraduate institutions awarded to LR (National Institutes of Health #1R15HD059927-01). We thank Andy Cameron and his intrepid crew at the Center for Computational Regulatory Genomics at Caltech's Beckman Institute for their assistance with sequences. EME conducted the spatiotemporal aspect of this research in the Davidson Laboratory and was funded by National Science Foundation

CREATIV grant #1240626. The authors wish to dedicate this paper to the memory of Eric Harris Davidson.

References

Davidson, E. H. and D. H. Erwin (2006). “Gene regulatory networks and the evolution of animal body plans.” In: *Science (New York, N.Y.)* 311.5762, pp. 796–800. ISSN: 1095-9203. doi: 10.1126/science.1113832. URL: <http://www.ncbi.nlm.nih.gov/pubmed/16469913>.

Erkenbrack, E. M. and E. H. Davidson (2015). “Evolutionary rewiring of gene regulatory network linkages at divergence of the echinoid subclasses”. In: *Proc Natl Acad Sci U S A* 112.30, E4075–84. ISSN: 1091-6490 (Electronic) 0027-8424 (Linking). doi: 10.1073/pnas.1509845112. URL: <http://www.ncbi.nlm.nih.gov/pubmed/26170318>.

Ettensohn, C. A. (2013). “Encoding anatomy: Developmental gene regulatory networks and morphogenesis”. In: *genesis* 51.6, pp. 383–409. ISSN: 1526954X. doi: 10.1002/dvg.22380. URL: <http://doi.wiley.com/10.1002/dvg.22380>.

Gao, F. and E. H. Davidson (2008). “Transfer of a large gene regulatory apparatus to a new developmental address in echinoid evolution”. English. In: *Proceedings of the National Academy of Sciences of the United States of America* 105.16, pp. 6091–6096. doi: 10.1073/pnas.0801201105. URL: %3CGo%20to%20ISI%3E://WOS:000255356000027.

Gao, F., J. R. Thompson, et al. (2015). “Juvenile skeletogenesis in anciently diverged sea urchin clades”. In: *Dev Biol* 400.1, pp. 148–158. doi: 10.1016/j.ydbio.2015.01.017. URL: <http://www.ncbi.nlm.nih.gov/pubmed/25641694>.

Howard-Ashby, M. et al. (2006). “Identification and characterization of homeobox transcription factor genes in *Strongylocentrotus purpuratus*, and their expression in embryonic development”. In: *Developmental Biology* 300.1, pp. 74–89. ISSN: 00121606. doi: 10.1016/j.ydbio.2006.08.039.

Jell, P. A. (2014). “A Tremadocian asterozoan from Tasmania and a late Llandovery edrioasteroid from Victoria”. In: *Alcheringa: An Australasian Journal of Palaeontology* 38.4, pp. 528–540. ISSN: 0311-5518. doi: 10.1080/03115518.2014.911642. URL: <http://www.tandfonline.com/doi/full/10.1080/03115518.2014.911642>.

Materna, S. C. et al. (2013). “Diversification of oral and aboral mesodermal regulatory states in pregastrular sea urchin embryos”. In: *Developmental Biology* 375.1, pp. 92–104. ISSN: 00121606. doi: 10.1016/j.ydbio.2012.11.033.

Mavrothalassitis, G. and J. Ghysdael (2000). “Proteins of the ETS family with transcriptional repressor activity.” In: *Oncogene* 19.55, pp. 6524–32. ISSN: 0950-9232. doi: 10.1038/sj.onc.1204045. URL: <http://www.ncbi.nlm.nih.gov/pubmed/11175368>.

McCauley, B. S., E. P. Weideman, and V. F. Hinman (2010). "A conserved gene regulatory network subcircuit drives different developmental fates in the vegetal pole of highly divergent echinoderm embryos". In: *Developmental Biology* 340.2, pp. 200–208. ISSN: 00121606. doi: 10.1016/j.ydbio.2009.11.020.

McCauley, B. S., E. P. Wright, et al. (2012). "Development of an embryonic skeletogenic mesenchyme lineage in a sea cucumber reveals the trajectory of change for the evolution of novel structures in echinoderms". In: *EvoDevo* 3.1, p. 17. ISSN: 2041-9139. doi: 10.1186/2041-9139-3-17. URL: <http://www.evodevojournal.com/content/3/1/17>.

Oliveri, P., Q. Tu, and E. H. Davidson (2008). "Global regulatory logic for specification of an embryonic cell lineage". In: *Proc Natl Acad Sci U S A* 105.16, pp. 5955–5962. doi: 10.1073/pnas.0711220105. URL: <http://www.ncbi.nlm.nih.gov/pubmed/18413610>.

Peter, I. S. and E. H. Davidson (2011). "A gene regulatory network controlling the embryonic specification of endoderm". In: *Nature* 474.7353, pp. 635–639. doi: 10.1038/nature10100. URL: <http://www.ncbi.nlm.nih.gov/pubmed/21623371>.

Poustka, A. J. et al. (2007). "A global view of gene expression in lithium and zinc treated sea urchin embryos: new components of gene regulatory networks". In: *Genome Biology* 8.5, R85. ISSN: 14656906. doi: 10.1186/gb-2007-8-5-r85. URL: <http://genomebiology.com/2007/8/5/R85>.

Rizzo, F. et al. (2006). "Identification and developmental expression of the ets gene family in the sea urchin (*Strongylocentrotus purpuratus*)". In: *Developmental Biology* 300.1, pp. 35–48. ISSN: 00121606. doi: 10.1016/j.ydbio.2006.08.012. URL: <http://linkinghub.elsevier.com/retrieve/pii/S0012160606010827>.

Schroeder, T. E. (1981). "Development of a 'primitive' sea urchin (*Eucidaris tribuloides*): irregularities in the hyaline layer, micromeres, and primary mesenchyme". In: *Biological Bulletin* 161.1, pp. 141–151.

Seidel, J. J. (2002). "An ERK2 docking site in the Pointed domain distinguishes a subset of ETS transcription factors". In: *Genes & Development* 16.1, pp. 127–137. ISSN: 08909369. doi: 10.1101/gad.950902. URL: <http://www.genesdev.org/cgi/doi/10.1101/gad.950902>.

Solek, C. M. et al. (2013). "An ancient role for Gata-1/2/3 and Scl transcription factor homologs in the development of immunocytes". In: *Developmental Biology* 382.1, pp. 280–292. ISSN: 00121606. doi: 10.1016/j.ydbio.2013.06.019.

Soufi, A. and P. S. Jayaraman (2008). "PRH/Hex: an oligomeric transcription factor and multifunctional regulator of cell fate." In: *The Biochemical journal* 412.3, pp. 399–413. ISSN: 1470-8728. doi: 10.1042/BJ20080035. URL: <http://www.ncbi.nlm.nih.gov/pubmed/18498250> <http://www.ncbi.nlm.nih.gov/articlerender.fcgi?artid=PMC2570084>.

Thompson, J.R. et al. (2015). “Reorganization of sea urchin gene regulatory networks at least 268 million years ago as revealed by oldest fossil cidaroid echinoid”. English. In: *Scientific Reports* 5. doi: ARTN1554110 . 1038/srep15541. URL: %3CGo%20to%20ISI%3E:/WOS:000363122100003.

Wray, G. A. and D. R. McClay (1988). “The origin of spicule-forming cells in a ‘primitive’ sea urchin (*Eucidaris tribuloides*) which appears to lack primary mesenchyme cells”. In: *Development* 103.2, pp. 305–315. URL: <http://www.ncbi.nlm.nih.gov/pubmed/3066611>.

Yamazaki, A. et al. (2014). “Larval mesenchyme cell specification in the primitive echinoid occurs independently of the double-negative gate”. In: *Development* 141.13, pp. 2669–2679. doi: 10.1242/dev.104331. URL: <http://www.ncbi.nlm.nih.gov/pubmed/24924196>.

EVOLUTION OF GENE REGULATORY NETWORK
TOPOLOGY AND DORSAL-VENTRAL AXIS SPECIFICATION
IN SEA URCHINS (ECHINOIDEA)

A version of this chapter was submitted to PNAS on 26 April 2016.

5.1 Abstract

Developmental gene regulatory networks (dGRNs) are assemblages of interacting regulatory factors that direct ontogeny of animal body plans. The hierarchical topology of these networks predicts that their nodes will evolve at different rates and consequently will bias the trajectories of embryonic evolution. To test these predictions, detailed, comparative analyses of dGRNs that specify early, global embryonic domains are required, but these are at best scant in the literature. The most extensively detailed dGRNs have been documented for one of the two subclasses of extant sea urchins, the euechinoids. Remarkably, these dGRNs show little appreciable change since their divergence approximately 90 million years ago (mya). Therefore, to better understand the rate, mechanisms, and ontogenetic consequences of change to dGRN topologies, comparative microdissection of dGRNs must be undertaken for sea urchins that diverged deeper in geological time. Recent studies have highlighted extensive divergence of skeletogenic mesoderm specification in the sister clade of euechinoids, the cidaroids, suggesting that extending comparative analyses to all cidaroid embryonic domains may prove insightful for understanding the dynamics of evolutionary change to dGRNs. Here, I report the spatial patterning of 19 regulatory factors involved in dorsal-ventral patterning of non-skeletogenic mesodermal and ectodermal domains in the early development of *Eucidaris tribuloides*, a cidaroid sea urchin. Endogenous spatiotemporal dynamics suggest that deployment of ectodermal regulatory factors is more impervious to change than mesodermal regulatory factors in the sea urchin lineage. This result is supported by perturbation experiments that inhibit proper dorsal-ventral patterning and by introduction of euechinoid ectodermal reporter constructs that, surprisingly, are expressed in homologous embryonic domains in *E. tribuloides*. Among these changes I specifically enumerate 19 heterochronic and heterotopic alterations to deployment of regulatory factors since the divergence of echinoids. Additionally, statistical analyses comparing the temporal expression dynamics of 55 *E. tribuloides* regulatory factors to their orthologues in two euechinoid sea urchins indicate that significantly more alterations have occurred to mesodermal than to endodermal and ectodermal GRN topologies. Whereas deployment of mesodermal regulatory factors has been altered at all levels of GRN topology since the divergence of the two echinoid subclasses, the same cannot be said for deployment of endodermal and ectodermal regulatory genes. These results provide a global view of early embryonic developmental processes in two clades that diverged at least 268.8 million years ago and show that the dGRNs controlling embryonic specification exhibit

differential lability, supporting the hypothesis that the topologies of dGRNs bias rates of evolutionary change and alter the developmental evolutionary trajectories of embryogenesis. Similar results may hold for all bilaterians due to the fundamental role of GRN topologies in developmental programs.

5.2 Introduction

From egg to embryo, early bilaterian development is the transformation of a single cell, the fertilized egg, into a dynamic gastrulating embryo with multiple cell types and embryonic domains. Integral to early development of a triploblastic bilaterian is the delineation of embryonic domains—endoderm, ectoderm, mesoderm—and their subdomains—dorsal, ventral, anterior, posterior, mesenchymal, etc. This partitioning sets the stage for specification of morphological features of the larva and/or adult. Asymmetrically distributed RNA and proteins in the egg provide the initial inputs into this process and thereby determine the spatial coordinates of domain formation (Davidson, 1986; Wikramanayake, Hong, et al., 2003). In the context of these maternal factors, zygotic transcription is initiated, and the interplay between the genetically encoded regulatory program and its output of regulatory factors, e.g. transcription factors and cell signaling pathways, delineates embryonic domains (Davidson, 2006). The deployment of evolutionarily conserved cohorts of transcription factors, or regulatory states, is the spatial readout of developmental gene regulatory networks (GRNs) and provides each embryonic domain with its molecularly distinct and functional identity (Peter and Davidson, 2015; Hashimshony et al., 2015).

The trajectories of change that can occur to developmental programs during evolution are affected both by the sequential unfolding of embryonic development and the hierarchical structure of GRNs (Peter and Davidson, 2011b). For example, that certain nodes in GRNs will evolve at different rates would seem to follow from their inherent hierarchical architecture and would provide a powerful mechanistic explanation as to why constraint occurs in some developmental processes and evolutionary change has occurred in others (Davidson and Erwin, 2006). However, despite the overt importance of the structure of developmental GRNs to effect change in developmental evolution in predictable ways, illustrative examples are scant in the literature. To address questions of the frequency and nature of change to developmental GRNs, the taxa sampled must be phylogenetically diverged enough to have undergone significant change to developmental GRNs and phylogenetically close enough so that similarity of developmental programs will afford meaningful

comparisons. Due to the cascading nature of early specification events and the rapid establishment of embryonic domains, early development is attractive in so far that it promises to provide fundamental insight into both its lineage-specific evolution and hierarchical change in developmental GRNs.

Sea urchins (class Echinodea) provide an excellent model system to study mechanisms of evolutionary change in early development. Specification of cell lineages and embryonic domains in sea urchin embryos depends on the canonical cleavage positions of their blastomeres (Davidson, 1991; Davidson, Cameron, and Ransick, 1998), thereby facilitating interpretation of mechanisms of spatial change. Also, a well-studied fossil record constrains the dating of evolutionary events (Kroh and A. B. Smith, 2010) and has established that the sister subclasses of sea urchins—cidaroids and euechinoids—diverged from one another at least 268.8 million years ago (mya) (Thompson et al., 2015). And yet, relative to their conspicuously diverged adult body plans, early embryonic development in these two clades is strikingly similar (Gao et al., 2015). This geologically ancient expanse combined with copious change of life history strategies in multiple sea urchin lineages provide a convenient framework, with experimental replicates, to investigate evolution and mechanisms of developmental programs (Wray and Bely, 1994). For indirect developing sea urchins (taxa with feeding larval forms), morphological and developmental heterochronies exhibited by cidaroids and euechinoids have long been a topic of interest, but only recently have become the subject of molecular research (Tennent, 1914; Mortensen, 1938; Schroeder, 1981; Wray and McClay, 1988; Wray and McClay, 1989; Yamazaki, Kidachi, Yamaguchi, et al., 2014; Erkenbrack and Davidson, 2015). Research on the early development of euechinoids has brought into high resolution the players and molecular logic directing the global embryonic developmental GRN that encompasses the varied embryonic domains and subdomains of the purple sea urchin *Strongylocentrotus purpuratus* (Angerer et al., 2000; Davidson, Rast, et al., 2002; Revilla-i-Domingo, Oliveri, and Davidson, 2007; Oliveri, Tu, and Davidson, 2008; Yaguchi et al., 2008; Su, 2009; Peter and Davidson, 2010; Peter and Davidson, 2011a; Materna, Ransick, et al., 2013; Barsi, Li, and Davidson, 2015; Nam et al., 2007). Additionally, abundant comparative evidence exists for other euechinoid taxa, including *Lytechinus variegatus* (Wikramanayake, Huang, and Klein, 1998; Sherwood and McClay, 1999; Logan et al., 1999; Sweet, Gehring, and Ettensohn, 2002; Flowers et al., 2004; Ettensohn et al., 2007; J. C. Croce and McClay, 2010) and *Paracentrotus lividus* (Duboc, Röttinger, Besnardreau, et al., 2004; Duboc, Lapraz, Besnardreau, et al., 2008; Saudemont et al.,

2010; Lhomond et al., 2012; Cavalieri and Spinelli, 2014). Remarkably, although these three indirect-development euechinoid sea urchins diverged from one another approximately 90 mya (Kroh and A. B. Smith, 2010; A. B. Smith et al., 2006), very little appreciable change to developmental GRNs has been observed in their early development (J. Croce, Range, et al., 2011; Ettensohn, 2009; Molina et al., 2013). Two questions arise from this observation: (1) how deep in geological time does this early developmental constraint extend, and (2) does this apparent calcification of GRN circuitry extend to specification of all embryonic domains or merely to some? Answers to these questions would afford fundamental insight into the ability of GRNs to buffer change, the evolutionary dynamics of GRN topology, and whether certain embryonic domains or subdomains have a greater propensity to change in early development than others. Such an analysis might also reveal the precise locations of and frequency in changes to GRN architecture over evolutionary time and would yield a more thorough understanding of the interplay of constraint and evolvability of early developmental programs.

Recently, studies of the cidaroid sea urchin *Eucidaris tribuloides* revealed that mesoderm specification in this clade is markedly different from that observed in euechinoids (Gao et al., 2015; Erkenbrack and Davidson, 2015; Erkenbrack, Ako-Asare, et al., 2016). Spatiotemporal and perturbation analyses of endomesodermal formation in *E. tribuloides* arrived at the conclusion that deployment of mesodermal regulatory factors has diverged more than deployment of endodermal regulatory factors since the cidaroid-euechinoid divergence. These studies provide insight into developmental process at the vegetal pole and bring within reach a global embryonic perspective that would afford a glimpse into rates of change to whole apparatus of developmental GRN throughout the early embryo. Here, I surveyed spatial and temporal expression patterns of non-skeletogenic mesodermal (NSM) and ectodermal regulatory factors in the cidaroid sea urchin *E. tribuloides* (Table 1). This study focused on dorsal-ventral (D-V; also called Aboral-Oral) patterning, which has consequences for both ectoderm and mesoderm. D-V axis specification is a well-documented process in the euechinoid GRN and is a highly conserved developmental mechanism in deuterostomes (Lapraz, Haillot, and Lepage, 2015; Duboc and Lepage, 2008). I present evidence that deployment of the primary regulatory factors specifying the sea urchin mesoderm have diverged substantially in indirect-developing echinoids. These alterations are overrepresented in specification of mesodermal SM and NSM subdomains. However, ectodermal and endodermal domains and subdomains show constraint relative to mesodermal domains. Spatiotemporal dynamics

of regulatory factors involved in *E. tribuloides* D-V axis specification are essentially congruent with that of euechinoids, suggesting constraint on deployment of these factors for sea urchin taxa with indirect-developing, feeding larval life strategies. Thus, I argue that in early development of indirect-developing sea urchins unequal

Gene	Maternal/zygotic	Zygotic activation	Spatial distribution
<i>bra</i>	zygotic	12 hpf	broad in early endomesoderm, then endodermal; perianal ectoderm and ventral ectoderm by mid-gastrula
<i>chordin</i>	zygotic	14 hpf	center of presumptive ventral ectoderm, then expanding slightly to most of presumptive ventral ectoderm
<i>ese</i>	zygotic	8 hpf	broad in ectoderm early; then by early gastrula broadly in NSM and restricted to presumptive ANE; later restricted in archenteron by mesenchyme gastrula and in ANE
<i>foxq2</i>	maternal	6 hpf	broadly in anterior/animal ectoderm early; subsequently restricted to ANE/lateral ectoderm by late blastula
<i>gatac</i>	zygotic	16 hpf	in SM by late blastula and later in NSM as well; later asymmetrical in NSM by gastrula stage
<i>gatae</i>	zygotic	12 hpf	first broadly in endomesoderm, then cleared from SM; later in endoderm and asymmetrical in NSM by gastrula stage
<i>gcm</i>	zygotic	10 hpf	first broadly in mesoderm; later asymmetrical in NSM and in a few ectodermal cells by early gastrula
<i>gsc</i>	zygotic	12 hpf	early spatial not observed; presumptive ventral ectoderm from late blastula onwards
<i>irxa</i>	zygotic	22 hpf	in dorsal ectoderm extending from border of ANE to blastopore; by gastrula stage excluded only from ventral ectoderm and pre-oral ANE
<i>lefty</i>	zygotic	10 hpf	early blastula distribution not observed; presumptive ventral ectoderm by late blastula and onwards
<i>msx</i>	zygotic	20 hpf	pregastrular distribution not observed; dorsal lateral ectoderm by early gastrula
<i>nodal</i>	zygotic	8 hpf	early blastula distribution not observed; center of presumptive ventral ectoderm at SB, expanding slightly to most of ventral ectoderm by gastrula stage
<i>not</i>	zygotic	10 hpf	early blastula distribution not observed; presumptive ventral ectoderm, then also in presumptive ventral mesoderm by mesenchyme gastrula
<i>onecut</i>	maternal	6 hpf	early blastula pattern not observed, by early gastrula in post-oral ventral ectoderm and expanding anteriorly in a band encompassing ventral ectoderm
<i>prox</i>	zygotic	16 hpf	SM early and subsequently in NSM; broadly in mesoderm by mid-gastrula
<i>scl</i>	zygotic	18 hpf	SM early and subsequently in NSM; partially restricted in mesoderm by mesenchyme gastrula
<i>tbx2/3</i>	maternal	8 hpf	early blastula distribution not observed; presumptive dorsal ectoderm by late blastula; later in dorsal lateral ectoderm as well as dorsal archenteron

Table 5.1: Regulatory factors in this study.

rates of change exist at specific nodes of early developmental GRNs. I enumerate specific examples of these changes at every level of GRN architecture. The lability

of developmental GRNs supports the notion that change can occur at all levels of their hierarchy in early development and offers an in principle mechanistic explanation for observations of rapid change to nearly all components of developmental process in the development of direct developing, nonfeeding sea urchins (Wray and Raff, 1991; M. S. Smith, Collins, and Raff, 2009; M. S. Smith, Turner, and Raff, 2008; Raff, 2008). These results suggest that, while early development is dependent on and constrained by cascading, sequential specification events, deployment of early developmental GRNs in bilaterian lineages may be biased towards alterations to specific embryonic domains or developmental programs.

5.3 Results

Dynamics of ectodermal D-V axis regulatory states in the cidaroid *E. tribuloides*

In euechinoids, numerous regulatory factors direct segregation of ectoderm into a diverse set of regulatory states (Molina et al., 2013; Su, 2009; Li, Cui, et al., 2014). *Nodal*, a member of the activin subfamily of the transforming growth factor- β (TGF- β) family of signaling molecules, is a critical factor in establishing dorsal-ventral (D-V) polarity in sea urchins (Duboc, Röttinger, Besnardreau, et al., 2004; Flowers et al., 2004). Nodal signaling directly regulates, among others, *nodal* (itself), *not*, *lefty* and *chordin* (Saudemont et al., 2010; Li, Materna, and Davidson, 2012). In *E. tribuloides*, zygotic transcription of *nodal*, *not* and *lefty* begins by early blastula stage (Figure 5.1A, 5.1B, 5.1C). In contrast, transcriptional activation of *chordin* is delayed by at least 5 hours from this initial cohort, indicative of an intermediate regulator between *nodal* and *chordin* in *E. tribuloides* (Figure 5.1A, 5.1E). From 17 hpf to 40 hpf, spatial expression of *nodal* is observed in a well-defined region in the ventral ectoderm (VE) that expands slightly as gastrulation proceeds (Figure 5.1A1-5.1A4, Figure 5.S1). Unlike *nodal*, the spatial distribution of its targets is not solely restricted to a small field of cells in the VE. *Lefty* (also known as Antivin), an antagonist of *nodal*, exhibits a broader pattern of expression that, by 50 hpf, expands into the ventral side of the archenteron (Figure 5.1B1-5.1B4, Figure 5.S1). Similarly, *chordin* transcripts are detected in VE throughout early *E. tribuloides* development (Figure 5.1E1-5.1E4, Figure 5.S1).

The homeobox gene *not*, known to play a role directly downstream of Nodal signaling in euechinoid D-V ectodermal and mesodermal polarization (Materna, Ransick, et al., 2013; Li, Materna, and Davidson, 2013), was observed spatially in VE during gastrulation, and later extends vegetally towards the perianal ectoderm and is observed in the archenteron (Figure 5.1C1-5.1C4, Figure 5.S1). While I do not

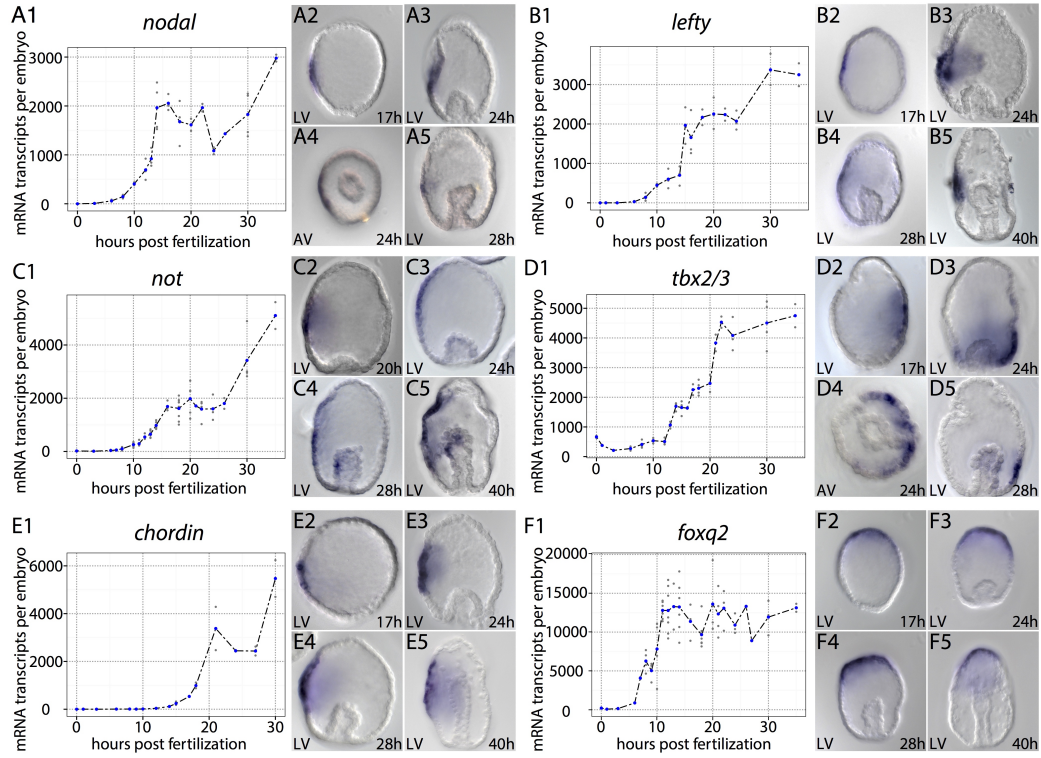


Figure 5.1: Spatiotemporal dynamics in *E. tribuloides* of six regulatory factors involved in euechinoid dorsal ventral (D-V) axis formation. See Materials and Methods for details on data acquisition. **(A1-A5)** *Nodal* is zygotically activated around 8 hpf and spatially restricted to a small field of cells in the ventral ectoderm (VE) up to early-mid gastrula stage. **(B1-B5)** *Lefty* is zygotically activated around 10 hpf and spatially restricted to a small field of cells in VE. **(C1-C5)** *Not* is zygotically activated around 10 hpf and its spatial distribution is first detected in a similar field of cells as nodal and lefty; however, the domain of *not* subsequently expands by 28 hpf where it is seen in the ventral side of the archenteron, where NSM and endoderm have been segregated. By 40 hpf, the spatial domain of *not* extends from ANE to perianal ectoderm, is clearly seen in NSM, and was not detected in endodermal domains. **(D1-D5)** Spatial distribution of *tbx2/3* at 17 hpf is detected broadly in dorsal ectoderm (DE) and later extends from the perianal ectoderm to lateral DE, but not past the embryonic equator. **(E1-E5)** *chordin* is zygotically activated around 14 hpf and is first observed in a few cells in VE at 17 hpf and subsequently expands to extend from the perianal ectoderm to ANE. **(F1-F5)** *Foxq2* is zygotically activated by 6 hpf and is seen broadly distributed in the ectoderm very early in development and is spatially restricted to ANE by 17 hpf.

present the spatial distribution of the critical Nodal-responsive regulatory factor *bmp2/4* here, qPCR timecourse data indicate that *bmp2/4* is upregulated with the *nodal-not-lefty* cohort (Figure 5.S2). In euechinoids, the Bmp2/4 ligand is a direct target of Nodal signaling and is translocated across the embryo to the dorsal

side, where it upregulates dorsal ectoderm (DE) specification genes such as *tbx2/3* (Duboc, Röttinger, Besnardeau, et al., 2004; Lapraz, Besnardeau, and Lepage, 2009; de-Leon et al., 2013). In *E. tribuloides*, *tbx2/3* is transcriptionally active very early with the *nodal-not-lefty* cohort. *Tbx2/3* exhibits spatial expression from late blastula stage onwards that is complementary to VE genes (Figure 5.1D1-5.1D4). By mid-gastrula stage, *tbx2/3* is also expressed in the archenteron and much later, by 70 hpf, is expressed in the bilateral clusters of cells synthesizing the larval skeleton (Figure 5.S1), which is similar to the spatial expression in two euechinoids with notably interesting heterochronic differences (J. Croce, Lhomond, and Gache, 2003; Gross et al., 2003). Lastly, the Forkhead family transcription factor *foxq2* is sequentially restricted to and specifically expressed in embryonic anterior neural ectoderm (ANE) territory in deuterostomes (Range, 2014). In euechinoids, *foxq2* restriction to ANE is a crucial component of D-V axis specification, setting the anterior boundary of VE by restricting expression of *nodal* (Yaguchi et al., 2008; Li, Cui, et al., 2014). In *E. tribuloides*, *foxq2* exhibited an expression pattern consistent with observations in euechinoids and other deuterostomes, suggesting conserved roles for this gene in ANE and D-V specification (Figure 5.1F, Figure 5.S1).

Dynamics of ciliated band regulatory states in the cidaroid *E. tribuloides*

Free-feeding, indirect-developing sea urchins possess a single neurogenic ciliated band (CB) early in development that circumnavigates the larval ventral face and facilitates feeding and locomotion (Strathmann, 1971). This structure has undergone frequent modification in the lineages leading to modern sea urchins, viz. in planktotrophic larvae (Wray, 1992). In euechinoids *goosecoid* (*gsc*), *onecut*, and *irxa* contribute to the geometric patterning of CB formation (Barsi, Li, and Davidson, 2015; Saudemont et al., 2010; Barsi and Davidson, 2016). In euechinoids, *gsc* is expressed in VE and is directly downstream of Nodal signaling on the ventral side of the embryo (Saudemont et al., 2010). *Onecut* (also known as *hnf6*) is a ubiquitous, maternally deposited factor that is restricted to the boundary of VE and DE, at which lies progenitor CB territory; and *irxa* is expressed exclusively in DE downstream of *Tbx2/3* (Saudemont et al., 2010; Poustka et al., 2007). In the cidaroid *E. tribuloides*, *gsc* is zygotically expressed with the *nodal-not-lefty* cohort by 12 hpf and is specifically expressed in VE (Figure 5.2A, Figure 5.S3).

Onecut is also a maternally deposited factor in *E. tribuloides*; early *onecut* spatial expression was difficult to interpret, as staining was only observed much later in development in a restricted band of cells encircling the VE. The spatial dynamics of

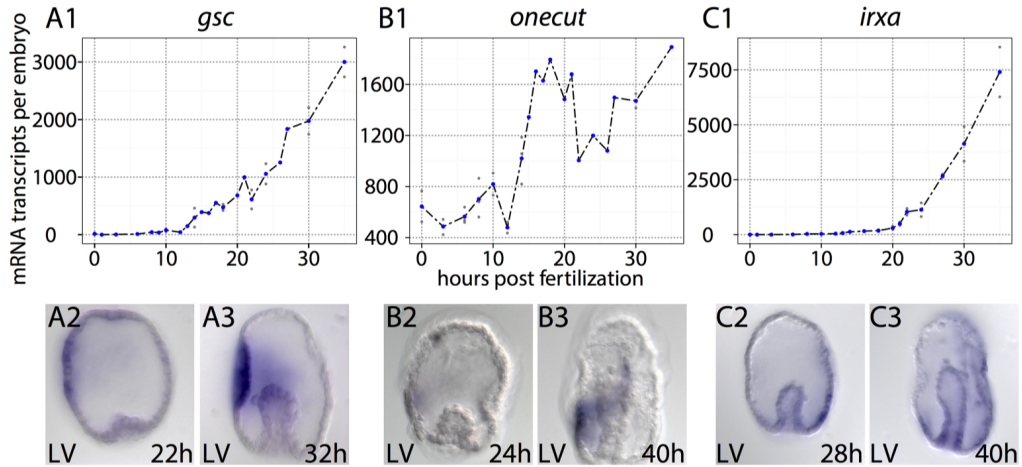


Figure 5.2: Spatiotemporal dynamics in *E. tribuloides* of three regulatory factors involved in euechinoid ciliary band (CB) formation. See Materials and Methods for details on data acquisition. **(A1-A3)** *Gsc* is zygotically activated around 12 hpf and from 22 hpf to 32 hpf is observed exclusively in ventral ectoderm. **(B1-B3)** Spatial distribution of *onecut* is negligible at 22 hpf though qPCR evidence indicates that there is abundance mRNA transcripts present, suggesting it may be ubiquitously expressed. By 40 hpf *onecut* is detected in the future post oral CB and is extending in a band towards ANE. **(C1-C3)** *Irxa* is zygotically activated by 22 hpf and by 28 hpf is detected in dorsal ectoderm, extending from the vegetal endodermal domains to ANE. By 40 hpf *irxa* is seen extending from a region proximal and circumnavigating ventral ectoderm thru ANE.

onecut in *E. tribuloides* is quite remarkable; however, insofar that whole-mount *in situ* hybridization (WMISH) timecourse revealed that its activation unfolds slowly and in a sequential manner that begins in the progenitor field of post oral CB and subsequently extends in a narrow band of 4-8 cell diameters towards progenitor pre oral CB (Figure 5.2B, Figure 5.S3). This observation is in stark contrast to that in euechinoids, in which *onecut* is observed to be ubiquitously expressed early and later delimited to the CB territory by transcriptional repressors in the VE and DE (Barsi, Li, and Davidson, 2015; Otim et al., 2004). *Irxa* initiates zygotic expression at mid-blastula stage (14 hpf) in *E. tribuloides*, and by 28 hpf is observed broadly in DE (Fig 5.2C). Unlike in euechinoids, *irxa* is broadly distributed in DE—much more so than *tbx2/3*—indicating that it is likely broadly activated in the ectoderm and repressed in VE and ANE. The spatial distributions of *gsc*, *onecut*, and *irxa* are highly suggestive of a conserved regulatory apparatus that spatially restricts CB to the boundary of VE and DE. To test for this, I assayed a series of endogenous and site-directed mutagenesis *onecut* BACs from *S. purpuratus* by

microinjection [67]. Remarkably, a BAC that has been shown to recapitulate the endogenous *S. purpuratus onecut* expression pattern faithfully expressed reporter GFP in the CB of *E. tribuloides* (Figure 5.S4). Further, a BAC harboring mutated repressor sites for the ventral repressor Gsc repeatedly exhibited ectopic expression in VE of *E. tribuloides* (Figure 5.S4). Taken together, the early specification of CB regulatory factors suggests divergence of initial activation and spatial distributions of *onecut* and *irxa* and is consistent with conserved circuitry of *gsc*. Later, *E. tribuloides* CB patterning exhibits congruence with spatial expression patterns and circuitry observed in euechinoids, suggesting stage-specific constraint during larval morphogenesis.

Dynamics of non-skeletogenic mesoderm regulatory states in the cidaroid *E. tribuloides*

Non-skeletogenic mesoderm (NSM) in euechinoids arises at the vegetal plate from early cleavage endomesodermal precursors and gives rise to four different cell types: blastocoelar cells, pigment cells, circumesophageal cells, and coelomic pouch cells (Cameron and Davidson, 1991). Experimental observations indicate that euechi-noids completely rely on presentation of Delta ligand in the adjacent SM to upregulate NSM regulatory factors in veg2 endomesodermal cells (Sherwood and McClay, 1999; Sweet, Hodor, and Ettensohn, 1999; Sweet, Gehring, and Ettensohn, 2002; Materna and Davidson, 2012). As gastrulation begins, euechinoid NSM has already become segregated into dorsal NSM and ventral NSM in response to Nodal signaling from VE (Materna, Ransick, et al., 2013; Duboc, Lapraz, Saudemont, et al., 2010). Mesodermal patterning in *E. tribuloides* also depends on Notch signaling, though by restricting SM fate to the micromere-descendants and, strikingly, not affecting the early expression of *gcm*, a regulatory factor involved in NSM segregation and pigment cell specification (Erkenbrack and Davidson, 2015). In *E. tribuloides*, *ese* and *gcm* are early euechinoid NSM regulatory factors that are zygotically activated at late cleavage/early blastula stage (Figure 5.3A, 5.3D).

In contrast to *S. purpuratus* spatial distribution, *ese* in *E. tribuloides* is observed both in the ANE and the NSM simultaneously (Figure 5.3A1-5.3A4, Figure 5.S5) (Rizzo et al., 2006). Indeed, very early in development *ese* is exclusively in an-imal blastomeres and later becomes zygotically expressed in NSM progenitors at the vegetal pole (Figure 5.S5). In NSM, *ese* expression first occurs broadly just prior to the onset of gastrulation and is subsequently restricted to one side of the archenteron (Figure 5.3A1-5.3A4). *Gcm* is co-expressed with *alx1* and *delta* in

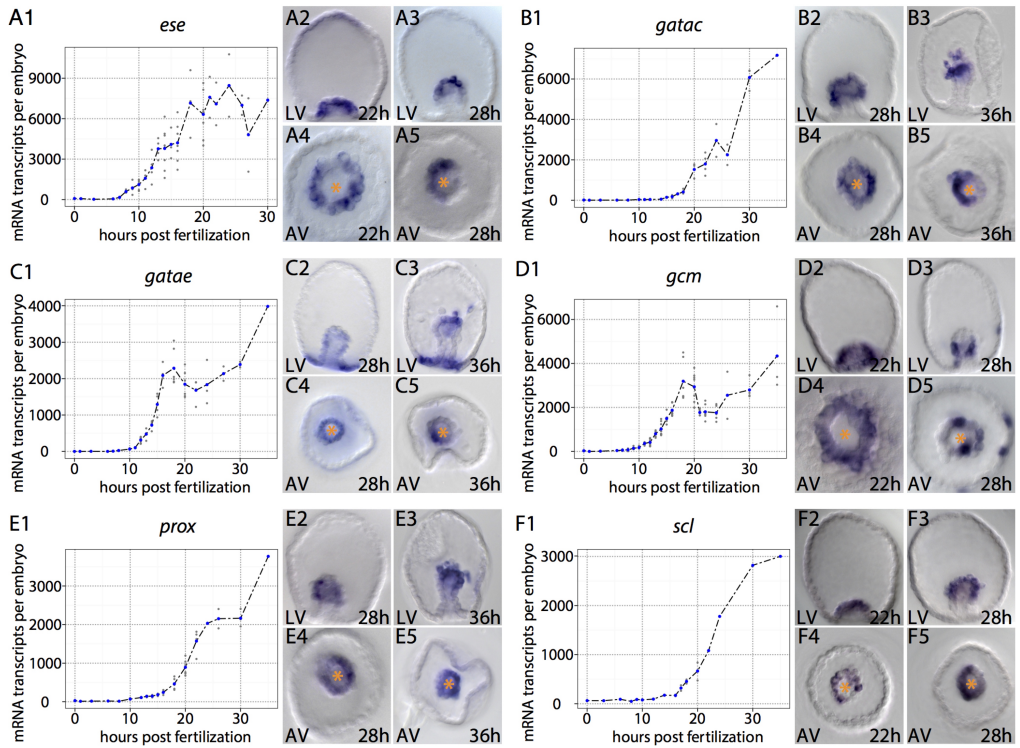


Figure 5.3: Spatiotemporal dynamics in *E. tribuloides* of six regulatory factors involved in euechinoid non-skeletogenic mesenchyme (NSM) domains. **(A1-A5)** *Ese* is zygotically activated by 8 hpf and by 22 hpf is detected in both the NSM and ANE. By 28 hpf, *ese* is observed asymmetrically polarized in NSM at the tip of the archenteron. **(B1-B5)** *Gatac* is zygotically activated by 16 hpf and by 28 hpf is expressed throughout the mesoderm and does not show polarity. By 36 hpf, *gatac* is detected in ingressing cells and is showing polarity at the tip of the archenteron. **(C1-C5)** *Gatae* is zygotically activated by 12 hpf and by 28 hpf is detected throughout the endomesoderm. Later at 36 hpf *gatae* is cleared from progenitor foregut endodermal domains and is expressed at the blastopore, in ingressing mesenchymal cells and at the tip of the archenteron, where it is polarized. **(D1-D5)** *Gcm* is zygotically activated by 10 hpf and as gastrulation begins is expressed broadly in NSM; however, by 28 hpf it is polarized in a field of cells that is proximal to the archenteron tip. *Gcm* is also observed in a few ectodermal cells prior to mesenchymal ingression. **(E1-E5)** *Prox* is zygotically activated by 16 hpf and its spatial distribution is throughout NSM at 28 hpf. By 36 hpf it is expressed in ingressing mesenchymal cells and polarity is not yet observed in NSM. **(F1-F5)** *Scl* is zygotically activated by 18 hpf and is observed throughout NSM at 22 hpf (though not in SM). At 28 hpf it is expressed in ingressing mesenchyme and throughout NSM, where it is polarized.

SM very early in development. After gastrulation begins, *gcm* is expressed transiently in ventral and dorsal NSM, and by 28 hpf is restricted to a cluster of cells just below the tip of the archenteron (Figure 5.3D1-5.3D4).

Later this expression is seen solely on one side of the archenteron as *gcm*-positive cells ingress rapidly into the blastocoel at 36 hpf (Figure 5.S5). In contrast to its spatial expression in euechinoids and similar to its expression in asteroids (Ransick, Rast, et al., 2002; Hinman and Davidson, 2007), *gcm* in *E. tribuloides* is upregulated in the ectoderm at late blastula/early gastrula stage (Figure 5.S5). While I cannot definitively preclude the possibility that these *gcm*-positive cells are mesodermal in origin, all observations of and experimental data on *E. tribuloides* supports the notion that SM is the first mesodermal lineage to ingress at 28 hpf. The data presented here are at least 6 hours prior to this initial ingestion event and are highly supportive of the hypothesis that *gcm* is activated in the ectoderm at the onset of gastrulation. Directly downstream of *gcm* in euechinoids is *gatae* (Materna, Ransick, et al., 2013). In both cidaroids and euechinoids, *gatae* is observed in the endomesoderm early in development (Lee and Davidson, 2004) [Erkenbrack, Davidson, Peter, forthcoming]. In *E. tribuloides* NSM, *gatae* is expressed throughout the endomesoderm at the time of SM ingestion (28 hpf) and later is observed restricted to one side near the tip of the archenteron, as well as in the second wave of ingressing mesenchyme (Figure 5.3C1-5.3C4). *Gatac* (*gata1/2/3*), *prox* and *scl*, all of which are ventral NSM genes in euechinoids (Materna, Ransick, et al., 2013), come off the baseline at similar times in *E. tribuloides* and are detectable by 18 hpf by WMISH (add to supp or unpublished data?). Of these three genes, *scl* was the first to show D-V NSM polarity followed by *gatac* (Figure 5.3B1-5.3B4, 5.3F1-5.3F4). Surprisingly, by 36 hpf *prox* did not exhibit an expression pattern that clearly indicated D-V polarity (Figure 5.3E1-5.3E4), suggesting that either *prox* is a general mesodermal regulatory factor in *E. tribuloides* or it is spatially restricted later in its development.

Double fluorescent WMISH (dfWMISH) indicate that *ese* is spatially restricted to the opposite side of *gcm* (Figure 5.S5), suggesting that diversification of at least two NSM regulatory states is underway by the time SM ingestion commences (28 hpf). The observation that *ese* is restricted to ventral NSM and *gcm* to dorsal NSM (Materna, Ransick, et al., 2013) is consistent with data in euechinoids. However, in *E. tribuloides* it is clear from the preceding data that the archenteron harbors multiple NSM regulatory states and that the sequential segregation of this territory is markedly different from that in euechinoids.

Effects of perturbation of D-V axis specification on ectodermal regulatory factors in *E. tribuloides*

The spatiotemporal data presented thus far are highly suggestive that D-V axis specification, as well as gastrular CB formation, in *E. tribuloides* is consistent with similar processes in euechinoids and that NSM specification has ostensibly diverged. To establish differences in the topology of these developmental GRNs, perturbation experiments disrupting initial inputs into D-V axis specification were conducted. In euechinoids, the primary molecular event responsible for animal-vegetal (A-V) axis polarity is nuclearization of β -catenin in micromere nuclei at the vegetal pole, and, unexpectedly, these experiments showed that perturbation of A-V axis formation disrupted D-V axis specification (Wikramanayake, Huang, and Klein, 1998; Logan et al., 1999). One mechanism underlying the crosstalk of these two deuterostome specification events was found to be restriction of *foxq2* to ANE, as its presence in VE blocked *nodal* transcription (Yaguchi et al., 2008). To test for this GRN linkage, I overexpressed dn-Cadherin RNA in *E. tribuloides* to block nuclearization of β -catenin at the vegetal pole. As in euechinoids, this perturbation led to upregulation of *foxq2*, whereas *nodal* and its euechinoid downstream components of D-V axis GRN circuitry—e.g. *bmp2/4*, *not*, and *tbx2/3*—were strongly downregulated (Figure 5.4A). This result suggests that the molecular crosstalk between and GRN topology of β -catenin/TCF, Foxq2 and Nodal signaling are conserved between euechinoid and cidaroid echinoids.

Next, I aimed to determine the spatiotemporal effects of perturbation of D-V specification by culturing *E. tribuloides* embryos in the presence of SB43152, a small molecule antagonist of the TGF- β (Nodal) receptor Alk4/5/7 (Duboc, Röttinger, Lapraz, et al., 2005). At four days post fertilization, these embryos exhibited strong dorsalization, archenterons that failed to make contact with VE, and supernumerary skeletal elements (Figure 5.4B). Quantitative PCR (qPCR) analysis at four different timepoints in *E. tribuloides* development showed strong downregulation of VE regulatory factors *chordin*, *gsc*, *lefty*, *nodal*, and *not* (Figure 5.4C). This result was confirmed spatially by WMISH for mRNA transcripts of *chordin*, *nodal*, and *not* (Figure 5A, 5B). Another critical VE regulatory factor is the secreted TGF- β ligand Bmp2/4. This gene was clearly not affected to the same degree as the aforementioned cohort of VE factors (Figure 5.4C). This result is strikingly different from the strong downregulation of *bmp2/4* observed in the euechinoid *P. lividus* when it was cultured in the presence of SB431542 or when injected with Nodal morpholino (MASO) (Duboc, Röttinger, Besnardreau, et al., 2004; Saudemont et al.,

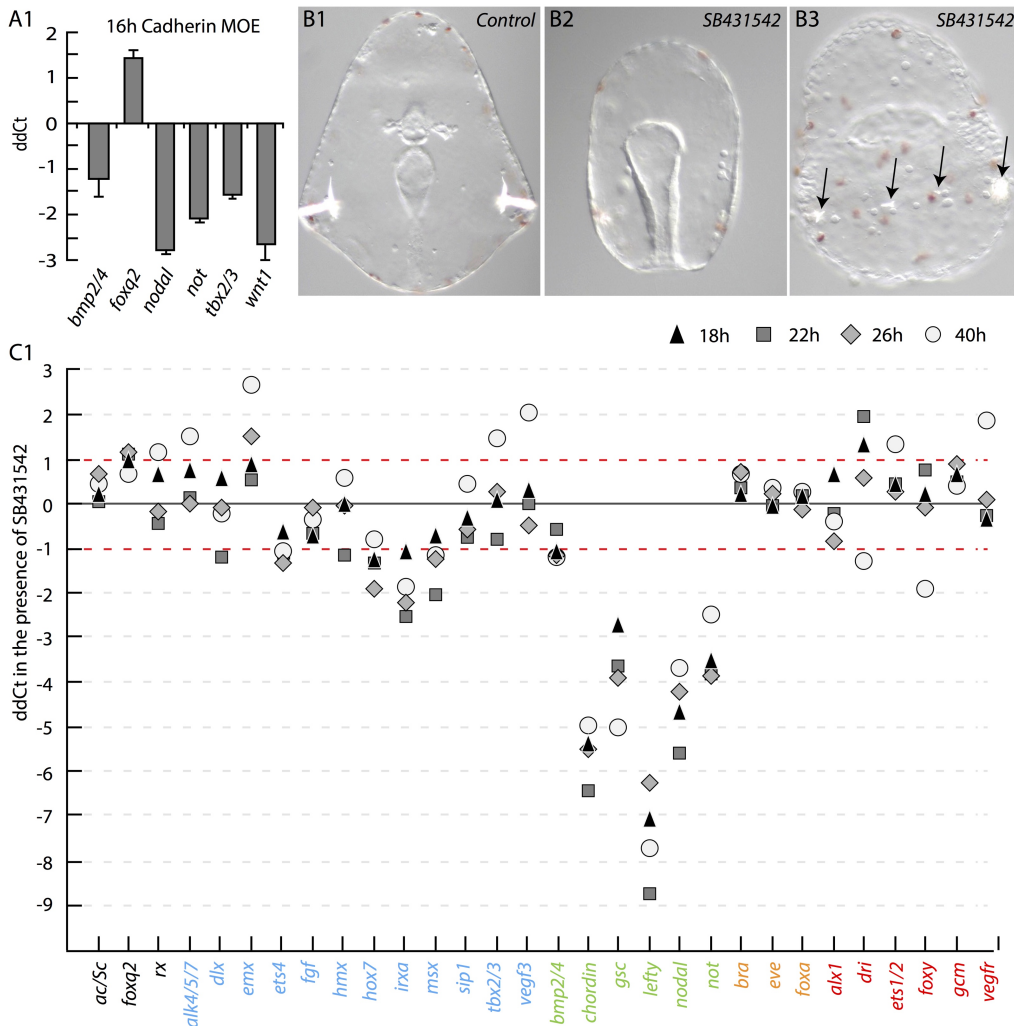


Figure 5.4: Early inputs and dynamics of dorsal-ventral (D-V) axis formation in *E. tribuloides* as revealed by cadherin mRNA overexpression (MOE) and development in the presence of the *alk4/5/7* small molecule inhibitor SB431542. **(A)** Cadherin MOE affects *nodal* and its downstream targets. ddCt values are listed on the y-ordinate. When cadherin is overexpressed in *E. tribuloides*, *nodal* and its targets are strongly downregulated. **(B1-B3)** Effect of SB431542, a small molecule antagonist of Nodal receptor *alk4/5/7*, on *E. tribuloides* embryogenesis. At 120 hpf, *E. tribuloides* shows two skeletal rods extending anteriorly and orally. When cultured in 15 μ M SB431542, *E. tribuloides* embryos are dorsally radialized and exhibit serial centers of spiculogenesis (black arrows). **(C)** Effect of SB431542 on expression of regulatory factors *E. tribuloides* as revealed by qPCR. Two timepoints from two independent replicates are shown. Regulatory factors are listed on the x-axis and font color designates their embryonic domain: black, ANE; blue, DE; green, VE; yellow, endoderm; red, mesoderm.

2010). Lastly for VE, this quantitative assay does not indicate disturbance in the regulation of *brachyury* (*bra*) and *foxa*, two euechinoid stomodeum (larval mouth) regulatory factors strongly downregulated upon Nodal perturbation in euechinoids (Figure 5.4C) (Saudemont et al., 2010; Oliveri, Walton, et al., 2006). However, there is a clear heterochrony in the onset of *bra* and *foxa* in VE of *E. tribuloides* as stomodeum-specific genes such as these are not activated in VE until, at least for *brachyury*, around 36 hpf in *E. tribuloides* development (Figure 5.S1). Notably, *foxa* expression was never observed in the *E. tribuloides* stomodeum up to 40 hpf.

On the dorsal side, a striking difference is the effect of this treatment on regulatory factor *tbx2/3*. In euechinoids, *tbx2/3* is downstream of Bmp2/4 ligand, which diffuses from VE to DE (Lapraz, Besnardieu, and Lepage, 2009; de-Leon et al., 2013; Bradham et al., 2009). Treatment of *P. lividus* embryos with SB431542 inhibitor completely and specifically extinguishes *tbx2/3* in DE while not interfering with its SM expression (Saudemont et al., 2010). In *E. tribuloides*, qPCR data suggest SB431542 inhibitor has no effect on *tbx2/3* regulation (Figure 5.4C). However, when I assayed *tbx2/3* by WMISH, its spatial distribution expanded into VE (Figure 5.5A, 5.5B). Similarly, whereas in *E. tribuloides* qPCR data indicate strong downregulation of the DE regulatory factor *irxa* (Figure 5.4C), its domain of expression expanded into VE in *P. lividus* embryos upon SB431542-treatment (Saudemont et al., 2010). These results suggest distinct GRN topologies exist immediately downstream of the initial *nodal* and *bmp2/4* circuitry in echinoids.

The preceding results detailing the effect of SB431542 on specification of VE and DE in *E. tribuloides* suggest that cidaroids and euechinoids share multiple transcriptional targets directly downstream of Nodal signaling in VE. However, the notable exception in the euechinoid VE cohort is *bmp2/4*, the spatial expression of which has not been detailed in *E. tribuloides* and was not detailed in this study. In DE it would appear that multiple euechinoid GRN linkages are different in *E. tribuloides*, including the spatial regulation of *tbx2/3* and *irxa*. Taken together these results suggest that the initial specification of regulatory factors immediately downstream of Nodal in euechinoid VE exhibit similar deployment than regulatory interactions that are immediately downstream of the ventral to dorsal signal.

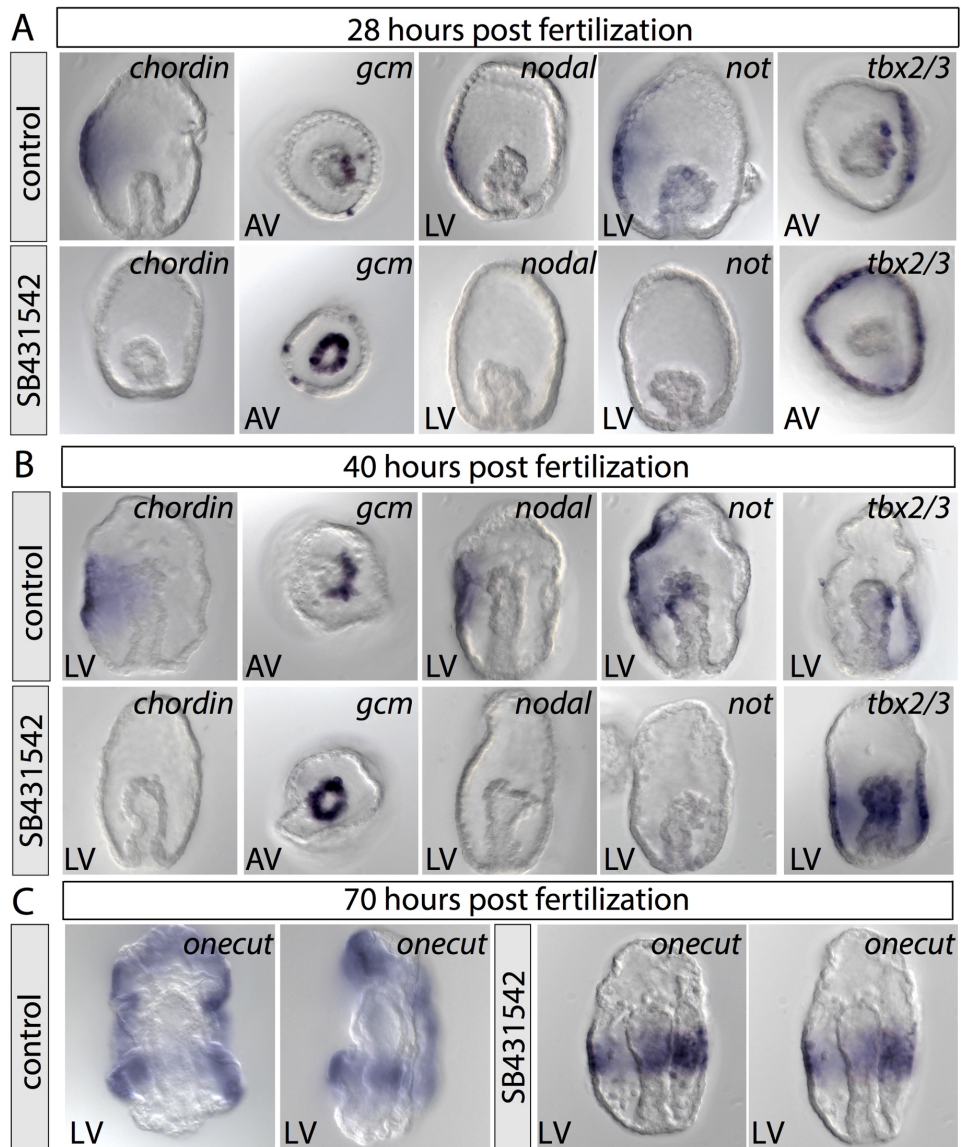


Figure 5.5: Spatial effect of SB431542 on expression of selected regulatory factors involved in ectodermal, mesodermal and ciliary band formation in *E. tribuloides*. **(A)** At 28 hpf expression of *chordin*, *nodal*, and *not* are completely extinguished. Whereas NSM regulatory factor *gcm* is regularly restricted to one side of the archen-teron, in the presence of SB431542 it exhibits expression throughout the archenteron. In the ectoderm, expression of DE regulatory factor *tbx2/3* expands into VE in the presence of the inhibitor. **(B)** Similar results were obtained for these regulatory factors at 40 hpf. **(C)** Endogenous expression of *onecut* is normally observed in a band of cells between the boundaries of VE and DE. However, in the presence of SB431542, *onecut* is expressed in an equatorial band that is 6-10 cell diameters across.

Effects of perturbation of D-V axis specification on mesodermal regulatory factors in *E. tribuloides*

In euechinoids studied thus far, polarity in NSM (D-V) lineages is also regulated by regulatory factors downstream of Nodal signaling (Materna, Ransick, et al., 2013; Duboc, Lapraz, Saudemont, et al., 2010). In *E. tribuloides*, qPCR data did not indicate consistent differences in mRNA abundance for NSM regulatory factors (Figure 5.4C). However, WMISH assays revealed that embryos treated with SB431542 failed to restrict *gcm* to the dorsal side (Figure 5A, 5B). This observation is consistent with the euechinoid GRN linkage of the Nodal-responsive *not* repressing dorsal NSM in the ventral-facing region of the archenteron (Materna, Ransick, et al., 2013). Indeed, in *E. tribuloides*, *not* can be seen observed in the archenteron throughout gastrulation (Figure 5.1C2-5.1C4). However, upon disruption of the Nodal signal, *not* expression is extinguished and *gcm* is not properly restricted (Figure 5.5A, 5.5B). These observations are consistent with a conserved role for Nodal signaling in NSM segregation in the archenteron of *E. tribuloides*.

Lastly, CB formation in euechinoids is dependent on repression of *gsc* in VE and *irxa* in DE (Saudemont et al., 2010; Barsi and Davidson, 2016). While little is known about CB formation in *E. tribuloides*, recent work indicated that *Onecut* is expressed in CB and that disruption of endomesoderm formation by treatment with zinc resulted in embryos exhibiting a ring of highly concentrated proneural Synaptotagmin-B positive cells at the equator of the embryo (Bishop et al., 2013). This result is remarkably similar to that shown in Figure 5.5C, which shows *onecut* mRNA transcripts detected by WMISH in an equatorial band in *E. tribuloides* embryos cultured with SB431542. Thus, by blocking D-V axis specification in *E. tribuloides*, embryos produce a single proneural CB encircling the embryo at the equator. However, this perturbation is drastically different in euechinoids, where treatment with SB431542 or injection of Nodal MASO markedly increases *onecut* expression throughout the ectoderm (Bradham et al., 2009). However, this is not the case in cidaroids, as perturbation data presented here and elsewhere (Bishop et al., 2013) suggest that, in the absence of proper D-V patterning, a proneural CB appears only at the equator in the cidaroid sister-clade. These conflicting results are consistent with the hypothesis that there are anteriorly positioned regulatory factors repressing *onecut* in cidaroids.

Comparative analysis of global developmental GRN dynamics in early echinoid embryos

Next I undertook a statistical comparative analysis between *E. tribuloides* and two euechinoids that would inform hypotheses on correlation of transcriptional activity of GRN regulatory factors and global developmental GRN topology. While there are multiple datasets published with timecourse data of transcript abundance in *S. purpuratus* (Materna, Nam, and Davidson, 2010; Tu, Cameron, and Davidson, 2014), until recently there were no large datasets for other euechinoids. However, a high density timecourse dataset of temporal expression dynamics and initiation times was recently published for early regulatory factors operating in *P. lividus*, and their inclusion with *S. purpuratus* data provided the foundation for a comparative analysis between three species (Gildor and de-Leon, 2015). To conduct this analysis, distinct ontogenetic rates between the species were corrected for by comparing the timing of major developmental events, e.g. gastrulation, between the species, and relative transcript abundance in each species combined with Spearman's rank correlation coefficients (ρ) were compiled for orthologues. Previous analyses had already posited the absence of a double-negative gate in cidaroids (Yamazaki, Kidachi, Yamaguchi, et al., 2014; Erkenbrack and Davidson, 2015), an observation that even without additional data supports the notion of large scale rewiring at the top of the SM GRN hierarchy. To determine if altered deployment of early GRN topologies is the rule and not the exception for early patterning of embryonic territories in echinoids, an analysis of 18 regulatory factors in *E. tribuloides*, *P. lividus*, and *S. purpuratus* was conducted. Plotting relative mRNA transcriptional dynamics for the three species were indicative of compelling correlation for ectodermal and endodermal regulatory factors and supported the notion of poor correlation for regulatory factors driving mesoderm specification (Figure 5.6).

To provide further support for the hypothesis of domain-specific change to GRN topology, a two-species comparison between *E. tribuloides* and *S. purpuratus* was conducted to analyze an increased sample size of 34 regulatory genes, the spatial distributions of which are all known in *S. purpuratus* and *E. tribuloides*. Spearman's rank correlation coefficients (ρ) were calculated pairwise for each orthologue. Values for ρ were then binned by their embryonic domain of expression in *S. purpuratus*. Comparison of the domain-specific ρ of regulatory factors expressed in each of the three canonical bilaterian embryonic domains (germ layers) against the mean of all ρ values, regulatory genes expressed in both *S. purpuratus* and *E. tribuloides* endoderm and ectoderm exhibited significantly higher ρ relative to the mean of all ρ

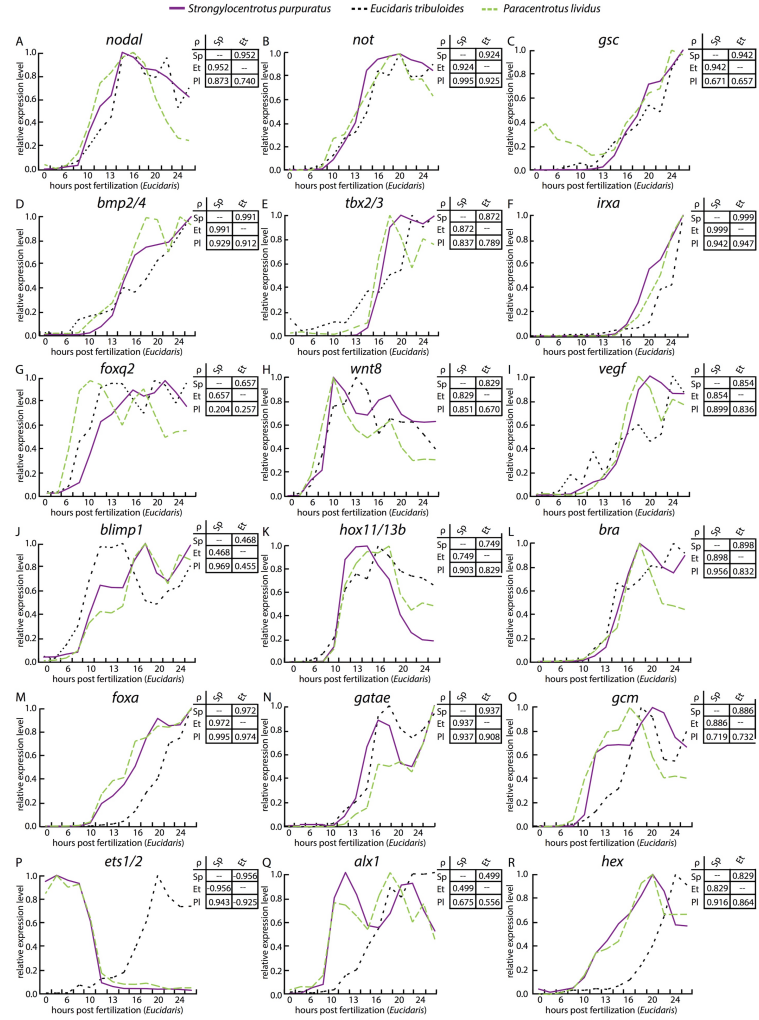


Figure 5.6: Comparative analysis of relative gene expression of early GRN regulatory factors expressed in each embryonic tissue layer in three different species of echinoids. Transcripts per embryo for each gene were normalized to their maximal expression over the first 30 hours of development and are plotted against *E. tribuloides* development on the x-ordinate. Comparative developmental staging for each species is listed in Supplemental Table 5.S4. Each analysis is accompanied by a matrix of Spearman correlation coefficient (marked as greek ρ). *S. purpuratus*, purple line; *P. lividus*, green dashed line; *E. tribuloides*, black dashed line.

values, suggesting strong conservation of transcriptional dynamics of these factors in echinoids (Figure 5.7A). However, regulatory factors expressed in *S. purpuratus* and *E. tribuloides* mesodermal germ layers did not depart significantly from the ρ mean, suggesting transcriptional dynamics of mesodermal regulatory factors have changed markedly since the cidaroid-euechinoid divergence (Figure 5.7A). To determine whether mesodermal subdomains had undergone changes to GRN de-

ployment, regulatory factors were further binned into embryonic subdomains. This finer-scale analysis revealed that whereas both SM and NSM regulatory factors showed significant variation in their transcriptional dynamics relative to the mean of all ρ values, the SM showed significantly more variation than the NSM (Figure 5.7B). In contrast to this, deployment of subdomains of ectodermal and endodermal regulatory factors exhibit statistically significant departures from the mean of all ρ values (Figure 5.7B).

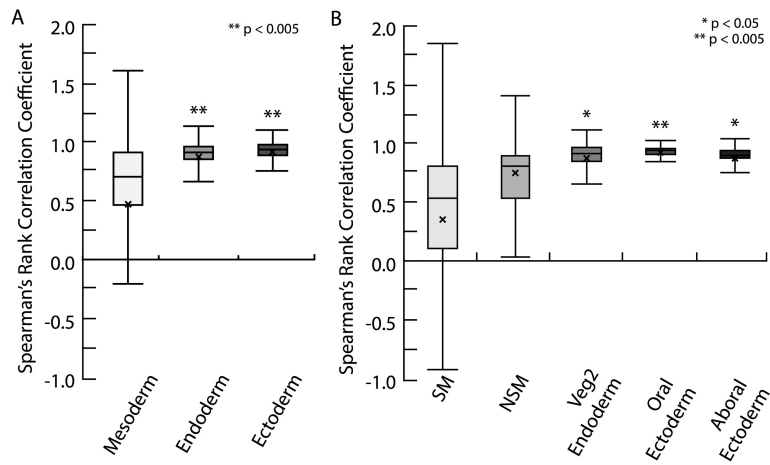


Figure 5.7: Distribution plots of Spearman's rank correlation coefficients (ρ) for *E. tribuloides* and *S. purpuratus* regulatory factors binned by embryonic domain of expression observed in *S. purpuratus*. Boxplot boundaries show interquartile range, means and standard deviation. Asterisks mark statistical significance as determined by a two-tailed t-test. **(A)** Boxplots for statistical distribution of endodermal, ectodermal and mesodermal regulatory factors in *E. tribuloides* and *S. purpuratus*. Mean ρ values for endodermal and ectodermal regulatory factors were significantly higher than the mean of all ρ values. Mesodermal regulatory factors did not significantly vary from the mean. **(B)** Boxplots for statistical distribution of subdomains of endodermal, ectodermal and mesodermal regulatory factors in *E. tribuloides* and *S. purpuratus*. Whereas veg2 endoderm and ventral and dorsal ectodermal domains were showed statistically significant differences from the mean, both skeletogenic and non-skeletogenic regulatory factors did not differ significantly from the mean of all ρ values.

5.4 Discussion

Divergence of embryonic domain specification in early development of echinoids

Since the divergence of cidaroids and euechinoids at least 268.8 mya, echinoid developmental GRNs have significantly diverged, as shown above by the large-scale survey of regulatory factors establishing D-V polarity in mesoderm and ectoderm

of *E. tribuloides*. Importantly, these networks are not so dissimilar as to be unrecognizable. Indeed, at all levels of GRN deployment there exist commonalities. By contrasting these observations with those in other echinoderms, we can begin to appreciate the degree to which embryonic developmental GRNs are constrained or malleable over vast evolutionary distances and can reconstruct the ancestral regulatory states that must have existed in the embryos of echinoderm ancestors (Erkenbrack, Ako-Asare, et al., 2016).

Regulatory states and polarity of NSM in *E. tribuloides*

The most conspicuous morphological differences during embryogenesis of cidaroids and euechinoids are the asymmetric cleavage of micromeres and the heterochrony of primary mesenchymal ingressions. Euechinoids exhibit asymmetric cleavage of vegetal blastomeres at 4th and 5th cleavage to yield large micromeres and small micromeres. Large micromeres present the Delta ligand to immediately adjacent cell layers, which give rise to mesodermal NSM anteriorly and the small micromere quartet (SMQ) posteriorly. In mesodermal NSM, *gcm* is directly downstream of Notch signaling and is restricted to dorsal NSM by the time that SM ingresses into the blastocoel prior to gastrulation (J. C. Croce and McClay, 2010; Duboc, Lapraz, Saudemont, et al., 2010; Ransick, Rast, et al., 2002; Ransick and Davidson, 2006). In cidaroids, mesodermal polarity of *gcm* occurs 4-6 hours prior to SM ingestion and does not occur until after gastrulation has begun. Thus, if *gcm* is near the top of the NSM GRN in cidaroids [19], as is the case in euechinoids (Ransick and Davidson, 2006), then this pregastrular NSM polarization can be viewed as a euechinoid synapomorphy. This hypothesis is supported by the observation that no significant polarity occurs in mesodermal specification in holothuroids (McCauley et al., 2012). Two observations make it likely that euechinoid regulatory linkages mediating *gcm* polarization via the transcription factor Not (Materna, Ransick, et al., 2013) are likely to exist in *E. tribuloides* as well: (1) *not* expression is observed at on the ventral side of the archenteron by early gastrula stage when *gcm* is spatially restricted (Figure 5.1C1, Figure 5.3D1-5.3D4) and (2) dorsal localization of *gcm* does not obtain when D-V axis patterning is perturbed (Figure 5.5A). Together these observations suggest a conserved role for VE regulatory factors in patterning the NSM of echinoids and that, in the lineage leading to modern euechinoids, deployment of GRN circuitry polarizing NSM underwent a heterochronic shift in the lineage leading to euechinoids.

Intriguingly, *gcm* expression is observed in the ectoderm prior to SM ingestion.

One hypothesis that would explain this observation in *E. tribuloides* is that NSM ingresses prior to SM ingress. However, as *gcm*-expressing cells have never been observed in the blastocoel prior to 30 hpf, these cells would not express *gcm* until they intercalate into ectoderm. This scenario is very unlikely, though, given that numerous independent observations show that the primary mesenchymal ingress event in *E. tribuloides* is executed by SM and occurs only after the archenteron has extended considerably into the blastocoel (Tennent, 1914; Mortensen, 1938; Schroeder, 1981; Wray and McClay, 1988; Erkenbrack and Davidson, 2015; Urben, Nislow, and Spiegel, 1988). A competing hypothesis is that ectodermal *gcm* expression in *E. tribuloides* is evolutionarily related to *gcm* expression seen in late blastula stages of asteroids (Hinman and Davidson, 2007). Indeed, follow up experiments indicated that perturbation of Notch signaling increased the spatial domain of ectodermal *gcm* and resulted in supernumerary pigment cell formation (Figure 5.S6). These observations support the hypothesis that *gcm* in *E. tribuloides* has roles both in mesodermal NSM and ectoderm. If this is the case, two more things are clear evolutionarily: (1) *gcm* was likely expressed in the ectoderm in the echinozoan ancestor at least 481 mya; and (2) the lineage leading to camarodont euechinoids lost ectodermally-derived *gcm* activity, which may have been a consequence of the endomesodermal Notch-dependent *gcm* linkage now observed. Further investigation disentangling the roles of *gcm* in cidaroids will provide insight into how the regulation and function of this gene has evolved in echinoderms.

The data presented on D-V polarity in the NSM of *E. tribuloides* suggest that multiple regulatory domains unfold at and around the tip of the archenteron as gastrulation proceeds. Similar to euechinoids, this study determined that *ese* operates in the ventral NSM exclusive of *gcm* in the dorsal NSM. While the regulatory states in *E. tribuloides* NSM need further refinement by two-color WMISH, for our purposes the overt disorder in its formation relative to the overt order of *S. purpuratus* NSM makes two salient points. First, early pregastrular or early gastrular polarity of NSM regulatory states represents an echinoid novelty, as no evidence for early mesodermal polarity exists in outgroup echinoderms (McCauley et al., 2012; Dylus et al., 2016). Second, if we take *E. tribuloides* as a proxy to the ancestral state for this character/regulatory state, then it is clear that the D-V polarity observed in the euechinoid NSM was shifted to occur prior to gastrulation in the lineage leading to modern euechinoids. On the other hand, an alternate evolutionary scenario is that NSM polarity manifested in these two modern echinoids is the result of two independent evolutionary trajectories with heterochronic and spatial differences,

but both meeting a similar end in the diversification of NSM cell types in early development. That at least two D-V regulatory states are common to these embryos and that *gcm* is downstream of Nodal and Notch signaling provide support for the first scenario. Further investigation into the developmental timing and regulatory states of cidaroid NSM will be required to parse out the most likely evolutionary scenario.

Ectodermal regulatory states in *E. tribuloides*

Correspondence between *E. tribuloides* and euechinoids in deployment of ectodermal regulatory factors provides support to the idea that ectodermal specification is constrained and that alteration to the circuitry is nontrivial in early development. However, major alterations have occurred to ectodermal patterning pathways in regards to deployment and rewiring of circuitry during the evolution of euechinoid lineages that possess direct-developing, non-feeding larvae (M. S. Smith, Turner, and Raff, 2008; Wilson, Andrews, and Raff, 2005; Wilson, Andrews, Turner, et al., 2005; Raff and M. S. Smith, 2009). These observations support the idea that the pressures of selection can overwhelm strong evolutionary constraint in early development. Of course there are very interesting differences in *E. tribuloides* ectodermal spatiotemporal dynamics and regulatory states relative to euechinoids. For instance, perturbation of Nodal signaling reveals that, while initial specification events are highly similar, alterations likely have occurred to the regulation of *bmp2/4* and *tbx2/3*. In *E. tribuloides* *tbx2/3* is expressed in DE and dorsal NSM by mid-gastrula. By late gastrula, it is expressed in the lateral clusters of skeletogenic synthesis, at the tip of the gut, in the gut endoderm, and residually in the ectoderm. This unfolding pattern of *tbx2/3* expression in *E. tribuloides* has essentially been compressed into the early stages of euechinoid development (J. Croce, Lhomond, and Gache, 2003). In euechinoids, perturbation of Nodal signaling with SB431542 extinguishes dorsal ectodermal *tbx2/3* specifically in *P. lividus*, while not affecting its expression in SM (Saudemont et al., 2010). In *E. tribuloides* I observed the expression domain of *tbx2/3* expand into VE upon perturbation with this inhibitor (Figure 5.5A, 5.5B). This observation combined with the result that *bmp2/4* responds differently to Nodal perturbation suggests altered GRN circuitry downstream of Nodal. However, the vast evolutionary distances between cidaroids and euechinoids and the conserved spatiotemporal deployment of regulatory factors strongly argue for developmental constraint of ectodermal patterning mechanisms.

Ciliary band formation and ANE patterning in *E. tribuloides* are evolutionarily inter-

esting evolutionarily given the fact that cidaroids lack the pan-deuterostome apical sensory organ (Mortensen, 1938; Schroeder, 1981; Emlet, 1988; Bennett, Young, and Emlet, 2012). Understanding the alterations in GRN circuitry that accompanied the loss of this embryonic structure and its downstream consequences would provide insight into the evolution of embryonic morphology and GRN architecture. Previous studies indicated that ANE patterning in *E. tribuloides* is more similar to outgroup echinoderms than it is in euechinoids, though expression of CB and anterior regulatory factors, e.g. *onecut* and *nk2.1*, exhibited spatial distributions similar to those seen in euechinoids (Bishop et al., 2013). Here, I observed patterning and regulation of CB that are consistent with the hypothesis that this process is conserved in echinoids. Additionally, I observed the sequential spatial restriction of *foxq2* to ANE, a pan-bilaterian observation driven by endomesodermal wnt factors (Yaguchi et al., 2008; Tu, Brown, et al., 2006; Santagata et al., 2012; Yu et al., 2008; Fritzenwanker et al., 2014). These data suggest that specification of the apical sensory organ in *E. tribuloides* is developmentally downstream of these events and that the loss of this embryonic structure had little effect on conserved patterning of CB and anterior localization of *foxq2*.

Lastly, perturbation of D-V patterning drastically altered the spatial distribution of CB regulatory factor *onecut* and resulted in a belt of 6-10 cells encircling the *E. tribuloides* embryo as a single dense ciliary band. A similar result was also obtained for Synaptotagmin in *E. tribuloides* by disruption of endomesodermal specification via zinc perturbation (Bishop et al., 2013). These results are consistent with the hypothesis that anteriorly positioned ANE repressors restrict CB fate to the equator when D-V patterning is disrupted. Indeed, in *S. purpuratus*, Foxq2 restricts CB positioning anteriorly in ANE (Barsi, Li, and Davidson, 2015). Although it is clear from work in euechinoids that ANE regulatory factors do not expand when D-V patterning is disrupted (Saudemont et al., 2010), this is likely not the case in *E. tribuloides*. While ANE is greatly expanded in *E. tribuloides* relative to other echinoderms (Tu, Brown, et al., 2006; Yankura et al., 2010), there is no evidence to indicate that it extends to the embryonic equator. The most likely scenario is that disruption of D-V patterning expands anteriorly positioned ANE repressors of CB, e.g. candidate regulatory factors being Foxq2 and Nk2.1, and CB positioning occurs at the equator where a pan-ectodermal driver, e.g. SoxB1 (Barsi, Li, and Davidson, 2015; Saudemont et al., 2010; de-Leon et al., 2013), is able to drive *onecut* expression. Elevated mRNA levels of *foxq2* in *E. tribuloides* upon disruption of D-V patterning support this hypothesis (Figure 5.4A, 5.4C).

Further, the sequential vegetal-to-animal zygotic activation of *onecut* seen during *E. tribuloides* early development is consistent with the hypothesis of anteriorly positioned ANE repressors that must be cleared for proper onecut expression.

Evolution of global embryonic domains in early development of echinoids

Previous analyses of embryonic domain regulatory states in *E. tribuloides* surveyed SM regulatory factors (Erkenbrack and Davidson, 2015), endomesodermal regulatory factors including early NSM up to early gastrula [Erkenbrack, Davidson and Peter, forthcoming], and anterior neural ectoderm specification (Bishop et al., 2013). Additionally, two previous studies investigated SM and early endomesodermal micromere regulatory factors in the Pacific-dwelling cidaroid *Prionocidaris baculosa* (Yamazaki, Kidachi, Yamaguchi, et al., 2014; Yamazaki, Kidachi, and Minokawa, 2012). Integrating these data into this study affords an analysis of global embryonic regulatory states and GRN linkages over 268.8 mya of evolution in indirect-developing sea urchins. From these studies, numerous alterations to deployment and GRN circuitry at all levels of GRN topology can be enumerated. Here, I enumerate 19 changes in spatiotemporal deployment or regulation of ectodermal and mesodermal embryonic regulatory factors since the cidaroid-euechinoid divergence (Table 2). Prominent among rewiring events are those that have occurred in establishing polarity in mesodermal embryonic domains. Endodermal and ectodermal specification and regulatory states also have undergone change, but to a lesser degree. One hypothesis that can accommodate these observations is that endodermal and ectodermal developmental programs may be more recalcitrant to change than mesodermal programs due to their more ancient evolutionary origin, suggesting that accretion of process over evolutionary time is a mechanism of constraint in developmental programs (Hashimshony et al., 2015). Indeed, in euechinoids there have been additional layers of GRN topology accrued in mesodermal specification, e.g. the *pmar1-hesc* double-negative gate novelty (Yamazaki, Kidachi, Yamaguchi, et al., 2014; Erkenbrack and Davidson, 2015; Oliveri, Tu, and Davidson, 2008), *delta*-dependent NSM specification (Erkenbrack and Davidson, 2015; Sweet, Gehring, and Ettensohn, 2002), etc., which cidaroids do not exhibit, and which may explain the observation that little to no appreciable change has been observed in the mesodermal developmental programs of *L. variegatus*, *P. lividus* and *S. purpuratus*, representatives of modern euechinoid lineages that diverged approximately 90 mya.

No.	Regulatory factor	Change in deployment	Description of change	Euechinoid citations
[1]	<i>bmp2/4</i>	heterotopy	Altered regulation in D-V perturbation background	(Saudemont et al., 2010)
[2]	<i>brachyury</i>	heterochrony	Heterochronic shift in VE	(Duboc, Lapraz, Besnardieu, et al., 2008)
[3]	<i>ese</i>	heterochrony	Heterochronic shift in NSM, <i>E. tribuloides</i> polarity prior to SM ingress	(Duboc, Lapraz, Saudemont, et al., 2010; Rizzo et al., 2006)
[4]	<i>ese</i>	heterotopy	Altered spatial distribution, first broadly mesodermal in <i>E. tribuloides</i> then polarized	(Materna, Ransick, et al., 2013)
[5]	<i>foxa</i>	heterochrony	Heterochronic shift in VE	(Saudemont et al., 2010; Oliveri, Walton, et al., 2006)
[6]	<i>foxq2</i>	heterotopy	Altered spatial distribution in ectoderm	(Tu, Brown, et al., 2006)
[7]	<i>gatac</i>	heterochrony	Heterochronic shift in NSM, <i>E. tribuloides</i> polarity after SM ingress	(Materna, Ransick, et al., 2013; Duboc, Lapraz, Saudemont, et al., 2010)
[8]	<i>gatac</i>	heterotopy	Altered spatial distribution, first broadly mesodermal then polarized	(Materna, Ransick, et al., 2013)
[9]	<i>gatae</i>	heterochrony	Heterochronic shift in NSM, <i>E. tribuloides</i> polarity after SM ingress	(Materna, Ransick, et al., 2013)
[10]	<i>gcm</i>	heterotopy	Altered spatial distribution in ectoderm	(Ransick and Davidson, 2006)
[11]	<i>gcm</i>	heterochrony	Heterochronic shift in NSM, <i>E. tribuloides</i> polarity prior to SM ingress	(Materna, Ransick, et al., 2013; Duboc, Lapraz, Saudemont, et al., 2010; Ransick and Davidson, 2006)
[12]	<i>onecut</i>	heterotopy	Altered spatial distribution in D-V perturbation background	(Saudemont et al., 2010)
[13]	<i>onecut</i>	heterochrony	Heterochronic shift in CB restriction/activation	(Barsi, Li, and Davidson, 2015; Otim et al., 2004)
[14]	<i>prox</i>	heterotopy	Altered maternal distribution, maternal in <i>S. purpuratus</i>	(Materna, Ransick, et al., 2013)
[15]	<i>prox</i>	heterotopy	Altered spatial distribution in NSM, no observed polarity in <i>E. tribuloides</i>	(Materna, Ransick, et al., 2013; Poustka et al., 2007)
[16]	<i>scl</i>	heterotopy	Altered spatial distribution, in <i>E. tribuloides</i> broadly mesodermal then polarized	(Materna, Ransick, et al., 2013)
[17]	<i>tbx2/3</i>	heterochrony	Heterochronic shift in SM	(J. Croce, Lhomond, and Gache, 2003; Gross et al., 2003)
[18]	<i>tbx2/3</i>	heterotopy	Altered spatial distribution in D-V perturbation background	(Saudemont et al., 2010)
[19]	<i>tbx2/3</i>	heterotopy	Altered spatial distribution in DE	(J. Croce, Lhomond, and Gache, 2003; Gross et al., 2003)

Table 5.2: Enumeration of heterotopic (spatial) and heterochronic (temporal) changes to deployment of regulatory factors in echinoids since the cidaroid-euechinoid divergence 268 mya.

Biased rates of change to GRN topology in early development

Davidson and Erwin (Davidson and Erwin, 2006) first proposed the hypothesis that the hierarchical nature of GRN structure would manifest unequal rates of change during developmental evolution. This hypothesis was formulated from experimental observations in multiple bilaterian lineages (Davidson, 2006; Levine and Davidson, 2005), and its underlying principle is to couch the systematic structure of Linnean phylogeny in terms of molecular mechanistic explanation (Peter and Davidson, 2011b; Davidson, 2011). Here evidence was presented that affords a first approximation of the lability of GRN deployment and circuitry underlying GRN topology in early echinoid development. I have presented a comparative analysis of developmental programs that diverged in the middle Permian and that argues for domain-specific, biased rates of change in deployment of GRN regulatory factors. While the genomic hardwired changes underlying this bias were not revealed here, the confluence of spatial, temporal, and experimental evidence strongly suggests that regulatory circuitry specifying mesodermal domains in early echinoid embryonic development has undergone substantially more alteration at all levels of GRN topology than endodermal and ectodermal domains. For the early embryo it is imperative to establish canonical domains that are tasked with highly conserved processes, e.g. boundary formation and gastrulation. Thus, rates of change to GRN topology will vary during embryonic development depending on the capacity of the domain to buffer the effect of any mutation. The prediction that recursively wired, hierarchical GRNs constrain the possible trajectories of change in future lineages was a prescient observation that we are only now beginning to appreciate.

5.5 Materials and Methods

Animals and embryo culture

Adult *E. tribuloides* were obtained from KP Aquatics (Tavernier, Florida). Eggs were collected by gravity and washed four times in Millipore filtered sea water (MFSW). Eggs were fertilized with a dilute sperm solution, and embryo cultures with less than 95% fertilization were discarded. Embryos were developed in glass pyrex dishes in a temperature-controlled setting of 22°C, and MFSW was refreshed daily.

Cloning and gene isolation

RNAseq and genomic databases of *E. tribuloides* reads were utilized for primer design using euechinoid sequences as seeds for BLAST searches and subsequent

verification of orthology. PCR products were cloned into PGEM-T vector (Promega) and sequence verified in house using an ABI 3730xl sequencer. WMISH antisense RNA probes were synthesized from restricted plasmid vectors using T7 or SP6 RNA polymerase with digoxigenin or fluorescein dUTP incorporation (Roche).

Whole-mount *in situ* hybridization and mRNA transcript abundance

Transcript abundance of mRNA was estimated as described (Erkenbrack, Ako-Asare, et al., 2016). Briefly, transcripts were estimated by counting the number of embryos and spiking in an external standard of quantified synthetic XenoRNA (Power SYBR Green Cells-to-Ct Kit, Thermo-Fisher Scientific) prior to RNA isolation (RNeasy, Qiagen). Thus, to each qPCR reaction a known amount of embryos and RNA were added and the transcript number is deduced by ddCt method. Additionally, some estimates were made with an internal standard that had been previously quantified. Primers qPCR are listed in Table 5.S1.

Whole-mount *in situ* hybridization (WMISH) was conducted as previously described (Erkenbrack and Davidson, 2015). The WMISH protocol slightly modified for double fluorescent WMISH (dfWMISH) with different antibodies and probe detection. Antibodies for dfWMISH were either Anti-DIG or Anti-FLU conjugated to horseradish peroxidase (Roche) at a concentration of 0.25 μ g/mL. Probes were detected with the Tyramide Signal Amplification Plus kit (Perkin Elmer) by using cyanine 5 or fluorescein conjugates at a dilution of 1:4000 in TBST. The amplification reaction was quenched by addition of 1% hydrogen peroxide. The protocol then cycled back to the blocking step and proceeded as described to detect the second probe. Primers for WMISH are listed in Table 5.S2.

Perturbations

Dominant-negative cadherin RNA overexpression (dnCad or δ -cadherin) was microinjected at a concentration of 1,000 ng/ μ L as previously described (Erkenbrack and Davidson, 2015). Translation blocking morpholino (MASO) targeting hesc mRNA transcript (AATCACAAAGGTAAGACGAGGATGGT) was purchased from Gene Tools (Philomath, OR, USA) and microinjected at a concentration of 1 mM as described (Erkenbrack and Davidson, 2015). BACs were microinjected at a concentration of 60 ng per mL nuclease-free water in the presence of 10 ng HindIII-digested genomic carrier DNA.

For perturbation of D-V patterning, both timing and concentration of treatment with the Alk4/5/7-antagonist SB431542 (Cat no. 1614, Tocris Bioscience) were deter-

mined. MFSW containing 2x concentration of the inhibitor was added to an equal volume of embryo culture in a 6-well tissue culture plate. To determine the optimum concentration, embryo cultures were reared in 5, 15 and 30 μ M SB431542. Embryos reared at 5 μ M showed no gross morphological deformities, whereas embryos reared at 30 μ M exhibited significant developmental delays and gross deformities. To determine the sensitive period of inhibitor exposure, embryo cultures were exposed to the inhibitor at 1, 12, and 24 hpf. Embryos cultured in the inhibitor from 1 hpf or 24 hpf onwards showed significant developmental delays or no significant morphological differences, respectively. Results of these manipulations showed that treatment with 15 μ M SB431542 at 12 hpf was the concentration and sensitive period at which a majority of larvae in the culture showed the characteristic phenotypes of dorsalization: multiple centers of skeletal synthesis and an hourglass phenotype. For Notch perturbation, embryos were cultured in the Notch-antagonist DAPT (Cat No. S2215, Selleck Chemicals) at a concentration of 12 μ M from 1 hpf onwards.

Comparative RNA timecourse analysis and statistics

Absolute mRNA transcript number was estimated as described above for regulatory genes in early development of *E. tribuloides*. Comparative analyses of this dataset were based on published data from two echinoids, *S. purpuratus* (Materna, Nam, and Davidson, 2010) and *P. lividus* (Gildor and de-Leon, 2015). As developmental timing differs between the three species, a one-to-one comparison of timecourse datapoints could not be obtained. This issue was resolved by utilizing the adjustments for *S. purpuratus* and *P. lividus* described in Gildor and Ben-Tabou de Leon (Gildor and de-Leon, 2015). The comparative timepoints used in this study are presented in Table 5.S3. Absolute transcript number for each timepoint was then ranked highest to lowest for each gene relative to itself. Spearman's rank correlation coefficient (ρ) was chosen over Pearson's correlation in order to reduce the influence of large differences sometimes observed in estimates of absolute mRNA transcript numbers. For each pair of orthologous genes for which data were available in two species ρ was calculated; these data are presented for three species in Figure 5.6 and are found in Table 5.S3. For comparative analysis of global embryonic regulatory factors shown in Figure 5.7, values for ρ were calculated for 34 regulatory genes in *E. tribuloides* and *S. purpuratus* and were compared. Only regulatory factors for which the embryonic domain of expression is known in *E. tribuloides* were used in the analysis, though data for 55 regulatory genes are presented in Table 5.S3. Values for ρ were binned by their expression in embryonic regulatory domains in the *S. pur-*

puratus global developmental GRN (available at <http://sugp.caltech.edu/endomes/>). The standard statistical distribution is represented in Figure 5.7. Statistical significance was calculated for each embryonic domain using the average of all ρ values (55 regulatory genes) as the expected mean. Conservation of regulatory gene deployment is then interpreted as ρ values near 1, i.e. high correlation of temporal deployment between two species.

5.6 Acknowledgments

I appreciatively acknowledge numerous colleagues for discussing various aspects of this work with me over the long course of its maturation: Dr. Julius C. Barsi kindly provided his advice and the *Sp onecut* wildtype and mutated BACs; Jennifer Wellman, M.S., for her insight on statistical analyses; Dr. Stefan Materna for providing raw data for *S. purpuratus* mRNA transcript abundance and reviewed early versions of the manuscript; Drs. David McClay, Tom Stewart, and Jeffrey R. Thompson for their critical commentary on figures and the manuscript; my colleagues in the Wagner Lab who critiqued early drafts of the figures; and Ms. Cong Liang for assisting in my computational analysis of the qPCR timecourse data. Research presented here was undertaken in the laboratory of the late Professor Eric Harris Davidson and was written in the laboratory of Professor Günter P. Wagner, the latter of whom provided critical insight into portions of the manuscript. Their support is unending and inestimable. This work was funded by National Science Foundation CREATIV grant #1240626.

5.7 Supplemental Figures

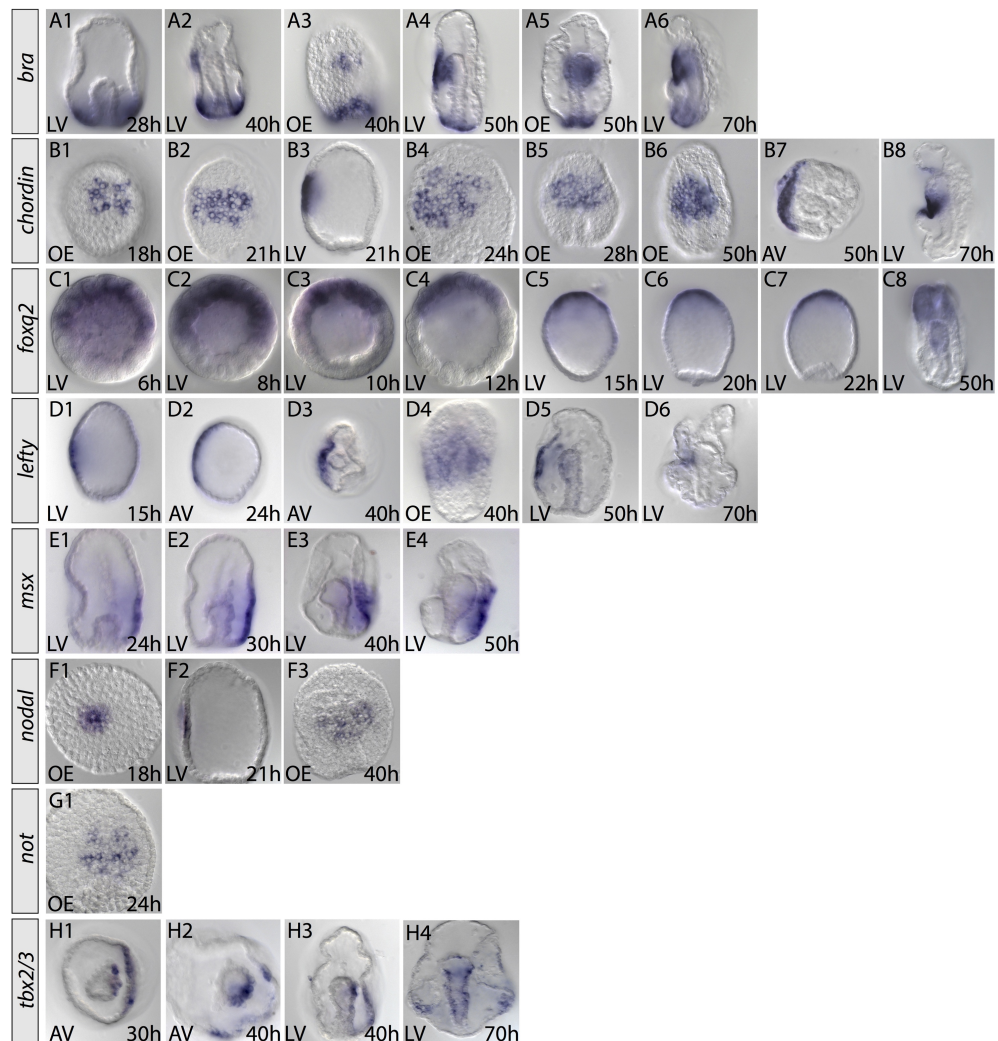


Figure 5.8: Spatial expression of *E. tribuloides* regulatory factors involved in dorsal-ventral (D-V) axis formation in euechinoids. Additional whole mount in situ hybridization images of selected timepoints for (A1-A6) *brachyury*, (B1-B8) *chordin*, (C1-C8) *foxq2*, (D1-D6) *lefty*, (E1-E4) *msx*, (F1-F3) *nodal*, (G1) *not*, and (H1-H4) *tbx2/3*.

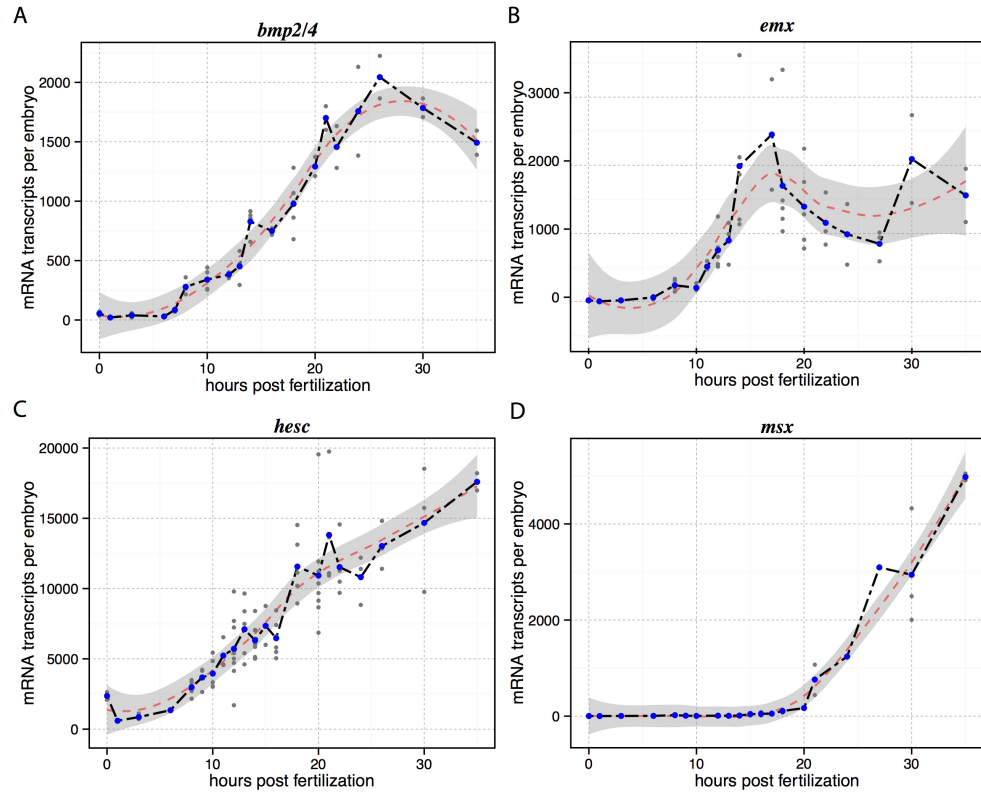


Figure 5.9: Temporal dynamics of selected regulatory factors during the first 35 hpf of *E. tribuloides* development. **(A)** *bmp2/4*, **(B)** *emx*, **(C)** *hesc*, and **(D)** *msx*.

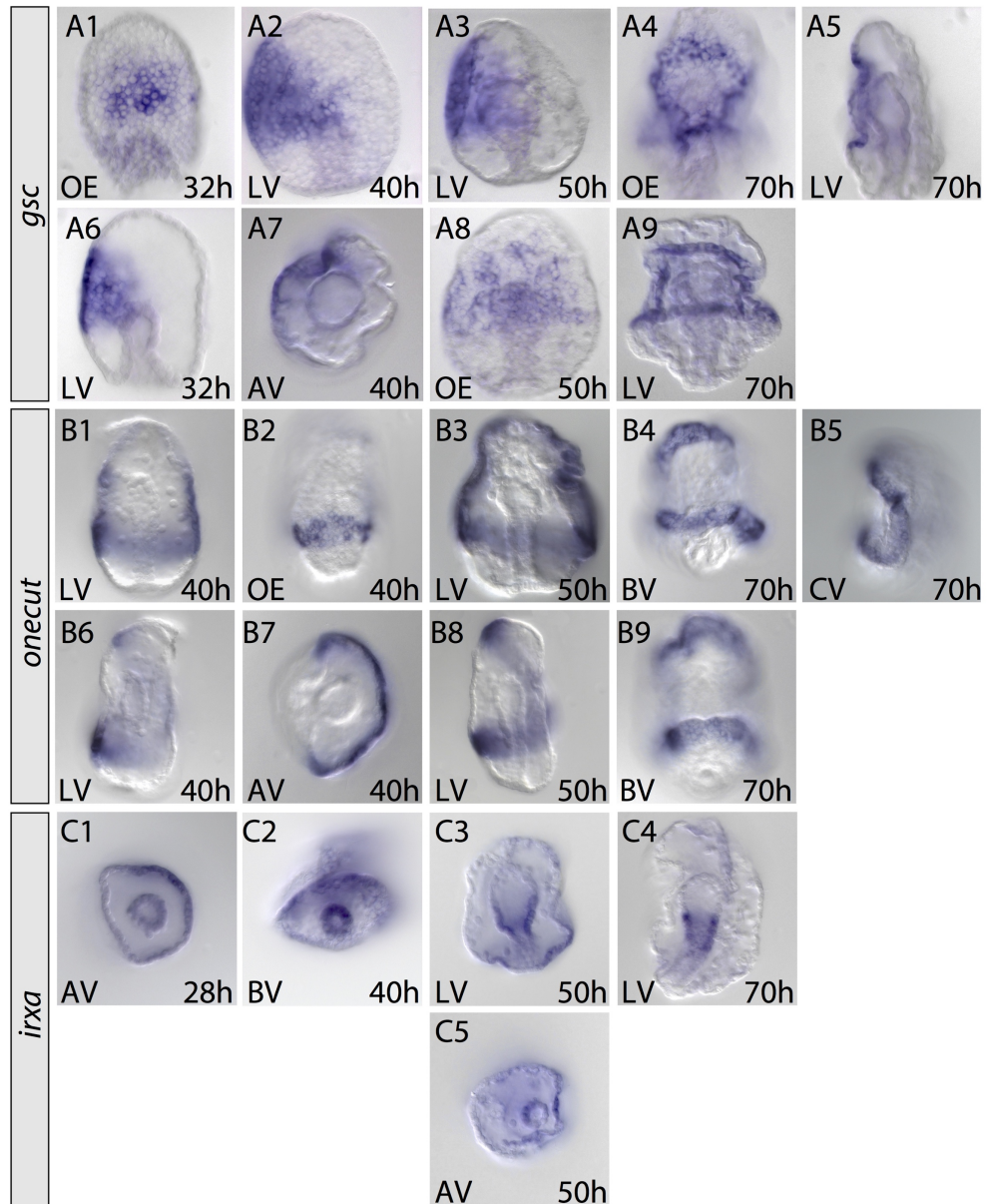


Figure 5.10: Spatial expression of *E. tribuloides* regulatory factors involved in ciliary band formation in euechinoids. Additional whole mount *in situ* hybridization images of selected timepoints for (A1-A9) *gsc*, (B1-B9) *onecut*, and (C1-C5) *irxa*.

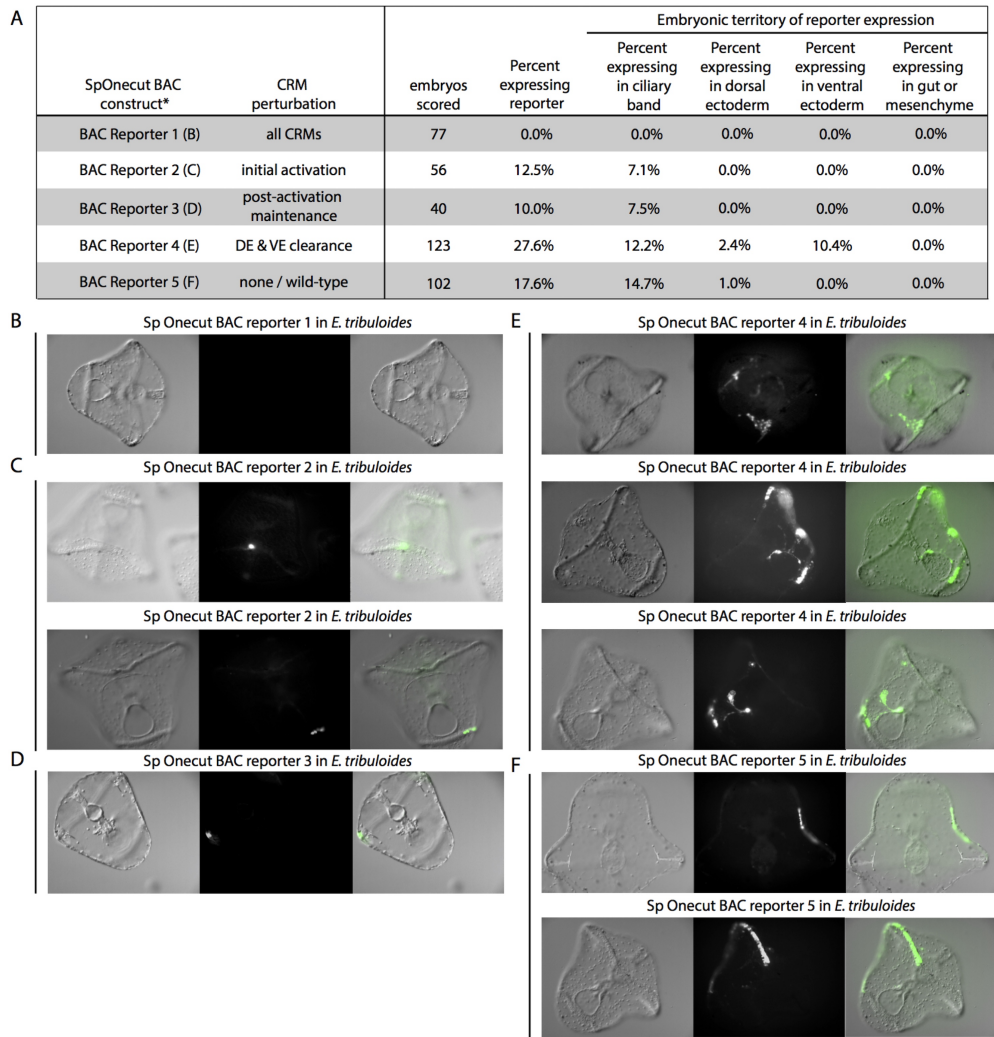


Figure 5.11: Microinjection data showing GFP reporter expression of *S. purpuratus* onecut BACs in *E. tribuloides*. **(A)** Table showing reporter activity in *E. tribuloides* of the *S. purpuratus* onecut BACs. Wild-type and mutated BACs were scored for reporter activity. For each BAC, a summary of its modifications, number of embryos scored, and percent of embryos showing reporter activity in each embryonic domain of *E. tribuloides* are shown. **(B-F)** Exemplary *E. tribuloides* larvae showing typical reporter activity for each BAC in 5 days post fertilization larvae.

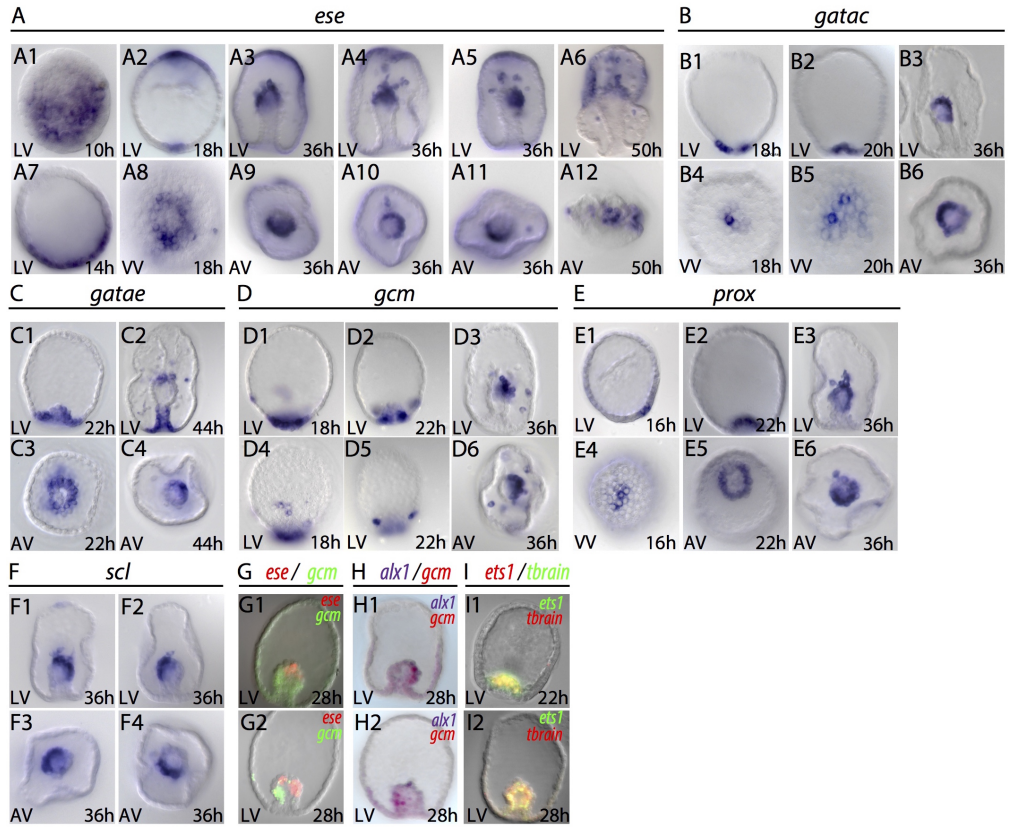


Figure 5.12: Spatial expression of *E. tribuloides* regulatory factors involved in specification of non-skeletogenic mesoderm in euechinoids. Additional whole mount *in situ* hybridization images of selected timepoints for (A1-A12) *ese*, (B1-B6) *gatac*, (C1-C4) *gatae*, (D1-D6) *gcm*, (E1-E6) *prox*, and (F1-F4) *scl*. (G-I) Two-color whole mount *in situ* hybridization of mesodermal regulatory factors at 28 hpf. (G1,G2) *ese* (red) and *gcm* (green). (H1,H2) *alx1* (purple) and *gcm* (red). (I1,I2) *ets1* (red) and *tbrain* (green).

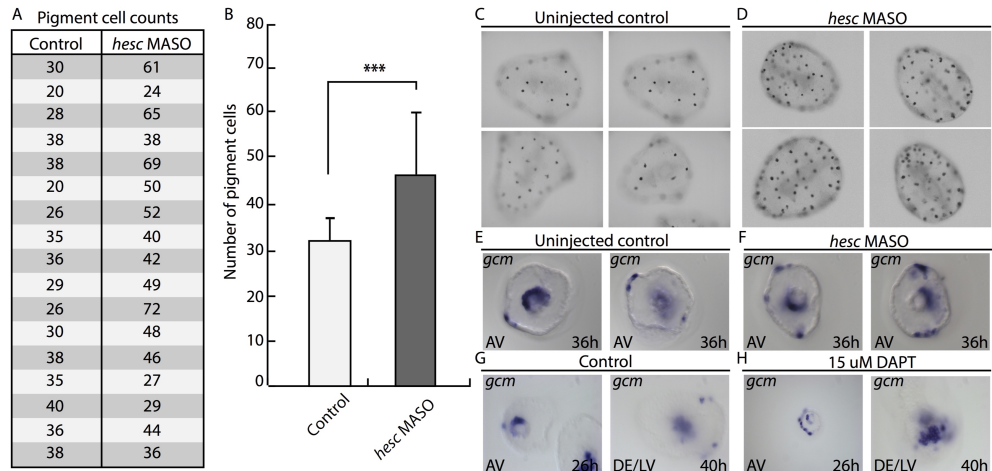


Figure 5.13: Ectodermal *gcm* expression and pigment cell abundance are altered in a Delta-Notch perturbed background in *E. tribuloides*. **(A)** *Gcm* Individual counts of pigment cells in uninjected control versus embryos injected with morpholino targeting the Delta-Notch responsive regulatory factor *hesc*. Knockdown of *hesc* induced supernumerary pigment cells. **(B)** Mann-Whitney rank-sum test of data compiled from (A). **(C,D)** Typical larval phenotypes of uninjected control and *hesc* MASO-treated larvae. **(E,F)** Ectodermal expression of *gcm* expands in the ectoderm when embryos are injected with MASO targeting *hesc*. **(G-H)** Ectodermal expression of *gcm* expands in the ectoderm when embryos are cultured in the presence of the small molecule Notch-antagonist DAPT.

5.8 Supplementary Tables

gene	qPCR forward primer	qPCR reverse primer
<i>ac/sc</i>	CAAGAGTGGATAAACTTCACGCT	CGCACTCGCTTGGGTAAT
<i>alk4/5/7</i>	ACGAGACGGAGATCAAGAGG	CCATCGCTCGTCAGATTGTC
<i>dlx1</i>	ATCCGGGTATGAAATGCCCA	TTCTGCAGATGCGGAGCATA
<i>blimp1</i>	AAGAGCCACCAAGTCCTCCA	TGTAAGTGCCTGGATCTCACGTGGT
<i>bmp2/4</i>	TCACGGAAACAGGACGATAG	AGAGTCCCAGATTACATGATGG
<i>bra</i>	GATAGGGTGACCTGACGGTACTT	CACATGCTGCCGTATTGGTT
<i>chordin</i>	CCAGGGTACGGCTTGACTGGTG	TAGCCGACATCTCGCTGAA
<i>delta</i>	AAATGTAACGTGCCGTGAGCCA	TACAGCTCACATTGGTCGCACCT
<i>dlx</i>	CGGACAGTGAATCATCTCTGG	CCTTGCCTTACCGGAACG
<i>dri</i>	AGCAGAGACGAATCATTGAGG	GGAGACTGATGCGACAAGAG
<i>emx</i>	GACGGCCTTTCACCTTCAC	AACAGCTGGCAGCGAGTCTA
<i>erg</i>	TTCGACGCCGAGGAAC	CCACTGGACCCACTGTTGA
<i>ese</i>	ACGAAAGAAGAACAAACCCGCAG	TTTGGCAAGAACGCTGATGGGT
<i>ets1/2</i>	TGAGTCATACCGAACTCGAACCA	GGTGTCCGTCAAACGTGTCAAA
<i>ets4</i>	CGACGGATGAAATTCAAGAAGG	GCTAGTCGTGACGTGG
<i>eve</i>	AACAGATCGGTCGTCTGGAGAA	AAGCGCCAACGAATGTCGATGT
<i>fgf</i>	AGACGGCGATCCGAGAAAGAC	AAGCACAGTTCATCCCCGTC
<i>foxa</i>	ATGGGTATGAATGCAGGGATGGGA	ATCCTGCTCTATGTCGATGAGGT
<i>foxb</i>	AAGCACCGTCATCTTCTT	AAAGATGGAGTCGAAGGAATG
<i>foxn2/3</i>	GTCCGCTCTCCAATATCTCAAG	CAGAATGGACTGGACATGGAA
<i>foxo</i>	CCAGTCCACAGACCAACTAAC	CTACAGTGGATCGGAAATGTCC
<i>foxq2</i>	TACGCCTATCCTTCCACCATC	GTGAAGGCAGCGACGAATATG
<i>foxy</i>	GTCGCCAGAGAGTGTTT	CCACTGCGTCACTGT
<i>gatac</i>	TCAACTGTGGAGGCCACATCGACA	GTCACCATGAAGAAGGAAGGA
<i>gatae</i>	GCAACATAACCGACGACCAAACA	ATGAACGGGTACAACAGACCGCT
<i>gcm</i>	ATCGATGCACGAAACATCTCAGC	TCCAACAATGTCAAACGAGTGC
<i>gsc</i>	GACATCGCACGATCTTCACC	CGAGTGGAGGTCTGGTCA
<i>hesc</i>	ACGTGAGAACAGAATCAACG	CACTGACTGGGTCTGTAATTCC
<i>hex</i>	CTCTACCGTACTCTAGGAATGA	ATCGTTGGAGAACCTGACTTG
<i>hmx</i>	CATAACCCAGCCCTGTACG	CGTCTCGAAACCAACTCA
<i>hox11/13b</i>	ATGGCCCACAGCAACATACA	GCGACCGTACTCGAAACTGCAAAT
<i>hox7</i>	GACGGGACGTACAGAAATAGG	GGATGCCTGTAGCAGGTC
<i>irxa</i>	AGAGGTTTGTGGCTGGAGGA	CGGTAGAGCGGTTAACCTGC
<i>lefty</i>	CCGAATTCCATCCCGATTCA	TTGTCTGTACGAAGGCGAAG
<i>msx</i>	CAGTCGGACATGGATTGTACC	GGAAGCCAATCTCAAATGTACATC
<i>myc</i>	CCGACTCTGAGGAGGAATC	ACAGAGCACACAGGTCTTA
<i>nodal</i>	GACGACGTGACAAGGAATG	TGATGTTACCGCGGTCTAC
<i>not</i>	TCGAGAAGGAATTGACCGACAGC	TCCAGAACAGACGCATCAAATGGC
<i>notch</i>	GACATGGTCAACGGCTACA	ACCTACACCTGCAACTGTC
<i>onecut</i>	TCTGCCGCAATAAACACTG	GGTATGAACATGGGGTTGG
<i>prox</i>	AACCCTAGTCTCCATCCAACGCTA	TACATGAGTGACCACCGTTCTCA
<i>rx</i>	AGAGGGCGAGGATCACAGAA	CGAGAGAACGCTGACGAC
<i>scl</i>	AGAGTCCTACTCTACCCACGGAC	TACTTGGACCTTCCACTGTC
<i>sip1</i>	AATTCTGCCTCGGACAACC	GCTAGAGTTACATGTGAGTGG
<i>tbr</i>	ATTCTCCAAGGTAGTGGGCTGCAT	ATGCACAAGTACCAACCTCGCATC
<i>tbx2/3</i>	TTTTCCCCCTACCCACCTTCC	TCTTCGGAGCCAATTGTT
<i>tel</i>	AAATTCACTGACGGAGGCG	TCGGTGTCTCTGATTCTGCTCT
<i>tgif</i>	GCGAGTAGTTCTGCTCCAAA	ATGGCGAATCTCACTCTCTG
<i>vegf3</i>	GCTGTGGATAGTGAAGAAGG	GCAACCTGCGACTACC
<i>vegfr</i>	TCCTCATGTGGCATCTTACG	CCTATGATCCAAGTGGGAGTT
<i>wnt1</i>	CGAGTCATGTACGTGTACTAC	GAAAGGACGAGACTTGAGATACC
<i>wnt5</i>	TGGATCCATCTCGGTACATCTAC	GATAACTGATGCTCTTCGCG
<i>wnt8</i>	TGTCCAAACTCTCGTGGATGCTG	TTGTAAATGCCATGGTGTCTCCGG
<i>wnt16</i>	ATAACGTGGATCACGGGATAAG	AAATCCCAGATGATGACGCA
<i>zic</i>	AAACGTCAGGACAGCCCAAT	AGCATGAGTAGCTACCCGC

Table 5.3: Sequences of primer sets for qPCR used in this study.

gene	WMISH forward primer	WMISH reverse primer
<i>alx1</i>	TGAAATGCCCATAGCTCCACGA	ATGCCCATGACTGAAGTGTGCT
<i>bra</i>	TGGACACGTGGCTCGTATTTGT	AAACGGGCTATCAGGACAGT
<i>chordin</i>	ACGTGACCTGCGCAATAGAA	GACGACAGCATTGGTACCGA
<i>ese</i>	AACAGCAGTACCGGTCGTTTC	TTTGGCAAGAACGCTGATGGGT
<i>ets1/2</i>	AATGAGGTGGACGAGTGCTGTCA	GTCCGTAAACGTGTCAAAGGGT
<i>foxq2</i>	GCTACACACGACAC	TCGTTCTGCATGTACCTTATGAAC
<i>gatac</i>	TCGCAAGCAGTCAAGTTGCAG	ATGGATTATGGGATGACGTCGGCA
<i>gatae</i>	AACCCACAACGGTCTGACGGGCTA	TGCCGTAGCCGTTCCGTAGATAA
<i>gcm</i>	GGCCATGCGAACACCAACAATCA	AGACGACACGACAACGTTACTGA
<i>gsc</i>	CACTGAGCCCGTCTCG	CCACAAACGGACTTGTAGAAAC
<i>irxa</i>	GGGAGAACATCCACACGTCA	CGGTAGAGCGGTTAACCTGC
<i>lefty</i>	GACCGTAAACGCCAACTCTT	AAGAAGACGTTCGCTGCTG
<i>msx</i>	ACCGGATGTGTGTTACTAGC	CCATCTCTGGITCCTCAGAAC
<i>nodal</i>	ACAAACCTCGAGCGAACGTGG	TAAAGCTCTGCTCGCTGTCG
<i>not</i>	TTCTCGCTCTCCATGTACCAACCA	AAGCTCAGTTGGTTCACTTCCGC
<i>onecut</i>	GCTTGGGGATGAACGGTTA	CGTTAAGATTGGCAGGCTCC
<i>prox</i>	TTACGAATAATCCGACCGACGTGC	AAATTCACTAGCCCCGATGC
<i>scl</i>	TGATTGACATGGCAACTCCTCCCA	GAACAGCGTTACTTCAGCGACGA
<i>tbr</i>	TGTTCCCTCAACTGGTCTTCAAGC	CATAGCGCCCTTTGTGATAGGAT
<i>tbx2/3</i>	CAGGAGGATGGACGCTAAGG	TCTTCGGAGCCAATTCGTT

Table 5.4: Sequences of primer sets for WMISH used in this study.

Timepoint	Species		
	<i>E. tribuloides</i>	<i>P. lividus</i>	<i>S. purpuratus</i>
1	0	0	0
2	3	2	3
3	6	5	7
4	8	6	8
5	10	8	10
6	12	10	13
7	13	11	14
8	14	12	16
9	16	14	18
10	18	15	20
11	20	18	24
12	22	20	26
13	24	22	29
14	26	24	31

Table 5.5: Comparative developmental timepoints in three species of echinoids used in this study.

References

Angerer, L. M. et al. (2000). “A BMP pathway regulates cell fate allocation along the sea urchin animal-vegetal embryonic axis.” In: *Development* 127.5, pp. 1105–14. ISSN: 0950-1991. URL: <http://www.ncbi.nlm.nih.gov/pubmed/10662649>.

Barsi, J. C. and E. H. Davidson (2016). “cis-Regulatory control of the initial neurogenic pattern of onecut gene expression in the sea urchin embryo.” In: *Developmental biology* 409.1, pp. 310–8. ISSN: 1095-564X. doi: 10.1016/j.ydbio.2015.10.021. URL: <http://www.ncbi.nlm.nih.gov/pubmed/26522848>.

Barsi, J. C., E. Li, and E. H. Davidson (2015). “Geometric control of ciliated band regulatory states in the sea urchin embryo.” In: *Development* 142.5, pp. 953–61. ISSN: 1477-9129. doi: 10.1242/dev.117986. URL: <http://www.ncbi.nlm.nih.gov/pubmed/25655703%20http://www.ncbi.nlm.nih.gov/articlerender.fcgi?artid=PMC4352983>.

Bennett, K. C., C. M. Young, and R. B. Emlet (2012). “Larval development and metamorphosis of the deep-sea cidaroid urchin *Cidaris blakei*.” In: *The Biological bulletin* 222.2, pp. 105–17. ISSN: 1939-8697. URL: <http://www.ncbi.nlm.nih.gov/pubmed/22589401>.

Bishop, C. D. et al. (2013). “Neural development in *Eucidaris tribuloides* and the evolutionary history of the echinoid larval nervous system.” In: *Developmental biology* 377.1, pp. 236–44. ISSN: 1095-564X. doi: 10.1016/j.ydbio.2013.03.006. URL: <http://www.ncbi.nlm.nih.gov/pubmed/23506838>.

Bradham, C. A. et al. (2009). “Chordin is required for neural but not axial development in sea urchin embryos.” In: *Developmental biology* 328.2, pp. 221–33. ISSN: 1095-564X. doi: 10.1016/j.ydbio.2009.01.027. URL: <http://www.ncbi.nlm.nih.gov/pubmed/19389361%20http://www.ncbi.nlm.nih.gov/articlerender.fcgi?artid=PMC2700341>.

Cameron, R. A. and E. H. Davidson (1991). “Cell type specification during sea urchin development.” In: *Trends in genetics* 7.7, pp. 212–8. ISSN: 0168-9525. URL: <http://www.ncbi.nlm.nih.gov/pubmed/1887502>.

Cavalieri, V. and G. Spinelli (2014). “Early asymmetric cues triggering the dorsal/ventral gene regulatory network of the sea urchin embryo.” In: *eLife* 3, e04664. ISSN: 2050-084X. doi: 10.7554/eLife.04664. URL: <http://www.ncbi.nlm.nih.gov/pubmed/25457050%20http://www.ncbi.nlm.nih.gov/articlerender.fcgi?artid=PMC4273433>.

Croce, J. C. and D. R. McClay (2010). “Dynamics of Delta/Notch signaling on endomesoderm segregation in the sea urchin embryo.” In: *Development* 137.1, pp. 83–91. ISSN: 1477-9129. doi: 10.1242/dev.044149. URL: <http://www.ncbi.nlm.nih.gov/pubmed/20023163%20http://www.ncbi.nlm.nih.gov/articlerender.fcgi?artid=PMC2796929>.

Croce, J., G. Lhomond, and C. Gache (2003). "Coquillette, a sea urchin T-box gene of the Tbx2 subfamily, is expressed asymmetrically along the oral-aboral axis of the embryo and is involved in skeletogenesis." In: *Mechanisms of development* 120.5, pp. 561–72. ISSN: 0925-4773. URL: <http://www.ncbi.nlm.nih.gov/pubmed/12782273>.

Croce, J., R. C. Range, et al. (2011). "Wnt6 activates endoderm in the sea urchin gene regulatory network." In: *Development* 138.15, pp. 3297–306. ISSN: 1477-9129. doi: 10.1242/dev.058792. URL: <http://www.ncbi.nlm.nih.gov/pubmed/21750039> http://www.ncbi.nlm.nih.gov/pmc/articles/PMC3133919.

Davidson, E. H. (1986). *Gene activity in early development*. 3rd. New York: Academic Press.

- (1991). "Spatial mechanisms of gene regulation in metazoan embryos". In: *Development* 113.1, pp. 1–26.
- (2006). *The regulatory genome: gene regulatory networks in development and evolution*. 1st. New York: Academic Press.
- (2011). "Evolutionary bioscience as regulatory systems biology". In: *Developmental biology* 357.1, pp. 35–40. ISSN: 1095-564X. doi: 10.1016/j.ydbio.2011.02.004. URL: <http://www.ncbi.nlm.nih.gov/pubmed/21320483> http://www.ncbi.nlm.nih.gov/pmc/articles/PMC3135751.

Davidson, E. H., R. A. Cameron, and A. Ransick (1998). "Specification of cell fate in the sea urchin embryo: summary and some proposed mechanisms." In: *Development* 125.17, pp. 3269–90. ISSN: 0950-1991. URL: <http://www.ncbi.nlm.nih.gov/pubmed/9693132>.

Davidson, E. H. and D. H. Erwin (2006). "Gene regulatory networks and the evolution of animal body plans." In: *Science (New York, N.Y.)* 311.5762, pp. 796–800. ISSN: 1095-9203. doi: 10.1126/science.1113832. URL: <http://www.ncbi.nlm.nih.gov/pubmed/16469913>.

Davidson, E. H., J. P. Rast, et al. (2002). "A genomic regulatory network for development." In: *Science* 295.5560, pp. 1669–78. ISSN: 1095-9203. doi: 10.1126/science.1069883. URL: <http://www.ncbi.nlm.nih.gov/pubmed/11872831>.

Duboc, V., F. Lapraz, L. Besnardieu, et al. (2008). "Lefty acts as an essential modulator of Nodal activity during sea urchin oral-aboral axis formation." In: *Developmental biology* 320.1, pp. 49–59. ISSN: 1095-564X. doi: 10.1016/j.ydbio.2008.04.012. URL: <http://www.ncbi.nlm.nih.gov/pubmed/18582858>.

Duboc, V., F. Lapraz, A. Saudemont, et al. (2010). "Nodal and BMP2/4 pattern the mesoderm and endoderm during development of the sea urchin embryo." In: *Development* 137.2, pp. 223–35. ISSN: 1477-9129. doi: 10.1242/dev.042531. URL: <http://www.ncbi.nlm.nih.gov/pubmed/20040489>.

Duboc, V. and T. Lepage (2008). "A conserved role for the nodal signaling pathway in the establishment of dorso-ventral and left-right axes in deuterostomes." In: *Journal of experimental zoology. Part B, Molecular and developmental evolution* 310.1, pp. 41–53. ISSN: 1552-5007. doi: 10.1002/jez.b.21121. URL: <http://www.ncbi.nlm.nih.gov/pubmed/16838294>.

Duboc, V., E. Röttinger, L. Besnardieu, et al. (2004). "Nodal and BMP2/4 signaling organizes the oral-aboral axis of the sea urchin embryo." In: *Developmental cell* 6.3, pp. 397–410. ISSN: 1534-5807. URL: <http://www.ncbi.nlm.nih.gov/pubmed/15030762>.

Duboc, V., E. Röttinger, F. Lapraz, et al. (2005). "Left-right asymmetry in the sea urchin embryo is regulated by nodal signaling on the right side." In: *Developmental cell* 9.1, pp. 147–58. ISSN: 1534-5807. doi: 10.1016/j.devcel.2005.05.008. URL: <http://www.ncbi.nlm.nih.gov/pubmed/15992548>.

Dylus, D. V. et al. (2016). "Large-scale gene expression study in the ophiuroid *Amphiura filiformis* provides insights into evolution of gene regulatory networks." In: *EvoDevo* 7, p. 2. ISSN: 2041-9139. doi: 10.1186/s13227-015-0039-x. URL: <http://www.ncbi.nlm.nih.gov/pubmed/26759711%20http://www.ncbi.nlm.nih.gov/articlerender.fcgi?artid=PMC4709884>.

Emlet, R. B. (1988). "Larval Form and Metamorphosis of a "Primitive" Sea Urchin, *Eucidaris thouarsi* (Echinodermata: Echinoidea: Cidaroida), with Implications for Developmental and Phylogenetic Studies". In: *The Biological Bulletin* 174.1, pp. 4–19. ISSN: 0006-3185.

Erkenbrack, E. M., K. Ako-Asare, et al. (2016). "Ancestral state reconstruction by comparative analysis of a GRN kernel operating in echinoderms". In: *Development, Genes and Evolution* 226.1, pp. 37–45. ISSN: 0949-944X. doi: 10.1007/s00427-015-0527-y. URL: <http://link.springer.com/10.1007/s00427-015-0527-y>.

Erkenbrack, E. M. and E. H. Davidson (2015). "Evolutionary rewiring of gene regulatory network linkages at divergence of the echinoid subclasses". In: *Proc Natl Acad Sci U S A* 112.30, E4075–84. ISSN: 1091-6490 (Electronic) 0027-8424 (Linking). doi: 10.1073/pnas.1509845112. URL: <http://www.ncbi.nlm.nih.gov/pubmed/26170318>.

Ettensohn, C. A. (2009). "Lessons from a gene regulatory network: echinoderm skeletogenesis provides insights into evolution, plasticity and morphogenesis." In: *Development* 136.1, pp. 11–21. ISSN: 0950-1991. doi: 10.1242/dev.023564. URL: <http://www.ncbi.nlm.nih.gov/pubmed/19060330>.

Ettensohn, C. A. et al. (2007). "Gene regulatory networks and developmental plasticity in the early sea urchin embryo: alternative deployment of the skeletogenic gene regulatory network." In: *Development* 134.17, pp. 3077–87. ISSN: 0950-1991. doi: 10.1242/dev.009092. URL: <http://www.ncbi.nlm.nih.gov/pubmed/17670786>.

Flowers, V. L. et al. (2004). "Nodal/activin signaling establishes oral-aboral polarity in the early sea urchin embryo." In: *Developmental dynamics : an official publication of the American Association of Anatomists* 231.4, pp. 727–40. ISSN: 1058-8388. doi: 10.1002/dvdy.20194. URL: <http://www.ncbi.nlm.nih.gov/pubmed/15517584>.

Fritzenwanker, J. H. et al. (2014). "The Fox/Forkhead transcription factor family of the hemichordate *Saccoglossus kowalevskii*." In: *EvoDevo* 5, p. 17. ISSN: 2041-9139. doi: 10.1186/2041-9139-5-17. URL: <http://www.ncbi.nlm.nih.gov/pubmed/24987514%20http://www.ncbi.nlm.nih.gov/articlerender.fcgi?artid=PMC4077281>.

Gao, F. et al. (2015). "Juvenile skeletogenesis in anciently diverged sea urchin clades". In: *Dev Biol* 400.1, pp. 148–158. doi: 10.1016/j.ydbio.2015.01.017. URL: <http://www.ncbi.nlm.nih.gov/pubmed/25641694>.

Gildor, T. and S. Ben-Tabou de-Leon (2015). "Comparative Study of Regulatory Circuits in Two Sea Urchin Species Reveals Tight Control of Timing and High Conservation of Expression Dynamics." In: *PLoS genetics* 11.7, e1005435. ISSN: 1553-7404. doi: 10.1371/journal.pgen.1005435. URL: <http://www.ncbi.nlm.nih.gov/pubmed/26230518%20http://www.ncbi.nlm.nih.gov/articlerender.fcgi?artid=PMC4521883>.

Gross, J. M. et al. (2003). "LvTbx2/3: a T-box family transcription factor involved in formation of the oral/aboral axis of the sea urchin embryo." In: *Development* 130.9, pp. 1989–99. ISSN: 0950-1991. URL: <http://www.ncbi.nlm.nih.gov/pubmed/12642501>.

Hashimshony, T. et al. (2015). "Spatiotemporal transcriptomics reveals the evolutionary history of the endoderm germ layer". In: *Nature* 519.7542, pp. 219–222. doi: 10.1038/nature13996.

Hinman, V. F. and E. H. Davidson (2007). "Evolutionary plasticity of developmental gene regulatory network architecture." In: *Proceedings of the National Academy of Sciences of the United States of America* 104.49, pp. 19404–9. ISSN: 1091-6490. doi: 10.1073/pnas.0709994104. URL: <http://www.ncbi.nlm.nih.gov/pubmed/18042699%20http://www.ncbi.nlm.nih.gov/articlerender.fcgi?artid=PMC2148302>.

Kroh, A. and A. B. Smith (2010). "The phylogeny and classification of post-Palaeozoic echinoids". English. In: *Journal of Systematic Palaeontology* 8.2, pp. 147–212. doi: Pii922467612Doi10.1080/14772011003603556. URL: %3CGo%20to%20ISI%3E:/WOS:000278007400001.

Lapraz, F., L. Besnardieu, and T. Lepage (2009). "Patterning of the dorsal-ventral axis in echinoderms: insights into the evolution of the BMP-chordin signaling network." In: *PLoS biology* 7.11, e1000248. ISSN: 1545-7885. doi: 10.1371/journal.pbio.1000248. URL: <http://www.ncbi.nlm.nih.gov/pubmed/19956794> %20http://www.ncbi.nlm.nih.gov/pmcarticlerender.fcgi?artid=PMC2772021.

Lapraz, F., E. Haillot, and T. Lepage (2015). "A deuterostome origin of the Spemann organiser suggested by Nodal and ADMPs functions in Echinoderms." In: *Nature communications* 6, p. 8927. ISSN: 2041-1723. doi: 10.1038/ncomms9927. URL: <http://www.ncbi.nlm.nih.gov/pubmed/26582589>.

Lee, P. Y. and E. H. Davidson (2004). "Expression of Spgatae, the Strongylocentrotus purpuratus ortholog of vertebrate GATA4/5/6 factors." In: *Gene expression patterns : GEP* 5.2, pp. 161–5. ISSN: 1567-133X. doi: 10.1016/j.modgep.2004.08.010. URL: <http://www.ncbi.nlm.nih.gov/pubmed/15567710>.

de-Leon, S. Ben-Tabou et al. (2013). "Gene regulatory control in the sea urchin aboral ectoderm: spatial initiation, signaling inputs, and cell fate lockdown." In: *Developmental biology* 374.1, pp. 245–54. ISSN: 1095-564X. doi: 10.1016/j.ydbio.2012.11.013. URL: <http://www.ncbi.nlm.nih.gov/pubmed/23211652> %20http://www.ncbi.nlm.nih.gov/pmcarticlerender.fcgi?artid=PMC3548969.

Levine, M. and E. H. Davidson (2005). "Gene regulatory networks for development." In: *Proceedings of the National Academy of Sciences of the United States of America* 102.14, pp. 4936–42. ISSN: 0027-8424. doi: 10.1073/pnas.0408031102. URL: <http://www.ncbi.nlm.nih.gov/pubmed/15788537> %20http://www.ncbi.nlm.nih.gov/pmcarticlerender.fcgi?artid=PMC555974.

Lhomond, G. et al. (2012). "Frizzled1/2/7 signaling directs β -catenin nuclearisation and initiates endoderm specification in macromeres during sea urchin embryogenesis." In: *Development* 139.4, pp. 816–25. ISSN: 1477-9129. doi: 10.1242/dev.072215. URL: <http://www.ncbi.nlm.nih.gov/pubmed/22274701> %20http://www.ncbi.nlm.nih.gov/pmcarticlerender.fcgi?artid=PMC3265065.

Li, E., M. Cui, et al. (2014). "Encoding regulatory state boundaries in the pre-gastrular oral ectoderm of the sea urchin embryo." In: *Proceedings of the National Academy of Sciences of the United States of America* 111.10, E906–13. ISSN: 1091-6490. doi: 10.1073/pnas.1323105111. URL: <http://www.ncbi.nlm.nih.gov/pubmed/24556994> %20http://www.ncbi.nlm.nih.gov/pmcarticlerender.fcgi?artid=PMC3956148.

Li, E., S. C. Materna, and E. H. Davidson (2012). "Direct and indirect control of oral ectoderm regulatory gene expression by Nodal signaling in the sea urchin embryo." In: *Developmental biology* 369.2, pp. 377–85. ISSN: 1095-564X. doi: 10.1016/j.ydbio.2012.06.022. URL: <http://www.ncbi.nlm.nih.gov/pmcarticlerender.fcgi?artid=PMC3548969>.

gov / pubmed / 22771578 %20http : / / www . pubmedcentral . nih . gov / articlerender . fcgi?artid=PMC3423475.

Li, E., S. C. Materna, and E. H. Davidson (2013). “New regulatory circuit controlling spatial and temporal gene expression in the sea urchin embryo oral ectoderm GRN.” In: *Developmental biology* 382.1, pp. 268–79. ISSN: 1095-564X. doi: 10 . 1016 / j . ydbio . 2013 . 07 . 027. URL: <http://www.ncbi.nlm.nih.gov/pubmed/23933172> %20http : / / www . pubmedcentral . nih . gov / articlerender . fcgi?artid=PMC3783610.

Logan, C. Y. et al. (1999). “Nuclear beta-catenin is required to specify vegetal cell fates in the sea urchin embryo”. English. In: *Development* 126.2, pp. 345–357. URL: %3CGo%20to%20ISI%3E://WOS:000078613200014.

Materna, S. C. and E. H. Davidson (2012). “A comprehensive analysis of Delta signaling in pre-gastrular sea urchin embryos.” In: *Developmental biology* 364.1, pp. 77–87. ISSN: 1095-564X. doi: 10 . 1016 / j . ydbio . 2012 . 01 . 017. URL: <http://www.ncbi.nlm.nih.gov/pubmed/22306924> %20http : / / www . pubmedcentral . nih . gov / articlerender . fcgi?artid=PMC3294105.

Materna, S. C., J. Nam, and E. H. Davidson (2010). “High accuracy, high-resolution prevalence measurement for the majority of locally expressed regulatory genes in early sea urchin development.” In: *Gene expression patterns : GEP* 10.4-5, pp. 177–84. ISSN: 1872-7298. doi: 10 . 1016 / j . gep . 2010 . 04 . 002. URL: <http://www.ncbi.nlm.nih.gov/pubmed/20398801> %20http : / / www . pubmedcentral . nih . gov / articlerender . fcgi?artid=PMC2902461.

Materna, S. C., A. Ransick, et al. (2013). “Diversification of oral and aboral mesodermal regulatory states in pregastrular sea urchin embryos”. In: *Developmental Biology* 375.1, pp. 92–104. ISSN: 00121606. doi: 10 . 1016 / j . ydbio . 2012 . 11 . 033.

McCauley, B. S. et al. (2012). “Development of an embryonic skeletogenic mesenchyme lineage in a sea cucumber reveals the trajectory of change for the evolution of novel structures in echinoderms”. In: *EvoDevo* 3.1, p. 17. ISSN: 2041-9139. doi: 10 . 1186 / 2041-9139-3-17. URL: <http://www.evodevojournal.com/content/3/1/17>.

Molina, M. D. et al. (2013). “Nodal: master and commander of the dorsal-ventral and left-right axes in the sea urchin embryo.” In: *Current opinion in genetics & development* 23.4, pp. 445–53. ISSN: 1879-0380. doi: 10 . 1016 / j . gde . 2013 . 04 . 010. URL: <http://www.ncbi.nlm.nih.gov/pubmed/23769944>.

Mortensen, T. (1938). “Contributions to the study of the development and larval forms of echinoderms. IV”. In: *Danske Vid Selsk Ser* 9.7(3), pp. 1–59.

Nam, J. et al. (2007). “Cis-regulatory control of the nodal gene, initiator of the sea urchin oral ectoderm gene network.” In: *Developmental biology* 306.2, pp. 860–9. ISSN: 0012-1606. doi: 10 . 1016 / j . ydbio . 2007 . 03 . 033. URL: <http://www.ncbi.nlm.nih.gov/pubmed/17451671> %20http : / / www . pubmedcentral . nih . gov / articlerender . fcgi?artid=PMC2063469.

Oliveri, P., Q. Tu, and E. H. Davidson (2008). “Global regulatory logic for specification of an embryonic cell lineage”. In: *Proc Natl Acad Sci U S A* 105.16, pp. 5955–5962. doi: 10.1073/pnas.0711220105. URL: <http://www.ncbi.nlm.nih.gov/pubmed/18413610>.

Oliveri, P., K. D. Walton, et al. (2006). “Repression of mesodermal fate by foxa, a key endoderm regulator of the sea urchin embryo.” In: *Development* 133.21, pp. 4173–81. ISSN: 0950-1991. doi: 10.1242/dev.02577. URL: <http://www.ncbi.nlm.nih.gov/pubmed/17038513>.

Otim, O. et al. (2004). “SpHnf6, a transcription factor that executes multiple functions in sea urchin embryogenesis.” In: *Developmental biology* 273.2, pp. 226–43. ISSN: 0012-1606. doi: 10.1016/j.ydbio.2004.05.033. URL: <http://www.ncbi.nlm.nih.gov/pubmed/15328009>.

Peter, I. S. and E. H. Davidson (2010). “The endoderm gene regulatory network in sea urchin embryos up to mid-blastula stage.” In: *Developmental biology* 340.2, pp. 188–99. ISSN: 1095-564X. doi: 10.1016/j.ydbio.2009.10.037. URL: <http://www.ncbi.nlm.nih.gov/pubmed/19895806%20http://www.ncbi.nlm.nih.gov/articlerender.fcgi?artid=PMC3981691>.

- (2011a). “A gene regulatory network controlling the embryonic specification of endoderm”. In: *Nature* 474.7353, pp. 635–639. doi: 10.1038/nature10100. URL: <http://www.ncbi.nlm.nih.gov/pubmed/21623371>.
- (2011b). “Evolution of Gene Regulatory Networks Controlling Body Plan Development”. In: *Cell* 144.6, pp. 970–985. ISSN: 00928674. doi: 10.1016/j.cell.2011.02.017.
- (2015). *Genomic Control Process, Development and Evolution*. Oxford: Academic Press.

Poustka, A. J. et al. (2007). “A global view of gene expression in lithium and zinc treated sea urchin embryos: new components of gene regulatory networks”. In: *Genome Biology* 8.5, R85. ISSN: 14656906. doi: 10.1186/gb-2007-8-5-r85. URL: <http://genomebiology.com/2007/8/5/R85>.

Raff, R. A. (2008). “Origins of the other metazoan body plans: the evolution of larval forms.” In: *Philosophical transactions of the Royal Society of London. Series B, Biological sciences* 363.1496, pp. 1473–9. ISSN: 0962-8436. doi: 10.1098/rstb.2007.2237. URL: <http://www.ncbi.nlm.nih.gov/pubmed/18192188%20http://www.ncbi.nlm.nih.gov/articlerender.fcgi?artid=PMC2614227>.

Raff, R. A. and M. S. Smith (2009). “Axis formation and the rapid evolutionary transformation of larval form.” In: *Current topics in developmental biology* 86, pp. 163–90. ISSN: 0070-2153. doi: 10.1016/S0070-2153(09)01007-2. URL: <http://www.ncbi.nlm.nih.gov/pubmed/19361693>.

Range, R. C. (2014). "Specification and positioning of the anterior neuroectoderm in deuterostome embryos." In: *Genesis* 52.3, pp. 222–34. ISSN: 1526-968X. doi: 10.1002/dvg.22759. URL: <http://www.ncbi.nlm.nih.gov/pubmed/24549984>.

Ransick, A. and E. H. Davidson (2006). "cis-regulatory processing of Notch signaling input to the sea urchin glial cells missing gene during mesoderm specification." In: *Developmental biology* 297.2, pp. 587–602. ISSN: 0012-1606. doi: 10.1016/j.ydbio.2006.05.037. URL: <http://www.ncbi.nlm.nih.gov/pubmed/16925988>.

Ransick, A., J. P. Rast, et al. (2002). "New early zygotic regulators expressed in endomesoderm of sea urchin embryos discovered by differential array hybridization." In: *Developmental biology* 246.1, pp. 132–47. ISSN: 0012-1606. doi: 10.1006/dbio.2002.0607. URL: <http://www.ncbi.nlm.nih.gov/pubmed/12027439>.

Revilla-i-Domingo, R., P. Oliveri, and E. H. Davidson (2007). "A missing link in the sea urchin embryo gene regulatory network: hesC and the double-negative specification of micromeres". In: *Proc Natl Acad Sci U S A* 104.30, pp. 12383–12388. doi: 10.1073/pnas.0705324104. URL: <http://www.ncbi.nlm.nih.gov/pubmed/17636127>.

Rizzo, F. et al. (2006). "Identification and developmental expression of the ets gene family in the sea urchin (*Strongylocentrotus purpuratus*)". In: *Developmental Biology* 300.1, pp. 35–48. ISSN: 00121606. doi: 10.1016/j.ydbio.2006.08.012. URL: <http://linkinghub.elsevier.com/retrieve/pii/S0012160606010827>.

Santagata, S. et al. (2012). "Development of the larval anterior neurogenic domains of *Terebratalia transversa* (Brachiopoda) provides insights into the diversification of larval apical organs and the spiralian nervous system." In: *EvoDevo* 3, p. 3. ISSN: 2041-9139. doi: 10.1186/2041-9139-3-3. URL: <http://www.ncbi.nlm.nih.gov/pubmed/22273002%20http://www.ncbi.nlm.nih.gov/articlerender.fcgi?artid=PMC3314550>.

Saudemont, A. et al. (2010). "Ancestral regulatory circuits governing ectoderm patterning downstream of Nodal and BMP2/4 revealed by gene regulatory network analysis in an echinoderm." In: *PLoS Genetics* 6.12, e1001259. ISSN: 1553-7404. doi: 10.1371/journal.pgen.1001259. URL: <http://www.ncbi.nlm.nih.gov/pubmed/21203442%20http://www.ncbi.nlm.nih.gov/articlerender.fcgi?artid=PMC3009687>.

Schroeder, T. E. (1981). "Development of a 'primitive' sea urchin (*Eucidaris tribuloides*): irregularities in the hyaline layer, micromeres, and primary mesenchyme". In: *Biological Bulletin* 161.1, pp. 141–151.

Sherwood, D. R. and D. R. McClay (1999). “LvNotch signaling mediates secondary mesenchyme specification in the sea urchin embryo.” In: *Development* 126.8, pp. 1703–13. ISSN: 0950-1991. URL: <http://www.ncbi.nlm.nih.gov/pubmed/10079232>.

Smith, A. B. et al. (2006). “Testing the molecular clock: molecular and paleontological estimates of divergence times in the Echinoidea (Echinodermata).” In: *Molecular biology and evolution* 23.10, pp. 1832–51. ISSN: 0737-4038. DOI: 10.1093/molbev/msl039. URL: <http://www.ncbi.nlm.nih.gov/pubmed/16777927>.

Smith, M. S., S. Collins, and R. A. Raff (2009). “Morphogenetic mechanisms of coelom formation in the direct-developing sea urchin *Heliocidaris erythrogramma*.” In: *Development genes and evolution* 219.1, pp. 21–9. ISSN: 1432-041X. DOI: 10.1007/s00427-008-0262-8. URL: <http://www.ncbi.nlm.nih.gov/pubmed/18958491>.

Smith, M. S., F. R. Turner, and R. A. Raff (2008). “Nodal expression and heterochrony in the evolution of dorsal-ventral and left-right axes formation in the direct-developing sea urchin *Heliocidaris erythrogramma*.” In: *Journal of experimental zoology. Part B, Molecular and developmental evolution* 310.8, pp. 609–22. ISSN: 1552-5015. DOI: 10.1002/jez.b.21233. URL: <http://www.ncbi.nlm.nih.gov/pubmed/18702078>.

Strathmann, R. R. (1971). “The feeding behavior of planktotrophic echinoderm larvae: Mechanisms, regulation, and rates of suspensionfeeding”. In: *Journal of Experimental Marine Biology and Ecology* 6.2, pp. 109–160. ISSN: 00220981. DOI: 10.1016/0022-0981(71)90054-2.

Su, Y. (2009). “Gene regulatory networks for ectoderm specification in sea urchin embryos.” In: *Biochimica et biophysica acta* 1789.4, pp. 261–7. ISSN: 0006-3002. DOI: 10.1016/j.bbagen.2009.02.002. URL: <http://www.ncbi.nlm.nih.gov/pubmed/19429544>.

Sweet, H. C., M. Gehring, and C. A. Ettensohn (2002). “LvDelta is a mesoderm-inducing signal in the sea urchin embryo and can endow blastomeres with organizer-like properties.” In: *Development* 129.8, pp. 1945–55. ISSN: 0950-1991. URL: <http://www.ncbi.nlm.nih.gov/pubmed/11934860>.

Sweet, H. C., P. G. Hodor, and C. A. Ettensohn (1999). “The role of micromere signaling in Notch activation and mesoderm specification during sea urchin embryogenesis.” In: *Development* 126.23, pp. 5255–65. ISSN: 0950-1991. URL: <http://www.ncbi.nlm.nih.gov/pubmed/10556051>.

Tennent, D. H. (1914). “The early influence of the spermatozoan upon the characters of echinoid larvae”. In: *Carn Inst Wash Publ* 182, pp. 129–138.

Thompson, J.R. et al. (2015). “Reorganization of sea urchin gene regulatory networks at least 268 million years ago as revealed by oldest fossil cidaroid echinoid”. URL: <http://www.ncbi.nlm.nih.gov/pubmed/26183000>.

English. In: *Scientific Reports* 5. doi: ARTN1554110 . 1038/srep15541. URL: %3C%20to%20ISI%3E:/WOS:000363122100003.

Tu, Q., C. T. Brown, et al. (2006). “Sea urchin Forkhead gene family: phylogeny and embryonic expression.” In: *Developmental biology* 300.1, pp. 49–62. ISSN: 0012-1606. doi: 10.1016/j.ydbio.2006.09.031. URL: <http://www.ncbi.nlm.nih.gov/pubmed/17081512>.

Tu, Q., R. A. Cameron, and E. H. Davidson (2014). “Quantitative developmental transcriptomes of the sea urchin *Strongylocentrotus purpuratus*.” In: *Developmental biology* 385.2, pp. 160–7. ISSN: 1095-564X. doi: 10.1016/j.ydbio.2013.11.019. URL: <http://www.ncbi.nlm.nih.gov/pubmed/24291147> http://www.ncbi.nlm.nih.gov/pmc/articles/PMC3898891.

Urben, S., C. Nislow, and M. Spiegel (1988). “The origin of skeleton forming cells in the sea urchin embryo”. In: *Roux's archives of developmental biology* 197.8, pp. 447–456. doi: 10.1007/BF00385678. URL: <http://link.springer.com/article/10.1007/BF00385678>.

Wikramanayake, A. H., M. Hong, et al. (2003). “An ancient role for nuclear [beta]-catenin in the evolution of axial polarity and germ layer segregation”. In: *Nature* 426.6965, pp. 446–450. ISSN: 0028-0836. URL: <http://dx.doi.org/10.1038/nature02113> http://www.nature.com/nature/journal/v426/n6965/supplinfo/nature02113%7B%5C_%7DS1.html.

Wikramanayake, A. H., L. Huang, and W. H. Klein (1998). “beta-Catenin is essential for patterning the maternally specified animal-vegetal axis in the sea urchin embryo.” In: *Proceedings of the National Academy of Sciences of the United States of America* 95.16, pp. 9343–8. ISSN: 0027-8424. URL: <http://www.ncbi.nlm.nih.gov/pubmed/9689082> http://www.ncbi.nlm.nih.gov/pmc/articles/PMC21340.

Wilson, K. A., M. E. Andrews, and R. A. Raff (2005). “Dissociation of expression patterns of homeodomain transcription factors in the evolution of developmental mode in the sea urchins *Heliocidaris tuberculata* and *H. erythrogramma*.” In: *Evolution & development* 7.5, pp. 401–15. ISSN: 1520-541X. doi: 10.1111/j.1525-142X.2005.05045.x. URL: <http://www.ncbi.nlm.nih.gov/pubmed/16174034>.

Wilson, K. A., M. E. Andrews, F. R. Turner, et al. (2005). “Major regulatory factors in the evolution of development: the roles of goosecoid and Msx in the evolution of the direct-developing sea urchin *Heliocidaris erythrogramma*.” In: *Evolution & development* 7.5, pp. 416–28. ISSN: 1520-541X. doi: 10.1111/j.1525-142X.2005.05046.x. URL: <http://www.ncbi.nlm.nih.gov/pubmed/16174035>.

Wray, G. A. (1992). “The Evolution of Larval Morphology During the Post-Paleozoic Radiation of Echinoids”. In: *Paleobiology* 18.3, pp. 258–287. ISSN: 00948373, 19385331. URL: <http://www.jstor.org/stable/2400816>.

Wray, G. A. and A. E. Bely (1994). "The evolution of echinoderm development is driven by several distinct factors." In: *Development* 1994 Suppl, pp. 97–106. URL: <http://www.ncbi.nlm.nih.gov/pubmed/7579528>.

Wray, G. A. and D. R. McClay (1988). "The origin of spicule-forming cells in a 'primitive' sea urchin (*Eucidaris tribuloides*) which appears to lack primary mesenchyme cells". In: *Development* 103.2, pp. 305–315. URL: <http://www.ncbi.nlm.nih.gov/pubmed/3066611>.

– (1989). "Molecular Heterochronies and Heterotopies in Early Echinoid Development". In: *Evolution* 43.4, pp. 803–813. ISSN: 00143820, 15585646. URL: <http://www.jstor.org/stable/2409308>.

Wray, G. A. and R. A. Raff (1991). "The evolution of developmental strategy in marine invertebrates." In: *Trends in ecology & evolution* 6.2, pp. 45–50. ISSN: 0169-5347. DOI: [10.1016/0169-5347\(91\)90121-D](https://doi.org/10.1016/0169-5347(91)90121-D). URL: <http://www.ncbi.nlm.nih.gov/pubmed/21232422>.

Yaguchi, S. et al. (2008). "A Wnt-FoxQ2-nodal pathway links primary and secondary axis specification in sea urchin embryos." In: *Developmental cell* 14.1, pp. 97–107. ISSN: 1534-5807. DOI: [10.1016/j.devcel.2007.10.012](https://doi.org/10.1016/j.devcel.2007.10.012). URL: <http://www.ncbi.nlm.nih.gov/pubmed/18194656>.

Yamazaki, A., Y. Kidachi, and T. Minokawa (2012). ""Micromere" formation and expression of endomesoderm regulatory genes during embryogenesis of the primitive echinoid *Prionocidaris baculosa*." In: *Development, growth & differentiation* 54.5, pp. 566–78. ISSN: 1440-169X. DOI: [10.1111/j.1440-169X.2012.01360.x](https://doi.org/10.1111/j.1440-169X.2012.01360.x). URL: <http://www.ncbi.nlm.nih.gov/pubmed/22680788>.

Yamazaki, A., Y. Kidachi, M. Yamaguchi, et al. (2014). "Larval mesenchyme cell specification in the primitive echinoid occurs independently of the double-negative gate". In: *Development* 141.13, pp. 2669–2679. DOI: [10.1242/dev.104331](https://doi.org/10.1242/dev.104331). URL: <http://www.ncbi.nlm.nih.gov/pubmed/24924196>.

Yankura, K. A. et al. (2010). "Uncoupling of complex regulatory patterning during evolution of larval development in echinoderms." In: *BMC biology* 8, p. 143. ISSN: 1741-7007. DOI: [10.1186/1741-7007-8-143](https://doi.org/10.1186/1741-7007-8-143). URL: [http://www.ncbi.nlm.nih.gov/articlerender.fcgi?artid=PMC3002323](http://www.ncbi.nlm.nih.gov/pubmed/21118544%20http://www.ncbi.nlm.nih.gov/articlerender.fcgi?artid=PMC3002323).

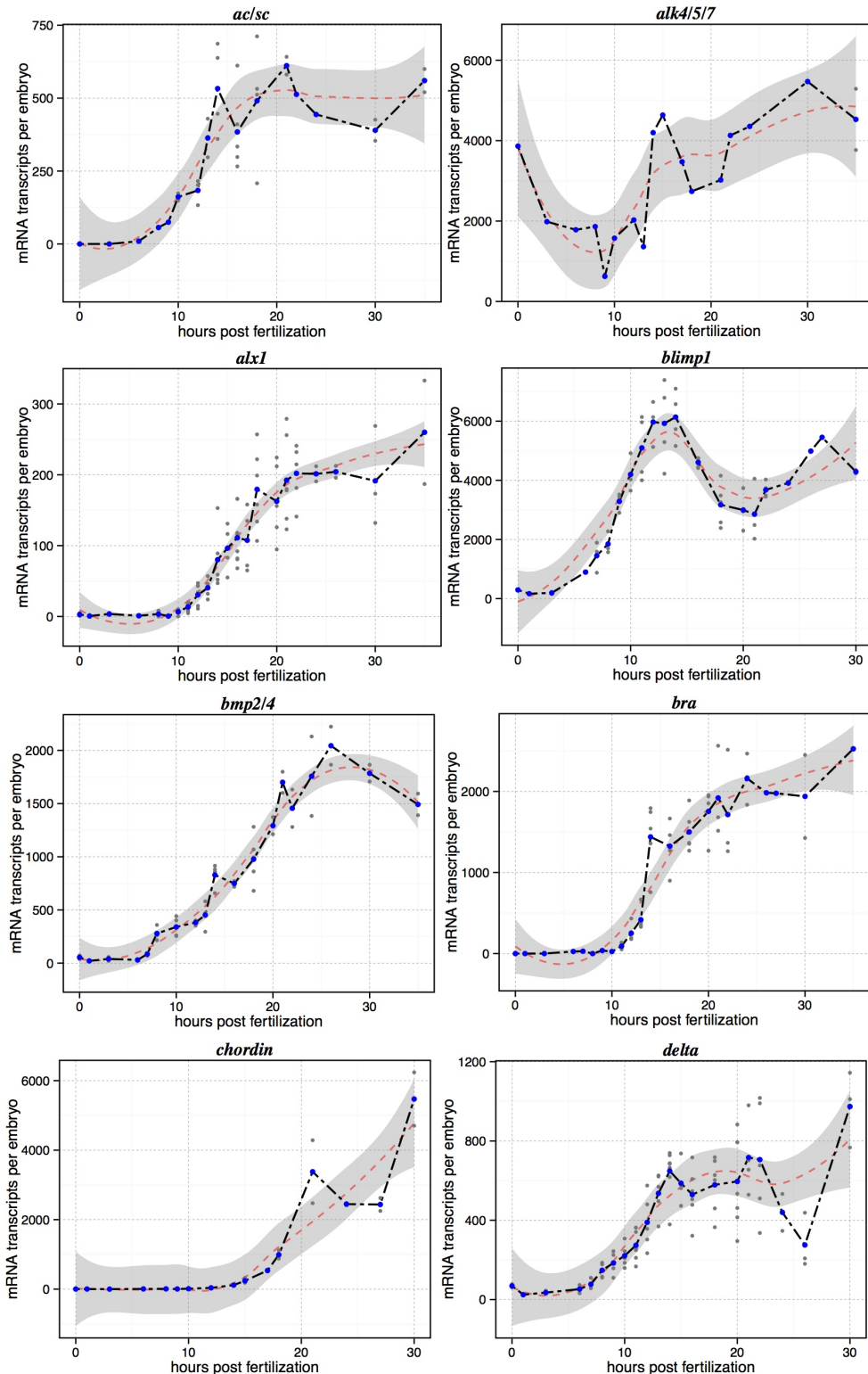
Yu, J. et al. (2008). "The Fox genes of *Branchiostoma floridae*." In: *Development genes and evolution* 218.11-12, pp. 629–38. ISSN: 1432-041X. DOI: [10.1007/s00427-008-0229-9](https://doi.org/10.1007/s00427-008-0229-9). URL: <http://www.ncbi.nlm.nih.gov/pubmed/18773219>.

Appendix A

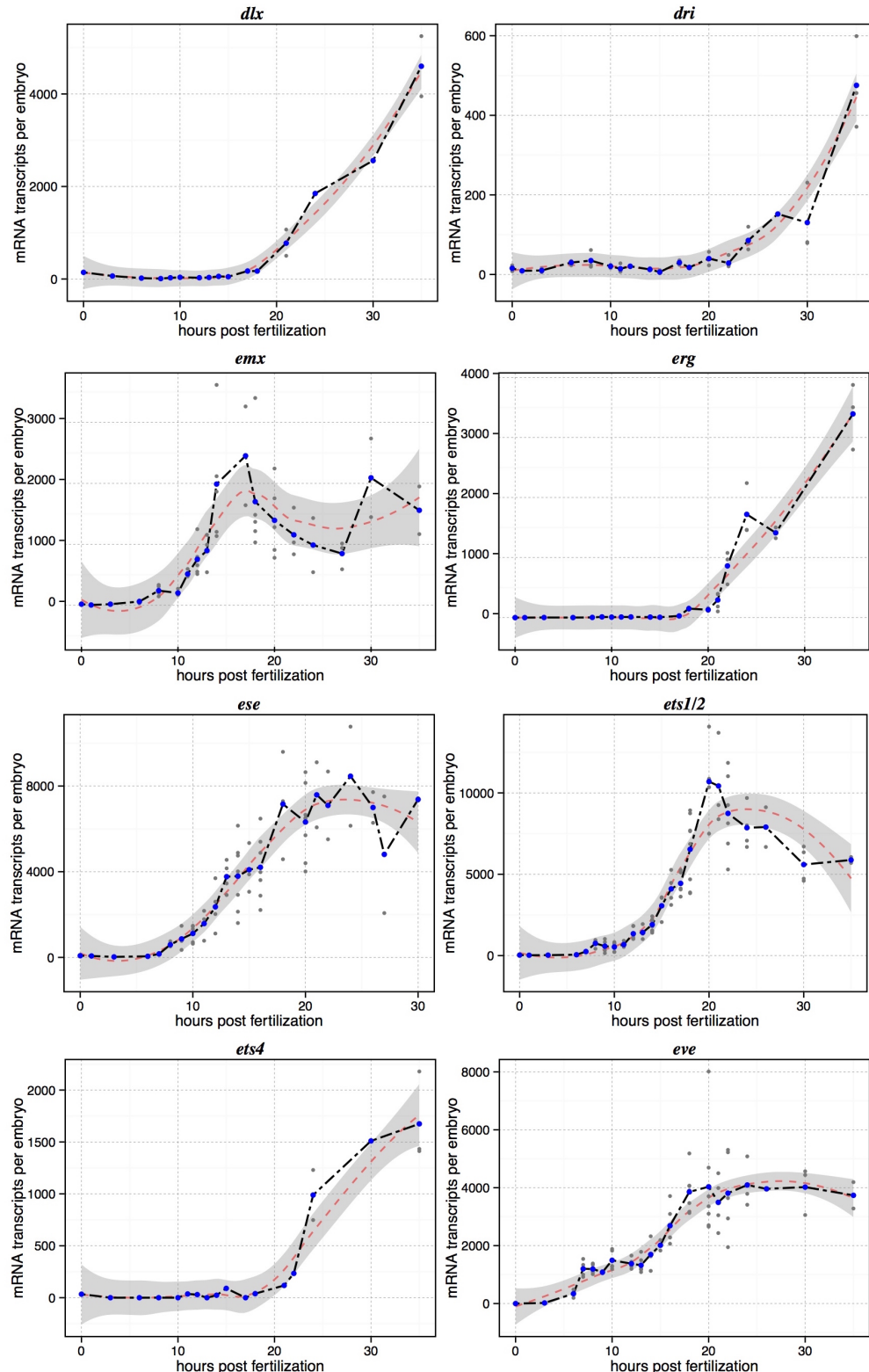
TEMPORAL DYNAMICS OF 63 REGULATORY FACTORS IN
EARLY DEVELOPMENT OF *EUCIDARIS TRIBULOIDES**Index of Genes*

1. <i>ac/sc</i>	156	33. <i>hnf6 (onecut)</i>	160
2. <i>alk4/5/7</i>	156	34. <i>hox7</i>	160
3. <i>alx1</i>	156	35. <i>hox11/13b</i>	160
4. <i>blimp1</i>	156	36. <i>irxa</i>	160
5. <i>bmp2/4</i>	156	37. <i>lefty</i>	160
6. <i>brachyury</i>	156	38. <i>msx</i>	160
7. <i>chordin</i>	156	39. <i>myc</i>	160
8. <i>delta</i>	156	40. <i>nlk</i>	160
9. <i>dlx</i>	157	41. <i>nodal</i>	161
10. <i>dri</i>	157	42. <i>not</i>	161
11. <i>emx</i>	157	43. <i>notch</i>	161
12. <i>erg</i>	157	33. <i>oncut (hnf6)</i>	160
13. <i>ese</i>	157	44. <i>pks</i>	161
14. <i>ets1/2</i>	157	45. <i>prox</i>	161
15. <i>ets4</i>	157	46. <i>rx</i>	161
16. <i>eve</i>	157	47. <i>scl</i>	161
17. <i>fgf</i>	158	48. <i>sip1</i>	161
18. <i>fgfr</i>	158	49. <i>sm29</i>	162
19. <i>foxa</i>	158	50. <i>tbrain</i>	162
20. <i>foxb</i>	158	51. <i>tbx2/3</i>	162
21. <i>foxg</i>	158	52. <i>tel</i>	162
22. <i>foxn2/3</i>	158	53. <i>tgif</i>	162
23. <i>foxo</i>	158	54. <i>univin</i>	162
24. <i>foxq2</i>	158	55. <i>vegf3</i>	162
25. <i>foxy</i>	159	56. <i>vegfr</i>	162
26. <i>gatac</i>	159	57. <i>wnt1</i>	163
27. <i>gatae</i>	159	58. <i>wnt5</i>	163
28. <i>gcm</i>	159	59. <i>wnt6</i>	163
29. <i>gsc</i>	159	60. <i>wnt7</i>	163
30. <i>hesc</i>	159	61. <i>wnt8</i>	163
31. <i>hex</i>	159	62. <i>wnt16</i>	163
32. <i>hmx</i>	159	63. <i>zic</i>	163

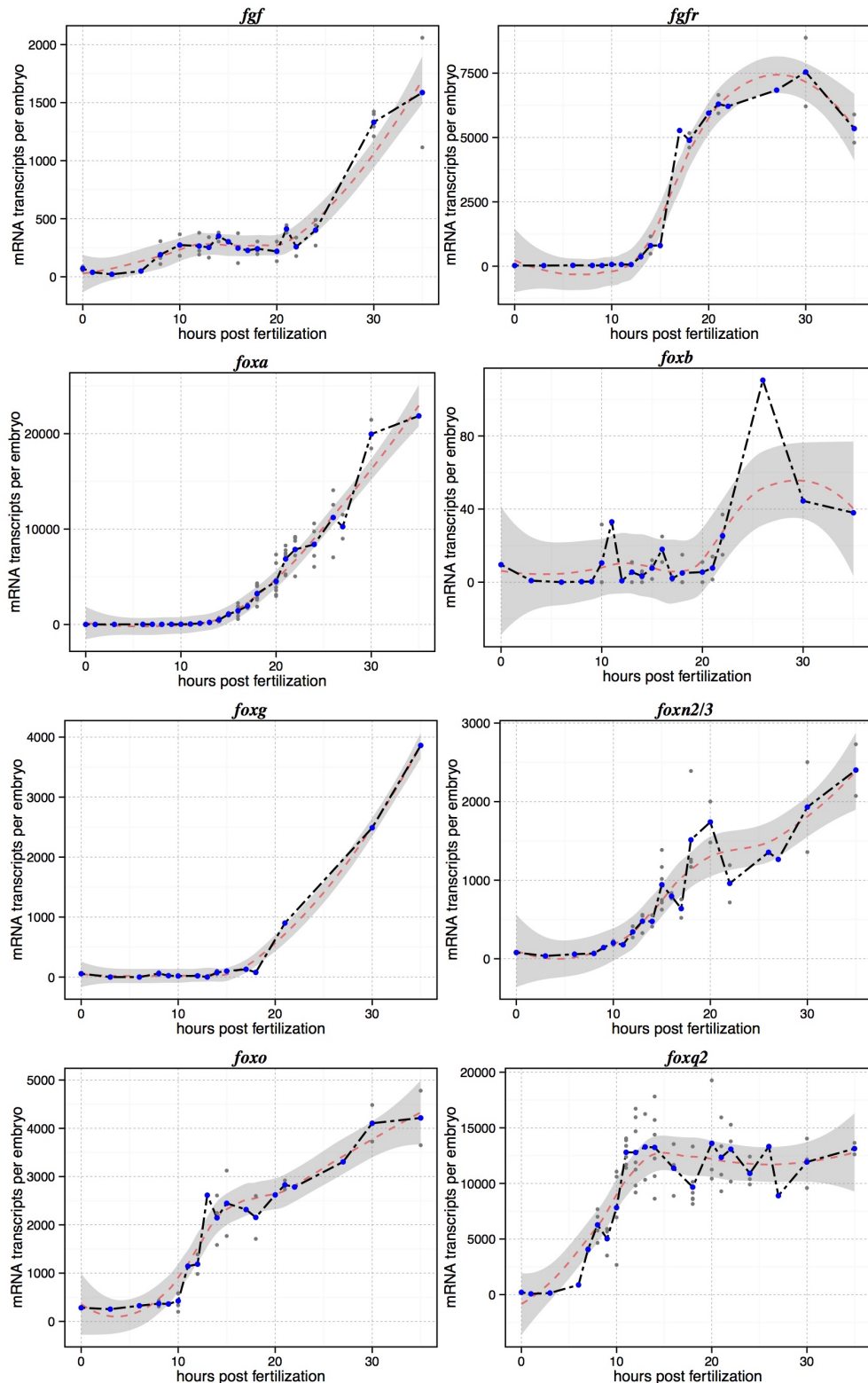
Appendix A



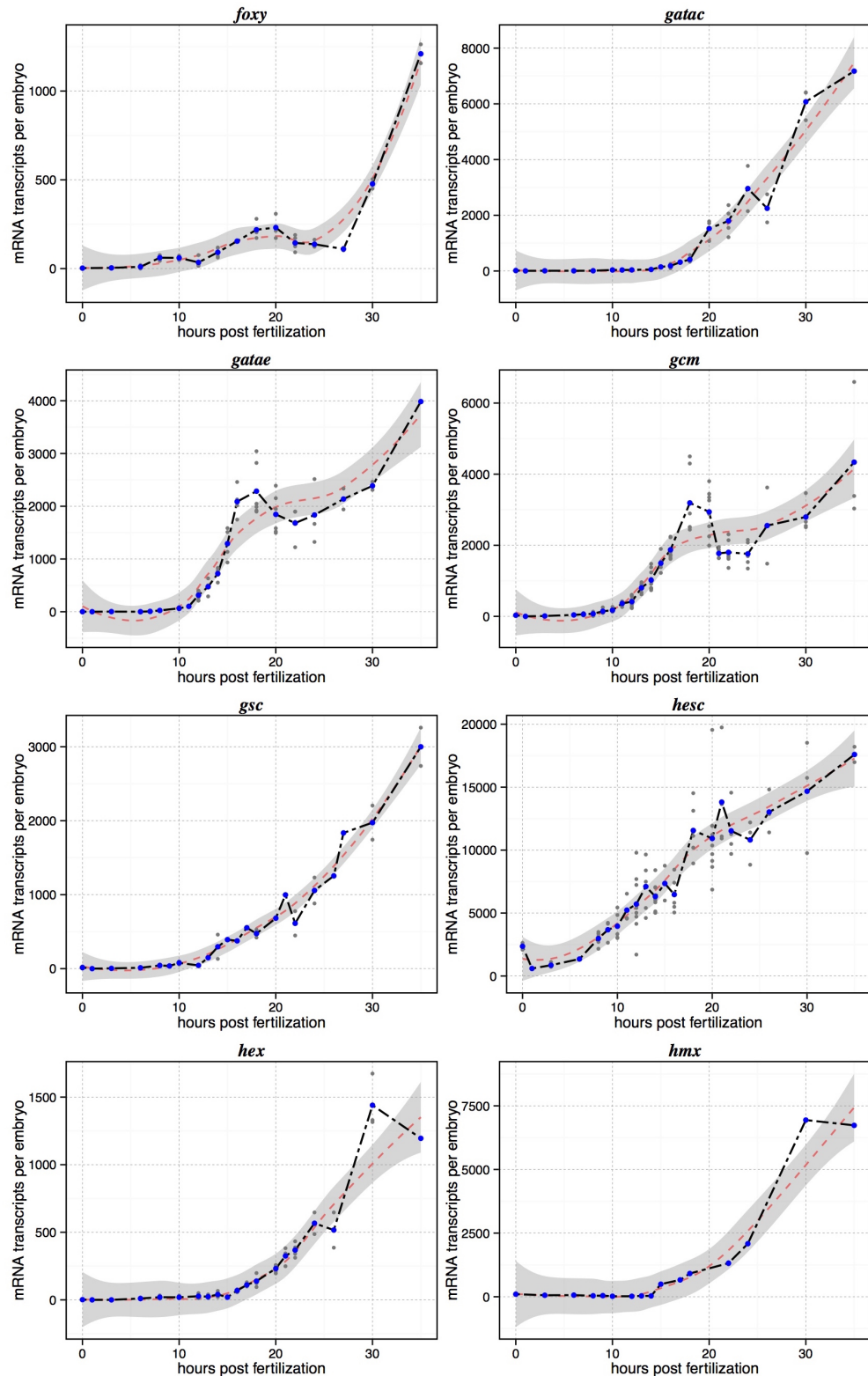
Appendix A



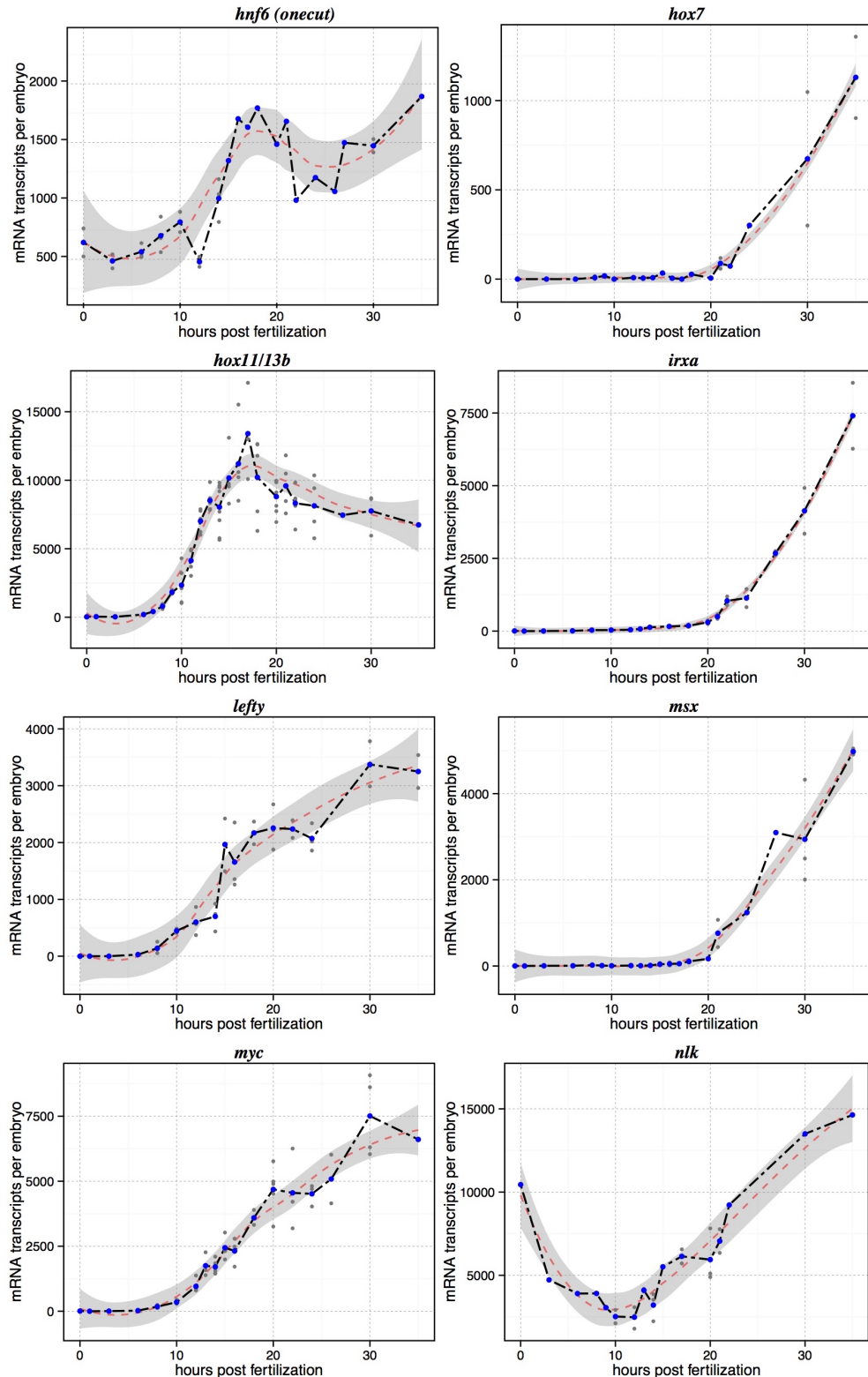
Appendix A



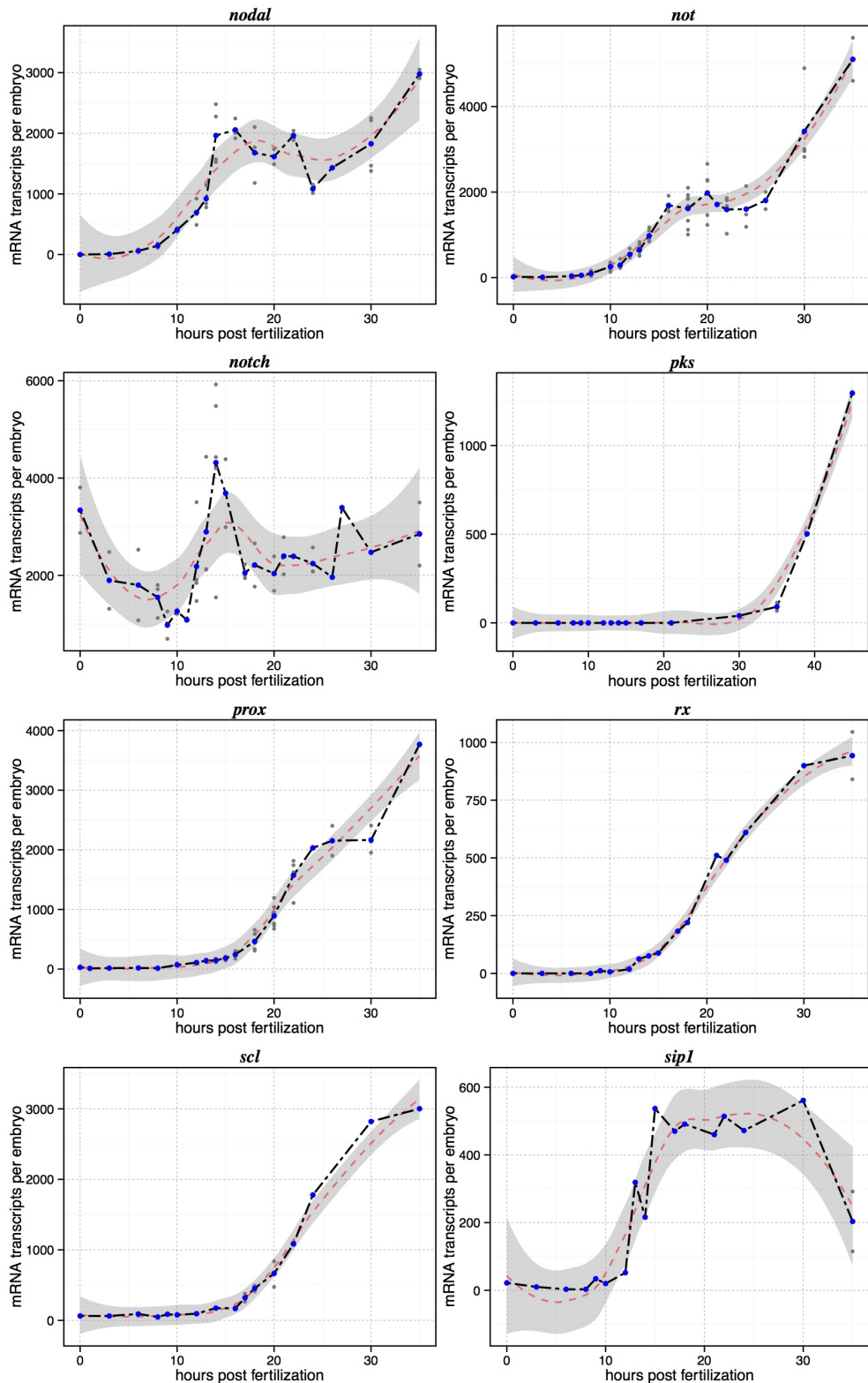
Appendix A



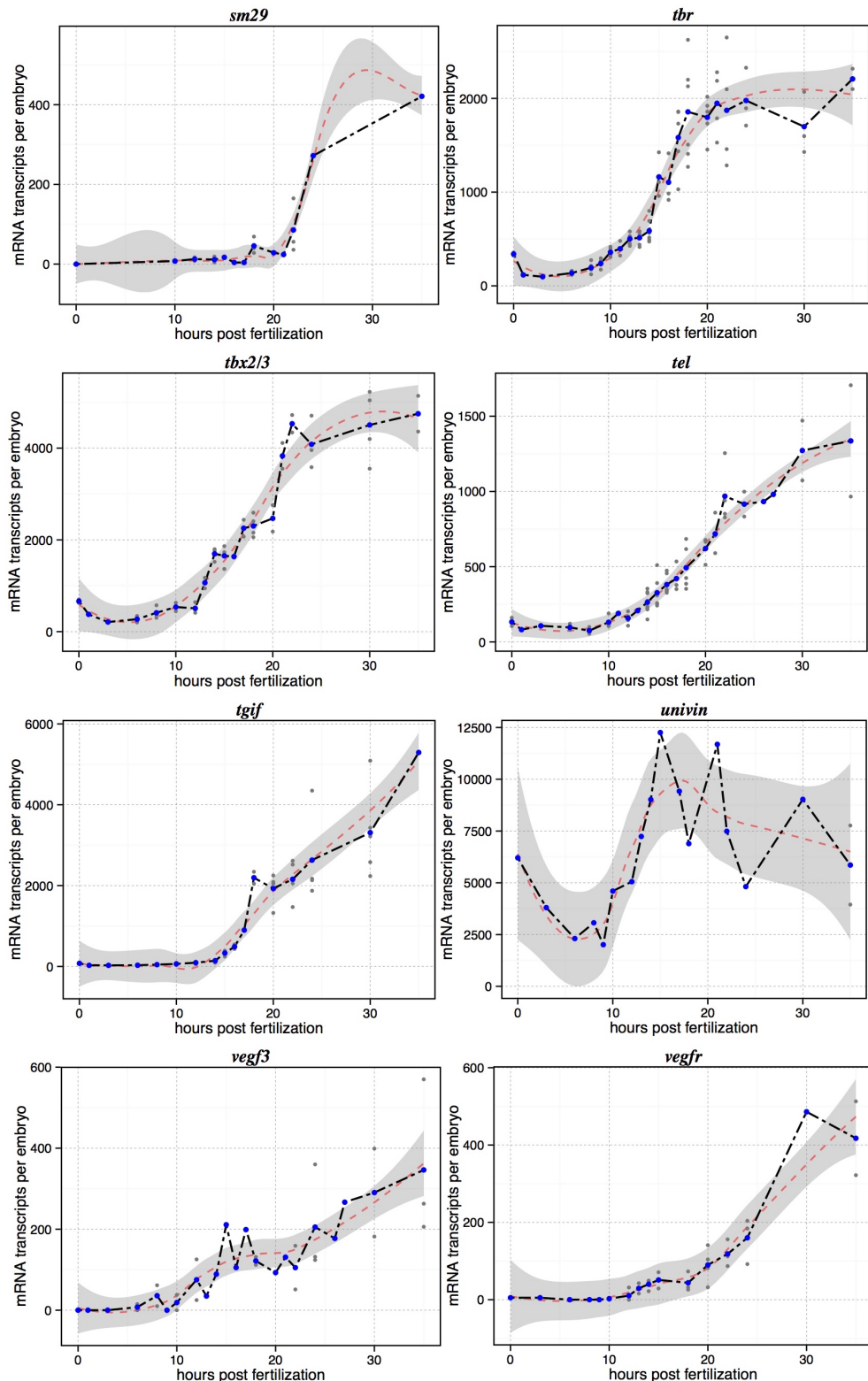
Appendix A



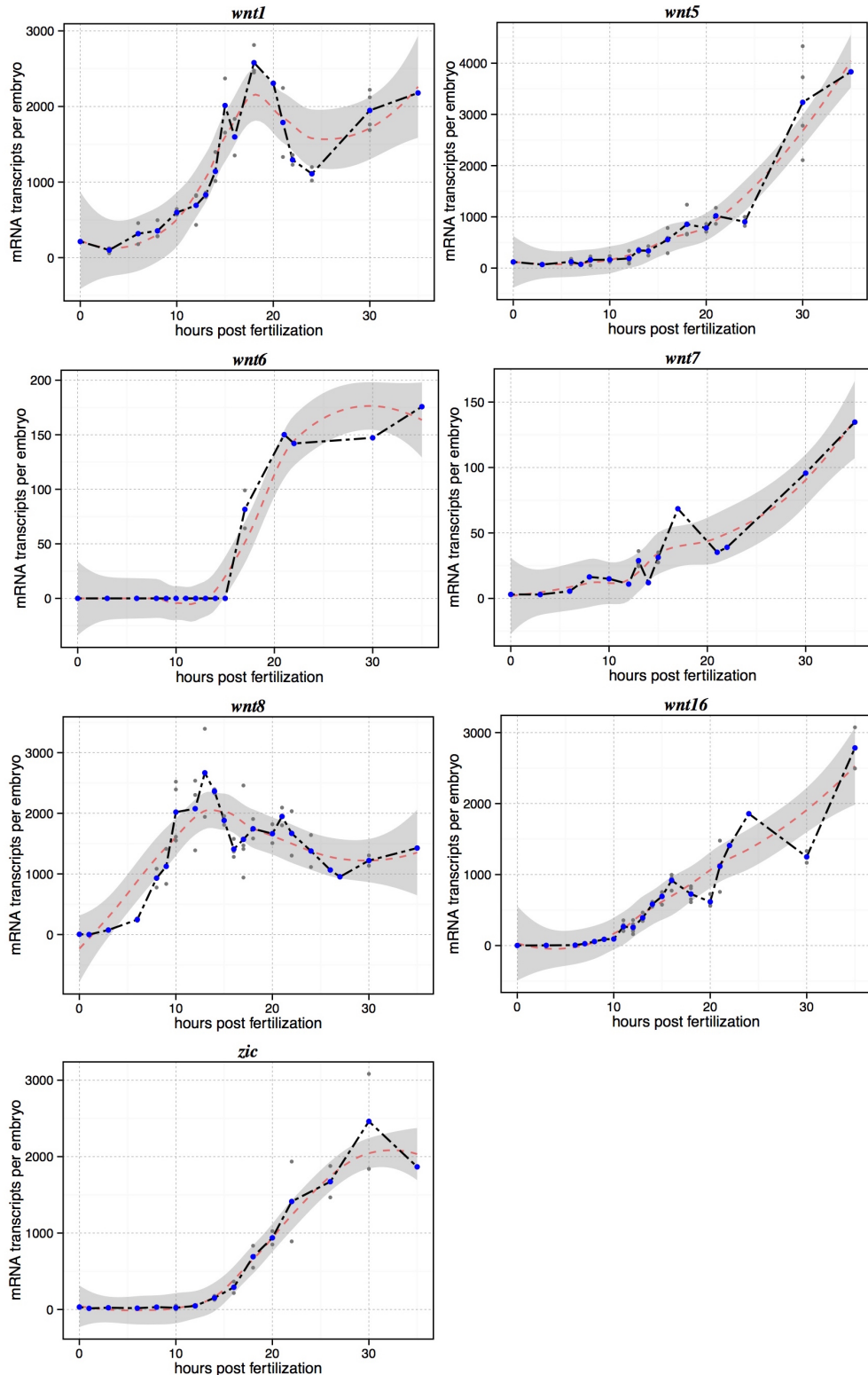
Appendix A



Appendix A



Appendix A



Appen dix B

BRIEF NOTES ON THE GRAVIDITY OF *EUCIDARIS TRIBULOIDES* OFF THE COAST OF KEY LARGO, FLORIDA, USA

During the course of this study, we collated data in the laboratory to determine the most opportune time of year to conduct research on *E. tribuloides*. Since sea urchins frequently spawn en route to their destination when shipped overnight in crates, we thought it important to find a way to acquire data on the reef. Few studies have looked at this closely in cedaroid sea urchins. But noteworthy studies on this question have been conducted (Pearse, 1969; McPherson, 1968; Holland, 1967; Lessios, 1991). These studies all suggest that there exists a seasonal periodicity in gravidity of cedaroid species around the world, as is the case with numerous if not all echinoderms.

With the help of Kara and Philipp Rauch of Key Largo, Florida, we spawned *E. tribuloides* and collected monthly data for over four years. Animals were spawned on the reef with 0.5M KCl subcutaneous injection. Organisms were very gravid, slightly gravid, or dry, as well as male or female. What follows is two figures representing our findings. Briefly, we also found a strong correlation with seasonal periodicity as did previous surveys. *E. tribuloides* off the coast of Florida are most gravid in early August to late December. Virtually no animals were gravid from mid-January to early June, and of those that were gravid, cultures frequently collapsed and were not worth the time.

We also spent copious effort in trying to establish a gravid colony in the laboratory, as was previously suggested possible by (McClintock and Watts, 1990; Lares and McClintock, 1991). However, the best we ever did in this regard was to maintain whatever gametes the urchins had in them when they arrived. While this strategy was at times useful, it was also frustrating and led to difficulties with lab cultures.

Thus, with this in mind, in our opinion the best strategy for working with this species is to collect as much data as you can during the fall and winter and spend the subsequent winter months collecting and analyzing the data. And we leave you with two figures on *E. tribuloides* gravidity off the coast of Key Largo, Florida, USA.

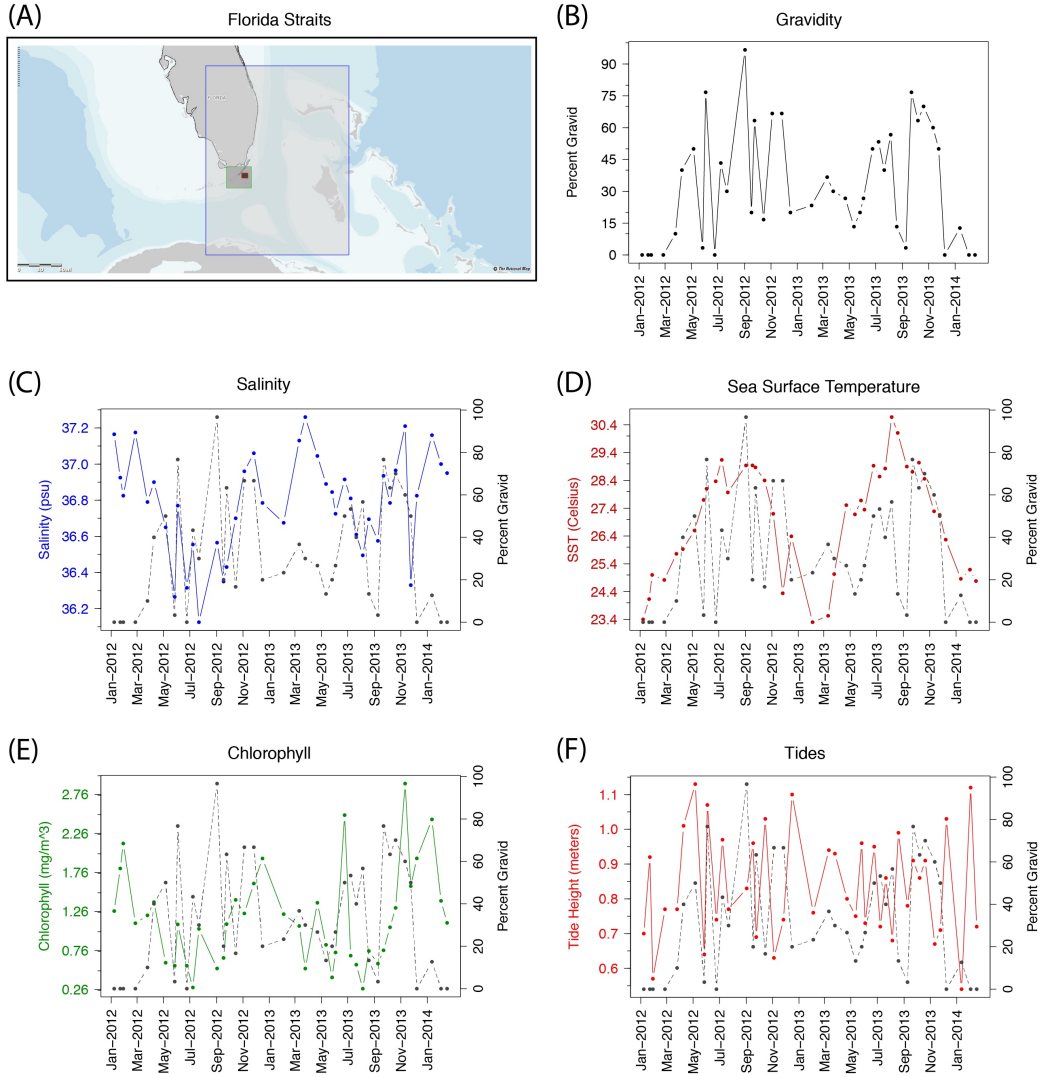


Figure B.1: Gravidity of *Eucidaris tribuloides* off the coast of Key Largo, Florida and its correlation to local environmental variables. (A) Geographic area in which the various datasets were collected: blue outlined box, salinity; green outlined box, chlorophyll; red outlined box, sea surface temperature and tides. (B) Gravidity of *E. tribuloides* from January 2012 to January 2014. (C) Gravidity data against environmental salinity (in practical salinity units) over the same time period. (D) Gravidity data against sea surface temperature over the same time period. (E) Gravidity data against environmental chlorophyll levels (in milligrams per cubic meter) over the same time period. (F) Gravidity data against local tidal levels over the same time period. Environmental data source: NOAA / Aquarius.

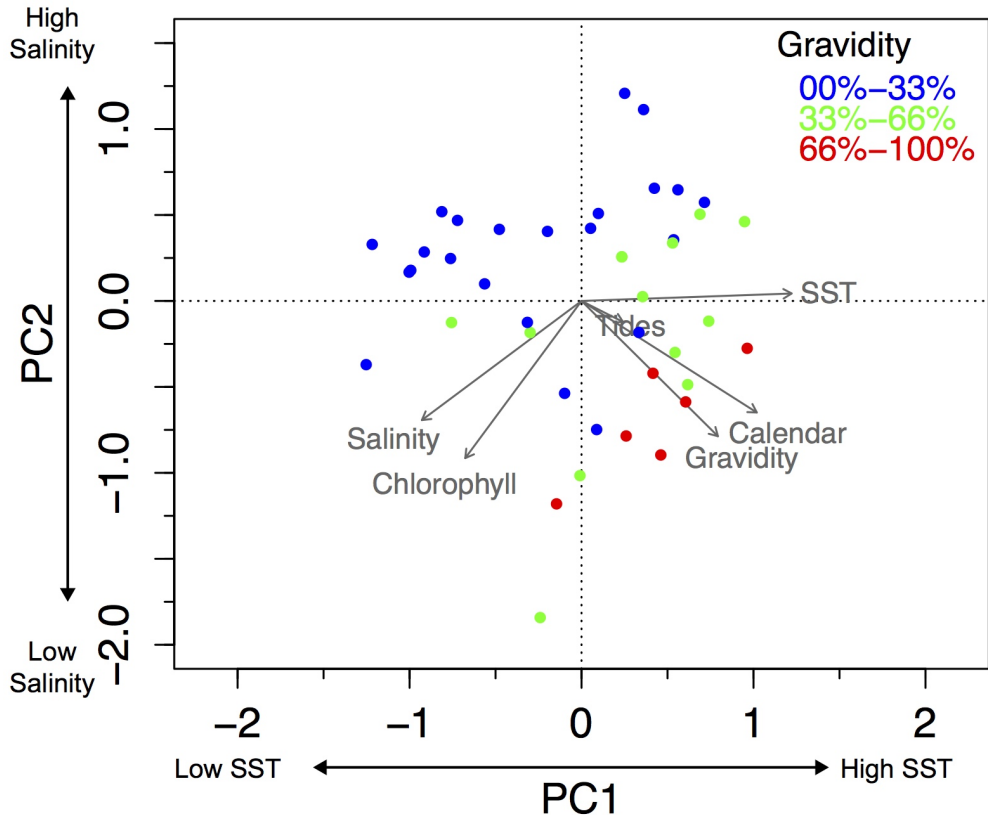


Figure B.2: Principal component analysis of environmental data against gravidity. Biplot of the first two principal components from principal component analysis of environmental variables and spawning events. Each point is a spawning event and is color coded to represent either low gravidity (0%-33%), medium gravidity (33%-66%), or high gravidity (66%-100%). The first principal component (PC1) was heavily influenced by sea surface temperature (SST). The second principal component (PC2) was heavily influenced by ocean salinity levels.

References

Holland, N. D. (1967). "Gametogenesis during the annual reproductive cycle in a cidaroid sea urchin (*Stylocidaris affinis*)". In: *Biological bulletin* 133.3, pp. 578–590.

Lares, M. T. and J. B. McClintock (1991). "The effects of temperature on the survival, organismal activity, nutrition, growth, and reproduction of the carnivorous, tropical sea urchin *Eucidaris tribuloides*". In: *Marine & Freshwater Behaviour & Phy* 19.2, pp. 75–96.

Lessios, H. A. (1991). "Presence and absence of monthly reproductive rhythms among eight Caribbean echinoids off the coast of Panama". In: *Journal of Experimental Marine Biology and Ecology* 153.1, pp. 27–47.

McClintock, J. B. and S. A. Watts (1990). "The effects of photoperiod on gametogenesis in the tropical sea urchin *Eucidaris tribuloides* (Lamarck)(Echinodermata: Echinoidea)". In: *Journal of Experimental Marine Biology and Ecology* 139.3, pp. 175–184.

McPherson, B. F. (1968). "Contributions to the biology of the sea urchin *Eucidaris tribuloides* (Lamarck)". In: *Bulletin of Marine Science* 18.2, pp. 400–443.

Pearse, J. S. (1969). "Reproductive periodicities of Indo-Pacific invertebrates in the Gulf of Suez. I. The echinoids *Prionocidaris baculosa* (Lamarck) and *Lovenia elongata* (Gray)". In: *Bulletin of marine science* 19.2, pp. 323–350.

Appendix C

QUESTIONNAIRE

*Appendix D***CONSENT FORM**

INDEX

F

figures, 26–30, 32, 35, 39, 42, 43, 61, 63–65, 67, 70, 73, 91, 92, 99, 112, 114, 116, 119, 121, 124, 125, 136–141

T

tables, 49, 79, 80, 93, 97, 101, 110, 131, 142, 143